

On the Fundamental Limits in High-dimensional Testing and Inference

by

Zheng Gao

A dissertation submitted in partial fulfillment
of the requirements for the degree of
Doctor of Philosophy
(Statistics)
in the University of Michigan
2020

Doctoral Committee:

Professor Stilian Stoev, Chair
Professor Tailen Hsing
Professor Roderick Little
Professor Ya'acov Ritov
Assistant Professor Jonathan Terhorst



For what is a man, what has he got?

Zheng Gao

gaozheng@umich.edu

ORCID iD: 0000-0003-1394-8741

© Zheng Gao 2020

All Rights Reserved

ACKNOWLEDGEMENTS

I am deeply indebted to my advisor Professor Stilian Stoev. He allowed me the luxury of autonomy and the freedom to pursue my own interests, while by some magic, was always able to give me the most incisive advice. This thesis is made possible only by his astute guidance and enthusiastic encouragements.

My gratitude also goes to collaborators and coauthors: Rafail Kartsioukas, Doctor Michalis Kallitsis, Doctor Cristopher Van Hout, and Assistant Professor Jonathan Terhorst. I would like to thank Professor Tailen Hsing, Professor Ya'acov Ritov, Professor Roderick Little, and Assistant Professor Jonathan Terhorst for serving on the dissertation committee and providing valuable feedback.

I was blessed with much needed help during a period of difficulty from my fellow students Yumu Liu, Yuanzhi Li, Yifan Jin, Xinzhou Guo, Jingshen Wang, and from my friends in the nursing profession Louise Crisostomo and Alice Del Valle. The Center for the Education of Women provided me with generous financial relief. I would not be here without them.

Finally, I would like to thank my parents for their unconditional love and support through the years. To my partner Ruirui, thank you for your sacrifice and companionship. It is a privilege to share this wonderful journey with you.

TABLE OF CONTENTS

Acknowledgements	ii
List of Figures	vi
List of Abbreviations	x
Abstract	xi
Chapter	
1 Introduction	1
1.1 The additive error model	2
1.2 Genome-wide association studies and the chi-square model	4
1.3 Contents	6
2 Background and Literature Review	9
2.1 Statistical risks	9
2.2 Statistical procedures	13
2.3 Related literature and our contributions	18
2.4 Relationships between the asymptotic risks	22
2.5 The asymptotic generalized Gaussian models	24
2.6 Rapid variation and relative stability	25
3 The Phase Transition Phenomena in Independent Gaussian Error Models . .	29
3.1 Sparse signal detection problems	30
3.2 Sparse signal support recovery problems	34
3.2.1 The exact support recovery problem	35
3.2.2 The approximate support recovery problem	36
3.2.3 The exact-approximate support recovery problem	38
3.2.4 The approximate-exact support recovery problem	39
3.2.5 Asymptotic power analysis	40
3.3 Proofs	41
3.3.1 Auxiliary facts of Gaussian distributions	41
3.3.2 Monotonicity of the Benjamini-Hochberg procedure	43
3.3.3 Proof of Theorem 3.1	45
3.3.4 Proof of Theorem 3.4	48
3.3.5 Proof of Theorems 3.5 and 3.7	53

4	Exact Support Recovery and Minimax Optimality	58
4.1	Exact support recovery under AGG errors	61
4.1.1	Sufficient conditions for exact support recovery	62
4.1.2	Dependence and uniform relative stability	66
4.1.3	Necessary conditions for exact support recovery	67
4.1.4	Dense signals	71
4.1.5	Numerical illustrations for independent errors	73
4.2	Bayes minimax optimality and (sub)optimality of thresholding procedures	75
4.2.1	Point-wise minimax optimality	75
4.2.2	Bayes optimality in support recovery problems	76
4.2.3	Bayes optimality under sub-exponential errors	79
4.2.4	Minimax optimality over all procedures	81
4.2.5	Bayes optimality of likelihood ratio thresholding	83
4.3	Strong classification boundaries in other light-tailed error models	85
4.3.1	Additive error models with heavier-than-AGG tails	86
4.3.2	Additive error models with lighter-than-AGG tails	87
4.4	Thresholding procedures under heavy-tailed errors	89
4.5	Additional proofs	93
4.5.1	Proof of the claims in Examples 4.3 and 4.10	93
4.5.2	Proofs of Propositions 4.19 and 4.27	95
4.5.3	Sub-optimality of data thresholding procedures	98
5	Characterization of Uniform Relative Stability for Gaussian Arrays	99
5.1	Ramsey’s Coloring theorem and structure of correlation matrices	104
5.2	URS implies UDD (‘only if’ part of Theorem 5.6)	107
5.3	UDD implies URS (‘if’ part of Theorem 5.6)	109
5.3.1	Bounding the upper tails of AGG maxima	111
5.3.2	Bounding the lower tails of Gaussian maxima	113
5.4	Numerical illustrations of exact support recovery under dependence	118
6	The Phase Transition Phenomena in Genome-wide Association Studies	124
6.1	Support recovery problems in chi-squared models	125
6.1.1	The exact support recovery problem	126
6.1.2	The exact-approximate support recovery problem	127
6.1.3	The approximate support recovery problem	127
6.1.4	The approximate-exact support recovery problem	128
6.1.5	Comparison of one- versus two-sided alternatives in additive error models	129
6.2	Odds ratios and statistical power	130
6.3	Optimal study designs and rare variants	134
6.4	Phase transitions in large-scale association screening studies	136
6.5	Numerical illustrations of the phase transitions in chi-square models	140
6.5.1	Exact support recovery	140
6.5.2	Approximate, and approximate-exact support recovery	142
6.6	Proofs	143

6.6.1	Auxiliary facts of chi-square distributions	143
6.6.2	Proof of Theorem 6.1	149
6.6.3	Proof of Theorem 6.4	153
6.6.4	Proof of Theorems 6.3 and 6.5	159
6.6.5	Proof of Proposition 6.6 and Corollary 6.7	164
Appendix A: U-PASS: A Software for Unified Power Analysis and Forensics for		
Qualitative Traits in Genetic Association Studies		167
A.1	Power analysis in genetic association studies	167
A.2	Specification of alternatives in power analysis	170
A.3	Use case illustrations	178
A.4	Download, installation, and usage	184
Bibliography		186

LIST OF FIGURES

FIGURE

- 3.1 The phase diagrams of the sparse signal detection problem. Signal size and sparsity are parametrized by r and β , respectively. The diagrams illustrate the regions where the signal detection problem can be solved asymptotically by some of the commonly used statistics: the maximum (M), the sum-of-squares (L_2), the sum-of-absolute values (L_1), and the sum (S). In each region of the diagram, the annotated statistics can make the detection risk (2.4) vanish, as dimension p diverges. Conversely, the risks has \liminf at least one. The detection problem is unsolvable for very sparse and weak signals in the undetectable regions. Notice that the L_1 and L_2 statistics are in fact sub-optimal for all sparsity levels. On the other hand, the max-statistic remains powerful for sparse signals ($\beta > 1/2$), and is fully efficient when the problem is very sparse ($\beta \geq 3/4$). The higher-criticism (HC) statistic can detect signals in all configurations in the detectable regions. See text and Theorem 3.1. 32
- 3.2 The phase diagram of support recovery problems for the high-dimensional chi-square model (3.1), illustrating the boundaries of the exact support recovery (FWER + FWNR; top curve; Theorem 3.3), the approximate-exact support recovery (FDR + FWNR; second curve from top; Theorem 3.7), the exact-approximate support recovery (FWER + FNR; horizontal line $r = 1$; Theorem 3.5), and the approximate support recovery problems (FDR + FNR; tilted line $r = \beta$; Theorem 3.4). The signal detection problem (Type I + Type II errors of the global test; lower curve) was studied in Donoho and Jin (2004). In each region of the diagram and above, the annotated statistical risk can be made to vanish, as dimension p diverges. Conversely, the risks has \liminf at least one. . . 37
- 4.1 The empirical probability of exact support recovery from numerical experiments, as a function of sparsity level β and signal sizes r , from Gaussian error models (upper panels), Laplace error models (middle panels), and generalized Gaussian with $\nu = 1/2$ (lower panels); darker color indicates higher probability of exact support recovery. The experiments were repeated 1000 times for each sparsity-signal size combination, and for dimensions $p = 100$ (left panels) and $p = 10000$ (right panels). Numerical results agree with the boundaries described in Theorem 4.1; convergence is noticeably slower for under generalized Gaussian ($\nu = 1/2$) errors. For reference, the dashed and dash-dotted lines represent the weak classification and detection boundaries (see Chapter 3). 74

5.1	The empirical probability of exact support recovery from numerical experiments, as a function of sparsity level β and signal sizes r . Darker colors indicate higher probability of exact support recovery. Three AR(1) models with autocorrelation functions $(-0.5)^k$ (upper), 0.5^k (middle), and 0.9^k (lower) are simulated. The experiments were repeated 1000 times for each sparsity-signal size combination. In finite dimensions ($p = 10000$), the Bonferroni procedures (left) suffers small loss of power compared to the oracle procedures (right). A phase transition in agreement with the predicted boundary (4.5) can be seen in the AR models. The boundaries (solid, dashed, and dash-dotted lines) are as in Fig 4.1.	120
5.2	The empirical probability of exact support recovery from numerical experiments, as a function of sparsity level β and signal sizes r . Darker colors indicate higher probability of exact support recovery. Two fGn models with Hurst parameter $H = 0.75$ (upper), $H = 0.9$ (middle), and the non-UDD errors in Example 5.9 (lower) are simulated. The experiments were repeated 1000 times for each sparsity-signal size combination. In finite dimensions ($p = 10000$), the oracle procedures (right) is able to recover support for weaker signals than the Bonferroni procedures (left) when errors are heavily dependent, although they have the same phase transition limit. The non-UDD errors demonstrate qualitatively different behavior, enabling support recovery for strictly weaker signals. The boundaries (solid, dashed, and dash-dotted lines) are as in Fig 4.1. In the non-UDD example, dashed lines represent the limit attained by Bonferroni's procedures. See text for additional comments.	122
6.1	Signal sizes per sample w^2 as functions of odds ratios in 2-by-2 multinomial distributions for selected genotype marginals in balanced (left) and unbalanced (right) designs; see Relation (6.11) in Proposition 6.6. For given marginal distributions, extreme odds ratios imply stronger statistical signals at a given sample size. However, the signal sizes are bounded above by constants that depend on the marginal distributions; see Relations (6.12) and (6.13).	133
6.2	The OR-RAF diagram visualizing the marginal power of discovery in genetic association studies, after applying Bonferroni's procedure with nominal FWER at 5% level. Sample sizes are marked in each panel, and the problem dimensions are, respectively, $p = 4$ (upper-left), $p = 10^2$ (upper-right), and $p = 10^6$ (lower-left), so that $n/\log p$ are roughly constant. Red curves mark the boundaries ($r = 1$) of the phase transition for the exact-approximate support recovery problem; dashed curves are the equi-signal (equi-power) curves. The phase transition in signal sizes λ translates into the phase transition in terms of (f, R) , and sharpens as $p \rightarrow \infty$; see Example 6.10. In the lower-right panel, we visualize discovered associations (blue circles) in a recent GWA study (Michailidou et al. (2017)); the estimated odds ratios and risk allele frequencies are subject to survival bias and should not be taken at their face values; see Remark 6.11.	137

6.3	The empirical probability of exact support recovery of Bonferroni's procedure in the chi-squared model (1.3). We simulate $\nu = 1, 2, 3, 6$ (first to last row), at dimensions $p = 10^2, 10^3, 10^4$ (left to right column), for a grid of sparsity levels β and signal sizes r . The experiments were repeated 1000 times for each sparsity-signal size combination; darker color indicates higher probability of exact support recovery. Numerical results are in general agreement with the boundaries described in Theorem 6.1; for large ν 's, the phase transitions take place somewhat above the predicted boundaries. The boundary for the approximate support recovery (Theorem 6.4) and the detection boundary (see Donoho and Jin (2004)) are plotted for comparison.	141
6.4	The empirical probability of exact support recovery of Bonferroni's procedure (solid curves) and the oracle procedure (dashed curves) in the chi-squared model with one degree of freedom (marked '2') in the additive Gaussian error model and under one-sided alternatives (marked '1'). We simulate at dimensions $p = 10^2, 10^3, 10^5$ (left to right) for a grid of signal sizes r and sparsity level $\beta = 0.6$. The experiments were repeated 1000 times for each method-model-signal-size combination. Numerical results show evidence of convergence to the 0-1 law as predicted by Theorem 6.1; regions where asymptotically exact support recovery can be achieved are shaded in grey. The difference in power between Bonferroni's procedure and the oracle procedure, as well as in the two types of alternatives both decrease as dimensionality increases. . . .	142
6.5	The empirical risk of approximate support recovery of Benjamini-Hochberg's procedure (solid curves) and the oracle procedure (dashed curves) in the chi-squared model with one degree of freedom (marked '2') and in the additive Gaussian error model under one-sided alternatives (marked '1'). We simulate at dimensions $p = 10^2, 10^3, 10^5$ (left to right) for a grid of signal sizes r and sparsity level $\beta = 0.6$. The experiments were repeated 1000 times for each method-model-signal-size combination. Numerical results show evidence of convergence to the 0-1 law as predicted by Theorem 6.4; regions where asymptotically approximate support recovery can be achieved are shaded in grey. The difference in risks between Benjamini-Hochberg's procedure and the oracle procedure, as well as in the two types of alternatives, both decrease as dimensionality increases.	144
6.6	The estimated risk of approximate support recovery risk ^A (see (2.7)) of the Benjamini-Hochberg procedure in the chi-squared model (1.3). We simulate $\nu = 1, 2, 3, 6$ (first to last row), at dimensions $p = 10^2, 10^3, 10^4$ (left to right column), for a grid of sparsity levels β and signal sizes r . The experiments were repeated 1000 times for each sparsity-signal size combination; darker color indicates higher larger risk ^A . Numerical results are generally in agreement with the boundaries described in Theorem 6.4; for large ν 's, the phase transitions take place somewhat above the predicted boundaries. The boundary for the exact support recovery problem (Theorem 6.1) and the detection boundary (see Donoho and Jin (2004)) are plotted for comparison.	145

6.7	The estimated risk of approximate-exact support recovery risk^{EA} (see (2.12)) of the Benjamini-Hochberg procedure in the chi-squared model (1.3). We simulate $\nu = 1, 2, 3, 6$ (first to last row), at dimensions $p = 10^2, 10^3, 10^4$ (left to right column), for a grid of sparsity levels β and signal sizes r . The experiments were repeated 1000 times for each sparsity-signal size combination; darker color indicates higher larger risk ^{EA} . Numerical results are generally in agreement with the boundaries described in Theorem 6.5; for small β 's and large ν 's, the phase transitions take place somewhat above the predicted boundaries. Other boundaries in the support recovery and the detection problems are plotted for comparison.	146
A.1	The process of a typical power analysis for genetic association tests. The quantities depend on, and can be calculated from the values of their parents in the directed graph. Power can be calculated as long as one set of parameters in each branch is known. While there is a one-to-one correspondence between the sample size specifications (n_1, n_2) and (ϕ, n) , the mapping from disease model specifications to (f, R) is many-to-one.	171
A.2	The OR-RAF diagram of two studies where gross misalignments were identified. Left: Dominguez-Cruz et al. (2018), right: Haryono et al. (2015). The reported odds ratios and risk allele frequencies of the discovered associations in these two papers are charted with orange (and red) circles. Dark regions represent f - R parameter combinations that are predicted to have low power of discovery under the current sample sizes. See text for more comments.	179
A.3	A screenshot of the user interface for the “Design my study” tab of the software. The inputs are as described in the numerical example in Section A.3.2. Results of the power calculation are visualized in an interactive plot in the application.	182
A.4	A screenshot of the user interface for the “Disease model converter” tab of the software. See Section A.2 for details of the conversion between disease models and canonical parameters in genome-wide association studies.	183

LIST OF ABBREVIATIONS

AGG asymptotically generalized Gaussian

BH Benjamini-Hochberg

CDF cumulative distribution function

FDR false discovery rate

FNR false non-discovery rate

FWER family-wise error rate

FWNR family-wise non-discovery rate

GWAS genome-wide association studies

HC higher-criticism

iid independent and identically distributed

LR likelihood-ratio

SNP single-nucleotide polymorphisms

URS uniform relatively stable/uniform relative stability

ABSTRACT

High-dimensional models that incorporate sparsity assumptions arise naturally in numerous modern applications ranging from cybersecurity to statistical genetics. In such data models, statisticians are typically tasked with (a) detecting the presence of sparse signals, and (b) estimating the support – i.e., locations of the non-zero components – of the signals. In the past two decades, researchers have studied the theoretical limits for the two statistical problems, and discovered interesting phase transition phenomena where the problems are found to be solvable if and only if the signals have certain configurations in terms of their sparsity and signal size. This dissertation contributes a spectrum of new phase-transition results under various statistical risks, providing a largely complete picture of the fundamental limits in the sparse signal detection and support recovery problems.

A major contribution of this thesis is a complete solution to the exact signal support recovery problem for the general class of thresholding estimators. Specifically, it is shown that if the signal magnitude is larger than a certain boundary as a function of the signal sparsity, then thresholding estimators can recover the signal support exactly as the signal dimension grows to infinity. Conversely, for signal magnitudes below that same boundary, no thresholding estimators can recover the support asymptotically. This phase-transition result is surprisingly universal and it holds under very general error-dependence models. Threshold-based support estimators were also shown to be finite-sample Bayes-optimal for errors with log-concave densities and sub-optimal for heavier tailed errors. As a result, complete minimax characterizations of the statistical difficulty in support recovery problems are obtained.

The study of exact support recovery under broad error-dependence conditions is a first of its kind. It is made possible by developing new probabilistic results on a concentration of maxima phenomenon known as relative stability. A complete characterization of the relative stability phenomenon for Gaussian error arrays in terms of their correlation structure is established.

Finally, the manifestation of the phase transition phenomena in the field of statistical genetics is studied. The established results provide a first theoretical explanation of the long empirically observed trade-off between allele frequency and penetrance, and quantifies the fundamental statistical limits of discoverability in genome-wide association studies. Moreover, one surprising result of practical significance is that balanced designs in association studies rarely deliver optimal power. Developed are explicit formulas for power calculations, as well as an interactive web-based software application for performing power analysis and finding optimal study designs.

CHAPTER 1

Introduction

The proliferation of information technology has enabled us to collect and consume huge volumes of data at unprecedented speeds and at very low costs. This fast and cheap access to data gave rise to fundamentally new ways of pursuing scientific questions. In contrast with the traditional hypothesis–experiment–analysis cycle where data are collected from the experiments, abundant information are often available before specific questions are even formulated. Such information can be used for not just evaluating hypotheses, but also for *generating*, and *selecting* the hypotheses to pursue. As a result, multiple testing — where a large number of hypotheses are formulated and screened for their plausibility simultaneously — has become a staple of modern data-driven studies.

An archetypal example of multiple testing problems is genetic association studies (Bush and Moore, 2012). In genetic association studies, scientists test hypotheses relating each of the hundreds of thousands of genetic marker locations to phenotypic traits of interest; the goal here is to select the set of most promising genetic markers for subsequent investigation. Another example of multiple testing problems arise in cybersecurity, where millions of IP addresses are monitored in real time. In this engineering application, statistics are collected and tests are performed for each IP address, in an attempt to locate the IP addresses with anomalous network activities, so that and malicious traffic and volumetric attacks can be filtered to protect end users of network services (Kallitsis et al., 2016).

We are motivated by the above examples in particular to study high-dimensional multi-

ple testing problems where a large number of hypotheses are tested simultaneously.

In the rest of the introduction, we shall review the main objectives of high-dimensional multiple testing, elaborate on these objectives in two classes of data models and in the context of the genetic applications, and briefly summarize the contents of this dissertation.

1.1 The additive error model

Consider the canonical signal-plus-noise model where the observation x is a high-dimensional vector in \mathbb{R}^p ,

$$x(i) = \mu(i) + \epsilon(i), \quad i = 1, \dots, p. \quad (1.1)$$

The signal, $\mu = (\mu(i))_{i=1}^p$, is a vector with s non-zero components supported on the set $S = \{i : \mu(i) \neq 0\}$; the second term ϵ is a random error vector. The goal of high-dimensional statistics is usually two-fold:

1. To detect the presence of non-zero components in μ . That is, to test the global hypothesis $\mu = 0$, which we call the *detection* problem, and
2. To estimate the support set S , which we call the *support recovery* problem.

To illustrate, in the engineering application of cybersecurity, Internet service providers (ISP) routinely collect statistics of network traffic to determine if there are abnormal surges or blackouts. The data vector x could represent, for example, incoming traffic volumes to each server node that the ISP maintains. In this case, the vector μ would be the average traffic volumes when under normal operating conditions, and ϵ 's the fluctuations around these normal levels of traffic. The signal detection problem in this context is then equivalent to determining if there are *any* anomalies among all servers, and the support recovery problem is equivalent to *identifying* the servers with anomalies. Similar questions of signal detection and support recovery are pursued in large-scale microarray experiments, brain imaging and fMRI analysis, and numerous other applications.

A common theme in such applications is that the errors are correlated, and that the signal vectors are believed to be sparse: the number of non-zero components in μ is small compared to the number of test performed — in the cybersecurity example, while monitoring is performed over a large number of servers, it is often believed that only very few servers will be experiencing problems at any time. Under such sparsity assumptions, it is natural to ask if and when one can reliably (1) detect the signals, and (2) recover the support set S . We explore both the *detection* and the *support recovery* problems in this thesis. More precisely, we are interested in the theoretical feasibility of both problems, and seek minimal conditions under which these problems can be consistently solved in large dimensions.

Model (1.1) is simple yet ubiquitous. Consider the linear model

$$Y = X\mu + \xi,$$

where μ is a p -dimensional vector of regression coefficients of interest to be inferred from observations of X and Y . If the design matrix X is of full column rank, then the ordinary least squares (OLS) estimator of μ can be formed

$$\hat{\mu} = (X'X)^{-1} X'Y = \mu + \epsilon, \tag{1.2}$$

where $\epsilon := (X'X)^{-1} X'\xi$. Hence we recover the generic problem (1.1). Signal detection is therefore equivalent to the problem of testing the global null model, and support recovery problem corresponds to the fundamental problem of variable selection.

Note that the components in the observation x (and equivalently, the noise ϵ) in (1.1) need not be independent. In the linear regression example, even when the components of the noise term ξ are independent, those of the OLS estimator (1.2) need not be, unless we have an orthogonal design. Indeed, in practice, independence is the exception rather than the rule. Therefore a general theory of feasibility must address the role of the error

dependence structures in such testing problems, and identify practical procedures that attain the performance limits in independent as well as dependent cases, as soon as the problems become theoretically feasible.

1.2 Genome-wide association studies and the chi-square model

The second data model we analyze is the high-dimensional chi-square model,

$$x(i) \sim \chi_{\nu}^2(\lambda(i)), \quad i = 1, \dots, p, \quad (1.3)$$

where the data $x(i)$'s follow independent (non-central) chi-square distributions with ν degrees of freedom and non-centrality parameter $\lambda(i)$.

Model (1.3) is motivated by large-scale categorical variable screening problems, typified by genome-wide association studies (GWAS) where millions of genetic factors are examined for their potential influence on phenotypic traits.

In a GWAS with a case-control design, a total of n subjects are recruited, consisting of n_1 subjects possessing some defined traits, and n_2 subjects without the traits serving as controls. The genetic compositions of the subjects are then examined for variations known as single-nucleotide polymorphisms (SNP) at an array of p genomic marker locations, and compared between the case and the control group. These physical traits are commonly referred to as *phenotypes*, and the genetic variations are known as *genotypes*.

Focusing on one specific genomic location, the counts of observed genotypes, if two variants are present, can be tabulated as follows.

# Observations	Genotype		Total by phenotype
	Variant 1	Variant 2	
Cases	O_{11}	O_{12}	n_1
Controls	O_{21}	O_{22}	n_2

Researchers test for associations between the genotypes and phenotypes using, for example, the Pearson chi-square test with statistic

$$x = \sum_{j=1}^2 \sum_{k=1}^2 \frac{(O_{jk} - E_{jk})^2}{E_{jk}}, \quad (1.4)$$

where $E_{jk} = (O_{j1} + O_{j2})(O_{1k} + O_{2k})/n$.

Under the mild assumption that the counts O_{jk} 's follow a multinomial distribution (or a product-binomial distribution, if we decide to condition on one of the marginals), the statistic x in (1.4) can be shown to have an approximate $\chi^2(\lambda)$ distribution with $\nu = 1$ degree of freedom at large sample sizes (see, e.g., classical results in Ferguson (2017) and Agresti (2018)). Independence between the genotypes and phenotypes would imply a non-centrality parameter λ value of zero; if dependence exists, we would have a non-zero λ where its value depends on the underlying multinomial probabilities. More generally, if we have a J phenotypes and K genetic variants, assuming a $J \times K$ multinomial distribution, the statistic will follow approximately a $\chi^2_{\nu}(\lambda)$ distribution with $\nu = (J-1)(K-1)$ degrees of freedom, when sample sizes are large.

The same asymptotic distributional approximations also apply to the likelihood ratio statistic, and many other statistics under slightly different modeling assumptions (Gao et al., 2019). These association tests are performed at each of the p SNP marker locations throughout the whole genome, and we arrive at p statistics having approximately (non-central) chi-square distributions, $\chi^2_{\nu(i)}(\lambda(i))$, for $i = 1, \dots, p$, where $\lambda = (\lambda(i))_{i=1}^p$ is the p -dimensional non-centrality parameter.

Although the number of tested genomic locations p can sometimes exceed 10^5 or even

10^6 , it is often believed that only a small set of genetic locations have tangible influences on the outcome of the disease or the trait of interest. Under the stylized assumption of sparsity, λ is assumed to have s non-zero components, with s being much smaller than the problem dimension p . The goal of researchers is again two-fold: (1) to test if $\lambda(i) = 0$ for all i , and (2) to estimate the set $S = \{i : \lambda(i) \neq 0\}$. In other words, we look to first determine if there are *any* genetic variations associated with the disease; and if there are associations, we want to locate them.

The chi-square model (1.3) also plays an important role in analyzing variable screening problems under omnidirectional alternatives. A primary example is multiple testing under two-sided alternatives in the additive error model (1.1) where the errors ϵ are assumed to have standard normal distributions.

Under two-sided alternatives, unbiased test procedures call for rejecting the hypothesis $\mu(i) = 0$ at locations where observations have large absolute values, or equivalently, large squared values. Taking squares on both sides of (1.1), and we arrive at Model (1.3) with non-centrality parameters $\lambda(i) = \mu^2(i)$ and degree-of-freedom parameter $\nu = 1$. In this case, the support recovery problem is equivalent to locating the set of observations with mean shifts, $S = \{i : \mu(i) \neq 0\}$, where the mean shifts could take place in both directions.

Therefore, a theory for the chi-square model (1.3) naturally lends itself to the study of two-sided alternatives in the Gaussian additive error model (1.1). In comparing such results with existing theory on one-sided alternatives, we will be able to quantify if, and how much of a price has to be paid for the additional uncertainty when we have no prior knowledge on the direction of the signals.

1.3 Contents

Important notions and definitions in high-dimensional testing problems are recalled in Chapter 2. We review related literature and place our contributions in context, as well

as key concepts and technical results used in our subsequent analyses.

In Chapter 3 we study the sparse signal detection and support recovery problems for the additive error model (1.1) when components of the noise term ϵ are independent standard Gaussian random variables. In particular, we discover three new *phase transitions* in support recovery problems. These results show that as the dimension $p \rightarrow \infty$, the tasks of identifying the support set S are either doable or impossible depending on the sparsity and signal sizes of the problems. We also identify commonly used procedures that attain the performance limits in both detection and support recovery problems.

Both the Gaussianity assumption and the independence assumption are relaxed in Chapter 4. Established are the necessary and sufficient conditions for exact support recovery in the high-dimensional asymptotic regime. This is a major theoretical contribution of the thesis, solving, and expanding on, open problems in the literature (see Butucea et al. (2018); Gao and Stoev (2019)). The analysis of support recovery problem is intimately related to a *concentration of maxima* phenomena in the analysis of extremes. The latter concept is key to understanding the role played by dependence in the phase transition phenomena of high-dimensional testing problems. Using this probabilistic concept, we establish minimax optimality results that hold for a very large class of dependence structures.

The dependence condition defined by the concentration of maxima concepts is further demystified in Chapter 5 for Gaussian errors. We offer a complete characterization of the concentration of maxima phenomenon, known as uniform relative stability, in terms of the covariance structures of the Gaussian arrays. This result may be of independent interest since it relates to the so-called *superconcentration* phenomenon coined by Chatterjee (2014). See also, Gao and Stoev (2019) and Kartsioukas et al. (2019).

Chapter 6 returns to high-dimensional multiple testing problems, and study the chi-square model (1.3) inspired by the marginal association screening problems. We establish four new phase-transition-type results in the chi-square model, and illustrate their practical implications in the GWAS application. Our theory enables us to explain the long-standing

empirical observation that small perturbations in the frequency and penetrance of genetic variations lead to drastic changes in the discoverability in genetic association studies. We also provide a user-friendly web-based software tool for planning, and reviewing, genome-wide association studies, published in Gao et al. (2019).

CHAPTER 2

Background and Literature Review

We establish the background necessary for the study of sparse signal detection and support recovery problems in this chapter. Sections 2.1 and 2.2 provide a refresher on the definitions of statistical risks and some commonly used statistical procedures. Section 2.3 describes the asymptotic regime under which we analyze these procedures, and reviews the related literature in high-dimensional statistics. We discuss in Section 2.4 the connections among the risk metrics, and point out some common fallacies. The remaining sections collect the technical preparations for this thesis. Section 2.5 defines an important class of error distributions. And finally, Section 2.6 introduces the concepts of concentration of maxima, which plays a crucial role in the analysis of high-dimensional support recovery problems.

2.1 Statistical risks

We define the statistical risk metrics for signal detection and signal support recovery problems in this section.

Signal detection. Recall that in sparse signal detection problems, our goal is to come up with a procedure, $\mathcal{R}(x)$, such that the null hypothesis is rejected if the data x is deemed incompatible with the null. In the example of additive error models (1.1), we wish to tell apart two hypotheses

$$\mathcal{H}_0 : \mu(i) = 0, \ i = 1, \dots, p, \quad \text{v.s.} \quad \mathcal{H}_1 : \mu(i) \neq 0, \text{ for some } i \in \{1, \dots, p\}, \quad (2.1)$$

based on the p -dimensional observation x . Similarly in the chi-square model (1.3), we look to test

$$\mathcal{H}_0 : \lambda(i) = 0, \ i = 1, \dots, p, \quad \text{v.s.} \quad \mathcal{H}_1 : \lambda(i) \neq 0, \text{ for some } i \in \{1, \dots, p\}. \quad (2.2)$$

Since the decision is binary, we may write the outcome of the procedure in the form of an indicator function, $T(\mathcal{R}(x)) \in \{0, 1\}$, where the function T takes on value 1 if the null is to be rejected in favor of the alternative, and 0 if we fail to reject the null. The Type I and Type II errors of the procedure, i.e., the probability of wrong decisions under the null hypothesis \mathcal{H}_0 and alternative hypothesis \mathcal{H}_1 , respectively, are defined as

$$\alpha(\mathcal{R}) := \mathbb{P}_{\mathcal{H}_0}(T(\mathcal{R}(x)) = 1) \quad \text{and} \quad \beta(\mathcal{R}) := \mathbb{P}_{\mathcal{H}_1}(T(\mathcal{R}(x)) = 0). \quad (2.3)$$

The Neyman-Pearson framework of hypothesis testing then seeks tests that minimize the Type II error of the test, while controlling the Type I error of the test at low levels. We are particularly interested in the sum of the two errors,

$$\text{risk}^D(\mathcal{R}) := \alpha(\mathcal{R}) + \beta(\mathcal{R}), \quad (2.4)$$

which shall be referred to as the risk of signal detection (of the procedure \mathcal{R}). It is trivial that a small risk^D would imply both small Type I and Type II errors of the procedure.

Signal support recovery. Turning to support recovery problems, our goal is to design a procedure \mathcal{R} that produces a set estimate \hat{S} of the true index set of relevant variables S . For example, in the sparse additive error model (1.1) we aim to estimate $S = \{i : \mu(i) \neq 0\}$, while in the sparse chi-square model (1.3) the goal is to estimate $S = \{i : \lambda(i) \neq 0\}$. Formally, one should write $\hat{S}(\mathcal{R}(x))$ to reflect the dependence of the set estimate on the procedure \mathcal{R} and on the test statistics x ; for notational convenience, we suppress this dependence and simply write \hat{S} .

For a given procedure \mathcal{R} , the false discovery rate (FDR) and the false non-discovery rate (FNR) of a procedure are defined as

$$\text{FDR}(\mathcal{R}) := \mathbb{E} \left[\frac{|\hat{S} \setminus S|}{\max\{|\hat{S}|, 1\}} \right] \quad \text{and} \quad \text{FNR}(\mathcal{R}) := \mathbb{E} \left[\frac{|S \setminus \hat{S}|}{\max\{|S|, 1\}} \right], \quad (2.5)$$

where the maxima in the denominators resolve the possible division-by-0 problem. Roughly speaking, FDR measures the expected fraction of false findings, while FNR describes the proportion of Type II errors among the true signals, and reflects the average marginal power of the procedure.

A more stringent criterion for false discovery is the family-wise error rate (FWER), and correspondingly, a more stringent criteria for false non-discovery is the family-wise non-discovery rate (FWNR), i.e.,

$$\text{FWER}(\mathcal{R}) := 1 - \mathbb{P}[\hat{S} \subseteq S] \quad \text{and} \quad \text{FWNR}(\mathcal{R}) := 1 - \mathbb{P}[S \subseteq \hat{S}]. \quad (2.6)$$

We introduce five different statistical risk metrics, each having different asymptotic limits in the support recovery problems as we will see later in this thesis. Following Arias-Castro and Chen (2017), we define the risk for *approximate* support recovery as

$$\text{risk}^A(\mathcal{R}) := \text{FDR}(\mathcal{R}) + \text{FNR}(\mathcal{R}). \quad (2.7)$$

Analogously, we define the risk for *exact* support recovery as

$$\text{risk}^E(\mathcal{R}) := \text{FWER}(\mathcal{R}) + \text{FWNR}(\mathcal{R}). \quad (2.8)$$

Two closely related measures of success in the exact support recovery risk are the probability of exact recovery,

$$\mathbb{P}[\hat{S} = S] = 1 - \mathbb{P}[\hat{S} \neq S], \quad (2.9)$$

and the Hamming loss

$$H(\hat{S}, S) := |\hat{S} \triangle S| = \sum_{i=1}^p |\mathbb{1}_{\hat{S}}(i) - \mathbb{1}_S(i)|. \quad (2.10)$$

which counts the number of mismatches between the estimated and true support sets.

The relationship between probability of support recovery $\mathbb{P}[\hat{S} = S]$, exact support recovery risk risk^E , and the expected Hamming loss $\mathbb{E}[H(\hat{S}, S)]$ will be discussed in Section 2.4 below.

Notice that all risk metrics introduced so far penalize false discoveries and missed signals somewhat symmetrically — the approximate support recovery risk combines proportions of errors, the exact support recovery risk combines probabilities of errors, and the Hamming loss increments the risk by one regardless of the types of errors made. In applications, however, attitudes towards Type I and Type II errors are often different. In the example of GWAS, where the number of candidate locations p could be in the millions, researchers are typically interested in the marginal (location-wise) power of discovery, while exercising stringent (family-wise) false discovery control — a situation not reflected in the above-mentioned risk metrics. This asymmetric consideration, and in particular the GWAS application, prompts us to consider risks that weigh both the family-wise error rate and the marginal power of discovery. One such risk metric is what shall be referred to as the *exact-approximate* support recovery risk

$$\text{risk}^{\text{EA}}(\mathcal{R}) := \text{FWER}(\mathcal{R}) + \text{FNR}(\mathcal{R}). \quad (2.11)$$

The somewhat cumbersome name and notation are chosen to reflect the asymmetry in dealing with the two types of errors in support recovery. Namely, when the risk metric (2.11) vanishes, we have “exact false discovery control, and approximate false non-discovery control” asymptotically.

Analogously, we consider the *approximate-exact* support recovery risk

$$\text{risk}^{\text{AE}}(\mathcal{R}) := \text{FDR}(\mathcal{R}) + \text{FWNR}(\mathcal{R}), \quad (2.12)$$

which places more emphasis on non-discovery control over false discovery.

Theoretical limits and performance of procedures in support recovery problems will be studied in terms of the five risk metrics (2.7), (2.8), (2.9), (2.11) and (2.12), in Chapters 3, 4, and 6. We are particularly interested in fundamental limits of signal detection and support recovery problems in terms of these metrics, as well as the optimality of commonly used procedures in high dimensional settings.

2.2 Statistical procedures

We review some popular procedures for signal detection and signal support recovery tasks in this section.

Signal detection. One of the commonly used statistics in sparse signal detection problems such as (2.1) and (2.2) are the L_q norms of the observations x ,

$$L_q(x) = \left(\sum_{i=1}^p |x(i)|^q \right)^{1/q}. \quad (2.13)$$

Typical choices of q include $q = 1, 2$ and ∞ , where $L_\infty(x)$ is interpreted as the limit of $L_q(x)$ norms as $q \rightarrow \infty$, and is equivalent to $\max_i |x(i)|$. Test procedures based on (2.13) may then be written as $T(\mathcal{R}(x)) = \mathbb{1}_{(t, +\infty)}(L_q(x))$, where the cutoff t can be chosen to control the Type I error at desired levels.

While (2.13) measures the deviation of the data from the origin in an omnidirectional manner, statistics that are tailored to the alternatives can be used in the hopes of power improvement if the directions of the alternatives are known. For example, if we were to

test positive mean shifts in the additive error model (1.1) in the one-sided alternative,

$$\mathcal{H}_1 : \mu(i) > 0, \text{ for some } i \in \{1, \dots, p\}, \quad (2.14)$$

one might consider monitoring the sum (or equivalently, the arithmetic average) of the observations,

$$S(x) := \sum_{i=1}^p x(i), \quad (2.15)$$

or the maximum of the observations,

$$M(x) := \max_{i=1, \dots, p} x(i). \quad (2.16)$$

Other tests based on the empirical cumulative distribution function (CDF) are also available. Assuming the same one-sided alternative, let

$$p(i) = 1 - \sup\{F_i(y) : y < x(i)\}, \quad i = 1, \dots, p, \quad (2.17)$$

be the p-values of the individual observations, where F_i is the CDF of the i -th component $x(i)$ under \mathcal{H}_0 . We define empirical CDF of the p-values as

$$\widehat{F}_p(t) = \frac{1}{p} \sum_{i=1}^p \mathbb{1}_{(-\infty, t]}(p(i)). \quad (2.18)$$

Viewed as random elements in the space of càdlàg functions with the Skorohod J_1 topology, the centered and scaled CDFs converge weakly to a Brownian bridge,

$$\left\{ \sqrt{p} \left(\widehat{F}_p(t) - t \right) \right\}_{t \in [0, 1]} \Longrightarrow \{ \mathbb{B}(t) \}_{t \in [0, 1]},$$

under the global null \mathcal{H}_0 and mild continuity assumptions on the F_i 's (Skorokhod, 1956). Therefore, goodness-of-fit statistics such as Kolmogorov-Smirnov distance (Smirnov, 1948),

Cramer-von Mises-type statistics (Cramér, 1928; Anderson and Darling, 1952) that measure the departure from this limiting behavior can be used for testing \mathcal{H}_0 against \mathcal{H}_1 . Of particular interest is the HC statistic, first proposed by Tukey (1976),

$$HC(x) = \max_{0 \leq t \leq \alpha_0} \frac{\widehat{F}_p(t) - t}{\sqrt{t(1-t)/p}}.$$

Performance of these statistics in high-dimensional sparse signal detection problems will be reviewed in Section 2.3, and analyzed in Chapter 3.

Signal support recovery. In signal support recovery tasks, we shall study the performance of five procedures, all of which belong to the broad class of thresholding procedures.

Definition 2.1 (Thresholding procedures). A thresholding procedure for estimating the support $S := \{i : \lambda(i) \neq 0\}$ is one that takes on the form

$$\widehat{S} = \{i \mid x(i) \geq t(x)\}, \quad (2.19)$$

where the threshold $t(x)$ may depend on the data x .

Examples of thresholding procedures include ones that aim to control FWER (2.6) — Bonferroni’s Dunn (1961), Sidák’s (Šidák, 1967), Holm’s (Holm, 1979), and Hochberg’s procedure (Hochberg, 1988) — as well as procedures that target FDR (2.5), such as the Benjamini-Hochberg Benjamini and Hochberg (1995) and the Candès-Barber procedure Barber and Candès (2015). Indeed, the class of thresholding procedures (2.19) is so general that it contains most (but not all) of the statistical procedures in the multiple testing literature.

We review five thresholding procedures, starting with the well-known Bonferroni’s procedure which aims at controlling family-wise error rates.

Definition 2.2 (Bonferroni’s procedure). Suppose the errors $\epsilon(i)$ ’s have a common marginal distribution F , Bonferroni’s procedure with level α is the thresholding procedure that uses

the threshold

$$t_p = F^{\leftarrow}(1 - \alpha/p). \quad (2.20)$$

where $F^{\leftarrow}(u) = \inf \{x : F(x) \geq u\}$ is the generalized inverse function.

The Bonferroni procedure is deterministic (i.e., non data-dependent), and only depends on the dimension of the problem and the null distribution. A closely related procedure is Sidák's procedure (Šidák, 1967), which is a more aggressive (and also deterministic) thresholding procedure that uses the threshold

$$t_p = F^{\leftarrow}((1 - \alpha)^{1/p}). \quad (2.21)$$

The third procedure, strictly more powerful than Bonferroni's, is the so-called Holm's procedure (Holm, 1979). On observing the data x , its coordinates can be ordered from largest to smallest $x(i_1) \geq x(i_2) \geq \dots \geq x(i_p)$, where (i_1, \dots, i_p) is a permutation of $\{1, \dots, p\}$. Denote the order statistics as $x_{[1]}, x_{[2]}, \dots, x_{[p]}$.

Definition 2.3 (Holm's procedure). Let i^* be the largest index such that

$$\overline{F}(x_{[i]}) \leq \alpha/(p - i + 1), \quad \text{for all } i \leq i^*.$$

Holm's procedure with level α is the thresholding procedure with threshold

$$t_p(x) = x_{[i^*]}. \quad (2.22)$$

In contrast to the Bonferroni procedure, Holm's procedure is data-dependent. A closely related, more aggressive (data-dependent) thresholding procedure is Hochberg's procedure (Hochberg, 1988) which replaces the index i^* in Holm's procedure with the largest index such that

$$\overline{F}(x_{[i]}) \leq \alpha/(p - i + 1).$$

Notice that both Holm's procedure and Hochberg's procedure compare p-values to the same thresholds $\alpha/(p - i + 1)$. However, Holm's procedure only rejects the set of hypotheses whose p-values are all smaller than their respective thresholds. On the other hand, Hochberg's procedure rejects the set of hypotheses as long as the largest of their p-values fall below its threshold, and therefore, can be more powerful than Holm's procedure.

It can be shown that Bonferroni's procedure and Holm's procedure both control FWER at their nominal levels, regardless of dependence in the data (Holm, 1979). In contrast, Sidák's procedure and Hochberg's procedure control FWER at nominal levels when data are independent (Šidák, 1967; Hochberg, 1988).

Last but not least, we review the Benjamini-Hochberg (BH) procedure, which aims at controlling false discovery rate (FDR) in (2.5), proposed by Benjamini and Hochberg (1995).

Recall the order statistics of our observations $x_{[1]} \geq x_{[2]} \geq \dots \geq x_{[p]}$.

Definition 2.4 (Benjamini-Hochberg's procedure). Let i^* be the largest index such that

$$\overline{F}(x_{[i]}) \leq \alpha i/p.$$

The Benjamini-Hochberg procedure with level α is the thresholding procedure with threshold

$$t_p(x) = x_{[i^*]}, \tag{2.23}$$

The BH procedure is shown to control the FDR at level α when the $x(i)$'s are independent (Benjamini and Hochberg, 1995). Variations of the BH procedure have been proposed to control the FDR under dependent observations (Benjamini and Yekutieli, 2001).

Performance of these procedures in high-dimensional sparse signal support recovery problems will be reviewed in Section 2.3, and analyzed in Chapters 3, 4, and 6.

2.3 Related literature and our contributions

We look to derive useful asymptotic approximations for high dimensional problems, and analyze the afore-mentioned procedures in the regime where the dimensionality of the observations diverge. Throughout this thesis, we consider triangular arrays of observations as described in Models (1.1) and (1.3), and study the performance of procedures in the signal detection and support recovery tasks when

$$p \rightarrow \infty.$$

The criteria for success and failure in support recovery problems under this high-dimensional asymptotic regime are defined as follows.

Definition 2.5. We say a sequence of procedures $\mathcal{R} = \mathcal{R}_p$ succeeds asymptotically in the detection problem (and respectively, exact, exact-approximate, approximate-exact, and approximate support recovery problem) if

$$\text{risk}^P(\mathcal{R}) \rightarrow 0, \quad \text{as } p \rightarrow \infty, \quad (2.24)$$

where $P = D$ (respectively, E, EA, AE, A).

Conversely, we say the exact support recovery fails asymptotically in the detection problem (and respectively, exact, exact-approximate, approximate-exact, and approximate support recovery problem) if

$$\liminf \text{risk}^P(\mathcal{R}) \geq 1, \quad \text{as } p \rightarrow \infty, \quad (2.25)$$

where $P = D$ (respectively, E, EA, AE, A).

The choice of the constant 1 in the definition (2.25) allows us to declare failure for trivial testing procedures. For example, trivial deterministic procedures that always reject,

and ones that always fail to reject, both have statistical risks 1 in either the detection or the support recovery problem. Similarly, a trivial randomized procedure that reject the nulls uniformly at random also has risk of 1, and is declared as a failure in both problems.

Signal detection. The asymptotic behavior of the statistical risk of signal detection problems (2.4) in high dimensions was first studied in Ingster (1998), where a so-called phase transition phenomena was discovered for sparse additive models (1.1) with independent and Gaussian components. That is, depending on the signal size and sparsity of the signal μ , the detection risk either vanishes, or has a liminf of 1 when we apply the theoretically optimal likelihood-ratio (LR) test, as dimensionality of the problem diverges. The LR test, unfortunately, relies on the knowledge of signal sparsity and signal sizes which are often unknown. The sparsity-and-signal-size-agnostic statistic HC was identified to attain such optimal performance limits in sparse Gaussian models in Donoho and Jin (2004). A modified goodness-of-fit test statistic in Zhang (2002), and two statistics based on thresholded- L_1 and L_2 norms in Zhong et al. (2013) were also shown to be asymptotically optimal in the detection problem. Recent studies have also focused on the behavior of detection risk (2.4) in dense and scale mixture models Cai et al. (2011), under general distributional assumptions (Cai and Wu, 2014; Arias-Castro and Wang, 2017), as well as when errors are dependent (Hall and Jin, 2010). A comprehensive review focusing on the role of HC in detection problems can be found in Donoho and Jin (2015). Notwithstanding the extensive literature on the detection problem, performances of simple statistics such as L_q norms (2.13) and sums (2.15), to the best of our knowledge, have only been sparingly documented. We gather relevant results and fill in the gaps in Chapter 3 of this thesis.

Exact support recovery. There is a wealth of literature on the so-called sparsistency (i.e., $\mathbb{P}[\hat{S} = S] \rightarrow 1$ as $p \rightarrow \infty$) problem in the regression context. Sparsistency problems were pursued, among many others, by Zhao and Yu (2006) and Wasserman and Roeder (2009) in the high-dimensional regression setting (where the number of samples $n \ll p$), and by Meinshausen and Bühlmann (2006) in graphical models. Although there have been

numerous studies on the sufficient conditions for sparsistency, efforts on necessary conditions have been scarce. Notable exceptions include Wainwright (2009a,b) and Comminges and Dalalyan (2012) in regression problems. We refer readers to the recent book by Wainwright (2019) (and in particular, the bibliographical sections of Chapters 7 and 15) for a comprehensive review.

Elaborate asymptotic minimax optimality results under the Hamming loss were derived for methods proposed in Ji and Jin (2012) and Jin et al. (2014) for regression problems. More recently, Butucea et al. (2018) also obtained similar minimax optimality results for a specific procedure in the Gaussian additive error model (1.1) in terms of the expected Hamming loss.

Nevertheless, two important questions remained unanswered. Namely, precise phase-transition-type results for the exact support recovery risk (2.8) and for the support recovery probability (2.9) have not been established. And secondly, performance of commonly used statistical procedures reviewed in Section 2.2 in terms of these risk metrics have not been studied. Resolving these two issues, we show in this thesis that several well-known FWER-controlling procedures — including Bonferroni’s procedure — are optimal in the additive error model under both one-sided and two-sided alternatives; these results have appeared in Gao and Stoev (2019) and Gao (2019).

Approximate support recovery. Performance limits of FDR-controlling procedures in the support recovery problem have been actively studied in recent years. The asymptotic optimality of the Benjamini-Hochberg procedure was analyzed under decision theoretic frameworks in Genovese and Wasserman (2002); Bogdan et al. (2011); Neuvial and Roquain (2012), with main focus on location/scale models. In particular, these papers show that the statistical risks of the procedures come close to that of the oracle procedures under suitable asymptotic regimes. Strategies for dealing with multiple testing under general distributional assumptions can be found in, e.g., Efron (2004), Storey (2007), and Sun and Cai (2007). The two-sided alternative in the additive error model was featured as the primary

example in Sun and Cai (2007).

In the additive error model (1.1) under independent Gaussian errors and one-sided alternatives (2.14), Arias-Castro and Chen (2017) showed that a phase transition exists for the approximate support recovery risk (2.7). The BH procedure Benjamini and Hochberg (1995), and the Candès-Barber procedure Barber and Candès (2015) was identified to be asymptotically optimal. However, Arias-Castro and Chen (2017), as all related work so far, assumed the non-nulls to follow a common alternative distribution. We state a slightly more general version of the phase transition result that relaxes this assumption on the alternatives in Chapter 3.

Asymmetric statistical risks. Although weighted sums of false discovery and non-discovery have been studied in the literature, asymmetric statistical risks such as (2.11) and (2.12) have not been investigated. As argued in Section 2.1, properties of these asymmetric risks are of important practical concern in applications such as GWAS. We study the asymptotic behavior of these risks in Chapters 3 and 6 of this thesis; the results therein have appeared in Gao (2019).

Chi-square models and GWAS. The high-dimensional chi-square model (1.3) seemed to have received little attention in the literature. While the sparse signal detection problem in the chi-square model has been studied Donoho and Jin (2004), to the best of our knowledge, asymptotic limits of the support recovery problems have not been studied. The chi-squared model and the motivating GWAS application are analyzed in Chapter 6 of this thesis. Results in Chapter 6 now appear in Gao (2019). We also analyzed asymptotic equivalences of several additional common association tests, and implement power calculations for GWAS in a software tool Gao et al. (2019). The software streamlines power analysis with a canonical disease model invariant parametrization, and therefore enables forensics of reported findings in genetic association studies. We introduce the software and illustrate its use in the appendix.

2.4 Relationships between the asymptotic risks

We now elaborate on the relationship between statistical risks, as promised in Section 2.1. The first lemma concerns the asymptotic relationship between the probability of exact recovery (2.9) and the risk of exact support recovery (2.8).

Lemma 2.6. *For any sequence of procedures for support recovery $\mathcal{R} = \mathcal{R}_p$, we have,*

$$\mathbb{P}[\widehat{S} = S] \rightarrow 1 \iff \text{risk}^E(\mathcal{R}) \rightarrow 0, \quad (2.26)$$

and

$$\mathbb{P}[\widehat{S} = S] \rightarrow 0 \implies \liminf \text{risk}^E(\mathcal{R}) \geq 1, \quad (2.27)$$

as $p \rightarrow \infty$. Dependence on p was suppressed for notational convenience.

Proof of Lemma 2.6. Notice that $\{\widehat{S} = S\}$ implies $\{\widehat{S} \subseteq S\} \cap \{\widehat{S} \supseteq S\}$, therefore we have for every fixed p ,

$$\text{risk}^E = 2 - \mathbb{P}[\widehat{S} \subseteq S] - \mathbb{P}[S \subseteq \widehat{S}] \leq 2 - 2\mathbb{P}[\widehat{S} = S]. \quad (2.28)$$

On the other hand, since $\{\widehat{S} \neq S\}$ implies $\{\widehat{S} \not\subseteq S\} \cup \{\widehat{S} \not\supseteq S\}$, we have for every fixed p ,

$$1 - \mathbb{P}[\widehat{S} = S] = \mathbb{P}[\widehat{S} \neq S] \leq 2 - \mathbb{P}[\widehat{S} \subseteq S] - \mathbb{P}[S \subseteq \widehat{S}] = \text{risk}^E. \quad (2.29)$$

Relation (2.26) follows from (2.28) and (2.29), and Relation (2.27) from (2.29). \square

By virtue of Lemma 2.6, it is sufficient to study the probability of exact support recovery $\mathbb{P}[\widehat{S} = S]$ in place of risk^E , if we are interested in the asymptotic properties of the risk in the sense of (2.24) and (2.25).

Keen readers must have noticed the asymmetry in Relation (2.27) when we discussed the relationship between the exact support recovery risk (2.8) and the probability of exact

support recovery (2.9).

While a trivial procedure that never rejects and a procedure that always rejects both have risk^E equal to 1, the converse is not true. For example, it is possible that a procedure selects the true index set S with probability $1/2$, but makes one false inclusion *and* one false omission simultaneously the other half of the time. In this case the procedure will have

$$\text{risk}^E = 1, \quad \text{and} \quad \mathbb{P}[\widehat{S} = S] = 1/2,$$

showing that the converse of Relation (2.27) is in fact false.

The same argument applies to risk^A : a procedure may select the true index set S with probability $1/2$, but makes enough false inclusions and omissions other half of the time, so that risk^A is equal to one. Therefore, although the class of methods with risks equal to or exceeding 1 certainly contains the trivial procedures that we mentioned, they are not necessarily “useless” as some researchers have claimed (c.f., Arias-Castro and Chen (2017), Remark 2).

Upper and lower bounds for FDR and false non-discovery rate (FNR) can be immediately derived by replacing the numerators in (2.5) with the Hamming loss,

$$\mathbb{E} \left[\frac{H(\widehat{S}, S)}{\max\{|\widehat{S}|, |S|, 1\}} \right] \leq \text{FDR} + \text{FNR} \leq \mathbb{E} \left[\frac{H(\widehat{S}, S)}{\max\{\min\{|\widehat{S}|, |S|\}, 1\}} \right]. \quad (2.30)$$

Therefore, it is sufficient, but not necessary, that the Hamming loss vanish in order to have vanishing approximate support recovery risks (2.7).

Turning to the relationship between the probability of exact support recovery (2.9) and Hamming loss (2.10), we point out a natural lower bound of the former using the expectation of the latter,

$$\mathbb{P}[\widehat{S} = S] \geq 1 - \mathbb{E}[H(\widehat{S}, S)] = 1 - \sum_{i=1}^p \mathbb{E} |\mathbb{1}_{\widehat{S}}(i) - \mathbb{1}_S(i)|. \quad (2.31)$$

A key observation in Relation (2.31) is that the expected Hamming loss decouples into p terms, and dependence of the estimates $\mathbb{1}_{\hat{S}}(i)$ among the p locations no longer plays a role in the sum. Therefore, studying support recovery problems via the expected Hamming loss is not very informative especially under severe dependence, as the bound (2.31) may become very loose. Vanishing Hamming loss is again sufficient, but not necessary for $\mathbb{P}[\hat{S} = S]$ or the exact support recovery risk to go to zero.

2.5 The asymptotic generalized Gaussian models

We introduce a fairly general class of distributions known as asymptotically generalized Gaussian (AGG) in this section, and state some properties about the tails of the AGG distributions.

Definition 2.7. A distribution F is called asymptotic generalized Gaussian with parameter $\nu > 0$ (denoted $\text{AGG}(\nu)$) if

1. $F(x) \in (0, 1)$ for all $x \in \mathbb{R}$, and
2. $\log \bar{F}(x) \sim -\frac{1}{\nu}x^\nu$ and $\log F(-x) \sim -\frac{1}{\nu}(-x)^\nu$,

where $\bar{F}(x) = 1 - F(x)$ is the survival function, and $a(x) \sim b(x)$ is taken to mean $\lim_{x \rightarrow \infty} a(x)/b(x) = 1$.

The AGG models include, for example, the Gaussian distribution ($\nu = 2$), and the Laplace distribution ($\nu = 1$) as special cases. Since the requirement is only placed on the tail behavior, this class encompasses a large variety of light-tailed models, and is commonly used in the literature on high-dimensional testing (Cai et al., 2007; Arias-Castro and Chen, 2017).

Proposition 2.8. *The $(1/p)$ -th upper quantile of $\text{AGG}(\nu)$ is*

$$u_p := F^{\leftarrow}(1 - 1/p) \sim (\nu \log p)^{1/\nu}, \quad \text{as } p \rightarrow \infty, \quad (2.32)$$

where $F^{\leftarrow}(q) = \inf_x \{x : F(x) \geq q\}$, $q \in (0, 1)$.

Proof of Proposition 2.8. By definition of AGG, for any $\epsilon > 0$, there is a constant $C(\epsilon)$ such that for all $x \geq C$, we have

$$-\frac{1}{\nu}x^\nu(1+\epsilon) \leq \log \bar{F}(x) \leq -\frac{1}{\nu}x^\nu(1-\epsilon).$$

Therefore, for all $x < x_l := ((1+\epsilon)^{-1}\nu \log p)^{1/\nu}$, we have

$$-\log p = -\frac{1}{\nu}x_l^\nu(1+\epsilon) \leq \log \bar{F}(x_l) \leq \log \bar{F}(x), \quad (2.33)$$

and for all $x > x_u := ((1-\epsilon)^{-1}\nu \log p)^{1/\nu}$, we have

$$\log \bar{F}(x) \leq \log \bar{F}(x_u) \leq -\frac{1}{\nu}x_u^\nu(1-\epsilon) = -\log p. \quad (2.34)$$

By definition of generalized inverse,

$$u_p := F^{\leftarrow}(1 - 1/p) = \inf\{x : \bar{F}(x) \leq 1/p\} = \inf\{x : \log \bar{F}(x) \leq -\log p\}.$$

We know from relations (2.33) and (2.34) that

$$[x_u, +\infty) \subseteq \{x : \log \bar{F}(x) \leq -\log p\} \subseteq [x_l, +\infty),$$

and so $x_l \leq u_p \leq x_u$, and the expression for the quantiles follow. \square

2.6 Rapid variation and relative stability

The behavior of the maxima of identically distributed random variables has been studied extensively in the literature (see, e.g., Leadbetter et al. (2012); Resnick (2013); Embrechts et al. (2013); De Haan and Ferreira (2007) and the references therein). The concept of rapid

variation plays an important role in the light-tailed case.

Definition 2.9 (Rapid variation). The survival function of a distribution, $\bar{F}(x) = 1 - F(x)$, is said to be rapidly varying if

$$\lim_{x \rightarrow \infty} \frac{\bar{F}(tx)}{\bar{F}(x)} = \begin{cases} 0, & t > 1 \\ 1, & t = 1 \\ \infty, & 0 < t < 1 \end{cases}. \quad (2.35)$$

When $F(x) < 1$ for all finite x , Gnedenko (1943) showed that the distribution F has rapidly varying tails if and only if the maxima of independent observations from F are *relatively stable* in the following sense.

Definition 2.10 (Relative stability). Let $\epsilon_p = (\epsilon_p(i))_{i=1}^p$ be a sequence of random variables with identical marginal distributions F . Define the sequence $(u_p)_{p=1}^\infty$ to be the $(1 - 1/p)$ -th generalized quantile of F , i.e.,

$$u_p = F^{\leftarrow}(1 - 1/p). \quad (2.36)$$

The triangular array $\mathcal{E} = \{\epsilon_p, p \in \mathbb{N}\}$ is said to have relatively stable (RS) maxima if

$$\frac{1}{u_p} M_p := \frac{1}{u_p} \max_{i=1, \dots, p} \epsilon_p(i) \xrightarrow{\mathbb{P}} 1, \quad \text{as } p \rightarrow \infty. \quad (2.37)$$

In the case of independent and identically distributed $\epsilon_p(i)$'s, Barndorff-Nielsen (1963) and Resnick and Tomkins (1973) obtained necessary and sufficient conditions for the *almost sure stability* of maxima, where the convergence in (2.37) holds almost surely.

While relative stability (and almost sure stability) is well-understood in the independent case, the role of dependence has not been fully explored. We start this investigation with a small refinement of Theorem 2 in Gnedenko (1943) valid under arbitrary dependence.

Proposition 2.11 (Rapid variation and relative stability). *Assume that the array \mathcal{E} consists of identically distributed random variables with cumulative distribution function F , where $F(x) < 1$ for all finite $x > 0$.*

1. *If F has rapidly varying right tail, then for all $\delta > 0$,*

$$\mathbb{P}\left[\frac{1}{u_p}M_p \leq 1 + \delta\right] \geq 1 - \frac{\overline{F}((1 + \delta)u_p)}{\overline{F}(u_p)} \rightarrow 1. \quad (2.38)$$

2. *If, in addition, the array \mathcal{E} has independent entries, then it is relatively stable if and only if F has rapidly varying tail.*

Proof of Proposition 2.11. By the union bound and the fact that $p\overline{F}(u_p) \leq 1$, we have

$$\mathbb{P}[M_p > (1 + \delta)u_p] \leq p\overline{F}((1 + \delta)u_p) \leq \frac{\overline{F}((1 + \delta)u_p)}{\overline{F}(u_p)}. \quad (2.39)$$

In view of (2.35) (rapid variation) and the fact that $u_p \rightarrow \infty$, as $p \rightarrow \infty$, the right-hand side of (2.39) vanishes as $p \rightarrow \infty$, for all $\delta > 0$. This completes the proof of (2.38). Part 2 is a re-statement of the classic result due to Gnedenko in Gnedenko (1943). \square

We next demonstrate that Gaussian, Exponential, Laplace, and Gamma distributions all have rapidly varying tails.

Example 2.12 (Generalized AGG). A distribution is said to have *Generalized AGG* right tail, if $\log \overline{F}$ is regularly varying,

$$\log \overline{F}(x) = -x^\nu L(x), \quad (2.40)$$

where $\nu > 0$ and $L : (0, +\infty) \rightarrow (0, +\infty)$ is a slowly varying function. (A function is said to be slowly varying if $\lim_{x \rightarrow \infty} L(tx)/L(x) = 1$ for all $t > 0$.) Note that the AGG(ν) model corresponds to the special case where $L(x) \rightarrow 1/\nu$, as $x \rightarrow \infty$.

Relation (2.38) holds for all arrays \mathcal{E} with *generalized* AGG marginals; if the entries are independent, the maxima are relatively stable. This follows directly from Proposition 2.11, once we show that F has rapidly varying tail. Indeed, by (2.40), we have

$$\log \left(\overline{F}(tx) / \overline{F}(x) \right) = -L(x)x^\nu \left(t^\nu \frac{L(tx)}{L(x)} - 1 \right),$$

which converges to $-\infty$, 0, and $+\infty$, as $x \rightarrow \infty$, when $t > 1$, $t = 1$, and $t < 1$, respectively, since $x^\nu L(x) \rightarrow \infty$ as $x \rightarrow \infty$ by definition of L .

The AGG class encompasses a wide variety of rapidly varying tail models such as Gaussian and double exponential distributions. The larger class (2.40) is needed, however, for the Gamma distribution.

More generally, distributions with heavier tails (e.g., log-normal) and lighter tails (e.g., Gompertz) outside the generalized AGG class (2.40) may also possess rapidly varying tails; heavy-tailed distributions like the Pareto and t-distributions, on the other hand, do not. These alternative classes of models are will be introduced when we study the phase transitions in Chapter 4.

CHAPTER 3

The Phase Transition Phenomena in Independent Gaussian Error Models

We study the fundamental limits of the signal detection and support recovery problems in the location models with independent Gaussian errors in this chapter. Specifically, we derive the conditions under which the detection and support recovery problems succeed and fail in the sense of (2.24) and (2.25), in the additive error model

$$x(i) = \mu(i) + \epsilon(i), \quad i = 1, \dots, p, \quad (3.1)$$

where the errors $\epsilon(i)$'s are independent and identically distributed (iid) standard Gaussians random variables. We restrict our analysis to models with independent and identically distributed Gaussian errors for the moment. Both the distributional assumption and the independence assumption will be relaxed in the following chapters.

As laid out in Section 2.3, we work under the asymptotic regime where the problem dimension p diverges to infinity. Let the signal vectors $\mu = \mu_p$ have

$$|S_p| = \lfloor p^{1-\beta} \rfloor, \quad \beta \in (0, 1] \quad (3.2)$$

non-zero entries, where β parametrizes the problem sparsity. The closer β is to 1, the sparser the support S ; conversely, when β is close to 0, the support is dense with many

non-null signals. We consider one-sided alternatives (2.14), and parametrize the range of the non-zero (and perhaps unequal) signals with

$$\underline{\Delta} = \sqrt{2\underline{r} \log p} \leq \mu(i) \leq \overline{\Delta} = \sqrt{2\overline{r} \log p}, \quad \text{for all } i \in S_p, \quad (3.3)$$

for some constants $0 < \underline{r} \leq \overline{r} \leq +\infty$.

The parametrization of signal sparsity (3.2) and signal sizes (3.3) in the Gaussian model was first introduced in Ingster (1998), and later adopted by Hall and Jin (2010), Cai et al. (2011), Zhong et al. (2013), Cai and Wu (2014), Arias-Castro and Wang (2017), and numerous others for studying the signal detection problem in Gaussian location-scale models. Similar scalings of sparsity and signal size are also used in, e.g., Ji and Jin (2012), Jin et al. (2014), Butucea et al. (2018) to study the phase transitions of the support recovery problems under Gaussianity assumptions.

3.1 Sparse signal detection problems

The optimality of sparse signal detection was first studied by Ingster (1998), who showed that a phase transition in the r - β plane exists for the signal detection problem. Specifically, assuming equal signal sizes with magnitude $\sqrt{2r \log p}$, if the signal size r is above a so-called detection boundary,

$$f(\beta) = \begin{cases} \max\{0, \beta - 1/2\} & 0 < \beta \leq 3/4, \\ (1 - \sqrt{1 - \beta})^2 & 3/4 < \beta \leq 1, \end{cases} \quad (3.4)$$

then the global null hypothesis $\mu(i) = 0$ for all $i = 1, \dots, p$ can be distinguished from the alternative as $p \rightarrow \infty$ in the sense of (2.24) using the likelihood ratio test; otherwise, when signal sizes fall below the boundary, no test can do better than a random guess. Adaptive tests such as Tukey's HC (Donoho and Jin, 2004) and a modified goodness-of-fit

test statistic of Zhang (2002) have been identified to attain this performance limit without knowledge of the sparsity and signal sizes. It is also known that the max-statistic (2.16) is only efficient when $r > (1 + \sqrt{1 - \beta})^2$, and is therefore sub-optimal for denser signals where $1/2 \leq \beta \leq 3/4$; see Cai et al. (2011). In contrast, the sum-of-square-type statistics such as L_2 was shown in Fan (1996) to be asymptotically powerless when the L_2 -norm of the signal $\|\mu\|_2^2$ is $o(\sqrt{p})$, or equivalently, when $\beta > 1/2$ in our parametrization.

Notice that the scaling for the signal magnitude $\Delta = \sqrt{2r \log p}$ is useful for studying very sparse signals ($\beta > 1/2$), but fails to reveal the difficulties of the detection problems when signals are relatively dense ($\beta < 1/2$). Indeed, a different scaling is needed for small but dense signals. With slight overloading of notation, we parametrize signal sizes as

$$\underline{\Delta} = p^{\underline{r}} \leq \mu(i) \leq \overline{\Delta} = p^{\bar{r}}, \quad \text{for all } i \in S_p, \quad (3.5)$$

where \underline{r} and \bar{r} are negative constants. In this scaling for the faint signals, Cai et al. (2011) showed that a similar phase transition characterized by the following boundary,

$$f_s(\beta) = \beta - 1/2, \quad 0 < \beta \leq 1/2, \quad (3.6)$$

exists. Specifically, if $\bar{r} < f_s(\beta)$, the signal detection fails in the sense of (2.25) regardless of the procedures, while the HC statistic continues to attain asymptotically perfect detection when $\underline{r} > f_s(\beta)$. We visualize this boundary in the lower panel of Figure 3.1.

To the best of our knowledge, performance of simple statistics such as L_1 , L_2 norms, and S in this weak signal setting have not been reported in the literature perhaps due to a perceived lack of novelty. Our first Theorem investigates the performance of these routine statistics for detecting sparse signals in high-dimensions, and summarizes the known results.

Theorem 3.1. *Consider the signal detection problem in the triangular array of Gaussian error models (3.1) where the sparsity is parametrized as in (3.2).*

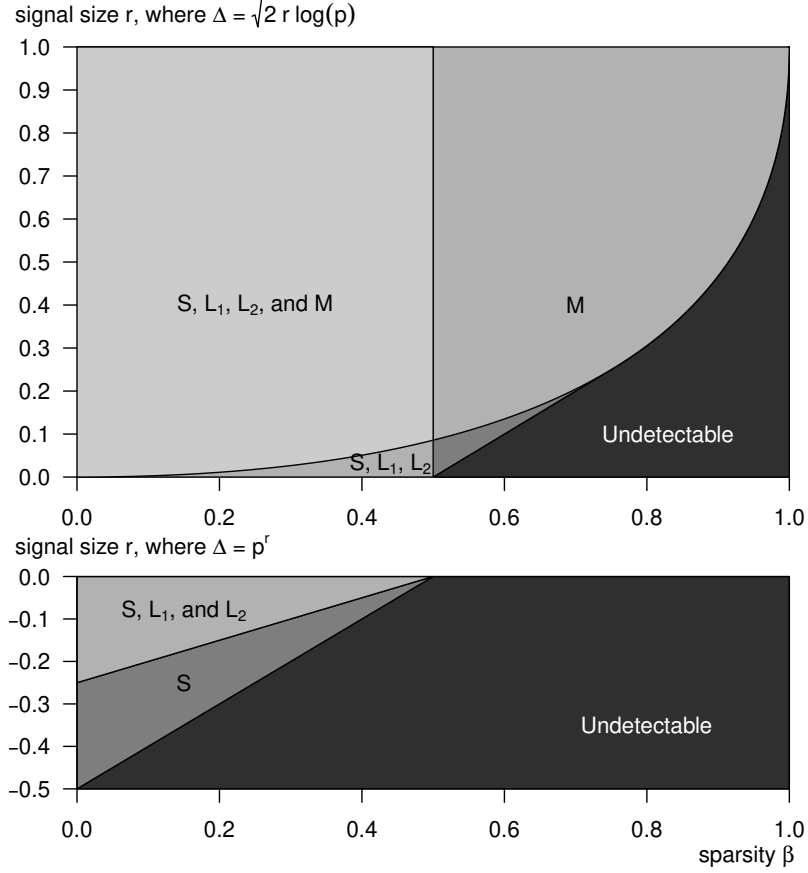


Figure 3.1: The phase diagrams of the sparse signal detection problem. Signal size and sparsity are parametrized by r and β , respectively. The diagrams illustrate the regions where the signal detection problem can be solved asymptotically by some of the commonly used statistics: the maximum (M), the sum-of-squares (L_2), the sum-of-absolute values (L_1), and the sum (S). In each region of the diagram, the annotated statistics can make the detection risk (2.4) vanish, as dimension p diverges. Conversely, the risks has liminf at least one. The detection problem is unsolvable for very sparse and weak signals in the undetectable regions. Notice that the L_1 and L_2 statistics are in fact sub-optimal for all sparsity levels. On the other hand, the max-statistic remains powerful for sparse signals ($\beta > 1/2$), and is fully efficient when the problem is very sparse ($\beta \geq 3/4$). The HC statistic can detect signals in all configurations in the detectable regions. See text and Theorem 3.1.

- For signals whose sizes are parametrized as in (3.3), the detection problem can be asymptotically solved in the sense of (2.24) with L_2 , L_1 , or S statistic when $\beta \leq 1/2$; on the other hand, these statistics are asymptotically powerless in the sense of (2.25) when $\beta > 1/2$.
- For small and dense signals whose signal sizes are parametrized as in (3.5), the detection problem can be asymptotically solved in the sense of (2.24) with L_2 or L_1 statistic when $\underline{r} > \beta/2 - 1/4$; on the other hand, these statistics are asymptotically powerless in the sense of (2.25) when $\bar{r} < \beta/2 - 1/4$. Further, tests based on the S statistic can succeed asymptotically in the sense of (2.24) when $\underline{r} > \beta - 1/2$, hence attaining the boundary of detectability in (3.6).

Theorem 3.1 is proved in Section 3.3 below. We visualize the results in Theorem in Figure 3.1. It is worth noting that the β - r parameter regions where L_1 and L_2 statistics are asymptotically powerful coincide, and these statistics are theoretically suboptimal for both sparse regimes ($\beta > 1/2$) and relatively dense regimes ($\beta \leq 1/2$).

Ideas have been proposed to combine statistics that are powerful for different alternatives to create adaptive tests that maintain high power for at all sparsity levels. Such adaptive tests can be constructed, for example, by leveraging the asymptotic independence of the sum- and supremum-type statistics (Hsing, 1995). Recently, Xu et al. (2016) showed that for dependent observations under mixing and moment conditions, the sum-of-power-type statistics

$$\tilde{L}_q(x) = \sum_{i=1}^p x^q(i) \quad (3.7)$$

with distinct positive integer powers (i.e., $q = 1, 2, \dots$) are asymptotically jointly independent, and proposed an adaptive test that monitors the minimum p-value of tests constructed with \tilde{L}_q 's. This idea is further developed in Wu et al. (2019) for generalized linear models and in He et al. (2018) with U-statistics.

Optimality properties of such adaptive tests and the optimal choice of the q -combinations,

however, remain open problems. Xu et al. (2016) suggested combine $q = 1, 2, 3, \dots, 6$, and $q = \infty$, based empirical evidence from numerical experiments. Theorem 3.1 here implies that, at least for detecting one-sided alternatives, the \tilde{L}_2 statistic (i.e., L_2 norm) and the L_1 norm are asymptotically dominated by the \tilde{L}_1 statistic (or equivalently, the sum S). Therefore it is sufficient to include only the latter in the construction of the adaptive test.

3.2 Sparse signal support recovery problems

Turning to support recovery problems in the Gaussian error model (3.1), we will analyze the asymptotic performance limits in terms of the risk metrics for exact, exact-approximate, approximate-exact support recovery problems (i.e., (2.8), (2.11), and (2.12), respectively), as well as the probability of support recovery (2.9). We will also review the recent result for exact support recovery risk (2.7) by Arias-Castro and Chen (2017), to reveal a rather complete landscape of support recovery problems in high-dimensional Gaussian error models.

We restrict our attention to the class of thresholding procedures in this section. Specifically, the lower bounds that we develop in Theorems 3.3 through 3.7 below are only meant to apply to thresholding procedures. Although it is intuitively appealing to consider only data-thresholding procedures in multiple testing problems, such procedures are not always optimal in more general settings. The optimality of thresholding procedures and the consequences of this restriction will be treated in Chapter 4.

A technical ingredient is needed in order to state our main results. We define a rate at which the nominal levels of FWER or FDR go to zero.

Definition 3.2. We say the nominal level of errors $\alpha = \alpha_p$ vanishes slowly, if

$$\alpha \rightarrow 0, \quad \text{and} \quad \alpha p^\delta \rightarrow \infty \text{ for any } \delta > 0. \quad (3.8)$$

As an example, the sequence of nominal levels $\alpha_p = 1/\log(p)$ is slowly vanishing,

while the sequence $\alpha_p = 1/\sqrt{p}$ is not.

3.2.1 The exact support recovery problem

Our study of the exact support recovery risk (2.8) begins with a brief review of existing results for the Hamming loss (2.10). Indeed, as discussions in Section 2.3 suggest, the latter can be informative of the exact support recovery problems for models with independent components.

Inspired by the phase transition results for the signal detection problem, Ji and Jin (2012), Genovese et al. (2012), and Jin et al. (2014) derived interesting sharp results on support recovery problems in linear models under the Hamming loss $H(\widehat{S}, S)$. Specifically, these papers establish minimax-type phase transition results in their respective settings. Under the sparsity parametrization in (3.2) and assuming equal signal sizes of $(2r \log p)^{1/2}$, Hamming losses were shown to diverge to $+\infty$ when r falls below the threshold

$$g(\beta) = (1 + (1 - \beta)^{1/2})^2, \quad (3.9)$$

for any method of support estimation. Conversely, under orthogonal, or near-orthogonal random designs, if $r > g(\beta)$, they showed that the methods they proposed achieve vanishing Hamming loss.

Very recently, Butucea et al. (2018) studied both asymptotics and non-asymptotics of support recovery problems in the additive noise model (3.1) under the assumption of equal signal sizes, using the Hamming loss. Again, the analysis of asymptotic optimality focused on a newly proposed procedure which is very specific to the Gaussian model. It is not at all clear if the optimality properties are a consequence of its mysterious construction.

We now show that commonly used and computationally efficient procedures can also be asymptotically optimal in the exact support recovery problem.

Theorem 3.3. *Consider the high-dimensional additive error model (3.1) under indepen-*

dent standard Gaussian errors, with signal sparsity and size as described in (3.2) and (3.3). The function (3.9) characterizes the phase transition of the exact support recovery problem. Specifically, if $\underline{r} > g(\beta)$, then Bonferroni's, Sidák's, Holm's, and Hochberg's procedures with slowly vanishing nominal FWER levels (as defined in Definition 3.2) all achieve asymptotically exact support recovery in the sense of (2.24).

Conversely, if $\bar{r} < g(\beta)$, then for any thresholding procedure \hat{S}_p , we have $\mathbb{P}[\hat{S}_p = S_p] \rightarrow 0$. Therefore, in view of Lemma 2.6, exact support recovery asymptotically fails for all thresholding procedures in the sense of (2.25).

We visualize the result in a β - r phase diagram in Figure 3.2.

Theorem 3.3 is in fact a special case of the more general Theorem 4.1 which covers dependent and non-Gaussian errors. We will study the exact support recovery problem in greater detail, and prove the more general version of the Theorem in Chapter 4.

3.2.2 The approximate support recovery problem

Arias-Castro and Chen (2017) studied the performance of the Benjamini-Hochberg procedure (Benjamini and Hochberg, 1995) and a stripped-down version of the Candès-Barber procedure (Barber and Candès, 2015) in approximate support recovery problems when the components of the noise term ϵ in (3.1) have independent and symmetric distributions. A phase transition phenomenon for the approximate support recovery risk (2.7) was established in the Gaussian additive error model, where the two aforementioned methods are both shown to be asymptotically optimal.

The analysis therein, however, assumed equal signal sizes for the alternatives. We generalize the main results of Arias-Castro and Chen (2017) to allow for unequal signal sizes.

Theorem 3.4. *In the context of Theorem 3.3, the function*

$$h(\beta) = \beta \tag{3.10}$$

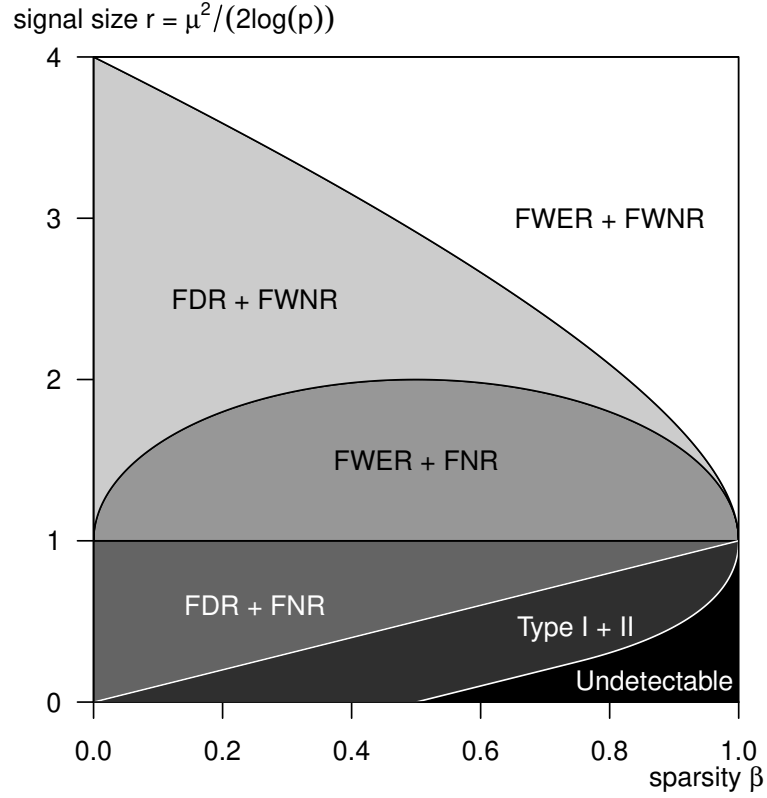


Figure 3.2: The phase diagram of support recovery problems for the high-dimensional chi-square model (3.1), illustrating the boundaries of the exact support recovery (FWER + FWNR; top curve; Theorem 3.3), the approximate-exact support recovery (FDR + FWNR; second curve from top; Theorem 3.7), the exact-approximate support recovery (FWER + FNR; horizontal line $r = 1$; Theorem 3.5), and the approximate support recovery problems (FDR + FNR; tilted line $r = \beta$; Theorem 3.4). The signal detection problem (Type I + Type II errors of the global test; lower curve) was studied in Donoho and Jin (2004). In each region of the diagram and above, the annotated statistical risk can be made to vanish, as dimension p diverges. Conversely, the risks has \liminf at least one.

characterizes the phase transition of approximate support recovery problem. Specifically, if $\underline{r} > h(\beta)$, then the Benjamini-Hochberg procedure (defined in Section 2.2) with slowly vanishing nominal FDR levels (as defined in Definition 3.2) achieves asymptotically approximate support recovery in the sense of (2.24).

Conversely, if $\bar{r} < h(\beta)$, then approximate support recovery asymptotically fails in the sense of (2.25) for all thresholding procedures.

Proof of Theorem 3.4 is presented in Section 3.3. The key to proving this generalization is a monotonicity property of the BH procedure. Namely, the power of the BH procedure in terms of FNR monotonically increases for stochastically larger alternatives. This fact will be formalized in Lemma 3.9, and may be of independent interest.

3.2.3 The exact-approximate support recovery problem

We now derive two new asymptotic phase transition results for the *asymmetric* statistical risks, (2.11) and (2.12), in the Gaussian error models. The next theorem describes the phase transition in the exact-approximate support recovery problem.

Theorem 3.5. *In the context of Theorem 3.3, the function*

$$\tilde{g}(\beta) = 1 \tag{3.11}$$

characterizes the phase transition of exact-approximate support recovery problem. Specifically, if $\underline{r} > \tilde{g}(\beta)$, then the procedures listed in Theorem 3.3 with slowly vanishing nominal FWER levels (as defined in Definition 3.2) achieve asymptotically exact-approximate support recovery in the sense of (2.24).

Conversely, if $\bar{r} < \tilde{g}(\beta)$, then for any thresholding procedure \hat{S} , the exact-approximate support recovery fails in the sense of (2.25).

Theorem 3.5 is proved in Section 3.3. The phase transition boundary (3.11) is visualized in Figure 3.2.

Remark 3.6. Boundary (3.11) was briefly suggested by Arias-Castro and Chen (2017). Unfortunately, it was falsely claimed that the boundary characterized the phase transition of the *exact* support recovery problem, and the alleged proof was left as an “exercise to the reader”. This exercise was completed in Chapter 4, where the correct boundary (6.4) was identified.

Theorem 3.5 here shows that the boundary (3.11) *does* exist, though for the slightly different *exact-approximate* support recovery problem. As we will see in Section 6.1, the boundary (3.11) also applies to the exact-approximate support recovery problem in chi-square models (1.3).

3.2.4 The approximate-exact support recovery problem

The last phase transition is in terms of the approximate-exact support recovery risk (2.12).

Theorem 3.7. *In the context of Theorem 3.3, the function*

$$\tilde{h}(\beta) = \left(\sqrt{\beta} + \sqrt{1 - \beta} \right)^2 \quad (3.12)$$

characterizes the phase transition of approximate-exact support recovery problem. Specifically, if $\underline{r} > \tilde{h}(\beta)$, then the Benjamini-Hochberg procedure with slowly vanishing nominal FDR levels (as defined in Definition 3.2) achieves asymptotically approximate-exact support recovery in the sense of (2.24).

Conversely, if $\bar{r} < \tilde{h}(\beta)$, then for any thresholding procedure \hat{S} , the approximate-exact support recovery fails in the sense of (2.25).

Theorem 3.7 is proved in Section 3.3. The phase transition boundary (3.12) is visualized in Figure 3.2.

3.2.5 Asymptotic power analysis

Theorems 3.3 through 3.7 allow us to asymptotically quantify the required signals sizes in support recovery problems, as well as in the global hypothesis testing problem in the Gaussian additive error model (3.1). Specifically, these results indicate that at all sparsity levels $\beta \in (0, 1)$, the difficulties of the problems in terms of the required signal sizes have the following ordering

$$f(\beta) < h(\beta) < \tilde{g}(\beta) < \tilde{h}(\beta) < g(\beta),$$

as previewed in Figure 3.2. The ordering aligns with our intuition that the required signal sizes must increase as we move from detection to support recovery problems. Similarly, more stringent criteria for error control (e.g., FWER compared to FDR) require larger signals. We can now also compare $\tilde{g}(\beta)$ and $\tilde{h}(\beta)$, whose ordering may not be clear from this line of reasoning.

Our last comment is on the gap between FDR and FWER under sparsity assumptions. Although it is believed that FWER control is sometimes too stringent compared to, say, FDR control in support recovery problems, the fact that all three thresholds (detection, weak, and strong classification) involve the same scaling indicates that the difficulties of the three problems (signal detection, approximate, and exact support recovery) are comparable when signals are very sparse, i.e., when β is close to 1. This is illustrated with the next example.

Example 3.8 (Power analysis for variable selection). For Gaussian errors (AGG with $\nu = 2$), when $\beta = 3/4$, the signal detection boundary (3.4) says that signals will have to be at least of magnitude $\sqrt{(\log p)/2}$, while approximate support recovery (3.10) requires signal sizes of at least $\sqrt{3(\log p)/2}$, and exact support recovery (3.9) calls for signal sizes of at least $\sqrt{9(\log p)/2}$. The required signal sizes increases, but are within the same order of magnitude.

If m independent copies x_1, \dots, x_m of the observations were made on the same set of p locations, then by taking location-wise averages, $\bar{x}_m(j) = \frac{1}{m} \sum_{i=1}^m x_i(j)$, we can reduce error standard deviation, and hence boost the signal-to-noise ratio, by a factor of \sqrt{m} . By the simple calculations above, if m samples are needed to detect (sparse) signals of a certain magnitude, then $3m$ samples will enable approximate support recovery with FDR control, and in fact, $9m$ samples would enable exact support recovery with FWER control.

On the other hand, the gap between FDR and FWER is much larger when signals are dense. For example, if the signals are only *approximately* sparse, i.e., having a few components above (3.9) but many smaller components above (3.10), then FDR-controlling procedures will discover substantially larger proportion of signals than FWER-controlling procedures.

Indeed, as $\beta \rightarrow 0$, the required signal size for approximate support recovery (3.10) tends to 0, while the required signal size for exact support recovery (3.9) tends to 4 in the Gaussian error models. While Example 3.8 indicates that the exact support recovery is not much more stringent than approximate support recovery when signals are sparse, the gap between required signal sizes widens when signals are dense.

3.3 Proofs

We first recall some basic properties of the Gaussian distribution in Section 3.3.1. Section 3.3.2 states and proves an interesting property of the BH procedure which may be of independent interest. Results on the signal detection problem (Theorem 3.1) are proved in Section 3.3.3, and the phase transition results on the support recovery problems (Theorems 3.3 through 3.7) are shown in Sections 3.3.4 and 3.3.5.

3.3.1 Auxiliary facts of Gaussian distributions

We recall three facts of Gaussian distributions that will be used in the proofs later.

We first state the relative stability of iid standard Gaussian random variables, Since the standard Gaussian distribution falls in the class of asymptotically generalized Gaussians (AGG; see Definition 2.7), by Example 2.12, we know that the triangular array $\mathcal{E} = \{(\epsilon_p(i))_{i=1}^p, p \in \mathbb{N}\}$ has relatively stable (RS) maxima in the sense of (2.37), i.e.,

$$\frac{1}{u_p} \max_{i=1, \dots, p} \epsilon_p(i) \xrightarrow{\mathbb{P}} 1, \quad \text{as } p \rightarrow \infty, \quad (3.13)$$

where u_p is the $(1/p)$ -th upper quantile as defined in (2.32). Similarly, since the array \mathcal{E} has distributions symmetric around 0, it also has relatively stable minima

$$\frac{1}{u_p} \min_{i=1, \dots, p} \epsilon_p(i) \xrightarrow{\mathbb{P}} -1, \quad \text{as } p \rightarrow \infty. \quad (3.14)$$

The second fact is on the well-known bounds for the Mill's ratio of Gaussian tails. Let Φ denote the CDF of the standard Gaussian distribution and ϕ its density. One can show that for all $x > 0$ we have

$$\frac{x}{1+x^2} \phi(x) \leq \bar{\Phi}(x) = 1 - \Phi(x) \leq \frac{1}{x} \phi(x), \quad (3.15)$$

using e.g., integration by parts.

The third fact is the stochastic monotonicity of the Gaussian location family. In fact, for all location families $\{F_\delta(x)\}_\delta$ where $F_\delta(x) = F(x - \delta)$, we have,

$$F_{\delta_1}(t) \geq F_{\delta_2}(t), \quad \text{for all } t \in \mathbb{R} \quad \text{and all } \delta_1 \leq \delta_2. \quad (3.16)$$

Relation (3.16) holds, of course, when F is the standard Gaussian distribution.

3.3.2 Monotonicity of the Benjamini-Hochberg procedure

We make a connection between power of the BH procedure and the stochastic ordering of distributions under the alternative. This result, though natural, seems new.

Lemma 3.9 (Monotonicity of the BH procedure). *Consider p independent observations $x(i)$, $i \in \{1, \dots, p\}$, where the $(p - s)$ coordinates in the null part have common distribution F_0 , and the remaining s signals have alternative distributions F_j^i , $i \in S$, respectively. Compare the two alternatives $j \in \{1, 2\}$, where the distributions in Alternative 2 are stochastically larger than those in Alternative 1, i.e.,*

$$F_2^i(t) \leq F_1^i(t), \quad \text{for all } t \in \mathbb{R}, \text{ and for all } i \in S.$$

If the BH procedure is applied at the same nominal level of FDR, then the FNR of the BH procedure under Alternative 2 is bounded above by the FNR under Alternative 1. Further, the threshold of the BH procedure under Alternative 2 is stochastically smaller than that under Alternative 1.

Loosely put, the power of the BH procedure is monotone increasing with respect to the stochastic ordering of the alternatives, yet (the distribution of) the BH threshold is monotone decreasing in the distributions of the alternatives.

Proof of Lemma 3.9. We first re-express the BH procedure in a different form. Recall that on observing $x(i)$, $i \in \{1, \dots, p\}$, the BH procedure is the thresholding procedure with threshold set at $x_{[i^*]}$, where $i^* := \max\{i \mid \overline{F}_0(x_{[i]}) \leq \alpha i/p\}$, and $x_{[1]} \geq \dots \geq x_{[p]}$ are the order statistics.

Let \widehat{G} denote the left-continuous empirical survival function

$$\widehat{G}(t) = \frac{1}{p} \sum_{i=1}^p \mathbb{1}\{x(i) \geq t\}. \quad (3.17)$$

By the definition, we know that $\widehat{G}(x_{[i]}) = i/p$. Therefore, by the definition of i^* , we have

$$\overline{F}_0(x_{[i]}) > \alpha \widehat{G}(x_{[i]}) = \alpha i/p \quad \text{for all } i > i^*.$$

Since \widehat{G} is constant on $(x_{[i^*+1]}, x_{[i^*]})$, the fact that $\overline{F}_0(x_{[i^*]}) \leq \alpha \widehat{G}(x_{[i^*]})$ and $\overline{F}_0(x_{[i^*+1]}) > \alpha \widehat{G}(x_{[i^*+1]})$ implies that $\alpha \widehat{G}$ and \overline{F}_0 must “intersect” on the interval by continuity of F_0 . We denote this “intersection” as

$$\tau = \inf\{t \mid \overline{F}_0(t) \leq \alpha \widehat{G}(t)\}. \quad (3.18)$$

Note that τ cannot be equal to $x_{[i^*+1]}$ since \overline{F}_0 is càdlàg. Since there is no observation in $[\tau, x_{[i^*]})$, we can write the BH procedure as the thresholding procedure with threshold set at τ .

Now, denote the observations under Alternatives 1 and 2 as $x_1(i)$ and $x_2(i)$. Since $x_2(i)$ stochastically dominates $x_1(i)$ for all $i \in \{1, \dots, p\}$, there exists a coupling $(\tilde{x}_1, \tilde{x}_2)$ of x_1 and x_2 such that $\tilde{x}_1(i) \leq \tilde{x}_2(i)$ almost surely for all i . We will replace \tilde{x}_1 and \tilde{x}_2 with x_1 and x_2 in what follows. Since we will compare the FNR’s, i.e., expectations with respect to the marginals of x ’s in the last step, this replacement does not affect the conclusions. To simplify notation, we still write x_1 and x_2 in place of \tilde{x}_1 and \tilde{x}_2 .

Let \widehat{G}_k be the left-continuous empirical survival function under Alternative k , i.e.,

$$\widehat{G}_k(t) = \frac{1}{p} \sum_{i=1}^p \mathbb{1}\{x_k(i) \geq t\}, \quad k \in \{1, 2\}. \quad (3.19)$$

We define the BH thresholds τ_1 and τ_2 by replacing \widehat{G} in (3.18) with \widehat{G}_1 and \widehat{G}_2 , respectively. Denote the set estimates of signal support $\widehat{S}_k = \{i \mid x_k(i) \geq \tau_k\}$ by the BH procedure. We claim that

$$\tau_2 \leq \tau_1 \quad \text{with probability 1.} \quad (3.20)$$

Indeed, by definition of the empirical survival function (3.19) and the fact that $x_1(i) \leq$

$x_2(i)$ almost surely for all i , we have $\widehat{G}_1(t) \leq \widehat{G}_2(t)$ for all t . Hence, $\overline{F}_0(t) \leq \alpha \widehat{G}_1(t)$ implies $\overline{F}_0(t) \leq \alpha \widehat{G}_2(t)$, and Relation (3.20) follows from the definition of τ in (3.18). The claim of stochastic ordering of the BH thresholds in Lemma 3.9 follows from (3.20).

Finally, when $\tau_2 \leq \tau_1$, we have $\tau_2 \leq \tau_1 \leq x_1(i) \leq x_2(i)$ with probability 1 for all $i \in \widehat{S}_1$. Therefore, it follows that $\widehat{S}_1 \subseteq \widehat{S}_2$ and hence $|S \setminus \widehat{S}_2| \leq |S \setminus \widehat{S}_1|$ almost surely. The first conclusion in Lemma 3.9 follows from the last inequality. \square

3.3.3 Proof of Theorem 3.1

Proof of Theorem 3.1. Statements about L_1 , L_2 , and sum statistics S in the case of diverging signal sizes (3.3) can be found in Fan (1996) and Candés (2018). We prove here the statements for the case where signals are dense and small, as parametrized in (3.5).

We first show that the sum statistic S , or equivalently, the simple arithmetic mean attains the sparse signal detection boundary.

Consider the case of vanishing signals as prescribed in (3.5), by normality of the summands, we have,

$$\frac{1}{\sqrt{p}} \sum_{i=1}^p x(i) \sim \begin{cases} N(0, 1), & \text{under } H_0 \\ N(p^{(r-\beta)+1/2}, 1), & \text{under } H_1. \end{cases} \quad (3.21)$$

It immediately follows that the two distributions can be distinguished perfectly if $p^{r-(\beta-1/2)}$ diverges, i.e., $r > \beta - 1/2$. This can be seen by simply setting the rejection region at $(p^{(r-\beta)+1/2}/2, +\infty)$ for the scaled statistic $\sum_{i=1}^p x(i)/\sqrt{p}$. According to the lower bound on the performance limit in detection problems (see Theorem 8 in Cai et al. (2011)), we have shown that S attains the optimal detection boundary (3.6).

We now turn to the L_2 -norms. Recall a non-central chi-square random variable $\chi_k^2(\lambda)$ has mean $(k + \lambda)$ and variance $2(k + 2\lambda)$. Since the observations have distributions $N(0, 1)$ under the null and $N(p^r, 1)$ under the alternative, we have $x^2(i) \sim \chi_1^2(0)$ for $i \notin S$ and

$x^2(i) \sim \chi_1^2(p^{2r})$ for $i \in S$. Therefore, mean and variance of the (centered and scaled) L_2 statistics are

$$\mathbb{E} \left[\frac{1}{\sqrt{p}} \sum_{i=1}^p (x(i)^2 - 1) \right] = \begin{cases} 0, & \text{under } H_0 \\ p^{1-\beta} p^{2r} p^{-1/2} = p^{1/2-\beta+2r} & \text{under } H_1, \end{cases} \quad (3.22)$$

and

$$\text{Var} \left(\frac{1}{\sqrt{p}} \sum_{i=1}^p (x(i)^2 - 1) \right) = \begin{cases} \frac{1}{p} 2p = 2, & \text{under } H_0 \\ \frac{1}{p} (2p + 2p^{1-\beta+2r}) = 2(1 + p^{2r-\beta}) & \text{under } H_1, \end{cases} \quad (3.23)$$

respectively. By the (Lyapunov) central limit theorem, we have

$$\frac{1}{2p} \sum_{i=1}^p (x(i)^2 - 1) \implies N(0, 1), \quad (3.24)$$

under the null, and

$$\frac{1}{2p} \left(\sum_{i=1}^p (x(i)^2 - 1) - p^{1/2-\beta+2r} \right) \implies N(0, 1), \quad (3.25)$$

under the alternative since $p^{2r-\beta} \rightarrow 0$ for all $r < 0$ and $\beta > 0$. Hence, perfect detection with the L_2 -norm is possible if $p^{1/2-\beta+2r}$ diverges, i.e., $r > \beta/2 - 1/4$. On the other hand, if $r < \beta/2 - 1/4$, the distributions of the (scaled) statistics merge under the null and the alternative.

The case of L_1 -norm is treated similarly. Let $Y = |X|$ where $X \sim |N(\mu, 1)|$. Using the expressions for the mean and variance of Y (see, e.g., Tsagris et al. (2014)),

$$\mu_Y = \mathbb{E}[Y] = \sqrt{\frac{2}{\pi}} e^{-\mu^2/2} + \mu(1 - \Phi(-\mu)), \quad (3.26)$$

$$\sigma_Y^2 = \text{Var}(Y) = \mu^2 + 1 - \mu_Y^2, \quad (3.27)$$

where Φ is the CDF of a standard normal random variable, we have, regardless of the value of μ ,

$$\sigma_Y^2 = \text{Var}(Y) = \mathbb{E}(Y - \mathbb{E}Y)^2 \leq \mathbb{E}(X - \mathbb{E}X)^2 = 1, \quad (3.28)$$

where the inequality holds because absolute value is a Lipschitz function with Lipschitz constant 1.

By the central limit theorem, we have,

$$\frac{1}{\sqrt{p}} \left(\sum_{i=1}^p |x(i)| - \sqrt{\frac{2}{\pi}} \right) \Rightarrow N(0, 1 - 2/\pi) \quad (3.29)$$

under the null. On the other hand, when the alternative hypothesis holds, we have

$$\begin{aligned} \mathbb{E} \left[\frac{1}{\sqrt{p}} \left(\sum_{i=1}^p |x(i)| - \sqrt{\frac{2}{\pi}} \right) \right] &= \frac{p^{1-\beta}}{\sqrt{p}} \left[\left(\sqrt{\frac{2}{\pi}} e^{-\mu^2/2} + \mu (1 - 2\Phi(-\mu)) \right) - \sqrt{\frac{2}{\pi}} \right] \\ &= p^{1/2-\beta} \left[\sqrt{\frac{2}{\pi}} (e^{-p^{2r}/2} - 1) + p^r (1 - 2\Phi(-\mu)) \right] \\ &= p^{1/2-\beta} \left[\sqrt{\frac{2}{\pi}} (-p^{2r}/2 - O(p^{4r})) + p^r \left(\sqrt{\frac{2}{\pi}} p^r + O(p^{3r}) \right) \right] \\ &= p^{1/2-\beta} \sqrt{\frac{2}{\pi}} (p^{2r}/2 + O(p^{4r})) \\ &= p^{1/2-\beta+2r} \sqrt{1/2\pi} + O(p^{1/2-\beta+4r}), \end{aligned}$$

and

$$\begin{aligned} \text{Var} \left(\frac{1}{\sqrt{p}} \left(\sum_{i=1}^p |x(i)| - \sqrt{\frac{2}{\pi}} \right) \right) &= (1 - p^{1-\beta})(1 - 2/\pi) + p^{1-\beta} \sigma_Y^2 \\ &\rightarrow 1 - 2/\pi, \end{aligned}$$

by boundedness of σ_Y^2 shown in (3.28). Again, by the (Lyapunov) central limit theorem, we conclude asymptotic normality of the centered and scaled L_1 -norms under the alternative.

In an entirely analogous argument to the L_2 -norm case, asymptotically perfect detection

can be achieved if $p^{1/2-\beta+2r}$ diverges, i.e., $r > \beta/2 - 1/4$. On the other hand, when $r < \beta/2 - 1/4$, the two hypotheses cannot be told apart by the L_1 -norms since the distributions of the (scaled) statistics merge under the two hypotheses. \square

3.3.4 Proof of Theorem 3.4

We first show the necessary condition. That is, when $\bar{r} < \beta$, no thresholding procedure is able to achieve approximate support recovery. The arguments are similar to that in Theorem 1 of Arias-Castro and Chen (2017), although we allow for unequal signal sizes.

Proof of necessary condition in Theorem 3.4. Denote the distributions of $N(0, 1)$, $N(\underline{\Delta}, 1)$, and $N(\overline{\Delta}, 1)$ as F_0 , $F_{\underline{a}}$, and $F_{\bar{a}}$ respectively.

Recall that thresholding procedures are of the form

$$\hat{S}_p = \{i \mid x(i) > t_p(x)\}.$$

Denote $\hat{S} := \{i \mid x(i) > t_p(x)\}$, and $\hat{S}(u) := \{i \mid x(i) > u\}$. For any threshold $u \geq t_p$ we must have $\hat{S}(u) \subseteq \hat{S}$, and hence

$$\text{FDP} := \frac{|\hat{S} \setminus S|}{|\hat{S}|} \geq \frac{|\hat{S} \setminus S|}{|\hat{S} \cup S|} = \frac{|\hat{S} \setminus S|}{|\hat{S} \setminus S| + |S|} \geq \frac{|\hat{S}(u) \setminus S|}{|\hat{S}(u) \setminus S| + |S|}. \quad (3.30)$$

On the other hand, for any threshold $u \leq t_p$ we must have $\hat{S}(u) \supseteq \hat{S}$, and hence

$$\text{NDP} := \frac{|S \setminus \hat{S}|}{|S|} \geq \frac{|S \setminus \hat{S}(u)|}{|S|}. \quad (3.31)$$

Since either $u \geq t_p$ or $u \leq t_p$ must take place, putting (3.30) and (3.31) together, we have

$$\text{FDP} + \text{NDP} \geq \frac{|\hat{S}(u) \setminus S|}{|\hat{S}(u) \setminus S| + |S|} \wedge \frac{|S \setminus \hat{S}(u)|}{|S|}, \quad (3.32)$$

for any u . Therefore it suffices to show that for a suitable choice of u , the RHS of (3.32)

converges to 1 in probability; the desired conclusion on FDR and FNR follows by the dominated convergence theorem.

Let $t^* = \sqrt{2q \log p}$ for some fixed q , we obtain an estimate of the tail probability by Mill's ratio (3.15),

$$\overline{F}_0(t^*) \sim \frac{1}{t^*} \phi(t^*) = \frac{1}{2\sqrt{\pi q \log p}} p^{-q}, \quad (3.33)$$

where $a_p \sim b_p$ is taken to mean $a_p/b_p \rightarrow 1$. Observe that $|\widehat{S}(t^*) \setminus S|$ has distribution $\text{Binom}(p - s, \overline{F}_0(t^*))$ where $s = |S|$, denote $X = X_p := |\widehat{S}(t^*) \setminus S|/|S|$, and we have

$$\mu := \mathbb{E}[X] = \frac{(p - s)\overline{F}_0(t^*)}{s}, \quad \text{and} \quad \text{Var}(X) = \frac{(p - s)\overline{F}_0(t^*)F_0(t^*)}{s^2} \leq \mu/s.$$

Therefore for any $M > 0$, we have, by Chebyshev's inequality,

$$\mathbb{P}[X < M] \leq \mathbb{P}[|X - \mu| > \mu - M] \leq \frac{\mu/s}{(\mu - M)^2} = \frac{1/(\mu s)}{(1 - M/\mu)^2}. \quad (3.34)$$

Now, from the expression of $\overline{F}_0(t^*)$ in (3.33), we obtain

$$\mu = (p^\beta - 1)\overline{F}_0(t^*) \sim \frac{1}{2\sqrt{\pi q \log p}} p^{\beta-q}.$$

Since $\bar{r} < \beta$, we can pick q such that $\bar{r} < q < \beta$. In turn, we have $\mu \rightarrow \infty$, as $p \rightarrow \infty$. Therefore the last expression in (3.34) converges to 0, and we conclude that $X \rightarrow \infty$ in probability, and hence

$$\frac{|\widehat{S}(t^*) \setminus S|}{|\widehat{S}(t^*) \setminus S| + |S|} = \frac{X}{X + 1} \rightarrow 1 \quad \text{in probability.} \quad (3.35)$$

On the other hand, we show that with the same choice of $u = t^*$, we have,

$$\frac{|S \setminus \widehat{S}(t^*)|}{|S|} \rightarrow 1 \quad \text{in probability.} \quad (3.36)$$

By the stochastic monotonicity of Gaussian location family (3.16), we have the following lower bound for the probability of missed detection for each signal $\mu(i)$, $i \in S$,

$$\mathbb{P}[\mathcal{N}(\mu(i), 1) \leq t^*] \geq F_{\bar{a}}(t^*). \quad (3.37)$$

Since $|S \setminus \widehat{S}(t^*)|$ can be written as the sum of s independent Bernoulli random variables,

$$|S \setminus \widehat{S}(t^*)| = \sum_{i \in S} \mathbb{1}_{(-\infty, t^*]}(x(i)),$$

using with (3.37), we conclude that $|S \setminus \widehat{S}(t^*)| \stackrel{d}{\geq} \text{Binom}(s, F_{\bar{a}}(t^*))$. Finally, we know that $F_{\bar{a}}(t^*)$ converges to 1 by our choice of diverging t^* , and the necessary condition is shown. \square

We now turn to the sufficient condition. That is, when $\underline{r} > \beta$, the Benjamini-Hochberg procedure with slowly vanishing FDR levels achieves asymptotic approximate support recovery.

Proof of the sufficient condition in Theorem 3.4. The FDR vanishes by our choice of α and the FDR-controlling property of the BH procedure (Benjamini and Hochberg, 1995). It only remains to show that FNR also vanishes.

To do so we compare the FNR under the alternative specified in Theorem 3.4 to one with all of the signal sizes equal to $\underline{\Delta}$. By Lemma 3.9, it suffices to show that the FNR under the BH procedure in this setting vanishes. Let $x(i)$ be vectors of independent observations with $p - s$ nulls having standard Gaussian distributions, and s signals having $\mathcal{N}(\underline{\Delta}, 1)$ distributions.

Denote the null and the alternative distributions as F_0 and F_a respectively. Let \widehat{G} denote the empirical survival function as in (3.17). Define the empirical survival functions for the

null part and signal part

$$\widehat{W}_{\text{null}}(t) = \frac{1}{p-s} \sum_{i \notin S} \mathbb{1}\{x(i) \geq t\}, \quad \widehat{W}_{\text{signal}}(t) = \frac{1}{s} \sum_{i \in S} \mathbb{1}\{x(i) \geq t\}, \quad (3.38)$$

where $s = |S|$, so that

$$\widehat{G}(t) = \frac{p-s}{p} \widehat{W}_{\text{null}}(t) + \frac{s}{p} \widehat{W}_{\text{signal}}(t).$$

We need the following result to describe the deviations of the empirical distributions.

Lemma 3.10 (Theorem 1 of Eicker (1979)). *Let Z_1, \dots, Z_k be iid with continuous survival function Q . Let \widehat{Q}_k denote their empirical survival function and define $\xi_k = \sqrt{2 \log \log(k)/k}$ for $k \geq 3$. Then*

$$\frac{1}{\xi_k} \sup_z \frac{|\widehat{Q}_k(z) - Q(z)|}{\sqrt{Q(z)(1-Q(z))}} \rightarrow 1,$$

in probability as $k \rightarrow \infty$. In particular,

$$\widehat{Q}_k(z) = Q(z) + O_{\mathbb{P}} \left(\xi_k \sqrt{Q(z)(1-Q(z))} \right),$$

uniformly in z .

Apply Lemma 3.10 to the two summands in \widehat{G} , we obtain $\widehat{G}(t) = G(t) + \widehat{R}(t)$, where

$$G(t) = \frac{p-s}{p} \overline{F}_0(t) + \frac{s}{p} \overline{F}_a(t), \quad (3.39)$$

and

$$\widehat{R}(t) = O_{\mathbb{P}} \left(\xi_p \sqrt{\overline{F}_0(t) F_0(t)} + \frac{s}{p} \xi_s \sqrt{\overline{F}_a(t) F_a(t)} \right), \quad (3.40)$$

uniformly in t .

Recall (see proof of Lemma 3.9) that the BH procedure is the thresholding procedure

with threshold set at

$$\tau = \inf\{t \mid \overline{F}_0(t) \leq \alpha \widehat{G}(t)\}. \quad (3.41)$$

The NDP may also be re-written as

$$\text{NDP} = \frac{|S \setminus \widehat{S}|}{|S|} = \frac{1}{s} \sum_{i \in S} \mathbb{1}\{x(i) < \tau\} = 1 - \widehat{W}_{\text{signal}}(\tau),$$

so that it suffices to show that

$$\widehat{W}_{\text{signal}}(\tau) \rightarrow 1 \quad (3.42)$$

in probability. Applying Lemma 3.10 to $\widehat{W}_{\text{signal}}$, we know that

$$\widehat{W}_{\text{signal}}(\tau) = \overline{F}_a(\tau) + O_{\mathbb{P}}\left(\xi_s \sqrt{\overline{F}_a(\tau) F_a(\tau)}\right) = \overline{F}_a(\tau) + o_{\mathbb{P}}(1).$$

So it suffices to show that $F_a(\tau) \rightarrow 0$ in probability. Now let $t^* = \sqrt{2q \log(p)}$ for some q such that $\beta < q < \underline{r}$. We have

$$F_a(t^*) = \Phi(t^* - \underline{\Delta}) = \Phi(\sqrt{2(q - \underline{r}) \log p}) \rightarrow 0. \quad (3.43)$$

Hence in order to show (3.42), it suffices to show

$$\mathbb{P}[\tau \leq t^*] \rightarrow 1. \quad (3.44)$$

By (3.39), the mean of the empirical process \widehat{G} evaluated at t^* is

$$G(t^*) = \frac{p-s}{p} \overline{F}_0(t^*) + \frac{s}{p} \overline{F}_a(t^*). \quad (3.45)$$

The first term, using Relation (3.33), is asymptotic to $p^{-q}L(p)$, where $L(p)$ is the logarithmic term in p . The second term, since $\overline{F}_a(t^*) \rightarrow 1$ by Relation (3.43), is asymptotic to $p^{-\beta}$.

Therefore, $G(t^*) \sim p^{-q}L(p) + p^{-\beta} \sim p^{-\beta}$, since $p^{\beta-q}L(p) \rightarrow 0$ where $q > \beta$.

The fluctuation of the empirical process at t^* , by Relation (3.40), is

$$\begin{aligned}\widehat{R}(t^*) &= O_{\mathbb{P}} \left(\xi_p \sqrt{\overline{F}_0(t^*) F_0(t^*)} + \frac{s}{p} \xi_s \sqrt{\overline{F}_a(t^*) F_a(t^*)} \right) \\ &= O_{\mathbb{P}} \left(\xi_p \sqrt{\overline{F}_0(t^*)} \right) + o_{\mathbb{P}}(p^{-\beta}).\end{aligned}$$

By (3.33) and the expression for ξ_p , the first term is $O_{\mathbb{P}}(p^{-(q+1)/2} L(p))$ where $L(p)$ is a poly-logarithmic term in p . Since $\beta < \min\{q, 1\}$, we have $\beta < (q+1)/2$, and hence $\widehat{R}(t^*) = o_{\mathbb{P}}(p^{-\beta})$.

Putting the mean and the fluctuation of $\widehat{G}(t^*)$ together, we obtain

$$\widehat{G}(t^*) = G(t^*) + \widehat{R}(t^*) \sim_{\mathbb{P}} G(t^*) \sim p^{-\beta},$$

and therefore, together with (3.33), we have

$$\overline{F}_0(t^*)/\widehat{G}(t^*) = p^{\beta-q} L(p)(1 + o_{\mathbb{P}}(1)),$$

which is eventually smaller than the FDR level α by the assumption (3.8) and the fact that $\beta < q$. That is,

$$\mathbb{P} \left[\overline{F}_0(t^*)/\widehat{G}(t^*) < \alpha \right] \rightarrow 1.$$

By definition of τ (recall (3.41)), this implies that $\tau \leq t^*$ with probability tending to 1, and (3.44) is shown. The proof for the sufficient condition is complete. \square

3.3.5 Proof of Theorems 3.5 and 3.7

Proof of Theorem 3.5 uses ideas from the proof of Theorem 3.4 and is substantially shorter.

Proof of Theorem 3.5. We first show the sufficient condition. Vanishing FWER is guaranteed by the properties of the procedures, and we only need to show that FNR also goes to

zero. Similar to the proof of Theorem 3.4, it suffices to show that

$$\text{NDP} = 1 - \widehat{W}_{\text{signal}}(t_p) \rightarrow 0, \quad (3.46)$$

where t_p is the threshold of Bonferroni's procedure.

Since α vanishes slowly (see Definition 3.8), for any $\delta > 0$, we have $p^{-\delta} = o(\alpha)$. Therefore, we have $-\log \alpha \leq \delta \log p$ for large p , and

$$1 \leq \limsup_{p \rightarrow \infty} \frac{2 \log p - 2 \log \alpha}{2 \log p} \leq 1 + \delta,$$

for any $\delta > 0$. Therefore, by the expression for normal quantiles, we know that

$$t_p = F^{\leftarrow}(1 - \alpha/p) \sim (2 \log p - 2 \log \alpha)^{1/2} \sim (2 \log p)^{1/2}.$$

Since $\underline{r} > \widetilde{g}(\beta) = 1$, we can pick q such that $1 < q < \underline{r}$. Let $t^* = \sqrt{2q \log p}$, we know that $t_p < t_p^*$ for large p . Therefore for large p , we have

$$\widehat{W}_{\text{signal}}(t_p) \geq \widehat{W}_{\text{signal}}(t^*) \geq \overline{F}_a(t^*) + o_{\mathbb{P}}(1),$$

where \overline{F}_a is the survival function of $N(\sqrt{2\underline{r} \log p}, 1)$; the last inequality follows from the stochastic monotonicity of the Gaussian location family (3.16), and Lemma 3.10. Indeed, by our choice of $q < \underline{r}$, we obtain

$$F_a(t^*) = \Phi\left(\sqrt{2(q - \underline{r}) \log p}\right) \rightarrow 0,$$

and (3.46) is shown. This completes the proof of the sufficient condition.

The proof of the necessary condition follows similar structure as in the proof of Theo-

rem 3.4, and uses the lower bound

$$\text{FWER}(\mathcal{R}) + \text{FNR}(\mathcal{R}) \geq \mathbb{P} \left[\max_{i \in S^c} x(i) > u \right] \wedge \mathbb{E} \left[\frac{|S \setminus \widehat{S}(u)|}{|S|} \right], \quad (3.47)$$

which holds for any arbitrary thresholding procedure \mathcal{R} and arbitrary real $u \in \mathbb{R}$.

By the assumption that $\bar{r} < \widetilde{g}(\beta) = 1$, we can pick q such that $\bar{r} < q < 1$ and let $u = t^* = \sqrt{2q \log p}$ in (3.47). By relative stability of iid Gaussian random variables (3.13), we have

$$\mathbb{P} \left[\frac{\max_{i \in S^c} x(i)}{\sqrt{2 \log p}} > \frac{t^*}{\sqrt{2 \log p}} \right] \rightarrow 1. \quad (3.48)$$

since the first fraction in (3.48) converges to 1, while the second converges to $q < 1$. Therefore, the first term on the right-hand side of (3.47) converges to 1.

On the other hand, by the stochastic monotonicity of Gaussian location family (3.16), the probability of missed detection for each signal is lower bounded by $\mathbb{P}[Z + \mu(i) \leq t^*] \geq F_{\bar{a}}(t^*)$, where Z is a standard Gaussian r.v., and $F_{\bar{a}}$ is the cdf of $N(\sqrt{2\bar{r} \log p}, 1)$. Therefore, $|S \setminus \widehat{S}(t^*)| \stackrel{d}{\geq} \text{Binom}(s, F_{\bar{a}}(t^*))$, and it suffices to show that $F_{\bar{a}}(t^*)$ converges to 1. Indeed,

$$F_{\bar{a}}(t^*) = \Phi(\sqrt{2(q - \bar{r}) \log p}) \rightarrow 1,$$

by our choice of $q > \bar{r}$. Hence both quantities in the minimum on the right-hand side of (3.47) converge to 1 in the limit, and the necessary condition is shown. \square

Proof of Theorem 3.7. We first show the sufficient condition. Since FDR control is guaranteed by the BH procedure, we only need to show that the FWNR also vanishes, that is,

$$\mathbb{P} \left[\min_{i \in S} x(i) \geq \tau \right] \rightarrow 1, \quad (3.49)$$

where τ is the threshold for the BH procedure.

By the assumption that $\underline{r} > \widetilde{h}(\beta) = (\sqrt{\beta} + \sqrt{1 - \beta})^2$, we have $\sqrt{\underline{r}} - \sqrt{1 - \beta} > \sqrt{\beta}$,

so we can pick $q > 0$, such that

$$\sqrt{r} - \sqrt{1 - \beta} > \sqrt{q} > \sqrt{\beta}. \quad (3.50)$$

We only need to show that with a specific choice of $t^* = \sqrt{2q \log p}$ where

$$\sqrt{r} - \sqrt{1 - \beta} > \sqrt{q} > \sqrt{\beta}, \quad (3.51)$$

we have both

$$\mathbb{P}[\tau \leq t^*] \rightarrow 1, \quad (3.52)$$

and

$$\mathbb{P}\left[\min_{i \in S} x(i) \geq t^*\right] \rightarrow 1, \quad (3.53)$$

so that

$$\mathbb{P}\left[\min_{i \in S} x(i) \geq \tau\right] \geq \mathbb{P}\left[\min_{i \in S} x(i) \geq t^*, t^* \geq \tau\right] \rightarrow 1.$$

Relation (3.52) follows in exactly the same way (3.44) did on page 52.

Dividing the left-hand-side in Relation (3.53) by $\sqrt{2 \log p}$, we have,

$$\begin{aligned} \frac{\min_{i \in S} x(i)}{\sqrt{2 \log p}} &= \frac{\min_{i \in S} \mu(i) + \epsilon(i)}{\sqrt{2 \log p}} \stackrel{d}{\geq} \frac{\sqrt{2r \log p} + \min_{i \in S} \epsilon(i)}{\sqrt{2 \log p}} \\ &\rightarrow -\sqrt{1 - \beta} + \sqrt{r}, \end{aligned}$$

where the last convergence follows from the relative stability of iid Gaussians minima (3.14). On the other hand, $t^*/\sqrt{2 \log p} = \sqrt{q} < \sqrt{r} - \sqrt{1 - \beta}$ by our choice of q , and Relation (3.53) follows.

The necessary condition follows from the lower bound

$$\text{FDR}(\mathcal{R}) + \text{FWNR}(\mathcal{R}) \geq \mathbb{E}\left[\frac{|\hat{S}(u) \setminus S|}{|\hat{S}(u) \setminus S| + |S|}\right] \wedge \mathbb{P}\left[\min_{i \in S} x(i) < u\right], \quad (3.54)$$

which holds for any thresholding procedure \mathcal{R} and for arbitrary $u \in \mathbb{R}$. In particular, we show that both terms in the minimum in (3.54) converge to 1 when we set $u = t^* = \sqrt{2q \log p}$ where

$$\sqrt{\bar{r}} - \sqrt{1 - \beta} < \sqrt{q} < \sqrt{\beta}. \quad (3.55)$$

On the one hand, we have,

$$\frac{\min_{i \in S} x(i)}{\sqrt{2 \log p}} \stackrel{d}{\leq} \frac{\min_{i \in S} \epsilon(i) + \sqrt{2\bar{r} \log p}}{\sqrt{2 \log p}} \rightarrow \sqrt{\bar{r}} - \sqrt{1 - \beta},$$

by relative stability of iid Gaussians (3.14). On the other hand, $t^*/\sqrt{2 \log p} = \sqrt{q} > \sqrt{\bar{r}} - \sqrt{1 - \beta}$ by our choice of q ; this shows that the second term on the right-hand side of (3.54) converges to 1.

Observe that $|\hat{S}(t^*) \setminus S|$ has distribution $\text{Binom}(p - s, \bar{\Phi}(t^*))$, and define $X = X_p := |\hat{S}(t^*) \setminus S|/|S|$, we obtain,

$$\begin{aligned} \mu := \mathbb{E}[X] &= (p^\beta - 1)\bar{\Phi}(t^*) \sim (p^\beta - 1) \frac{\phi(t^*)}{t^*} \\ &\sim \frac{1}{\sqrt{2\pi}} (2q \log p)^{-1/2} p^{\beta-q} \rightarrow \infty, \end{aligned}$$

where the divergence follows from our choice of $q < \beta$. Using again Relations (3.34) and (3.35), we conclude that the first term on the right-hand side of (3.54) also converges to 1.

This completes the proof of the necessary condition. \square

CHAPTER 4

Exact Support Recovery and Minimax Optimality

We focus on exact support recovery problems in this chapter, and generalize the results we obtained in Chapter 3 to additive error models with much relaxed distributional and dependence assumptions.

Consider the additive error model (1.1) with the triangular array of errors,

$$\mathcal{E} = \{(\epsilon_p(i))_{i=1}^p, p = 1, 2, \dots\}, \quad (4.1)$$

where the $\epsilon_p(i)$'s have common cumulative distribution function $F(x) = \mathbb{P}[\epsilon_p(i) \leq x]$. In contrast to the assumptions in Chapter 3, we only require the errors to have common marginal distributions, and allow them to have potentially arbitrary dependence.

Although our method of analysis applies to all light-tailed error distributions with rapidly varying tails (see Definition 2.9), to be concrete and better convey the main ideas, we will focus on the class of AGG(ν) laws (see Definition 2.7). Extensions of the results to other error models are presented in Section 4.3.

As in Chapter 3, we assume the signals in model (1.1) to be a sparse vector $\mu = (\mu(i))_{i=1}^p$ where the sparsity, with a few exceptions which will be explicitly stated, is parametrized as

$$s = |S_p| = \lfloor p^{1-\beta} \rfloor, \quad (4.2)$$

with $0 < \beta \leq 1$ fixed.

We assume that the non-zero entries of μ are positive and take values in the interval $[\underline{\Delta}, \overline{\Delta}] \subset (0, \infty)$. That is, $0 < \underline{\Delta} \leq \mu(i) < \overline{\Delta} \leq +\infty$, for all $i \in S_p$. The lower and upper bound on the signal sizes $\underline{\Delta}$ and $\overline{\Delta}$ are parametrized as

$$\underline{\Delta} = \underline{\Delta}(p) = (\nu \underline{r} \log p)^{1/\nu} \quad \text{and} \quad \overline{\Delta} = \overline{\Delta}(p) = (\nu \bar{r} \log p)^{1/\nu}, \quad (4.3)$$

with parameters $0 < \underline{r} \leq \bar{r} \leq +\infty$. Notice that the parametrization now depends on the shape of the assumed error distributions $\text{AGG}(\nu)$ through the parameter ν .

According to Lemma 2.6, in order to study the asymptotic behaviors of risk^E , it is sufficient to establish minimal conditions under which the support sets can be consistently estimated, i.e.,

$$\mathbb{P}[\widehat{S}_p = S_p] \longrightarrow 1 \quad \text{as } p \rightarrow \infty, \quad (4.4)$$

where \widehat{S}_p is an estimate of the true signal support set S_p .

Several authors have studied the support recovery problem in terms of the Hamming loss and obtained minimax optimality results (see, e.g., Ji and Jin (2012); Genovese et al. (2012); Jin et al. (2014); Butucea et al. (2018)). In the special case of Gaussian marginals, Butucea et al. (2018) showed that the boundary (3.9) exists in a minimax sense. That is, when errors are *independent* Gaussians, the Hamming loss cannot be made to vanish if signal sizes fall below the boundary (3.9) by any procedure. Conversely, if signal size falls below, the Hamming loss can be made to vanish with a specific thresholding procedure.

Unfortunately, as pointed out in Section 2.4, vanishing Hamming loss is only sufficient, not necessary for support recovery (4.4), and the sharp result does not carry over directly to the study of the probability of support recovery or exact support recovery risk. More importantly, despite their elegance, these Hamming loss-minimax studies naturally amounts to the analysis of the elementary case of iid data, and is by design blind to non-trivial error-dependence structures. This prevents us from fully exploring of the phase transition

phenomena under other dependence conditions.

So far in the literature, the role of dependence, and that of the distributional assumptions in model (1.1) remain largely unexplored. This chapter offers advances in both directions, and provides a close-to-complete solution of the exact support recovery problem. (See also, Chapter 5.) We briefly summarize our contributions next.

In Section 4.1, we study exact support recovery in the sense of (4.4) directly, under general distributional and dependence assumptions. In particular, we describe the phase transition phenomena in the dependent AGG model, under the scaling described in (4.2) and (4.3). Consider the function

$$g(\beta) = g_\nu(\beta) = (1 + (1 - \beta)^{1/\nu})^\nu, \quad \nu > 0, \quad (4.5)$$

which we refer to as the *strong classification boundary*. In Theorem 4.1 we show that, if the signal sizes are above the boundary (i.e., $\underline{r} > g(\beta)$), the FWER-controlling procedures described in Section 2.2 with appropriately calibrated levels achieve *exact support recovery* as in (4.4).

Conversely, we show in Theorem 4.8, that for a surprisingly large class of dependence structures characterized by the concept of *uniform relative stability* (URS, see Definition 4.6 below), when the signal size is below the boundary (i.e., $r < g(\beta)$), no thresholding procedure can achieve the asymptotically perfect support recovery (4.4). In fact,

$$\mathbb{P} \left[\widehat{S}_p = S_p \right] \longrightarrow 0, \quad \text{as } p \rightarrow \infty, \quad (4.6)$$

for all \widehat{S}_p in the form of (2.19).

These two results show that the thresholding procedures obey a phase transition phenomenon in a strong, *point-wise* sense over the class of URS dependence structures, and over the class of $\text{AGG}(\nu)$, $\nu > 0$ error distributions. The conclusions are fundamentally stronger and more informative than the minimax statements in the literature (see, e.g., Bu-

tucea et al. (2018)). The techniques developed in this here are also entirely different from those in Ji and Jin (2012) or Butucea et al. (2018), and transparent characterizations of the dependence conditions under which the phase transition type result holds will be established in the Chapter 5 later.

We show in Section 4.2 that data thresholding procedures are not only asymptotically, but in fact, finite sample optimal when the errors are independent and identically distributed (iid) with log-concave densities. In this case, no estimator can achieve perfect support recovery when the signal is below the strong classification boundary (4.5). Consequently, in the case of $\text{AGG}(\nu)$ errors with $\nu \geq 1$, the strong classification boundary is shown to hold in the minimax sense for *all* procedures. This is formalized in Theorem 4.23 and Corollary 4.24.

The phase transition phenomena for two additional classes of error distributions with either heavier or lighter tails than the AGG distributions will be described in Section 4.3.

A final surprising result that had only recently been noticed by the statistical community is that thresholding procedures, including data-dependent ones, are not optimal in general in the support recovery problem when the errors have heavy (regularly-varying) tails. Arias-Castro and Ying (2019) discussed the phenomena in approximate support recovery problems. In this case, we also demonstrate the absence of a phase transition phenomenon in exact support recovery by thresholding, in Section 4.4.

4.1 Exact support recovery under AGG errors

We present the sufficient condition under which exact support recovery (4.4) can be achieved in Section 4.1.1. A very general class of dependence structures characterized by the uniform relative stability concept will be introduced in Section 4.1.2, to prepare us for the necessary condition in Section 4.1.3.

Section 4.1.4 discusses the case in which signals are denser than parametrized in (4.2), and Section 4.1.5 illustrates the phase transition phenomena with numerical examples.

4.1.1 Sufficient conditions for exact support recovery

Following Butucea et al. (2018), we define the parameter space for the signals μ as

$$\Theta_p^+(\beta, \underline{r}) = \{\mu \in \mathbb{R}^p : \text{there exists a set } S_p \subseteq \{1, \dots, p\} \text{ such that } |S_p| \leq \lfloor p^{1-\beta} \rfloor, \\ \mu(i) \geq (\nu \underline{r} \log p)^{1/\nu} \text{ for all } i \in S_p, \text{ and } \mu(i) = 0 \text{ for all } i \notin S_p\}. \quad (4.7)$$

Our first result states that, when $F \in \text{AGG}(\nu)$ with $\nu > 0$, regardless of the error dependence structure, (asymptotic) perfect support recovery is achieved by applying Bonferroni's procedure with appropriately calibrated FWER, as long as the minimum signal size \underline{r} is above the strong classification boundary (4.5).

Theorem 4.1. *Let the errors have common marginal distribution $F \in \text{AGG}(\nu)$ with $\nu > 0$. Let \widehat{S}_p be the Bonferroni's procedure (2.20) with vanishing FWER $\alpha = \alpha(p) \rightarrow 0$, such that $\alpha p^\delta \rightarrow \infty$ for every $\delta > 0$. If*

$$\underline{r} > g(\beta) = (1 + (1 - \beta)^{1/\nu})^\nu, \quad (4.8)$$

then we have

$$\lim_{p \rightarrow \infty} \sup_{\mu \in \Theta_p^+(\beta, \underline{r})} \mathbb{P}[\widehat{S}_p \neq S_p] = 0. \quad (4.9)$$

Corollary 4.2 (Classes of procedures attaining the boundary). *Relation (4.9) holds for any FWER-controlling procedure that is strictly more powerful than Bonferroni's procedure. This includes Holm's procedure (Holm, 1979), and in the case of independent errors, Hochberg's procedure (Hochberg, 1988), and the Šidák procedure (Šidák, 1967).*

Example 4.3. Under Gaussian errors, the particular choice of the thresholding at $t_p = \sqrt{2 \log p}$ in (2.20) corresponds to a Bonferroni's procedure with FWER decreasing at a rate

of $(\log p)^{-1/2}$, and hence Theorem 4.1 applies. By Corollary 4.2, Holm's procedure — and when the errors are independent, the Šidák, and Hochberg procedures — with FWER controlled at $(\log p)^{-1/2}$ all achieve perfect support recovery provided that $\underline{r} > g(\beta)$.

The claims in Example 4.3 are verified in Section 4.5.

We now turn to the proof of Theorem 4.1.

Proof of Theorem 4.1. Throughout the proof, dependence on p will be suppressed to simplify notations when such omissions do not lead to ambiguity.

Under the $\text{AGG}(\nu)$ model, it is easy to see from equation (2.32) that the thresholds in Bonferroni's procedure are

$$t_p = F^{\leftarrow}(1 - \alpha/p) = (\nu \log(p/\alpha))^{1/\nu}(1 + o(1)). \quad (4.10)$$

It is known that Bonferroni's procedure $\widehat{S}_p = \{i : x(i) > t_p\}$ controls the FWER. Indeed,

$$\begin{aligned} \mathbb{P}[\widehat{S} \subseteq S] &= 1 - \mathbb{P}\left[\max_{i \in S^c} x(i) > t_p\right] = 1 - \mathbb{P}\left[\max_{i \in S^c} \epsilon(i) > t_p\right] \\ &\geq 1 - \sum_{i=1}^p \mathbb{P}[\epsilon(i) > t_p] \geq 1 - \alpha(p) \rightarrow 1, \end{aligned} \quad (4.11)$$

where we used the union bound in the first inequality. Notice that the lower bound (4.11) is independent of the parameter μ (as well as the dependence structures), and hence holds uniformly over the parameter space, i.e.,

$$\lim_{p \rightarrow \infty} \inf_{\mu \in \Theta_p^+(\beta, \underline{r})} \mathbb{P}[\widehat{S}_p \subseteq S_p] = 1. \quad (4.12)$$

On the other hand, for the probability of no missed detection, we have:

$$\mathbb{P}[\widehat{S} \supseteq S] = \mathbb{P}\left[\min_{i \in S} x(i) > t_p\right] = \mathbb{P}\left[\min_{i \in S} x(i) - (\nu \underline{r} \log p)^{1/\nu} > t_p - (\nu \underline{r} \log p)^{1/\nu}\right].$$

Since the signal sizes are no smaller than $(\nu \underline{r} \log p)^{1/\nu}$, we have

$$x(i) - (\nu \underline{r} \log p)^{1/\nu} \geq \epsilon(i), \quad \text{for all } i \in S,$$

and hence we obtain

$$\mathbb{P}[\widehat{S} \supseteq S] \geq \mathbb{P}\left[\min_{i \in S} \epsilon(i) > (\nu \log(p/\alpha))^{1/\nu}(1 + o(1)) - (\nu \underline{r} \log p)^{1/\nu}\right], \quad (4.13)$$

where we plugged in the expression for t_p in (4.10). Now, since the minimum signal size is bounded below by $\underline{r} > (1 + (1 - \beta)^{1/\nu})^\nu$, we have $\underline{r}^{1/\nu} - (1 - \beta)^{1/\nu} > 1$, and so we can pick a $\delta > 0$ such that

$$\delta < (\underline{r}^{1/\nu} - (1 - \beta)^{1/\nu})^\nu - 1. \quad (4.14)$$

Since by assumption, for all $\delta > 0$, we have $p^{-\delta} = o(\alpha(p))$, there is an $M = M(\delta)$ such that $p/\alpha(p) < p^{1+\delta}$ for all $p \geq M$. Thus, from (4.13), we further conclude that for $p \geq M$ we have

$$\begin{aligned} \mathbb{P}[\widehat{S} \supseteq S] &\geq \mathbb{P}\left[\min_{i \in S} \epsilon(i) > ((1 + \delta)\nu \log p)^{1/\nu}(1 + o(1)) - (\nu \underline{r} \log p)^{1/\nu}\right] \\ &= \mathbb{P}\left[\max_{i \in S} (-\epsilon(i)) < \underbrace{(\underline{r}^{1/\nu} - (1 + \delta)^{1/\nu})(\nu \log p)^{1/\nu}(1 + o(1))}_{=: A}\right] \\ &\geq 1 - \lfloor p^{1-\beta} \rfloor \times \overline{F}_-(A), \end{aligned} \quad (4.15)$$

where $\overline{F}_-(x) = \mathbb{P}[-\epsilon(i) > x]$ is the survival function of the $(-\epsilon(i))$'s. Notice that (4.15) follows from the union bound and the assumption that $|S_p| \leq \lfloor p^{1-\beta} \rfloor$. Therefore, the lower bound does not depend on μ (nor on the error dependence structure), and holds uniformly in the parameter space. In turn, we obtain

$$\inf_{\mu \in \Theta_p^+(\beta, \underline{r})} \mathbb{P}[\widehat{S}_p \supseteq S_p] \geq 1 - \lfloor p^{1-\beta} \rfloor \times \overline{F}_-(A). \quad (4.16)$$

If $\beta = 1$, we conclude that the right-hand-side of (4.16) converges to 1, since $A \rightarrow +\infty$.

Let now $\beta \in (0, 1)$ and $u_p^- := F_-^{\leftarrow}(1 - 1/p)$. The fact that $p\overline{F}_-(u_p^-) \leq 1$, implies

$$\lfloor p^{1-\beta} \rfloor \times \overline{F}_-(A) \leq \frac{\overline{F}_-(\mathbf{B} \times u_{\lfloor p^{1-\beta} \rfloor}^-)}{\overline{F}_-(u_{\lfloor p^{1-\beta} \rfloor}^-)} \quad (4.17)$$

where $\mathbf{B} := A/u_{\lfloor p^{1-\beta} \rfloor}^-$.

Notice that by assumption, the $-\epsilon(i)$'s are also $\text{AGG}(\nu)$ distributed and by Proposition 2.8, $u_p^- := F_-^{\leftarrow}(1 - 1/p) \sim (\nu \log(p))^{1/\nu}$, as $p \rightarrow \infty$. Therefore, we have

$$u_{\lfloor p^{1-\beta} \rfloor}^- \sim (\nu(1 - \beta) \log p)^{1/\nu} \quad (4.18)$$

and

$$\mathbf{B} = \frac{A}{u_{\lfloor p^{1-\beta} \rfloor}^-} = \frac{r^{1/\nu} - (1 + \delta)^{1/\nu}}{(1 - \beta)^{1/\nu}} (1 + o(1)) \rightarrow c > 1$$

as $p \rightarrow \infty$, by our choice of δ in (4.14).

Finally, since the distribution F_- has *rapidly varying* tails (by Definition 2.9 and Example 2.12), applying Proposition 2.11, we conclude that (4.17) vanishes. Consequently, the lower bound on the right-hand-side of (4.16) converges to 1. This, combined with (4.12), entails $\lim_{p \rightarrow \infty} \inf_{\mu \in \Theta_p^+(\beta, \underline{r})} \mathbb{P}[\widehat{S}_p = S_p] = 1$, and hence the desired conclusion (4.9), which completes the proof. \square

The statements in Theorem 4.1 can be strengthened, to prepare us for a minimax result given in Section 4.2 below.

Remark 4.4. In the proof of Theorem 4.1, both (4.11) and (4.15) hold uniformly over all error dependence structures. Therefore, (4.12) and (4.16) may be strengthened to yield

$$\lim_{p \rightarrow \infty} \sup_{\substack{\mu \in \Theta_p^+(\beta, \underline{r}) \\ \mathcal{E} \in D(F)}} P[\widehat{S}_p \neq S_p] = 0, \quad (4.19)$$

for $\underline{r} > g(\beta)$, where $D(F)$ is the collection of all arrays with common marginal F , i.e.,

$$D(F) = \{\mathcal{E} = (\epsilon_p(i))_p : \epsilon_p(i) \sim F \text{ for all } i = 1, \dots, p, \text{ and } p = 1, 2, \dots\}. \quad (4.20)$$

Remark 4.5. We emphasize that Theorem 4.1 holds for errors with *arbitrary* dependence structures. Intuitively, this is because the maxima of the errors grow at their fastest in the case of independence. Formally, the light-tailed nature of the error distribution allowed us to obtain sharp tail estimates via simple union bounds, valid under arbitrary dependence.

4.1.2 Dependence and uniform relative stability

An important ingredient needed for a converse of Theorem 4.1 is an appropriate characterization of the error dependence structure under which the strong classification boundary (4.5) is tight. The notion of *uniform relative stability* turns out to be the key.

Definition 4.6 (Uniform Relative Stability). Under the notations established in Definition 2.10, the triangular array \mathcal{E} is said to have uniform relatively stable (URS) maxima if for every sequence of subsets $S_p \subseteq \{1, \dots, p\}$ such that $|S_p| \rightarrow \infty$, we have

$$\frac{1}{u_{|S_p|}} M_{S_p} := \frac{1}{u_{|S_p|}} \max_{i \in S_p} \epsilon_p(i) \xrightarrow{\mathbb{P}} 1, \quad (4.21)$$

as $p \rightarrow \infty$, where u_q , $q \in \{1, \dots, p\}$ is the generalized quantile in (2.36). The collection of arrays $\mathcal{E} = \{\epsilon_p(i)\}$ with URS maxima is denoted $U(F)$.

Uniform relative stability is, as its name suggests, a stronger requirement on dependence than relative stability (recall Definition 2.10). Proposition 2.11 states that an array with iid components sharing a marginal distribution F with rapidly varying tails (Definition 2.9) has relatively stable maxima; it is easy to see that URS also follows, by independence of the entries.

Corollary 4.7. *An independent array \mathcal{E} with common marginals $F \in \text{AGG}(\nu)$, $\nu > 0$, is URS; in this case, URS holds with $u_{|S_p|} \sim (\nu \log |S_p|)^{1/\nu}$.*

On the other hand, RS and URS hold under much broader dependence structures than just independent errors. These conditions are extremely mild and can be shown to hold for many classes of error models. In Chapter 5, we will focus extensively on the Gaussian case, which is of great interest in applications and is rather challenging. We will provide simple necessary and sufficient condition for uniform relative stability in terms of the covariance structures.

The relative stability concepts are important because they characterize the dependence structures under which the maxima of error sequences *concentrate* around the quantiles (2.36) in the sense of (2.37). This concentration of maxima phenomena, in turn, is the key to establishing the necessary conditions of the phase transition results in support recovery problems.

4.1.3 Necessary conditions for exact support recovery

With the preparations from Section 4.1.2, we are ready to state the necessary conditions for exact support recovery (4.4) by thresholding procedures. It turns out that the strong classification boundary (4.5) is tight, under the general dependence structure characterized by URS (Definition 4.6).

Formally, we define the parameter space for the signals μ to be

$$\begin{aligned} \Theta_p^-(\beta, \bar{r}) = \{ \mu \in \mathbb{R}^p : \text{there exists a set } S_p \subseteq \{1, \dots, p\} \text{ such that } |S_p| = \lfloor p^{1-\beta} \rfloor, \\ 0 < \mu(i) \leq (\nu \bar{r} \log p)^{1/\nu} \text{ for all } i \in S_p, \text{ and } \mu(i) = 0 \text{ for all } i \notin S_p \}. \end{aligned} \quad (4.22)$$

Theorem 4.8. *Let \mathcal{E} be a triangular array with common $\text{AGG}(\nu)$ marginal F , $\nu > 0$. Assume further that the errors \mathcal{E} have uniform relatively stable maxima and minima, i.e.,*

$\mathcal{E} \in U(F)$, and $(-\mathcal{E}) = \{-\epsilon_p(i)\} \in U(F)$. If

$$\bar{r} < g(\beta) = (1 + (1 - \beta)^{1/\nu})^\nu, \quad (4.23)$$

then

$$\lim_{p \rightarrow \infty} \inf_{\hat{S}_p \in \mathcal{T}} \inf_{\mu \in \Theta_p^-(\beta, \bar{r})} \mathbb{P}[\hat{S}_p \neq S_p] = 1, \quad (4.24)$$

where \mathcal{T} is the class of all thresholding procedures (2.19).

Our first comment is on the signal sizes, and in particular, the gap between the sufficient conditions (Theorem 4.1) and the necessary conditions (Theorem 4.8).

Remark 4.9. The sufficient condition in Theorem 4.1 requires that *all* signals be larger than the strong classification boundary $g(\beta)$ in order to achieve exact support recovery (4.4), while Theorem 4.8 states that exact support recovery fails (in the sense of (4.6)) when *all* signal sizes are below the boundary — the two conditions are *not* complements of each other. This gap between the sufficient and necessary conditions on signal sizes, however, may be difficult to bridge. Indeed, in general, when signal sizes straddle the boundary $g(\beta)$, either outcome is possible, as we demonstrate in Example 4.10 below.

Example 4.10 (Signals straddling the boundary). Let the signal μ have $|S_p| = \lfloor p^{(1-\beta)} \rfloor$ non-zero entries, composed of two disjoint sets $S_p = S_p^{(1)} \cup S_p^{(2)}$. Let also the magnitude of the signals be equal within the two sets, i.e., $\mu(i) = \sqrt{2r^{(k)} \log p}$ if $i \in S_p^{(k)}$ for some constants $r^{(k)} > 0$ for $k = 1, 2$. For simplicity, assume that the errors are iid standard Gaussians.

Consider two scenarios

1. $r^{(1)} = (1 + \delta)g(\beta)$, $r^{(2)} = (1 + \delta)$ with $|S_p^{(1)}| = |S_p| - 1$, $|S_p^{(2)}| = 1$,
2. $r^{(1)} = (1 + \delta)g(\beta)$, $r^{(2)} = (1 - \delta)g(\beta)$ with $|S_p^{(1)}| = \lfloor |S_p|/2 \rfloor$, $|S_p^{(2)}| = |S_p| - |S_p^{(1)}|$.

for some constants $0 < \delta < 1 - \beta < 1$. In both cases, signals in $S_p^{(1)}$ (respectively, $S_p^{(2)}$) are above (respectively, below) the strong classification boundary (4.5). However, in the first

scenario, we have $\mathbb{P}[\widehat{S}_p^{\text{Bonf}} = S_p] \rightarrow 1$ where $\widehat{S}_p^{\text{Bonf}}$ is the Bonferroni's procedure described in Theorem 4.1, while in the second scenario, we have $\mathbb{P}[\widehat{S}_p = S_p] \rightarrow 0$ for *all* thresholding procedures \widehat{S}_p .

The claims in Example 4.10 are verified in Section 4.5.

Our second comment is on the interplay between thresholding procedures and the dependence class characterized by URS.

Remark 4.11. Paraphrasing Theorems 4.1 and 4.8: if we consider only thresholding procedures, then for a very large class of dependence structures, we cannot improve upon the Bonferroni procedure $\widehat{S}_p^{\text{Bonf}}$. Specifically, for all $\mathcal{E} \in U(F)$ and $-\mathcal{E} \in U(F)$, and for all $S_p \in \mathcal{S}$, where $\mathcal{S} = \{S \subseteq \{1, \dots, p\}; |S| = \lfloor p^{1-\beta} \rfloor\}$, we have

$$\lim_{p \rightarrow \infty} \mathbb{P}[\widehat{S}_p^{\text{Bonf}} \neq S_p] = \begin{cases} \limsup_{p \rightarrow \infty} \inf_{\widehat{S}_p \in \mathcal{T}} \mathbb{P}[\widehat{S}_p \neq S_p] = 0, & \text{if } \underline{r} > g(\beta), \\ \liminf_{p \rightarrow \infty} \inf_{\widehat{S}_p \in \mathcal{T}} \mathbb{P}[\widehat{S}_p \neq S_p] = 1, & \text{if } \bar{r} < g(\beta) \end{cases} \quad (4.25)$$

where \mathcal{T} is the set of all thresholding procedures (2.19).

Theorem 4.8 also yields an answer the question raised in Butucea et al. (2018). In particular, the authors of (Butucea et al., 2018) commented that independent error is the ‘least favorable model’ in the problem of support recovery, and conjectured that the support recovery problem may be easier to solve under dependence, similar to how the problem of signal detection is easier under dependent errors (see Hall and Jin (2010)). Surprisingly, our results here state that asymptotically, *all* error dependence structures in the large URS class are equally difficult for *thresholding procedures*. Therefore, the phase transition behavior is universal in the class of dependence structures characterized by URS.

To facilitate comparison with results in existing literature, we will formulate explicit minimax statements in Section 4.2.

We must emphasize that the restriction to the URS dependence class is *not* an assumption of convenience. The condition on dependence characterized by uniform relative sta-

bility is, in fact, the weakest of its kind in the literature. We will characterize the class URS dependence class in Chapter 5 below.

We conclude with the proof of Theorem 4.8.

Proof of Theorem 4.8. To avoid cumbersome double subscript notations, we will sometimes suppress dependence on p of the set sequences \widehat{S}_p and S_p in the proof.

Since the estimator $\widehat{S}_p = \{x(i) \geq t_p(x)\}$ is thresholding, exact support recovery takes place if and only if the threshold separates the signals and null part, i.e.,

$$\mathbb{P}[\widehat{S}_p = S_p] = \mathbb{P} \left[\max_{i \in S^c} x(i) < t_p(x) \leq \min_{i \in S} x(i) \right] \leq \mathbb{P} \left[\max_{i \in S^c} x(i) < \min_{i \in S} x(i) \right].$$

Since the right-hand-side does not depend on the procedure \widehat{S}_p , we also have

$$\sup_{\widehat{S}_p \in \mathcal{T}} \mathbb{P}[\widehat{S}_p = S_p] \leq \mathbb{P} \left[\max_{i \in S^c} x(i) < \min_{i \in S} x(i) \right] \leq \mathbb{P} \left[\max_{i \in S^c} \epsilon(i) < \overline{\Delta} + \min_{i \in S} \epsilon(i) \right], \quad (4.26)$$

where we used the assumption that the signal sizes are no greater than $\overline{\Delta}$. Let $S^* = S_p^*$ be a sequence of support sets that maximize the right-hand-side of (4.26), i.e., let

$$S_p^* = \arg \max_{S \subseteq \{1, \dots, p\} : |S| = \lfloor p^{1-\beta} \rfloor} \mathbb{P} \left[\max_{i \in S^c} \epsilon(i) < \overline{\Delta} + \min_{i \in S} \epsilon(i) \right],$$

where ties can be broken lexicographically if multiple maximizers exist. Then, we obtain the following bound which only depends on \bar{r} and the distribution of \mathcal{E} ,

$$\begin{aligned} \sup_{\widehat{S}_p \in \mathcal{T}} \sup_{\mu \in \Theta_{\bar{r}}(\beta, \bar{r})} \mathbb{P}[\widehat{S}_p = S_p] &\leq \mathbb{P} \left[\max_{i \in S^{*c}} \epsilon(i) < \overline{\Delta} + \min_{i \in S^*} \epsilon(i) \right] \\ &= \mathbb{P} \left[\frac{M_{S^{*c}}}{u_p} < \frac{\overline{\Delta} - m_{S^*}}{u_p} \right], \end{aligned} \quad (4.27)$$

where $M_{S^{*c}} = \max_{i \in S^{*c}} \epsilon(i)$ and $m_{S^*} = \max_{i \in S^*} (-\epsilon(i))$. Since the error arrays \mathcal{E} and

$(-\mathcal{E})$ are URS by assumption, using the expression for the AGG quantiles (2.32), we have

$$\frac{M_{S^{*c}}}{u_p} = \frac{M_{S^{*c}}}{u_{|S^{*c}|}} \frac{u_{|S^{*c}|}}{u_p} \xrightarrow{\mathbb{P}} 1, \quad \text{and} \quad \frac{m_{S^*}}{u_p} = \frac{m_{S^*}}{u_{|S^*|}} \frac{u_{|S^*|}}{u_p} \xrightarrow{\mathbb{P}} (1 - \beta)^{1/\nu}, \quad (4.28)$$

so that the two random terms in probability (4.27) converge to constants. Notice that the second relation in (4.28) holds by URS for any $\beta \in (0, 1)$; when $\beta = 1$, the relation holds since $u_{|S^*|}/u_p$ vanishes while $\{m_{S^*}/u_{|S^*|}\}$ is tight.

Since signal sizes are bounded above by $\bar{r} < (1 + (1 - \beta)^{1/\nu})^\nu$, we can write $\bar{r}^{1/\nu} = 1 + (1 - \beta)^{1/\nu} - d$ for some $d > 0$. By our parametrization of $\bar{\Delta}$, we have

$$\frac{\bar{\Delta}}{u_p} = (1 + (1 - \beta)^{1/\nu} - d) (1 + o(1)). \quad (4.29)$$

Combining (4.28) and (4.29), we conclude that the right-hand-side of the probability (4.27) converges in probability to a constant strictly less than 1, that is,

$$\frac{\bar{\Delta} - m_S}{u_p} \xrightarrow{\mathbb{P}} 1 - d, \quad (4.30)$$

while $M_{S^{*c}}/u_p \xrightarrow{\mathbb{P}} 1$. Therefore, the probability in (4.27) must go to 0. \square

4.1.4 Dense signals

We treat briefly the case of dense signals, where the size of the support set is proportional to the problem dimension, i.e. $s \sim cp$ for some constant $c \in (0, 1)$. We show that in this case, a phase-transition-type result still holds, independently of the value of c . Analogous to the set-up of Theorems 4.1 and 4.8, let

$$\Theta_p^{\text{d}+}(c, \underline{r}) = \{\mu \in \mathbb{R}^p : \text{there exists a set } S_p \subseteq \{1, \dots, p\} \text{ such that } |S_p| \leq \lfloor cp \rfloor, \\ \mu(i) \geq (\nu \underline{r} \log p)^{1/\nu} \text{ for all } i \in S_p, \text{ and } \mu(i) = 0 \text{ for all } i \notin S_p\}, \quad (4.31)$$

where “d” in the notation Θ_p^{d+} stands for “dense”. Similarly, define

$$\begin{aligned}\Theta_p^{d-}(c, \bar{r}) &= \{\mu \in \mathbb{R}^p : \text{there exists a set } S_p \subseteq \{1, \dots, p\} \text{ such that } |S_p| = \lfloor cp \rfloor, \\ &\quad 0 < \mu(i) \leq (\nu \bar{r} \log p)^{1/\nu} \text{ for all } i \in S_p, \text{ and } \mu(i) = 0 \text{ for all } i \notin S_p\}.\end{aligned}\tag{4.32}$$

Theorem 4.12. *Let $c \in (0, 1)$ be a fixed constant, and let $\widehat{S} = \widehat{S}_p^{\text{Bonf}}$ denote the Bonferroni’s procedure as described in Theorem 4.1. In the context of Theorem 4.1, if $\underline{r} > 1$, then we have*

$$\lim_{p \rightarrow \infty} \sup_{\mu \in \Theta_p^{d+}(c, \underline{r})} \mathbb{P}[\widehat{S}_p \neq S_p] = 0.\tag{4.33}$$

While in the context of Theorem 4.8, if $\bar{r} < 1$, then

$$\lim_{p \rightarrow \infty} \inf_{\widehat{S}_p \in \mathcal{T}} \inf_{\mu \in \Theta_p^{d-}(c, \bar{r})} \mathbb{P}[\widehat{S}_p \neq S_p] = 1,\tag{4.34}$$

where \mathcal{T} is the class of all thresholding procedures (2.19).

Remark 4.13. Notice that the boundary for the signal size parameter is identically 1 in this dense regime. Therefore, if we interpret $\beta = 0$ of the parametrization (4.2) as $s \sim cp$, where $c \in (0, 1)$, then the strong classification boundary (4.5) may be continuously extended to the left-end point where $g(0) = 1$.

Proof of Theorem 4.12. The proof is entirely analogous to that of Theorems 4.1 and 4.8. Specifically, (4.33) follows by replacing $\lfloor p^{1-\beta} \rfloor$ with $\lfloor cp \rfloor$ in Relation (4.15) onward, and replacing (4.18) with

$$u_s^- \sim (\nu \log cp)^{1/\nu} \sim (\nu \log p)^{1/\nu}.$$

in the proof of Theorem 4.1. Similarly, (4.34) follows the proof of Theorem 4.8. Indeed, by using the fact that

$$\frac{u_{|S^*c|}}{u_p} \sim \frac{(\nu \log (1-c)p)^{1/\nu}}{(\nu \log p)^{1/\nu}} \rightarrow 1$$

and $u_{|S^*|}/u_p \rightarrow 1$ for all $c \in (0, 1)$, we see that Relation (4.28) holds with $\beta = 0$, and the rest of Theorem 4.8 applies. \square

4.1.5 Numerical illustrations for independent errors

We examine numerically the boundaries (4.5) under several error tail assumptions for independence errors in this section. Numerical experiments for dependent errors will be deferred until we characterize the uniform relatively stable/uniform relative stability (URS) conditions in Chapter 5.

To demonstrate the phase transition phenomenon under different error tail densities, we simulate from the additive error model (1.1) with

- Gaussian errors, where the density is given by $f(x) = \frac{1}{\sqrt{2\pi}} \exp\{-x^2/2\}$.
- Laplace errors, where the density is given by $f(x) = \frac{1}{2} \exp\{-|x|\}$.
- Generalized Gaussian $\nu = 1/2$, with density $f(x) = \frac{1}{2} \exp\{-2|x|^{1/2}\}$.

The sparsity and signal size of the sparse mean vector are parametrized as in equations (4.2) and (4.3), respectively. The support set S is estimated with $\tilde{S} = \{i : x(i) > \sqrt{2 \log p}\}$ under the Gaussian errors, $\tilde{S} = \{i : x(i) > \log p + (\log \log p)/2\}$ under the Laplace errors, and with $\tilde{S} = \{i : x(i) > \frac{1}{4} (W(-c/(ep \log p)) + 1)^2\}$ under the generalized Gaussian ($\nu = 1/2$) errors. Here W is the Lambert W function, i.e., $W = f^{-1}$ where $f(x) = x \exp(x)$. The choices of thresholds correspond to Bonferroni's procedures with FWER decreasing at a rate of $1/\sqrt{\log p}$, therefore satisfying the assumptions in Theorem 4.1. Experiments were repeated 1000 times under each sparsity-and-signal-size combination.

The results of the numerical experiments are shown in Figure 4.1. The numerical results illustrate that the predicted boundaries are not only accurate in high-dimensions ($p = 10000$, right panels of Figure 4.1), but also practically meaningful even at moderate dimensions ($p = 100$, left panels of Figure 4.1).

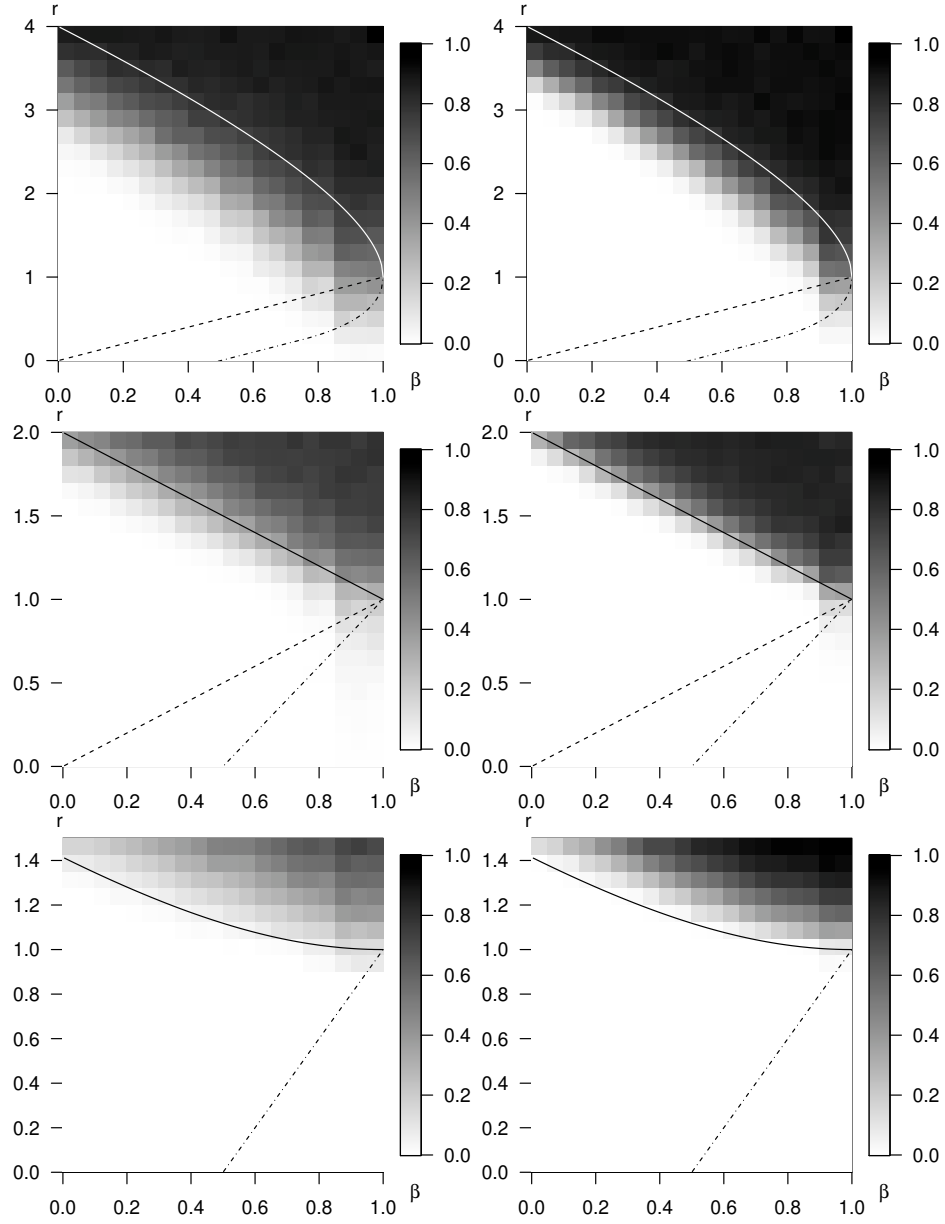


Figure 4.1: The empirical probability of exact support recovery from numerical experiments, as a function of sparsity level β and signal sizes r , from Gaussian error models (upper panels), Laplace error models (middle panels), and generalized Gaussian with $\nu = 1/2$ (lower panels); darker color indicates higher probability of exact support recovery. The experiments were repeated 1000 times for each sparsity-signal size combination, and for dimensions $p = 100$ (left panels) and $p = 10000$ (right panels). Numerical results agree with the boundaries described in Theorem 4.1; convergence is noticeably slower for under generalized Gaussian ($\nu = 1/2$) errors. For reference, the dashed and dash-dotted lines represent the weak classification and detection boundaries (see Chapter 3).

4.2 Bayes minimax optimality and (sub)optimality of thresholding procedures

We establish in this section minimax versions of our results from Section 4.1. Specifically, if we restrict ourselves to *the class of thresholding procedures* \mathcal{T} (defined in (2.19)), then Bonferroni's procedure is minimax optimal, for *any* fixed dependence structures in the URS class. This is formalized in Corollary 4.14 in Section 4.2.1. We refer to this result as *point-wise* minimax, to emphasize the fact that this optimality holds for every *fixed* URS array.

Meanwhile, if we search over *all procedures*, but expand the parameter space to include all dependence structures, then a different minimax optimality statement holds for Bonferroni's procedure. This result, formally stated in Section 4.2.4, is a consequence of our characterization of the finite-sample Bayes optimality of thresholding procedures in Sections 4.2.2 and 4.2.3.

Finally, we offer some insights into the support recovery problem in the case when errors have heavier-than-exponential tails in Section 4.2.5.

4.2.1 Point-wise minimax optimality

Theorems 4.1 and 4.8 can be cast in the form of an asymptotic minimax statement.

Corollary 4.14 (Point-wise minimax). *Let \widehat{S}_p^{Bonf} be the sequence of Bonferroni's procedure described in Theorem 4.1. Let also the errors have common $AGG(\nu)$ distribution F with parameter $\nu > 0$, and Θ_p^+ be as defined in (4.7). If $\underline{\tau} > g(\beta)$, then we have*

$$\limsup_{p \rightarrow \infty} \sup_{\mu \in \Theta_p^+(\beta, \underline{\tau})} \mathbb{P}(\widehat{S}_p^{Bonf} \neq S_p) = 0, \quad (4.35)$$

for arbitrary dependence structure of the error array $\mathcal{E} = \{\epsilon_p(i)\}_p$. Let \mathcal{T} be the class of

thresholding procedures (2.19). If $\underline{r} < g(\beta)$, then we have

$$\liminf_{p \rightarrow \infty} \inf_{\hat{S}_p \in \mathcal{T}} \sup_{\mu \in \Theta_p^+(\beta, \underline{r})} \mathbb{P}(\hat{S}_p \neq S_p) = 1, \quad (4.36)$$

for any error dependence structure such that $\mathcal{E} \in U(F)$ and $(-\mathcal{E}) \in U(F)$.

Proof of Corollary 4.14. The first conclusion (4.35) is a restatement of Theorem 4.1.

For the second statement (4.36), since $\underline{r} < g(\beta)$, we can pick a sequence $\mu^* \in \Theta_p^+(\beta, \underline{r})$ such that $|S_p| = \lfloor p^{1-\beta} \rfloor$, with signals having the same signal size $\mu(i) = (2r \log p)^{1/\nu}$ for all $i \in S_p$, where $\underline{r} < r < g(\beta)$. For this particular choice of μ^* we have $\mu^* \in \Theta_p^-(\beta, \bar{r})$ where $r < \bar{r} < g(\beta)$, and according to Theorem 4.8, we obtain $\lim_{p \rightarrow \infty} \inf_{\hat{S}_p \in \mathcal{T}} \mathbb{P}[\hat{S}_p \neq S_p] = 1$, for all dependence structures in the URS class. \square

Remark 4.15. Theorem 4.8 is a stronger result than the traditional minimax claim in Relation (4.36). Indeed, (4.24) involves an infimum (over the class Θ_p^-) while (4.36) has a supremum (over the class Θ_p^+).

On the other hand, Corollary 4.14 is more informative than many minimax-type statements, since it applies “point-wise” to any fixed error dependence structure in the URS class.

Remark 4.16. Corollary 4.14 echoes Remark 4.11: for a very large class of dependence structures, we cannot improve upon Bonferroni’s procedure in exact support recovery problems (asymptotically), unless we look beyond thresholding procedures.

4.2.2 Bayes optimality in support recovery problems

In studying support recovery problems (e.g., Arias-Castro and Chen (2017)), restrictions to the thresholding procedures are sometimes justified by arguing that such procedures are the “reasonable” choice for estimating the support set. We show in this section that, perhaps surprisingly, for general error models, thresholding procedures are not always optimal, even when the observations are independent.

We shall identify the optimal procedure for support recovery problems under a Bayesian setting with general distributional assumptions (including but not limited to additive models (1.1)). Specifically, we assume that there is an ordered set $P = (i_1, \dots, i_s)$, $i_i \in \{1, \dots, p\}$, and s (not necessarily equal) densities f_1, \dots, f_s , such that the observations indexed by P have corresponding densities. That is,

$$x(i_j) \sim f_j, \quad j = 1, \dots, s. \quad (4.37)$$

Let also the rest $(p - s)$ observations have common density f_0 , i.e., $x(i) \sim f_0$ for $i \notin S$. We further assume that the observations x are mutually independent.

We adopt here a Bayesian framework to measure statistical risks. Let the ordered support $P = (i_1, \dots, i_s)$ have prior

$$\pi((i_1, \dots, i_s)) = (p - s)!/p!, \quad (4.38)$$

for all distinct $1 \leq i_1, \dots, i_s \leq p$. Consequently, the unordered support $S = \{i_1, \dots, i_s\}$ is distributed uniformly in the collection of all set of size s , with the unordered uniform distribution π^u . That is, for all for all $S \in \mathcal{S} := \{S \subseteq \{1, \dots, p\}; |S| = s\}$, we have

$$\pi^u(\{i_1, \dots, i_s\}) = \sum_{\sigma} \pi((i_{\sigma(1)}, \dots, i_{\sigma(s)})) = (p - s)!s!/p!, \quad (4.39)$$

where the sum is taken over all permutations of $\{1, 2, \dots, s\}$.

For any fixed configuration P , consider the loss function,

$$\ell(\hat{S}, S) := \mathbb{P}[\hat{S} \neq S] = \mathbb{P}_P[\hat{S} \neq S],$$

where the probability is taken over the randomness in the observations only. The Bayes

optimal procedures should minimize

$$\mathbb{E}_\pi \mathbb{P}[\widehat{S} \neq S], \quad (4.40)$$

where the expectation is taken over the random configurations P , with a uniform distribution π as specified in (4.38).

If, however, the sparsity $s = |S|$ of the problem is known, then a natural estimator for S would be based on the set of top s order statistics.

Definition 4.17 (Oracle data thresholding). We call $\widehat{S}^* = \{i \mid x(i) \geq x_{[s]}\}$ the oracle data thresholding procedure, where $x_{[1]} \geq \dots \geq x_{[p]}$ are the order statistics of x .

The finite-sample optimality of the oracle thresholding procedure \widehat{S}^* is intimately linked with the *monotone likelihood ratio* (MLR) property.

Definition 4.18 (Monotone Likelihood Ratio). A family of positive densities on \mathbb{R} , $\{f_\delta, \delta \in U\}$, is said to have the MLR property if, for all $\delta_0, \delta_1 \in U \subseteq \mathbb{R}$ such that $\delta_0 < \delta_1$, the likelihood ratio $(f_{\delta_1}(x)/f_{\delta_0}(x))$ is an increasing function of x .

Their relationship is summarized in the following lemma.

Proposition 4.19. *Let the observations $x(i)$, $i = 1, \dots, p$ be as prescribed as in (4.37) through (4.38). If each of $\{f_0, f_1\}, \dots, \{f_0, f_s\}$ form an MLR family, then the oracle data thresholding procedure $\widehat{S}^* = \{i \mid x(i) \geq x_{[s]}\}$ is finite-sample optimal in terms of Bayes risk $\mathbb{E}_\pi \mathbb{P}[\widehat{S} \neq S]$. That is,*

$$\widehat{S}^* \in \arg \min_{\widehat{S}} \mathbb{E}_\pi \mathbb{P}[\widehat{S} \neq S]. \quad (4.41)$$

for all s and p .

The proof of Proposition 4.19 is found in Section 4.5.

We emphasize that the oracle thresholding procedures are in fact *finite-sample optimal* in the above Bayesian context. Further, our setup allows for different alternative distribu-

tions, and relaxes the assumptions of Butucea et al. (2018) when studying distributional generalizations, where the alternatives are assumed to be identically distributed.

It remains to understand when the key MLR property holds. We elaborate on this question next.

4.2.3 Bayes optimality under sub-exponential errors

Returning to the more concrete signal-plus-noise model (1.1), it turns out that the error tail behavior is what determines the optimality of data thresholding procedures. In this setting, log-concavity of the error densities is *equivalent* to the MLR property (Lemma 4.20). This, in turn, yields the finite-sample optimality of data thresholding procedures (Proposition 4.21).

Lemma 4.20. *Let δ be the magnitude of the non-zero signals in the signal-plus-noise model (1.1) with positive error density f_0 , and let $f_\delta(x) = f_0(x - \delta)$. The family $\{f_\delta, \delta \in \mathbb{R}\}$ has the MLR property if and only if the error density f_0 is log-concave.*

Proof of Lemma 4.20. Suppose MLR holds, we will show that $f_0(t) = \exp\{\phi(t)\}$ for some concave function ϕ . By the assumption of MLR, for any $x_1 < x_2$, setting $\delta_0 = 0$, and $\delta_1 = (x_2 - x_1)/2 > 0$, we have

$$\log \frac{f_{\delta_1}(x_2)}{f_{\delta_0}(x_2)} = \phi\left(\frac{(x_1 + x_2)}{2}\right) - \phi(x_2) \geq \phi(x_1) - \phi\left(\frac{(x_1 + x_2)}{2}\right) = \log \frac{f_{\delta_1}(x_1)}{f_{\delta_0}(x_1)}.$$

This implies that the log-density $\phi(t)$ is midpoint-concave, i.e., for all x_1 and x_2 , we have,

$$\phi\left(\frac{(x_1 + x_2)}{2}\right) \geq \frac{1}{2}\phi(x_1) + \frac{1}{2}\phi(x_2). \quad (4.42)$$

For Lebesgue measurable functions, midpoint concavity is equivalent to concavity by the Sierpinski Theorem (see, e.g., Sec I.3 of Donoghue (2014)). This proves the ‘only-if’ part.

For the ‘if’ part, when $\phi(t) = \log(f_0(t))$ is log-concave, then for any $\delta_0 < \delta_1$, and any

$x < y$, we have

$$\log \frac{f_{\delta_1}(y)}{f_{\delta_0}(y)} - \log \frac{f_{\delta_1}(x)}{f_{\delta_0}(x)} = \phi(y - \delta_1) - \phi(y - \delta_0) - \phi(x - \delta_1) + \phi(x - \delta_0) \geq 0, \quad (4.43)$$

where the last inequality is a simple consequence of concavity (see Lemma 4.37). This proves the ‘if’ part. \square

Proposition 4.19 and Lemma 4.20 yield immediately the following.

Proposition 4.21. *Consider the additive error model (1.1). Let the errors ϵ be independent with common distribution F . Let the signal μ have s positive entries with magnitudes $0 < \delta_1 \leq \dots \leq \delta_s$, located on $\{1, \dots, p\}$ as prescribed in (4.38). If F has a positive, log-concave density f , then the oracle thresholding procedure $\widehat{S}^* = \{i; x(i) \geq x_{[s]}\}$ is finite-sample optimal in terms of Bayes risk in the sense of (4.41).*

Notice that under MLR (or equivalently, log-concavity of the errors in additive models), the oracle thresholding procedure is finite-sample optimal even in the case where the signals have different (positive) sizes.

The assumption of log-concavity of the densities is compatible with the AGG model when $\nu \geq 1$, as demonstrated in the next example.

Example 4.22. The generalized Gaussian density $f(x) \propto \exp\{-|x|^\nu/\nu\}$ is log-concave for all $\nu \geq 1$. Therefore in the additive error model (1.1), according to Proposition 4.21, the oracle thresholding procedure is Bayes optimal in the sense of (4.41).

Consider the asymptotic Bayes risk as defined in (4.40), the statement for the necessary condition of support recovery, with the help of Proposition 4.21, can be strengthened to include all procedures (in the Bayesian context), regardless of whether they are thresholding.

Theorem 4.23. *Consider the additive model (1.1) where the $\epsilon_p(i)$ ’s are independent and identically distributed with log-concave densities in the AGG class. Let the signals be*

as prescribed in Proposition 4.21. If the signal sizes fall below the strong classification boundary (4.5), i.e. $\bar{r} < g(\beta)$, then we have

$$\liminf_{p \rightarrow \infty} \inf_{\hat{S}_p} \mathbb{E}_\pi \mathbb{P}[\hat{S}_p \neq S_p] = 1, \quad (4.44)$$

where the infimum on \hat{S}_p is taken over all procedures.

Proof of Theorem 4.23. When errors are independent with log-concave density, the oracle thresholding procedure \hat{S}_p^* , by Proposition 4.21, minimizes the Bayes risk (4.40) among all procedures. That is,

$$\liminf_{p \rightarrow \infty} \inf_{\hat{S}_p} \mathbb{E}_\pi \mathbb{P}[\hat{S}_p \neq S_p] \geq \liminf_{p \rightarrow \infty} \mathbb{E}_\pi \mathbb{P}[\hat{S}_p^* \neq S_p].$$

Since \hat{S}_p^* belongs to the class of all thresholding procedures, we have

$$\begin{aligned} \liminf_{p \rightarrow \infty} \mathbb{E}_\pi \mathbb{P}[\hat{S}_p^* \neq S_p] &\geq \liminf_{p \rightarrow \infty} \inf_{\hat{S}_p \in \mathcal{T}} \mathbb{E}_\pi \mathbb{P}[\hat{S}_p \neq S_p] \\ &\geq \liminf_{p \rightarrow \infty} \inf_{\hat{S}_p \in \mathcal{T}} \inf_{S_p} \mathbb{P}[\hat{S}_p \neq S_p] = 1, \end{aligned}$$

when $\bar{r} < g(\beta)$, where the last line follows from Theorem 4.8. \square

4.2.4 Minimax optimality over all procedures

Theorem 4.23 allows us to state another minimax conclusion — one in which we search over *all procedures*, by allowing the supremum in the minimax statement to be taken over the dependence structures.

Corollary 4.24. *Let $D(F)$ be the collection of error arrays with common marginal F as defined in (4.20) where F is an $\text{AGG}(\nu)$ distribution. Let also \hat{S}_p^{Bonf} be Bonferroni's*

procedure as described in Theorem 4.1. If $\underline{r} > g(\beta)$, then we have

$$\limsup_{p \rightarrow \infty} \sup_{\substack{\mu \in \Theta_p^+(\beta, \underline{r}) \\ \mathcal{E} \in D(F)}} \mathbb{P}(\widehat{S}_p^{Bonf} \neq S_p) = 0. \quad (4.45)$$

Further, when $\underline{r} < g(\beta)$, and F has a positive log-concave density f , we have

$$\liminf_{p \rightarrow \infty} \inf_{\widehat{S}_p} \sup_{\substack{\mu \in \Theta_p^+(\beta, \underline{r}) \\ \mathcal{E} \in D(F)}} \mathbb{P}(\widehat{S}_p \neq S_p) = 1, \quad (4.46)$$

where the infimum on \widehat{S}_p is taken over all procedures.

Remark 4.25. Since the class $\text{AGG}(\nu)$, $\nu \geq 1$ contains distributions with log-concave densities (Example 4.22), the minimax statement (4.46) continues to hold if the supremum is taken over the entire class $F \in \text{AGG}(\nu)$, $\nu \geq 1$. We opted for a more informative formulation which emphasizes the log-concavity condition on the density of F .

Remark 4.26. Corollary 4.24 is no stronger than Corollary 4.14. In Corollary 4.14 we search over only the class of thresholding procedures, but offer a tight, point-wise lower bound on the asymptotic risk over the class of URS dependence structures. On the other hand, Corollary 4.24 provides a uniform lower bound for the asymptotic risk over all dependence structures, which may not be tight except in the case of independent errors.

Proof of Corollary 4.24. Relation (4.45) is a re-statement of Remark 4.4.

For any distribution π (with a slight abuse of notation) over the parameter space $\Theta_p^+ \times D(F)$, we have

$$\liminf_{p \rightarrow \infty} \inf_{\widehat{S}_p} \sup_{\substack{\mu \in \Theta_p^+(\beta, \underline{r}) \\ \mathcal{E} \in D(F)}} \mathbb{P}(\widehat{S}_p \neq S_p) \geq \liminf_{p \rightarrow \infty} \inf_{\widehat{S}_p} \mathbb{E}_\pi \mathbb{P}(\widehat{S}_p \neq S_p), \quad (4.47)$$

since the supremum is bounded from below by expectations. In particular, define π to be

the uniform distribution over the configurations $\Theta_p^* \times I(f)$, where

$$\begin{aligned} \Theta_p^* = \{ \mu \in \mathbb{R}^d : |S_p| = \lfloor p^{1-\beta} \rfloor, \mu(i) = 0 \text{ for all } i \notin S, \text{ and} \\ \mu(i) = (\nu r \log p)^{1/\nu} \text{ for all } i \in S, \text{ where } \underline{r} < r < g(\beta) \}, \end{aligned}$$

and

$$I(f) = \{ \mathcal{E} = (\epsilon_p(i))_p : \epsilon_p(i) \text{ iid with density } f(x) \propto \exp\{-|x|^\nu/\nu\} \}.$$

Since the density f of F is log-concave, the distribution of the signal configurations satisfies the conditions in Theorem 4.23. Thus, the desired conclusion (4.46) follows from Theorem 4.23 and (4.47). \square

4.2.5 Bayes optimality of likelihood ratio thresholding

The following result provides the general form of finite-sample Bayes optimal procedures. It turns out that in general, *likelihood ratio thresholding* is optimal.

Proposition 4.27. *Let the observations $x(i)$, $i = 1, \dots, p$ have s signals as prescribed in (4.38) having common density f_a , and let the rest $(p - s)$ locations have common density f_0 . Define the likelihood ratios*

$$L(i) := f_a(x(i))/f_0(x(i)),$$

and let $L_{[1]} \geq L_{[2]} \geq \dots \geq L_{[p]}$ be the order statistics of the $L(i)$'s. Then the procedure $\hat{S}_{opt} = \{i \mid L(i) \geq L_{[s]}\}$ is finite-sample optimal in terms of Bayes risk. That is,

$$\hat{S}_{opt} \in \arg \min_{\hat{S}} \mathbb{E}_\pi \mathbb{P}[\hat{S} \neq S]. \quad (4.48)$$

for all s and p , where the infimum on \hat{S}_p is taken over all procedures.

The proof of Proposition 4.27 is found in Section 4.5.

The characterization of optimal likelihood ratio thresholding procedures in Proposition 4.27 may not always yield practical estimators, as the density of alternatives, and number of signals are typically unknown. Still, some insights can be gained by virtue of Proposition 4.27. In particular, when MLR fails (or equivalently, when the errors in model (1.1) do not have log-concave densities), data thresholding is sub-optimal.

Example 4.28 (Sub-optimality of data thresholding). Let the errors have iid generalized Gaussian density with $\nu = 1/2$, i.e., $\log f_0(x) \propto -x^{1/2}$. Let dimension $p = 2$, sparsity $s = 1$ with uniform prior, and signal size $\delta = 1$. That is, $\mathbb{P}[\mu = (0, 1)^T] = \mathbb{P}[\mu = (1, 0)^T] = 1/2$. If the observations take on values $x = (x_1, x_2)^T = (1, 2)^T$, we see from a comparison of the likelihoods (and hence, the posteriors),

$$\log \frac{f(x|\{1\})}{f(x|\{2\})} = 2x_1^{1/2} + 2(x_2 - 1)^{1/2} - 2x_2^{1/2} - 2(x_1 - 1)^{1/2} = 4 - 2\sqrt{2} > 0,$$

that even though $x_1 < x_2$, the set $\{1\}$ is a better estimate of support than $\{2\}$, i.e., $\mathbb{P}[S = \{1\} \mid x] > \mathbb{P}[S = \{2\} \mid x]$.

This simple example shows that, in the case when the errors have super-exponential tails, the optimal procedures are in general *not* data thresholding. A slightly more general conclusion can be found in Corollary 4.39.

Remark 4.29. Consider the model (1.1) with independent errors, Proposition 4.27, and indeed, Example 4.28 demonstrate that thresholding procedures are in fact *sub-optimal* for $\text{AGG}(\nu)$ models with $\nu < 1$. Therefore, the optimality of thresholding procedures (specifically, Bonferroni's procedure) only applies to $\text{AGG}(\nu)$ models with $\nu \geq 1$.

If we restrict the space of methods to only thresholding procedures, then results in Section 4.2.1 state that the phase transition phenomenon — the 0-1 law in the sense of Corollary 4.14 — is universal in all error models with rapidly varying tails. This includes $\text{AGG}(\nu)$ models *for all* $\nu > 0$. In contrast, models with heavy (regularly varying) tailed errors do not exhibit this phenomenon (see Theorem 4.34). We summarize the properties

of thresholding procedures in Table 4.1.

Table 4.1: Properties of thresholding procedures under different error distributions when errors are independent. Properties of the error distributions are listed in brackets.

Thresholding procedure (Error distributions)	Bayes optimality (Log-concave density)	Phase transition (Rapidly-varying tails)
AGG(ν), $\nu \geq 1$	Yes (Yes)	Yes (Yes)
AGG(ν), $0 < \nu < 1$	No (No)	Yes (Yes)
Power laws	No (No)	No (No)

4.3 Strong classification boundaries in other light-tailed error models

The strong classification boundaries extend beyond the AGG models. As our analysis in Section 4.1 suggests, all additive error models where the errors have URS maxima demonstrate this phase transition phenomenon under appropriate parametrization of the sparsity and signal sizes. We derive explicit boundaries for two additional classes of models under the general form of the additive noise models (1.1), with heavier and lighter tails than the AGG models, respectively.

We would like to point out that the sparsity and signal sizes can be re-parametrized for the boundaries to have different shapes. For example in the case of Gaussian errors, if we re-parametrize sparsity s with $\tilde{\beta} = 2 - (1 + \sqrt{1 - \beta})^2$ where $\tilde{\beta} \in (0, 1)$, then the signal sparsity would have a slightly more complicated form:

$$|S_p| = \lfloor p^{1-\beta} \rfloor = \left\lfloor p \left(\sqrt{2-\tilde{\beta}} - 1 \right)^2 \right\rfloor,$$

while the strong classification boundary would take on the simpler form:

$$g(\beta) = \tilde{g}(\tilde{\beta}) = 2 - \tilde{\beta}. \quad (4.49)$$

In the next two classes of models we will adopt parametrizations such that the boundaries are of the form \tilde{g} in (4.49).

4.3.1 Additive error models with heavier-than-AGG tails

Distributions such as the log-normal have heavier tails than the AGG model, yet the tails are nevertheless rapidly-varying. Therefore, Proposition 2.11 applies, and we expect to see phase-transition-type results when the additive errors have these heavier-than-AGG tails.

Example 4.30 (Heavier than AGG). Let $\gamma > 1$, $c > 0$, and suppose that

$$\log \overline{F}(x) = -(\log x)^\gamma (c + M(x)), \quad (4.50)$$

where $\lim_{x \rightarrow \infty} M(x) \log^\gamma x = 0$. Then, Relation (2.38) holds under model (4.50). Further, if the entries in the array are independent, the maxima are relatively stable.

The behavior of the quantiles u_p in this model is as follows. As $p \rightarrow \infty$,

$$u_p \sim \exp \left\{ (c^{-1} \log p)^{1/\gamma} \right\} \iff c (\log u_p)^\gamma + o(1) = \log(p) = -\log \overline{F}(u_p).$$

since u_p diverges, and $M(u_p)$ is $o((\log^\gamma u_p)^{-1})$.

Following Example 4.30, assume that the errors in Model (1.1) have rapidly varying right tails

$$\log \overline{F}(x) = -(\log x)^\gamma (c + M(x)), \quad (4.51)$$

as $x \rightarrow \infty$, and left tails

$$\log F(x) = -(\log(-x))^\gamma (c + M(-x)), \quad (4.52)$$

as $x \rightarrow -\infty$.

Theorem 4.31. *Suppose the marginals F follows (4.51) and (4.52). Let*

$$k(\beta) = \log p - ((\log p)^{1/\gamma} + \log(1 - \beta))^\gamma,$$

and let the signal μ have

$$|S_p| = \lfloor pe^{-k(\beta)} \rfloor$$

non-zero entries. Assume the magnitudes of non-zero signal entries are in the range between

$$\underline{\Delta} = \exp\{(\log p)^{1/\gamma}\}\underline{r} \quad \text{and} \quad \overline{\Delta} = \exp\{(\log p)^{1/\gamma}\}\bar{r}.$$

If $\underline{r} > \tilde{g}(\beta) = 2 - \beta$, then Bonferroni's procedure \hat{S}_p (defined in (2.20)) with appropriately calibrated FWER $\alpha \rightarrow 0$ achieves asymptotic perfect support recovery, under arbitrary dependence of the errors.

On the other hand, when the errors are uniformly relatively stable, if $\bar{r} < \tilde{g}(\beta) = 2 - \beta$, then no thresholding procedure can achieve asymptotic perfect support recovery with positive probability.

4.3.2 Additive error models with lighter-than-AGG tails

Similar to how Proposition 2.11 applies to models with heavier-than-AGG tails, it also to error models with lighter tails than the AGG class.

Example 4.32 (Lighter than AGG). With $\nu > 0$, and $L(x)$ a slowly varying function, the class of distributions

$$\log \overline{F}(x) = -\exp\{x^\nu L(x)\}, \tag{4.53}$$

is rapidly varying. The quantiles can be derived explicitly in a subclass of (4.53) where $L(x) \rightarrow 1$, or equivalently, when $\log |\log \overline{F}(x)| \sim x^\nu$,

$$u_p \sim (\log \log p)^{1/\nu} \iff \exp\{u_p^\nu (1 + o(1))\} = \log(p) = -\log \overline{F}(u_p).$$

Following Example 4.32, assume that errors in Model (1.1) has rapidly varying right tails

$$\log \overline{F}(x) = -\exp \{x^\nu L(x)\}, \quad (4.54)$$

where $L(x)$ is a slowly varying function, as $x \rightarrow \infty$, and left tails

$$\log \overline{F}(x) = -\exp \{-x^\nu L(-x)\}, \quad (4.55)$$

as $x \rightarrow -\infty$.

The phase transition results in multiple testing problems under such tail assumptions is characterizes as follows.

Theorem 4.33. *Suppose marginals F follow (4.54) and (4.55). Let*

$$k(\beta) = \log p - (\log(p))^{(1-\beta)^\nu},$$

and let the signal μ have

$$|S_p| = \lfloor pe^{-k(\beta)} \rfloor$$

non-zero entries. Assume the magnitudes of non-zero signal entries are in the range between

$$\underline{\Delta} = \log \log p^{1/\nu} \underline{r} \quad \text{and} \quad \overline{\Delta} = \log \log p^{1/\nu} \overline{r}.$$

If $\underline{r} > \widetilde{g}(\beta) = 2 - \beta$, then Bonferroni's procedure \widehat{S}_p (defined in (2.20)) with appropriately calibrated FWER $\alpha \rightarrow 0$ achieves asymptotic perfect support recovery, under arbitrary dependence of the errors.

On the other hand, when the errors are uniformly relatively stable, if $\overline{r} < \widetilde{g}(\beta) = 2 - \beta$, then no thresholding procedure can achieve asymptotic perfect support recovery with positive probability.

4.4 Thresholding procedures under heavy-tailed errors

We analyze the performance of thresholding estimators under heavy-tailed models in this section, and illustrate its lack of phase transition. Suppose we have iid errors with Pareto tails in Model (1.1), that is, $\epsilon(i)$'s have common marginal distribution F where

$$\overline{F}(x) \sim x^{-\alpha} \quad \text{and} \quad F(-x) \sim x^{-\alpha}, \quad (4.56)$$

as $x \rightarrow \infty$. It is well-known (see, e.g., Theorem 1.6.2 of (Leadbetter et al., 2012)) that the maxima of iid Pareto random variables have Frechet-type limits. Specifically, we have

$$\frac{\max_{i \in \{1, \dots, p\}} \epsilon(i)}{u_p} \implies Y, \quad (4.57)$$

in distribution, where $u_p = F^{\leftarrow}(1 - 1/p) \sim p^{1/\alpha}$, and Y is a standard α -Frechet random variable, i.e.,

$$\mathbb{P}[Y \leq t] = \exp\{-t^{-\alpha}\}, \quad t > 0.$$

By symmetry in our assumptions, the same argument applies to the minima as well.

Theorem 4.34. *Let errors in Model (1.1) be as described in Relation (4.56). Let the signal have $s = |S| = fp$ non-zero entries, with magnitude $\Delta = rp^{1/\alpha}$, where both $f \in (0, 1)$ and $r \in (0, +\infty)$ may depend on p , so that no generality is lost.*

Under these assumptions, the necessary condition for thresholding procedures \widehat{S} to achieve exact support recovery ($\mathbb{P}[\widehat{S} = S] \rightarrow 1$) is

$$\liminf_{p \rightarrow \infty} r = \infty. \quad (4.58)$$

Condition (4.58) is also sufficient for the oracle thresholding procedure to succeed in the exact support recovery problem.

On the other hand, the necessary and sufficient condition for all thresholding proce-

dures to fail exact support recovery ($\mathbb{P}[\widehat{S} = S] \rightarrow 0$) is

$$\limsup_{p \rightarrow \infty} r = 0.$$

In other words, Theorem 4.34 states that there does not exist a non-trivial phase transition for thresholding procedures when errors have (two-sided) α -Pareto tails.

Proof of Theorem 4.34. Recall the oracle thresholding procedure $\widehat{S}^* = \{i : x(i) \geq x_{[s]}\}$, and the set of all thresholding procedures, denoted \mathcal{S} (see Definition 2.19). The probability of exact support recovery by any thresholding procedure $\widehat{S} \in \mathcal{S}$ is bounded above by that of \widehat{S}^* , that is,

$$\begin{aligned} \max_{\widehat{S} \in \mathcal{S}} \mathbb{P}[\widehat{S} = S] &= \mathbb{P}[\widehat{S}^* = S] = \mathbb{P}\left[\max_{i \in S^c} x(i) \leq \min_{i \in S} x(i)\right] \\ &= \mathbb{P}\left[\frac{\max_{i \in S^c} x(i)}{u_p} \leq \frac{\min_{i \in S} x(i)}{u_p}\right] \\ &= \mathbb{P}\left[\frac{M_{S^c}}{u_p} \leq \frac{m_S}{u_p} + r_p\right], \end{aligned} \quad (4.59)$$

where $M_{S^c} = \max_{i \in S^c} \epsilon(i)$ and $m_S = \min_{i \in S} \epsilon(i)$. For any $\alpha > 0$, the following elementary relations hold,

$$0 < L \leq (1 - f)^{1/\alpha} + f^{1/\alpha} \leq U < \infty, \quad \text{for all } f \in (0, 1),$$

where $L = \min \{1, 2(1/2)^{1/\alpha}\}$ and $U = \max \{1, 2(1/2)^{1/\alpha}\}$. Therefore we have,

$$U \max \left\{ \frac{M_{S^c}}{u_p}, -\frac{m_S}{u_p} \right\} < r_p \implies (1 - f)^{1/\alpha} \frac{M_{S^c}}{u_p} - f^{1/\alpha} \frac{m_S}{u_p} < r_p, \quad (4.60)$$

and

$$L \min \left\{ \frac{M_{S^c}}{u_p}, -\frac{m_S}{u_p} \right\} < r_p \iff (1 - f)^{1/\alpha} \frac{M_{S^c}}{u_p} - f^{1/\alpha} \frac{m_S}{u_p} < r_p. \quad (4.61)$$

Putting together (4.59), (4.60), and (4.61), we have

$$\mathbb{P}\left[\max\left\{\frac{M_{S^c}}{u_p}, -\frac{m_S}{u_p}\right\} < r_p/U\right] \leq \mathbb{P}[\widehat{S}^* = S] \leq \mathbb{P}\left[\min\left\{\frac{M_{S^c}}{u_p}, -\frac{m_S}{u_p}\right\} < r_p/L\right]. \quad (4.62)$$

We know from the weak convergence result (4.57) that for any $\epsilon > 0$ there is a constant N such that for all $p > N$ we have

$$\mathbb{P}\left[\max\left\{\frac{M_{S^c}}{u_p}, -\frac{m_S}{u_p}\right\} < r_p/U\right] \geq \mathbb{P}\left[\max\{Y^{(1)}, Y^{(2)}\} < r_p/U\right] - \epsilon, \quad (4.63)$$

where $Y^{(1)}$ and $Y^{(2)}$ are independent α -Frechet random variables with scale coefficients $(1-f)^{1/\alpha}$ and $f^{1/\alpha}$ respectively. That is,

$$\mathbb{P}[Y^{(1)} \leq t] = \exp\{-(1-f)/t^\alpha\}, \quad \text{and} \quad \mathbb{P}[Y^{(2)} \leq t] = \exp\{-f/t^\alpha\}.$$

Since the distributional limit in (4.63) has a density (with respect to the Lebesgue measure), we know that density is bounded above by a finite constant, say, K . For the same choice of ϵ as before, we can find a further constant N' such that for all $p > \max\{N, N'\}$ we have

$$\liminf r_p < \epsilon/K + r_p,$$

so that the right hand side of (4.63) is bounded by

$$\mathbb{P}\left[\max\{Y^{(1)}, Y^{(2)}\} < r_p/U\right] - \epsilon \geq \mathbb{P}\left[\max\{Y^{(1)}, Y^{(2)}\} < \frac{\liminf r_p}{U}\right] - 2\epsilon. \quad (4.64)$$

By the arbitrariness in the choice of ϵ , we conclude from (4.63) and (4.64) that

$$\liminf \mathbb{P}\left[\max\left\{\frac{M_{S^c}}{u_p}, -\frac{m_S}{u_p}\right\} < r_p/U\right] \geq \mathbb{P}\left[\max\{Y^{(1)}, Y^{(2)}\} < \frac{\liminf r_p}{U}\right]. \quad (4.65)$$

Combining Relations (4.62) and (4.65), we know that if $\liminf r_p = \infty$, we must have

$$\liminf \mathbb{P} \left[\hat{S}^* = S \right] \geq \mathbb{P} \left[\max \{Y^{(1)}, Y^{(2)}\} < \frac{\liminf r_p}{U} \right] = 1.$$

Conversely, if $\liminf \mathbb{P} \left[\hat{S}^* = S \right] < 1$, we must have $\liminf r_p < \infty$.

Similarly, we can obtain the upper bound of exact support recovery probability for the optimal thresholding procedure,

$$\limsup \mathbb{P} \left[\min \left\{ \frac{M_{S^c}}{u_p}, -\frac{m_S}{u_p} \right\} < r_p/L \right] \leq \mathbb{P} \left[\min \{Y^{(1)}, Y^{(2)}\} < \frac{\limsup r_p}{L} \right]. \quad (4.66)$$

The conclusions of the second part of Theorem 4.34 follow from (4.62) and (4.66). \square

The probability of exact recovery can be approximated if the parameters r and f converge. The next result follows from a small modification of the arguments in the proof of Theorem 4.34.

Corollary 4.35. *Under the assumptions in Theorem 4.34, if $\lim r = r^*$, and $\lim f = f^*$, for some constant $r^* \geq 0$ and $f^* \in [0, 1]$, then*

$$\lim \mathbb{P}[\hat{S}^* = S] = \mathbb{P} \left[(1 - f^*)^{1/\alpha} Z_1 + (f^*)^{1/\alpha} Z_2 < r^* \right].$$

where Z_1 and Z_2 are independent standard α -Frechet random variables, i.e., $\mathbb{P}[Z_i \leq t] = \exp \{-t^{-\alpha}\}$, $x > 0$.

Remark 4.36. Of course one might wonder if it would be meaningful to derive a “phase transition” under a different parametrization of the signal sizes, say

$$\Delta = p^{r/\alpha}. \quad (4.67)$$

In this case, Theorem 4.34 suggests that a “phase transition” takes place at $r = 1$. However, this non-multiplicative parametrization of the signal sizes would make power analysis (like

in Example 3.8) dimension-dependent.

To illustrate, in the case of Gaussian errors with variance 1, if we were interested in small signals of size $\sqrt{2r \log p}$, where $r < 1$ is below the boundary (4.5), then we only need $n > 2/r$ samples to guarantee discovery of their support. In the Pareto case with parametrization (4.67), however, if we were interested in small signals of size $p^{r/\alpha}$, where $r < 1$, then the “boundary” says that we will need $n > p^{2(1-r)/\alpha}$ samples, which is exponential in the dimension p and quickly diverges. Recall that the “boundary” is really an asymptotic result in p . Such an approximation in finite dimensions becomes invalid.

4.5 Additional proofs

4.5.1 Proof of the claims in Examples 4.3 and 4.10

Proof of claims in Example 4.3. By the Mill’s ratio for the standard Gaussian distribution,

$$\frac{t_p \mathbb{P}[Z > t_p]}{\phi(t_p)} \rightarrow 1, \quad \text{as } t_p \rightarrow \infty,$$

where $Z \sim \mathcal{N}(0, 1)$. Using the expression for $t_p = \sqrt{2 \log p}$, we have

$$p \mathbb{P}[Z > t_p] \sim \sqrt{2\pi}^{-1} (2 \log p)^{-1/2} \rightarrow 0,$$

as desired. The rest of the claims follow from Corollary 4.2. □

Proof of claims in Example 4.10. In the first scenario, signal sizes in $S_p^{(1)}$ are by definition above the strong classification boundary (4.5). The signal in $S_p^{(2)}$ has size parameter $1 + \delta < 2 - \beta < (1 + \sqrt{1 - \beta})^2$, and therefore falls below the boundary.

It remains to show that $\mathbb{P}[\widehat{S}_p^{\text{Bonf}} = S_p] \rightarrow 1$. To do so, we define two new arrays

$$\mathcal{Y}^{(k)} = \{y_p^{(k)}(j), j = 1, 2, \dots, p\}, \quad k \in \{1, 2\}_p,$$

where $y_p^{(k)}(j) = x_p(j)$ if $j \notin S_p^{(k)}$, and $y_p^{(k)}(j) = \tilde{\epsilon}_p(j)$ if $j \in S_p^{(k)}$, using an independent error array $\{\tilde{\epsilon}_p(j), j = 1, \dots, p\}$ with iid standard Gaussian elements. That is, we replace the elements in $S_p^{(1)}$ and $S_p^{(2)}$ with iid standard Gaussian noise. Notice both arrays $\mathcal{Y}^{(1)}$ and $\mathcal{Y}^{(2)}$ satisfy the conditions in Theorem 4.1 (with sparsity parameter equal to β and 1, respectively). Hence, we have

$$\mathbb{P}[\widehat{S}_p^{\text{Bonf}} \subseteq S_p] = \mathbb{P}\left[\max_{j \in S^c} x(j) \leq t_p\right] \leq \mathbb{P}\left[\max_{j \in S^c} y^{(1)}(j) \leq t_p\right] \rightarrow 0,$$

and

$$\begin{aligned} \mathbb{P}[\widehat{S}_p^{\text{Bonf}} \supseteq S_p] &= \mathbb{P}\left[\min_{j \in S} x(j) > t_p\right] \geq 1 - \mathbb{P}\left[\min_{j \in S^{(1)}} x(j) \leq t_p\right] - \mathbb{P}\left[\min_{j \in S^{(2)}} x(j) \leq t_p\right] \\ &\geq 1 - \mathbb{P}\left[\min_{j \in S^{(1)}} y_p^{(2)}(j) \leq t_p\right] - \mathbb{P}\left[\min_{j \in S^{(2)}} y_p^{(1)}(j) \leq t_p\right] \rightarrow 1, \end{aligned}$$

where t_p is the threshold in Bonferroni's procedure. The conclusion follows.

In the second scenario, the signal sizes in $S^{(2)}$ by definition falls below the strong classification boundary (4.5). To see that no thresholding procedure succeeds, we adapt the proof of Theorem 4.8. In particular, we obtain

$$\mathbb{P}[\widehat{S}_p = S_p] \leq \mathbb{P}\left[\max_{j \in S^c} x(j) \leq t_p < \min_{j \in S} x(j)\right] \leq \mathbb{P}\left[\max_{j \in S^c} x(j) < \min_{j \in S^{(2)}} x(j)\right].$$

By the assumption that signals in $S^{(2)}$ have size parameter $(1 - \delta)g(\beta)$, we have

$$\mathbb{P}\left[\max_{j \in S^c} x(j) < \min_{j \in S^{(2)}} x(j)\right] = \mathbb{P}\left[\frac{M_{S^c}}{u_p} < \frac{\sqrt{2(1 - \delta)g(\beta) \log p} - m_{S^{(2)}}}{u_p}\right], \quad (4.68)$$

where $M_{S^c} = \max_{j \in S^c} \epsilon(j)$ and $m_{S^{(2)}} = \max_{j \in S^{(2)}} (-\epsilon(j))$. The ratio on the left-hand-side of the inequality converges to 1 as in (4.28) in the main text, whereas the term on the

right-hand-side

$$\begin{aligned} \frac{\sqrt{2(1-\delta)g(\beta)\log p} - m_{S^{(2)}}}{u_p} &= \sqrt{(1-\delta)g(\beta)} - \frac{m_{S^{(2)}}}{u_{|S^{(2)}|}} \frac{u_{|S^{(2)}|}}{u_p} \\ &\stackrel{\mathbb{P}}{\rightarrow} \sqrt{(1-\delta)} + \sqrt{1-\beta}(\sqrt{(1-\delta)} - 1) < 1. \end{aligned}$$

where we used the URS of the error arrays, and that

$$u_{|S^{(2)}|} \sim \sqrt{2 \log(p^{1-\beta}/2)} = \sqrt{2((1-\beta)\log p - \log 2)} \sim \sqrt{2(1-\beta)\log p}.$$

to conclude the convergence in probability. \square

4.5.2 Proofs of Propositions 4.19 and 4.27

Proof of Proposition 4.19. The problem of support recovery can be equivalently stated as a classification problem, where the discrete parameter space is $\mathcal{S} = \{S \subseteq \{1, \dots, p\} : |S| = s\}$, and the observation $x \in \mathbb{R}^p$ has likelihood $f(x|S)$ indexed by the support set S .

By the optimality of the Bayes classifier (see, e.g., (Domingos and Pazzani, 1997)), a set estimator that maximizes the probability of support recovery is such that

$$\hat{S} \in \arg \max_{S \in \mathcal{S}} f(x|S)\pi(S).$$

Since we know from (4.39) that $\pi(S)$ is uniform, the problem in our context reduces to showing that $f(x|\hat{S}^*) = f(x|\hat{S})$, where $f(x|S)$ is the conditional distribution of data given the unordered support S ,

$$f(x|S) = \sum_{P \in \sigma(S)} f(x|P) \pi^{\text{ord}}(P|S) = \frac{1}{s!} \left(\sum_{P \in \sigma(S)} \prod_{i=1}^s f_i(x(P(i))) \right) \prod_{k \notin S} f_0(x(k)),$$

where $\sigma(S)$ is the set of all permutations of the indices in the support set S .

Suppose $\widehat{S} \neq \widehat{S}^*$, then there must be indices $j \in \widehat{S}$ and $j' \in \widehat{S}^c$ such that $x(j) \leq x(j')$. We exchange the labels of $x(j)$ and $x(j')$, and form a new estimate $\widehat{S}' = (\widehat{S} \setminus \{j\}) \cup \{j'\}$. Comparing the likelihoods under \widehat{S} and \widehat{S}' , we have

$$\begin{aligned}
f(x|\widehat{S}) - f(x|\widehat{S}') &= \frac{1}{s!} \sum_{P \in \sigma(\widehat{S})} \prod_{i=1}^s f_i(x(P(i))) f_0(x(j')) \prod_{k \notin \widehat{S} \cup \{j'\}} f_0(x(k)) - \\
&\quad - \frac{1}{s!} \sum_{P' \in \sigma(\widehat{S}')} \prod_{i=1}^s f_i(x(P'(i))) f_0(x(j)) \prod_{k \notin \widehat{S}' \cup \{j\}} f_0(x(k)) \\
&= \frac{1}{s!} \left(\sum_{i=1}^s a_i \left(f_i(x(j)) f_0(x(j')) - f_i(x(j')) f_0(x(j)) \right) \right) \prod_{k \notin \widehat{S} \cup \{j'\}} f_0(x(k)),
\end{aligned} \tag{4.69}$$

where the last equality follows by first summing over all permutations fixing $P(i) = j$ and $P'(i) = j'$, and setting $a_i = \sum_{P \in \sigma(\widehat{S} \setminus \{j\})} \prod_{i' \neq i} f_{i'}(x(P(i')))$. Notice that the a_i 's are non-negative.

Since $x(j) \leq x(j')$, and that each of $\{f_0, f_i\}$ is an MLR family, we have

$$\frac{f_i(x(j))}{f_0(x(j))} - \frac{f_i(x(j'))}{f_0(x(j'))} \leq 0 \implies f_i(x(j)) f_0(x(j')) - f_i(x(j')) f_0(x(j)) \leq 0.$$

Using Relation (4.69), we conclude that $f(x|\widehat{S}) \leq f(x|\widehat{S}')$. This implies that any estimator that is not \widehat{S}^* may be improved, and the optimality follows. \square

Lemma 4.37. *Let ϕ be any concave function on \mathbb{R} . For any $x < y \in \mathbb{R}$, and $\delta > 0$ we have*

$$\phi(x) + \phi(y + \delta) \leq \phi(y) + \phi(x + \delta).$$

Proof of Lemma 4.37. Pick $\lambda = \delta/(y - x + \delta)$, by concavity of f we have

$$\lambda \phi(x) + (1 - \lambda) \phi(y + \delta) \leq \phi(\lambda x + (1 - \lambda)(y + \delta)) = \phi(y), \tag{4.70}$$

and

$$(1 - \lambda)\phi(x) + \lambda\phi(y + \delta) \leq \phi((1 - \lambda)x + \lambda(y + \delta)) = \phi(x + \delta). \quad (4.71)$$

Summing up (4.70) and (4.71) and we arrive at the conclusion as desired. \square

Proof of Proposition 4.27. The proof is entirely analogous to that of Proposition 4.19. Since we know from (4.39) that $\pi(S)$ is uniform, the problem reduces to showing that $f(x|\hat{S}_{\text{opt}}) = f(x|\hat{S})$, where

$$\hat{S} \in \arg \max_{S \in \mathcal{S}} f(x|S)\pi(S).$$

and $f(x|S)$ is the conditional distribution of data given the unordered support S ,

$$f(x|S) = \sum_P f(x|P)\pi^{\text{ord}}(P|S) = \prod_{j \in S} f_a(x(j)) \prod_{j \notin S} f_0(x(j)). \quad (4.72)$$

Suppose $\hat{S} \neq \hat{S}_{\text{opt}}$, then there must be indices $j \in \hat{S}$ and $j' \in \hat{S}^c$ such that $L(j) \leq L(j')$. If we exchange the labels of $L(j)$ and $L(j')$, that is, we form a new estimate $\hat{S}' = (\hat{S} \setminus \{j\}) \cup \{j'\}$, comparing the log-likelihoods under \hat{S} and \hat{S}' , we have

$$\log f(x|\hat{S}) - \log f(x|\hat{S}') = \log f_a(x(j)) + \log f_0(x(j')) - \log f_a(x(j')) - \log f_0(x(j)).$$

By the definition of $L(j)$'s, and the order relations, we obtain

$$\log f(x|\hat{S}) - \log f(x|\hat{S}') = \log L(j) - \log L(j') \leq 0$$

This implies that any estimator that is not \hat{S}_{opt} may be improved, and the optimality follows. \square

Remark 4.38. In the non-log-concave setting, where we know that thresholding procedures are suboptimal, likelihood thresholding procedures are promising, thanks to Proposition 4.27. However, in the case where signals have difference sizes, likelihood thresholding

procedures are undefined; in such settings, existence of an optimal procedure is an open problem.

Indeed, in the proof of Proposition 4.27, identical the signal densities are needed so that the relation (4.72) holds.

4.5.3 Sub-optimality of data thresholding procedures

We provide a slightly more general result on the sub-optimality of data thresholding procedures.

Corollary 4.39. *Consider the additive error model (1.1). Let the errors ϵ be independent with common distribution F . Let each of the s signals be located on $\{1, \dots, p\}$ uniformly at random with equal magnitude $0 < \delta < \infty$. If errors ϵ are iid with density f log-convex on $[K, +\infty)$, then whenever $j \in \hat{S}_{opt}$ for some $x(j) > K + \delta$, we must have $j' \in \hat{S}_{opt}$ for all j' such that $K + \delta \leq x(j') < x(j)$.*

Specifically, if there are m observations exceeding $K + \delta_s$, with $m > s$, then the top $m - s$ observations will *not* be included in the optimal estimator \hat{S}_{opt} . This shows that, in the case when the errors have super-exponential tails, the optimal procedures are in general *not* data thresholding.

Proof of Corollary 4.39. Since the alternative $f_a(t) = f(t - \delta)$ are log-convex on $[K + \delta, \infty)$, by Relation (4.43) in the proof of Lemma 4.20 and appealing to log-convexity (rather than log-concavity), the likelihood ratio

$$L(j) := \frac{f_a(x(j))}{f_0(x(j))}$$

is decreasing in $x(j)$ on $[K + \delta, \infty)$. The proof is complete by applying Proposition 4.27.

□

CHAPTER 5

Characterization of Uniform Relative Stability for Gaussian Arrays

In this chapter, we establish a complete characterization of URS for Gaussian arrays in terms of a simple condition on the covariance structures. The condition is as follows.

Definition 5.1 (Uniformly decreasing dependence (UDD)). Consider a triangular array of jointly Gaussian distributed errors $\mathcal{E} = \{(\epsilon_p(i))_{i=1}^p, p = 1, 2, \dots\}$ with unit variances,

$$\epsilon_p \sim N(0, \Sigma_p), \quad p = 1, 2, \dots$$

The array \mathcal{E} is said to be uniform decreasingly dependent (UDD) if for every $\delta > 0$ there exists a finite $N(\delta) < \infty$, such that for every $i \in \{1, \dots, p\}$, and $p \in \mathbb{N}$, we have

$$\left| \{k \in \{1, \dots, p\} : \Sigma_p(i, k) > \delta\} \right| \leq N(\delta) \quad \text{for all } \delta > 0. \quad (5.1)$$

That is, for every coordinate i , the number of elements which are more than δ -correlated with $\epsilon_p(i)$ does not exceed $N(\delta)$.

Note that the bound in (5.1) holds uniformly in i and p , and only depends on δ . Also observe that on the left-hand side of (5.1), we merely count in each row of Σ_p the number of exceedances of covariances (not their absolute values!) over level δ .

Remark 5.2. Without loss of generality, we may require that $N(\delta)$ be a monotone non-increasing function of δ , for we can take

$$N(\delta) = \sup_{p,i} \left| \{k : \Sigma_p(i, k) > \delta\} \right|,$$

which is non-increasing in δ . Definition 5.1 therefore states that the array is UDD when $N(\delta) < \infty$ for all $\delta > 0$.

Observe that the UDD condition does not depend on the order of the coordinates in the error vector $\epsilon_p = (\epsilon_p(i))_{i=1}^p$. Often times, however, the errors are thought of coming from a stochastic process indexed by time or space. To illustrate the generality of the UDD condition, we formulate next a simple sufficient condition (UDD') that is easier to check in a time-series context.

Definition 5.3 (UDD'). For $\epsilon_p \sim N(0, \Sigma_p)$ with unit variances, an array $\mathcal{E} = (\epsilon_p(i))_{i=1}^p$ is said to satisfy the UDD' condition if there exist:

- (i) permutations $l = l_p$ of $\{1, \dots, p\}$, for all $p \in \mathbb{N}$, and
- (ii) a non-negative sequence $(r_n)_{n=1}^\infty$ converging to zero $r_n \rightarrow 0$, as $n \rightarrow \infty$,

such that

$$\sup_{p \in \mathbb{N}} |\Sigma_p(i', j')| \leq r_{|i-j|}. \quad (5.2)$$

where $i' = l(i)$, $j' = l(j)$, for all $i, j \in \{1, \dots, p\}$.

Remark 5.4. Without loss of generality, we may also require that r_n be non-increasing in n , for we can replace r_n with the non-increasing sequence $r'_n = \sup_{m \geq n} r_m$.

Proposition 5.5. *UDD' implies UDD.*

Proof. Since $r_n \rightarrow 0$, for any $\delta > 0$, there exists an integer $M = M(\delta) < \infty$ such that $r_n \leq \delta$, for all $n \geq M$. Thus, by (5.2), for every fixed $j' \in \{1, \dots, p\}$, we can have

$|\text{Cov}(\epsilon_p(k'), \epsilon_p(j'))| > \delta$, only if k' belongs to the set:

$$\{k' \in \{1, \dots, p\} : j - M \leq k := l_p^{-1}(k') \leq j + M\},$$

where $j := l_p^{-1}(j')$. That is, there are at most $2M + 1 < \infty$ indices $k' \in \{1, \dots, p\}$, whose covariances with $\epsilon(j')$ may exceed δ . Since this holds uniformly in $j' \in \{1, \dots, p\}$, Condition UDD follows with $N(\delta) = 2M + 1$. \square

We now state the main result of this section: a Gaussian sequence is URS if and only if it is UDD. The URS condition essentially requires that the dependencies decay in a uniform fashion, the rate at which dependence decay does *not* matter.

Theorem 5.6. *Let \mathcal{E} be a Gaussian triangular array with standard normal marginals. The array \mathcal{E} has uniformly relatively stable (URS) maxima if and only if it is uniformly decreasing dependent (UDD).*

Specifically, for stationary Gaussian arrays, we have the following corollary.

Corollary 5.7. *Let $\mathcal{E} = \{\epsilon_p(i) = Z(i)\}$ for a stationary Gaussian time series $\mathcal{Z} = \{Z(i)\}$. Then \mathcal{E} is URS if and only if the autocovariance function $\text{Cov}(Z(k), Z(0)) \rightarrow 0$, as $k \rightarrow \infty$.*

Corollary 5.7 follows by Theorem 5.6 and the observation that UDD is equivalent to vanishing autocovariance of \mathcal{Z} . A slightly weaker form of the “if” part was established in Theorem 3 of Berman (1964).

Returning again to the study of support recovery problems, Theorem 5.6 and the necessary condition for exact support recovery in Theorem 4.8 yields the following result.

Corollary 5.8. *For UDD Gaussian errors, the result in Theorem 4.8 holds.*

As a counterpart to Remark 4.11, we demonstrate the tightness of the dependence conditions in Theorem 4.8. Specifically, we demonstrate that if the URS dependence condition is violated, then it may be possible to recover the support of weaker signals below the boundary.

Example 5.9. Suppose $\mathcal{E} = (\epsilon_p(i))_{i=1}^p$ is Gaussian, and is comprised of $\lfloor p^{1-\beta} \rfloor$ blocks, each of size at least $\lfloor p^\beta \rfloor$; let the elements of each block have correlation 1, and let elements from different blocks be independent. If $r \geq 4(1 - \beta)$, then the procedure $\widehat{S} = \{i : x(i) > \sqrt{2(1 - \beta) \log p}\}$ yields $\mathbb{P}[\widehat{S} = S] \rightarrow 1$. This requirement on signal size is strictly weaker than that of the strong classification boundary, since $4(1 - \beta) < (1 + \sqrt{1 - \beta})^2$ on $\beta \in (0, 1)$.

The above example shows that if the correlations of the Gaussian errors do not decay in a uniform fashion (UDD fails), then we can do substantially better in terms of support recovery. The claims in the example are verified in Section 4.5, while numerical simulations of this example can be found in Section 4.1.5.

We conclude with a brief discussion on the relationships between UDD and other dependence conditions in the context of extreme value theory, before proceeding to the proof of Theorem 5.6.

Suppose that the array of errors \mathcal{E} comes from a stationary Gaussian time series $\epsilon(i)$, $i \in \mathbb{N}$, with auto-covariance $r_p = \text{Cov}(\epsilon(i + p), \epsilon(i))$. One is interested in the asymptotic behavior of the maxima $M_p := \max_{i=1, \dots, p} \epsilon(i)$.

In this setting, the Berman's condition, introduced in Berman (1964), requires that

$$r_p \log p \rightarrow 0, \quad \text{as } p \rightarrow \infty. \quad (5.3)$$

This condition entails that

$$a_p(M_p - b_p) \xrightarrow{d} Z, \quad \text{as } p \rightarrow \infty, \quad (5.4)$$

with the Gumbel limit distribution $\mathbb{P}[Z \leq x] = \exp\{-e^{-x}\}$, $x \in \mathbb{R}$, where

$$a_p = \sqrt{2 \log p}, \quad b_p = \sqrt{2 \log p} - \frac{1}{2} \left(\sqrt{2 \log p} \right)^{-1} (\log \log(p) + \log(4\pi)),$$

are *the same* centering and normalization sequences as in the case of iid $\epsilon(i)$'s. Berman's condition is one of the weakest dependence conditions in the literature for which this result holds. See, e.g., Theorem 4.4.8 in Embrechts et al. (2013), where (5.3) is described as “very weak”.

For dependence conditions weaker than (5.3), the sequences of normalizing and centering constants in (5.4) are *different* from the iid case, and the corresponding limit is no longer Gumbel; see, for example, Theorems 6.5.1 and 6.6.4 in Leadbetter et al. (2012), and McCormick and Mittal (1976).

On the other hand, in our high dimensional support estimation context, the notion of relative stability is sufficient and more natural than the finer notions of distributional convergence. If one is merely interested in the asymptotic relative stability of the Gaussian maxima, then Berman's condition can be relaxed significantly (see also, Theorem 4.1 of Berman (1964)). Observe that by Proposition 5.5, the Berman condition (5.3) implies UDD and hence relative stability (Theorem 5.6), i.e.,

$$\frac{1}{b_p} M_p \xrightarrow{\mathbb{P}} 1, \quad \text{as } p \rightarrow \infty. \quad (5.5)$$

This *concentration of maxima* property can be readily deduced from (5.4), since $a_p b_p \sim 2 \log(p) \rightarrow \infty$ as $p \rightarrow \infty$. Theorem 5.6 shows that (5.5) holds if the much weaker uniform dependence condition UDD holds. Note that our condition is coordinate free — neither monotonicity of the sequence r_p nor stationarity of the underlying array is required.

The rest of this chapter is devoted to the proof of the main result, i.e., Theorem 5.6. We first introduce a key lemma regarding the structure of correlation matrix of high-dimensional random variables. The proof uses a surprising, yet elegant application of Ramsey's Theorem from the study of combinatorics. The ‘only if’ part of Theorem 5.6 follows from this lemma, in Section 5.2.

The proof of the ‘if’ part is detailed in Section 5.3. The arguments there was recently

extended to establish bounds on the rate of concentration of maxima in Kartsioukas et al. (2019); see also, Tanguy (2015) and references therein for related work on this topic.

5.1 Ramsey's Coloring theorem and structure of correlation matrices

Given any integer $k \geq 1$, there is always an integer $R(k, k)$ called the *Ramsey number*:

$$k \leq R(k, k) \leq \binom{2k-2}{k-1} \quad (5.6)$$

such that the following property holds: every undirected graph with at least $R(k, k)$ vertices will contain *either* a clique of size k , or an *independent set* of k nodes. Recall that a clique is a complete sub-graph where all pairs of nodes are connected, and an independent set is a set of nodes where no two nodes are connected.

This result is a consequence of the celebrated work of Ramsey (2009), which gave birth to Ramsey Theory (see e.g., Conlon et al. (2015)). The Ramsey Theorem and the upper bound (5.6) (established first in Erdős and Szekeres (1935)) are at the heart of the proof of the following result.

Proposition 5.10. *Fix $\gamma \in (0, 1)$ and let $P = (\rho(i, j))_{n \times n}$ be an arbitrary correlation matrix. If*

$$k := \lfloor \log_2(n)/2 \rfloor \geq \lceil 1/\gamma \rceil + 1, \quad (5.7)$$

then there is a set of k indices $K = \{l_1, \dots, l_k\} \subseteq \{1, \dots, n\}$ such that

$$\rho(i, j) \geq -\gamma, \text{ for all } i, j \in K. \quad (5.8)$$

Proof of Proposition 5.10. By using (5.6) and a refinement of the Stirling's formula, we

will show at the end of the proof that for $k \leq \log_2(n)/2$, we have

$$R(k, k) \leq n, \quad (5.9)$$

where $R(k, k)$ is the Ramsey number.

Now, construct a graph with vertices $\{1, \dots, n\}$ such that there is an edge between nodes i and j if and only if $\rho(i, j) > -\gamma$. In view of (5.9) and Ramsey's theorem (see e.g., Theorem 1 in Fox (2009) or Conlon et al. (2015) for a recent survey on Ramsey theory), there is a subset of k nodes $K = \{l_1, \dots, l_k\}$, which is either a *complete graph* or an *independent set*.

If K is a complete graph, then by our construction of the graph, Relation (5.8) holds.

Now, suppose that K is a set of independent nodes. This means, again by the construction of our graph, that

$$\rho(i, j) < -\gamma, \quad \text{for all } i \neq j \in K.$$

Let Z_i , $i \in K$ be zero-mean random variables such that $\rho(i, j) = \mathbb{E}[Z_i Z_j]$. Observe that

$$\text{Var} \left(\sum_{i \in K} Z_i \right) = \sum_{i \in K} \text{Var}(Z_i) + \sum_{\substack{i \neq j \\ i, j \in K}} \text{Cov}(Z_i, Z_j) < k - k(k-1)\gamma, \quad (5.10)$$

since $\text{Var}(Z_i) = 1$ and $\rho(i, j) < -\gamma$ for $i \neq j$. By our assumption, $k \geq (\lceil 1/\gamma \rceil + 1)$, or equivalently, $(k-1) \geq 1/\gamma$, the variance in (5.10) is negative. This is a contradiction showing that there are no independent sets K with cardinality k .

To complete the proof, it remains to show that Relation (5.9) holds. In view of the upper bound on the Ramsey numbers (5.6), it is enough to show that $k \leq \log_2(\sqrt{n})$ implies

$$\binom{2k-2}{k-1} \leq n.$$

This follows from a refinement of the Stirling formula, due to Robbins (1955):

$$\sqrt{2\pi}m^{m+1/2}e^{-m}e^{\frac{1}{(12m+1)}} \leq m! \leq \sqrt{2\pi}m^{m+1/2}e^{-m}e^{\frac{1}{12m}}.$$

Indeed, letting $\tilde{k} := k - 1$, and applying the above upper and lower bounds to the terms $(2\tilde{k})!$ and $\tilde{k}!$, respectively, we obtain:

$$\binom{2k-2}{k-1} \equiv \frac{(2\tilde{k})!}{(\tilde{k}!)^2} \leq \frac{2^{2\tilde{k}}}{\sqrt{\pi\tilde{k}}} \exp \left\{ \frac{1}{24\tilde{k}} - \frac{2}{12\tilde{k}+1} \right\} < 2^{2k}$$

where the last two inequalities follow by simply dropping positive factors less than 1. Since $2k \leq \log_2(n)$, the above bound implies Relation (5.9) and the proof is complete. \square

Using Proposition 5.10, we establish the key lemma used in the proof of Theorem 5.6.

Lemma 5.11. *Let $c \in (0, 1)$, and $P = (\rho(i, j))_{(n+1) \times (n+1)}$ be a correlation matrix such that*

$$\rho(1, j) > c \quad \text{for all } j = 1, \dots, n+1. \quad (5.11)$$

If $n \geq 2^{2\lceil 2/c^2 \rceil + 4}$, then there is a set of indices $K = \{l_1, \dots, l_k\} \subseteq \{2, \dots, n+1\}$ of cardinality $k = |K| = \lfloor \log_2 \sqrt{n} \rfloor$, such that

$$\rho(i, j) > \frac{c^2}{2} \quad \text{for all } i, j \in K. \quad (5.12)$$

That is, all entries of the $k \times k$ sub-correlation matrix $P_K := (\rho(i, j))_{i, j \in K}$ are larger than $c^2/2$.

Proof of Lemma 5.11. Let Z_1, \dots, Z_{n+1} be random variables with covariance matrix P .

Denote $\rho_j = \rho(1, j)$ and define

$$R(j) = \begin{cases} \frac{1}{\sqrt{1-\rho_j^2}} (Z(j) - \rho_j Z(1)), & \text{if } \rho_j < 1, \\ R^* & \text{if } \rho_j = 1, \end{cases} \quad (5.13)$$

where R^* is an arbitrary zero-mean, unit-variance random variable. It is easy to see that $\text{Var}(R(j)) = 1$, and

$$\begin{aligned}\text{Cov}(Z(i), Z(j)) &= \text{Cov}\left(\rho_i Z(1) + \sqrt{1 - \rho_i^2} R(i), \rho_j Z(1) + \sqrt{1 - \rho_j^2} R(j)\right) \\ &= \rho_i \rho_j + \sqrt{1 - \rho_i^2} \sqrt{1 - \rho_j^2} \text{Cov}(R(i), R(j)) \\ &\geq c^2 + \min\{\text{Cov}(R(i), R(j)), 0\}.\end{aligned}$$

Therefore, Relation (5.12) would hold if we can find a set of indices $K = \{l_1, \dots, l_k\}$ such that $\text{Cov}(R(i), R(j)) > -c^2/2$ for all $i, j \in K$, where $k = |K| = \lfloor \log_2 \sqrt{n} \rfloor$. This, however, follows from Proposition 5.10 applied to $(R(j))_{j=2}^{n+1}$ with $\gamma = c^2/2$, provided that

$$k = \lfloor \log_2 \sqrt{n} \rfloor \geq \lceil 2/c^2 \rceil + 1.$$

The last inequality indeed follows from the assumption that $n \geq 2^{2\lceil 2/c^2 \rceil + 4}$. □

5.2 URS implies UDD (‘only if’ part of Theorem 5.6)

In view of Remark 5.2, UDD is equivalent to the requirement that $N(\delta) := 1 + \sup_p N_p(\delta) < \infty$ for all $\delta \in (0, 1)$, where

$$N_p(\delta) := \max_{j \in \{1, \dots, p\}} \left| \{i : i \neq j, \Sigma_p(j, i) > \delta\} \right|. \quad (5.14)$$

Therefore, if \mathcal{E} is not UDD, then there must exist a constant $c \in (0, 1)$ for which $N(c)$ is infinite, i.e., there is a subsequence $\tilde{p} \rightarrow \infty$ such that $N_{\tilde{p}}(c) \rightarrow \infty$. Without loss of generality, we may assume that $\tilde{p} = p$.

Let $j_p(c)$ be the maximizers of (5.14), and let

$$S_p(c) := \{i \in \{1, \dots, p\} : \Sigma_p(j_p(c), i) > c\}. \quad (5.15)$$

Observe that $|S_p(c)| = N_p(c) + 1 \rightarrow \infty$, as $p \rightarrow \infty$ (note $j_p(c) \in S_p(c)$).

Applying Lemma 5.11 to the set of random variables indexed by $S_p(c)$, we conclude, for $N_p(c) \geq 2^{2\lceil 2/c^2 \rceil + 4}$, there must be a further subset

$$K_p(c) \subseteq S_p(c), \quad (5.16)$$

of cardinality

$$k_p(c) := |K_p(c)| \geq \log_2 \sqrt{N_p(c)}, \quad (5.17)$$

such that all pairwise correlations of the random variables indexed by $K_p(c)$ are greater than $c^2/2$. Since the sequence $N_p(c) \rightarrow \infty$, by (5.17), we have $k_p(c) \rightarrow \infty$ as $p \rightarrow \infty$.

Therefore, we have identified a sequence of subsets $K_p(c) \subseteq \{1, \dots, p\}$ with the following two properties:

1. $k_p(c) := |K_p(c)| \rightarrow \infty$, as $p \rightarrow \infty$, and
2. For all $i, j \in K_p(c)$, we have

$$\Sigma_p(i, j) > c^2/2. \quad (5.18)$$

Without loss of generality, we may assume $K_p(c) = \{1, \dots, k_p(c)\} \subseteq \{1, \dots, p\}$, upon re-labeling of the coordinates.

Now consider a Gaussian sequence $\epsilon^* = \{\epsilon^*(j), j = 1, 2, \dots\}$, independent of \mathcal{E} , defined as follows:

$$\epsilon^*(j) := Z \left(c/\sqrt{2} \right) + Z(j) \sqrt{1 - c^2/2}, \quad j = 1, 2, \dots,$$

where Z and $Z(j), j = 1, 2, \dots$ are independent standard normal random variables. Hence,

$$\text{Var}(\epsilon^*(j)) = 1 = \text{Var}(\epsilon_p(j)), \quad (5.19)$$

and

$$\text{Cov}(\epsilon^*(i), \epsilon^*(j)) = \frac{c^2}{2} \leq \text{Cov}(\epsilon_p(i), \epsilon_p(j)), \quad (5.20)$$

for all p , and all $i \neq j, i, j \in K_p(c)$. Thus we have, as $p \rightarrow \infty$,

$$\frac{1}{u_{k_p(c)}} \max_{j \in K_p(c)} \epsilon^*(j) = \frac{c/\sqrt{2}}{u_{k_p(c)}} Z + \frac{\sqrt{1-c^2/2}}{u_{k_p(c)}} \max_{j \in K_p(c)} Z(j) \xrightarrow{\mathbb{P}} \sqrt{1 - \frac{c^2}{2}}, \quad (5.21)$$

where the convergence in probability follows from Proposition 2.11 part 2.

Relations (5.19) and (5.20), by Slepian's Lemma Slepian (1962), also imply,

$$\frac{1}{u_{k_p(c)}} \max_{j \in K_p(c)} \epsilon^*(j) \stackrel{d}{\geq} \frac{1}{u_{k_p(c)}} \max_{j \in K_p(c)} \epsilon_p(j). \quad (5.22)$$

Therefore, by (5.22) and (5.21), for all $\sqrt{1-c^2/2} \leq \delta < 1$, we have,

$$\mathbb{P} \left[\frac{1}{u_{k_p(c)}} \max_{j \in K_p(c)} \epsilon_p(j) < \delta \right] \rightarrow 1 \quad \text{as } p \rightarrow \infty.$$

This contradicts the definition of URS (with the particular choice of $S_p := K_p(c)$), and the proof of the ‘only if’ part is complete.

5.3 UDD implies URS (‘if’ part of Theorem 5.6)

Recall that our objective is to show (4.21). We will do so in two stages; namely, we will prove that for all $\delta > 0$, we have

$$\mathbb{P} \left[\frac{M_{S_p}}{u_{|S_p|}} > 1 + \delta \right] \rightarrow 0, \quad (5.23)$$

and

$$\mathbb{P} \left[\frac{M_{S_p}}{u_{|S_p|}} < 1 - \delta \right] \rightarrow 0, \quad (5.24)$$

for any sequence of subsets S_p such that $|S_p| \rightarrow \infty$. Although the first step (5.23) was already shown in Proposition 2.11, regardless of the dependence structure, we provide in this section a more refined result. Specifically, the following result states that for the AGG model, the constant δ in Proposition 2.11 can be replaced by a vanishing sequence $c_p \rightarrow 0$.

Lemma 5.12 (Upper tails of AGG maxima). *Let \mathcal{E} be an array with marginal distribution $F \in \text{AGG}(\nu)$, $\nu > 0$. If we pick*

$$c_p = \frac{u_p \log p}{u_p} - 1, \quad (5.25)$$

where $u_p = F^{\leftarrow}(1 - 1/p)$, then we have $c_p > 0$, $c_p \rightarrow 0$, and

$$\mathbb{P} \left[\frac{M_p}{u_p} - (1 + c_p) > 0 \right] \rightarrow 0. \quad (5.26)$$

The proof can be found in Section 5.3.1 below.

Since Lemma 5.12 holds regardless of the dependence structure, the same conclusions hold if one replaces M_p by $M_{S_p} = \max_{j \in S_p} \epsilon(j)$ and p by $q = q(p) = |S_p|$, where S_p is any sequence of sets such that $q \equiv |S_p| \rightarrow \infty$. This entails (5.23).

On the other hand, the proof of (5.24) uses a more elaborate argument based on the Sudakov-Fernique bound. We proceed by first bounding the probability by an expectation. For all $\delta > 0$, we have

$$\begin{aligned} \mathbb{P} \left[\frac{M_{S_p}}{u_q} < 1 - \delta \right] &= \mathbb{P} \left[- \left(\frac{M_{S_p}}{u_q} - (1 + c_q) \right) > \delta + c_q \right] \\ &\leq \mathbb{P} \left[\left(\frac{M_{S_p}}{u_q} - (1 + c_q) \right)_- > \delta + c_q \right] \\ &\leq \frac{1}{\delta + c_q} \mathbb{E} \left[\left(\frac{M_{S_p}}{u_q} - (1 + c_q) \right)_- \right], \end{aligned} \quad (5.27)$$

where $(x)_- := \max\{-x, 0\}$ and the last line follows from the Markov inequality. The next result shows that the upper bound in (5.27) vanishes.

Lemma 5.13. *Let \mathcal{E} be a Gaussian UDD array and $S_p \subseteq \{1, \dots, p\}$ be an arbitrary*

sequence of sets such that $q = q(p) = |S_p| \rightarrow \infty$. Then, for $M_{S_p} := \max_{j \in S_p} \epsilon_p(j)$ and c_q as in (5.25), we have

$$\mathbb{E} \left[\left(\frac{M_{S_p}}{u_q} - (1 + c_q) \right)_- \right] \rightarrow 0, \quad \text{as } p \rightarrow \infty. \quad (5.28)$$

The proof of the lemma is given in Section 5.3.2 below.

Going back to the proof of Theorem 5.6, we observe that Relations (5.27) and (5.28) imply (5.24), which completes the proof of the ‘if’ part. \square

Remark 5.14. Only the Sudakov-Fernique minorization argument used in the proof of Lemma 5.13, relies on the Gaussian assumption. We expect the techniques and results here to be useful in extending Theorem 5.6 to more general class of distributions, say, the AGG model.

5.3.1 Bounding the upper tails of AGG maxima

Proof of Lemma 5.12. Recall by (2.32) that

$$u_q \sim (\nu \log q)^{1/\nu}, \quad q \rightarrow \infty,$$

so that

$$c_p = \frac{u_{p \log p}}{u_p} - 1 = \left(\frac{\log p + \log \log p}{\log p} \right)^{1/\nu} (1 + o(1)) - 1 \rightarrow 0 \quad \text{as } p \rightarrow \infty. \quad (5.29)$$

By the union bound, we have

$$\begin{aligned} \mathbb{P} \left[\frac{M_p}{u_p} > 1 + c_p \right] &\leq \sum_{j=1}^p \mathbb{P} \left[\frac{\epsilon_p(j)}{u_p} > 1 + c_p \right] = p \bar{F}(u_{p \log p}) \\ &= p \bar{F} \left(F^{\leftarrow} \left(1 - \frac{1}{p \log p} \right) \right) \leq \frac{1}{\log p} \rightarrow 0. \end{aligned} \quad (5.30)$$

where the last inequality follows from the fact that $F(F^{\leftarrow}(u)) \geq u$ for all $u \in [0, 1]$. \square

In addition to Lemma 5.12, which says the upper tail vanishes in probability, we will also prepare a result which states that the upper tail also vanishes in expectation.

Lemma 5.15. *Let M_p and c_p be as in Lemma 5.12, and denote*

$$\xi_p := \frac{M_p}{(1 + c_p)u_p}.$$

Then there exists $p_0, t_0 > 0$, and absolute constant $C > 0$ such that

$$\mathbb{P}[\xi_p > t] \leq \exp\{-Ct^\nu\}, \quad \text{for all } p > p_0, t > t_0. \quad (5.31)$$

In particular, the set of random variables $\{(\xi_p)_+, p \in \mathbb{N}\}$ is uniformly integrable.

Proof of Lemma 5.15. Recalling that $(1 + c_p)u_p = u_{p \log p}$, and by applying the union bound as in (5.30), we have

$$\begin{aligned} \log \mathbb{P}[\xi_p > t] &\leq \log p + \log \bar{F}(u_{p \log p} t) \\ &\leq \log p - \frac{1}{\nu} (u_{p \log p} t)^\nu (1 - \delta). \end{aligned} \quad (5.32)$$

for $t > t_0(\delta) > 0$, where $\delta \in (0, 1)$ is an arbitrarily small number fixed in advance. This follows from the assumption that $F \in \text{AGG}(\nu)$ and the Definition 2.7 of AGG tails. Using in (5.32) the explicit expressions for quantiles in (2.32), we obtain

$$\log \mathbb{P}[\xi_p > t] \leq \log p - \underbrace{(1 + o(1))(1 - \delta)t^\nu}_{\text{greater than 1 for large } t} \log p - t^\nu \underbrace{\log \log p (1 + o(1))(1 - \delta)}_{\text{greater than } C \text{ for large } p}. \quad (5.33)$$

For large t , we have $(1 + o(1))(1 - \delta)t^\nu > 1$, so that sum of the first two terms on the right-hand side of (5.33) is negative. Also, for p larger than some constant $p_0(\delta)$, we have $\log \log p (1 + o(1))(1 - \delta) > C$ for some constant C that does not depend on p . Therefore (5.31) holds for $t > t_0(\delta)$ and $p > p_0(\delta)$, and the proof is complete. \square

Corollary 5.16. *The upper tails of AGG maxima vanish in expectation, i.e.,*

$$\mathbb{E} \left[\left(\frac{M_p}{u_p} - (1 + c_p) \right)_+ \right] \rightarrow 0 \quad \text{as } p \rightarrow \infty, \quad (5.34)$$

where $(a)_+ := \max\{a, 0\}$.

Proof of Corollary 5.16. Since $c_p \geq 0$ is a sequence converging to 0, we have $c_p < 1$ for $p \geq p_0$. Hence for any $t > 0$, we have

$$\begin{aligned} \mathbb{P} \left[\left(\frac{M_p}{u_p} - (1 + c_p) \right)_+ > t \right] &= \mathbb{P} \left[(1 + c_p) (\xi_p - 1)_+ > t \right] \\ &\leq \mathbb{P} \left[(\xi_p - 1)_+ > t/2 \right] \leq \mathbb{P} \left[\xi_p > t/2 \right]. \end{aligned} \quad (5.35)$$

By Lemma 5.15, $\{(\xi_p)_+\}$ is u.i., therefore by Relation (5.35), $\{(M_p/u_p - (1 + c_p))_+, p \in \mathbb{N}\}$ is u.i. as well. Since by Lemma 5.12, $(M_p/u_p - (1 + c_p))_+ \rightarrow 0$ in probability, Relation (5.34) follows from the established uniform integrability. \square

5.3.2 Bounding the lower tails of Gaussian maxima

The main goal of this section is to establish the following result.

Proposition 5.17. *For every UDD Gaussian array \mathcal{E} , and any sequence of subsets $S_p \subseteq \{1, \dots, p\}$ such that $q = q(p) = |S_p| \rightarrow \infty$, we have*

$$\liminf_{p \rightarrow \infty} \mathbb{E} \left[\frac{M_{S_p}}{u_q} \right] \geq 1, \quad (5.36)$$

where $M_S = \max_{j \in S} \epsilon(j)$.

Lemma 5.13, which is the key to the proof of the ‘if’ part of Theorem 5.6, follows immediately from this proposition.

Proof of Lemma 5.13. We start with the identity

$$\mathbb{E} \left[\frac{M_{S_p}}{u_q} - (1 + c_q) \right] = \mathbb{E} \left[\left(\frac{M_{S_p}}{u_q} - (1 + c_q) \right)_+ \right] - \mathbb{E} \left[\left(\frac{M_{S_p}}{u_q} - (1 + c_q) \right)_- \right].$$

By re-arranging terms and taking limsup/liminf, we obtain

$$\begin{aligned} 0 &\leq \limsup_{p \rightarrow \infty} \mathbb{E} \left[\left(\frac{M_{S_p}}{u_q} - (1 + c_q) \right)_- \right] \\ &\leq \limsup_{p \rightarrow \infty} \mathbb{E} \left[\left(\frac{M_{S_p}}{u_q} - (1 + c_q) \right)_+ \right] - \liminf_{p \rightarrow \infty} \mathbb{E} \left[\frac{M_{S_p}}{u_q} - (1 + c_q) \right] \end{aligned} \quad (5.37)$$

$$= - \liminf_{p \rightarrow \infty} \mathbb{E} \left[\frac{M_{S_p}}{u_q} - (1 + c_q) \right], \quad (5.38)$$

where the last equality follows from the fact that the lim-sup in (5.37) vanishes by Corollary 5.16. On the other hand, since $c_q \rightarrow 0$, we have

$$\liminf_{p \rightarrow \infty} \mathbb{E} \left[\frac{M_{S_p}}{u_q} - (1 + c_q) \right] = \liminf_{p \rightarrow \infty} \mathbb{E} \left[\frac{M_{S_p}}{u_q} - 1 \right] \geq 0,$$

where the last inequality follows from Proposition 5.17. This shows that the right-hand side of (5.38) is non-positive and hence (5.28) holds. \square

A interesting fact on the relationship between the upper quantiles and the expectation of iid maxima will be needed for the proof of Proposition 5.17. The following lemma may be of independent interest.

Lemma 5.18. *Let $(X_i)_{i=1}^p$ be p iid random variables with distribution F such that $\mathbb{E}[(X_i)_-]$ exists, i.e.,*

$$\mathbb{E}[\max\{-X_i, 0\}] < \infty.$$

Let $M_p = \max_{i=1, \dots, p} X_i$. Assume that F has a density f , which is eventually decreasing. More precisely, we suppose there exists a C_0 such that $0 < F(C_0) < 1$, and $f(x_1) \geq f(x_2)$

whenever $C_0 < x_1 \leq x_2$. Under these assumptions, we have,

$$\liminf_{p \rightarrow \infty} \frac{\mathbb{E}M_p}{u_{p+1}} \geq 1,$$

where $u_{p+1} = F^{\leftarrow}(1 - 1/(p+1))$.

Proof of Lemma 5.18. Write

$$X_i = F^{\leftarrow}(U_i)$$

where U_i are iid uniform random variables on $(0, 1)$. Denote M_p^U as the maximum of the U_i 's, we have $\mathbb{E}M_p = \mathbb{E}[F^{\leftarrow}(M_p^U)]$, and by conditioning, we obtain

$$\begin{aligned} \mathbb{E}M_p &= \mathbb{E}[F^{\leftarrow}(M_p^U) \mid M_p^U \geq F(C_0)] \mathbb{P}[M_p^U \geq F(C_0)] + \\ &\quad + \mathbb{E}[F^{\leftarrow}(M_p^U) \mid M_p^U < F(C_0)] \mathbb{P}[M_p^U < F(C_0)]. \end{aligned} \quad (5.39)$$

We first handle the first term in the summation. Since f is decreasing beyond C_0 , F is concave on (C_0, ∞) , and F^{\leftarrow} is convex on $(F(C_0), 1)$. By Jensen's inequality, we have

$$\mathbb{E}[F^{\leftarrow}(M_p^U) \mid M_p^U \geq F(C_0)] \geq F^{\leftarrow}(\mathbb{E}[M_p^U \mid M_p^U \geq F(C_0)]).$$

With a direct calculation, one can show that

$$F^{\leftarrow}(\mathbb{E}[M_p^U \mid M_p^U \geq F(C_0)]) = F^{\leftarrow}\left(\left(1 - \frac{1}{p+1}\right) \left(\frac{1 - F(C_0)^{p+1}}{1 - F(C_0)^p}\right)\right),$$

and hence

$$\begin{aligned} \mathbb{E}[F^{\leftarrow}(M_p^U) \mid M_p^U \geq F(C_0)] &\geq F^{\leftarrow}\left(\left(1 - \frac{1}{p+1}\right) \left(\frac{1 - F(C_0)^{p+1}}{1 - F(C_0)^p}\right)\right) \\ &\geq F^{\leftarrow}\left(1 - \frac{1}{p+1}\right) = u_{p+1}. \end{aligned}$$

Since $\mathbb{P}[M_p^U \leq m \mid M_p^U < F(C_0)] = (m/F(C_0))^p \leq m/F(C_0)$ for $m \leq F(C_0)$, we have

$$(M_p^U \mid M_p^U < F(C_0)) \stackrel{d}{\geq} (U_1 \mid U_1 < F(C_0)),$$

where the latter is the uniform distribution on $(0, F(C_0))$. Therefore, for the second term of the sum in (5.39), by monotonicity of F^{\leftarrow} , we obtain

$$\begin{aligned} \mathbb{E}[F^{\leftarrow}(M_p^U) \mid M_p^U < F(C_0)] &\geq \mathbb{E}[F^{\leftarrow}(U_1) \mid U_1 < F(C_0)] \\ &= \mathbb{E}[X_1 \mid X_1 < C_0]. \end{aligned}$$

Finally, since $\mathbb{P}[M_p^U < F(C_0)] = F(C_0)^p = 1 - \mathbb{P}[M_p^U \geq F(C_0)]$, by (2.32), we have

$$\frac{\mathbb{E}M_p}{u_{p+1}} \geq (1 - F(C_0)^p) + \frac{\mathbb{E}[X_1 \mid X_1 < C_0]}{u_{p+1}} F(C_0)^p.$$

The conclusion follows since the right-hand-side of the last inequality converges to 1. \square

We now ready to prove Proposition 5.17. This is where the UDD dependence assumption is used.

Proof of Proposition 5.17. Define the canonical (pseudo) metric on S_p ,

$$d(i, j) = \sqrt{\mathbb{E}[(\epsilon(i) - \epsilon(j))^2]}.$$

It can be easily checked that the canonical metric takes values between 0 and 2. For arbitrary $\delta \in (0, 1)$, take $\gamma = \sqrt{2(1 - \delta)}$, and let \mathcal{N} be a γ -packing of S_p . That is, let \mathcal{N} be a subset of S_p , such that for any $i, j \in \mathcal{N}$, $i \neq j$, we have $d(i, j) \geq \gamma$, i.e.,

$$d(i, j) = \sqrt{2(1 - \Sigma_p(i, j))} \geq \gamma = \sqrt{2(1 - \delta)}, \quad (5.40)$$

or equivalently, $\Sigma_p(i, j) \leq \delta$. We claim that we can find a γ -packing \mathcal{N} whose number of

elements is at least

$$|\mathcal{N}| \geq q/N(\delta). \quad (5.41)$$

Indeed, \mathcal{N} can be constructed iteratively as follows:

Step 1: Set $S_p^{(1)} := S_p$ and $\mathcal{N} := \{j_1\}$, where $j_1 \in S_p^{(1)}$ is an arbitrary element. Set $k := 1$.

Step 2: Set $S_p^{(k+1)} := S_p^{(k)} \setminus B_\gamma(j_k)$, where

$$B_\gamma(j_k) := \{i \in S_p : d(i, j_k) < \gamma \equiv \sqrt{2(1-\delta)}\}.$$

Step 3: If $S_p^{(k)} \neq \emptyset$, pick an arbitrary $j_{k+1} \in S_p^{(k)}$, set $\mathcal{N} := \mathcal{N} \cup \{j_{k+1}\}$, and $k := k + 1$, go to step 2; otherwise, stop.

By the definition of UDD (see Definition 5.1), there are at most $N(\delta)$ coordinates whose covariance with $\epsilon(j)$ exceed δ . Therefore at each iteration, $|B_\gamma(j_k)| \leq N(\delta)$, and hence

$$|S_p^{(k+1)}| \geq |S_p^{(k)}| - |B_\gamma(j_k)| \geq q - kN(\delta).$$

The construction can continue for at least $q/N(\delta)$ iterations, and we have $|\mathcal{N}| \geq \lfloor q/N(\delta) \rfloor$ as desired.

Now we define on this γ -packing \mathcal{N} an independent Gaussian process $(\eta(j))_{j \in \mathcal{N}}$,

$$\eta(j) = \frac{\gamma}{\sqrt{2}} Z(j) \quad j \in \mathcal{N},$$

where $Z(j)$'s are iid standard normal random variables. Observe that by the definition of γ -packing in (5.40), the increments of the new process are smaller than those of the original process in the following sense,

$$\mathbb{E} [(\eta(i) - \eta(j))^2] = \gamma^2 \leq d^2(i, j) = \mathbb{E} [(\epsilon(i) - \epsilon(j))^2]$$

for all $i \neq j$, $i, j \in \mathcal{N}$. Applying the Sudakov-Fernique inequality (see, e.g., Theorem 2.2.3 in (Adler and Taylor, 2009)) to $(\eta(j))_{j \in \mathcal{N}}$ and $(\epsilon(j))_{j \in \mathcal{N}}$, we have

$$\mathbb{E} \left[\max_{j \in \mathcal{N}} \eta(j) \right] \leq \mathbb{E} \left[\max_{j \in \mathcal{N}} \epsilon(j) \right] \leq \mathbb{E} \left[\max_{j \in S_p} \epsilon(j) \right]. \quad (5.42)$$

Since the $(\eta(j))_{j \in \mathcal{N}}$ are independent Gaussians, Lemma 5.18 yields the lower bound,

$$\liminf_{p \rightarrow \infty} \mathbb{E} \left[\frac{\max_{j \in \mathcal{N}} \eta(j)}{u_{|\mathcal{N}|}} \right] \geq \frac{\gamma}{\sqrt{2}} = \sqrt{1 - \delta}. \quad (5.43)$$

Using the expressions (2.32) for the quantiles of AGG models (with $\nu = 2$ here), we have

$$\frac{u_{|\mathcal{N}|}}{u_q} \geq \left(\frac{\log q - \log N(\delta)}{\log q} \right)^{1/2} (1 + o(1)) \rightarrow 1, \quad (5.44)$$

since $N(\delta)$ does not depend on $q = q(p) \rightarrow \infty$, and that $|\mathcal{N}| \geq q/N(\delta)$.

By combining (5.42), (5.43) and (5.44), we conclude that

$$\begin{aligned} \liminf_{p \rightarrow \infty} \mathbb{E} \left[\frac{\max_{j \in S_p} \epsilon(j)}{u_q} \right] &\geq \liminf_{p \rightarrow \infty} \mathbb{E} \left[\frac{\max_{j \in \mathcal{N}} \eta(j)}{u_q} \right] && \text{by (5.42)} \\ &\geq \liminf_{p \rightarrow \infty} \mathbb{E} \left[\frac{\max_{j \in \mathcal{N}} \eta(j)}{u_{|\mathcal{N}|}} \right] && \text{by (5.44)} \\ &\geq \sqrt{1 - \delta}. && \text{by (5.43)} \end{aligned}$$

Since $\delta > 0$ is arbitrary, (5.36) follows as desired. \square

5.4 Numerical illustrations of exact support recovery under dependence

The characterization of URS with the UDD condition allows us to simulate Gaussian errors and illustrate the effect of dependence on the phase transition behavior in finite dimensions.

We shall compare the performance of the Bonferroni's procedure, which is agnostic to both sparsity and signal size, with the oracle procedure which picks the top- s observations.

The first set of experiments explores short-range dependent errors from an auto-regressive (AR) models.

- AR(1) Gaussian errors with parameter $\rho = -0.5$, $\rho = 0.5$, and $\rho = 0.9$, where the autocovariance functions decay exponentially, $\rho_k = \rho^k$.

We again apply both the sparsity- and signal-size agnostic Bonferroni's procedure, i.e., $\hat{S} = \{i : x(i) > \sqrt{2 \log p}\}$, as well as the oracle procedure $\hat{S}^* = \{i : x(i) \geq x_{[s]}\}$, $s = |S|$, to all settings. Results of the numerical experiments for the AR models are shown in Figure 5.1.

As was commented in the main text, for dependent errors the oracle procedures is able to recover support of signals with higher probability than the Bonferroni procedures in finite dimensions; compare left and right columns of Figure 5.1. Short range dependent observations, however, there is not a pronounced difference. The results of the experiments are very similar to that of the independent Gaussian case.

The second set of experiments explores exact support recovery in additive error models in the cases of long-range dependent but UDD, as well as non-UDD errors. In particular we simulate

- Fractional Gaussian noise (fGn) with Hurst parameter $H = 0.75$ and $H = 0.9$. The autocovariance functions are

$$\rho_k \sim 0.75k^{-0.6} \quad \text{and} \quad \rho_k \sim 1.44k^{-0.2},$$

as $k \rightarrow \infty$. Both fGn models represent the regime of long-range dependence, where covariances decay very slowly to zero, so that $\sum |\rho_k| = \infty$; see, e.g., (Taqqu, 2003). Observe that every stationary Gaussian process with vanishing autocovariance gives rise to an UDD array as concluded in Corollary 5.7.

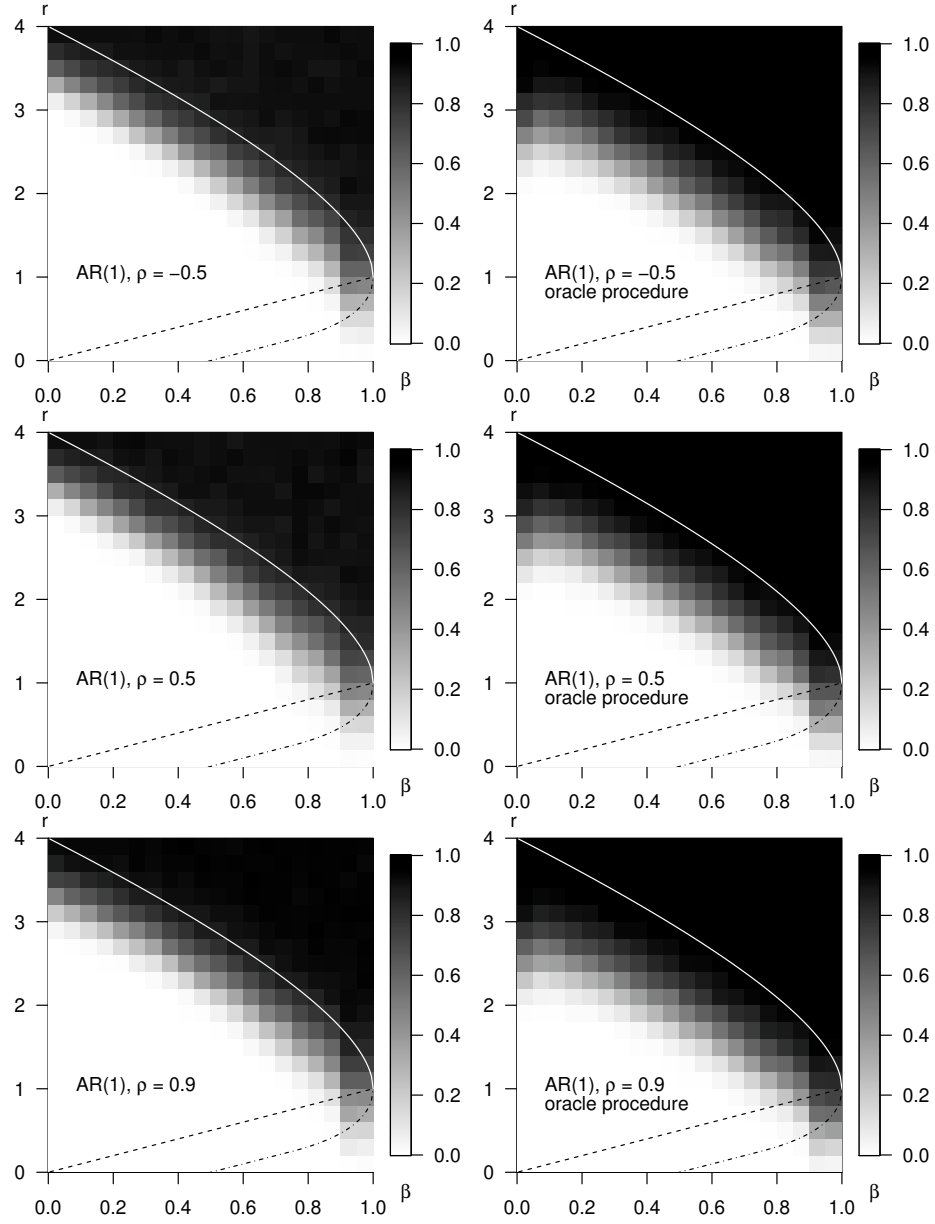


Figure 5.1: The empirical probability of exact support recovery from numerical experiments, as a function of sparsity level β and signal sizes r . Darker colors indicate higher probability of exact support recovery. Three AR(1) models with autocorrelation functions $(-0.5)^k$ (upper), 0.5^k (middle), and 0.9^k (lower) are simulated. The experiments were repeated 1000 times for each sparsity-signal size combination. In finite dimensions ($p = 10000$), the Bonferroni procedures (left) suffers small loss of power compared to the oracle procedures (right). A phase transition in agreement with the predicted boundary (4.5) can be seen in the AR models. The boundaries (solid, dashed, and dash-dotted lines) are as in Fig 4.1.

- The non-UDD Gaussian errors described in Example 5.9.

We will apply both the sparsity-and-signal-size-agnostic Bonferroni's procedure, i.e., $\tilde{S} = \{i : x(i) > \sqrt{2 \log p}\}$, as well as the oracle procedure $\hat{S}^* = \{i : x(i) \geq x_{[s]}\}$, $s = |S|$, to all settings. Results of the numerical experiments for the fGn and non-UDD models are shown in Figure 5.2.

Notice that the oracle procedure sets its thresholds more aggressively (at roughly $\sqrt{2 \log s}$) than the Bonferroni procedure (at $\sqrt{2 \log p}$). Although this difference vanishes as $p \rightarrow \infty$, in finite dimensions ($p = 10\,000$) the advantage can be felt. Indeed, in all our experiments the oracle procedure is able to recover support of signals with higher probability than the Bonferroni procedures; compare left and right columns of Figure 5.2. Notice also that there is an increase in probability of recovery near $\beta = 0$ for oracle procedures. This is an artifact in finite dimensions due to the fact that $s = \lfloor p^{1-\beta} \rfloor < p/2$, and there are more signals than nulls. The oracle procedure is able to adjust to this reversal by lowering its threshold accordingly.

For UDD errors, Theorem 4.8 predicts that exact recovery of the support is impossible when signal sizes are below the boundary (4.5), even with oracle procedures. However, the rate of this convergence (i.e., $\mathbb{P}[\hat{S}^* = S] \rightarrow 0$ or 1) can be very slow when the errors are heavily dependent, even though all AR and fGn models demonstrate qualitatively the same behavior in line with the predicted boundary (4.5). In finite dimensions ($p = 10\,000$), as dependence in the errors increases (fGN(H=0.75) to fGN(H=0.9)), the oracle procedure becomes more powerful at recovering signal support with high probability for weaker signals.

On the other hand, as demonstrated in Example 5.9, non-UDD errors yield qualitatively different behavior; exact support recovery is possible for signal sizes strictly weaker than that in the UDD case. Lower-right panel of Figure 5.2 demonstrates in this example that the signal support can be recovered as long as the signal sizes are larger than $4(1 - \beta)$.

For completeness, we verify the claims in Example 5.9.

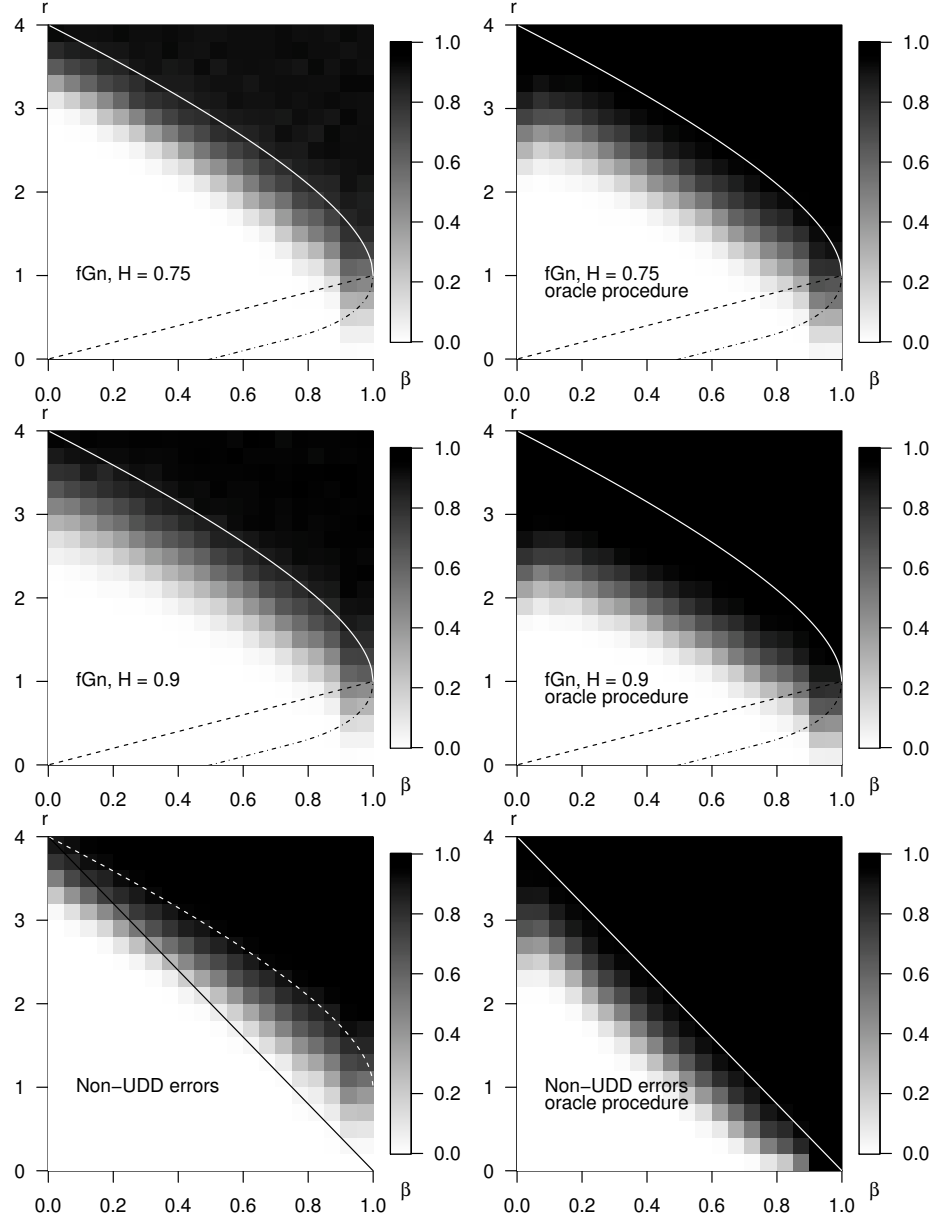


Figure 5.2: The empirical probability of exact support recovery from numerical experiments, as a function of sparsity level β and signal sizes r . Darker colors indicate higher probability of exact support recovery. Two fGn models with Hurst parameter $H = 0.75$ (upper), $H = 0.9$ (middle), and the non-UDD errors in Example 5.9 (lower) are simulated. The experiments were repeated 1000 times for each sparsity-signal size combination. In finite dimensions ($p = 10000$), the oracle procedures (right) is able to recover support for weaker signals than the Bonferroni procedures (left) when errors are heavily dependent, although they have the same phase transition limit. The non-UDD errors demonstrate qualitatively different behavior, enabling support recovery for strictly weaker signals. The boundaries (solid, dashed, and dash-dotted lines) are as in Fig 4.1. In the non-UDD example, dashed lines represent the limit attained by Bonferroni's procedures. See text for additional comments.

Proof of claims in Example 5.9. Recall that $\widehat{S}^* = \{j : x(j) > t_p^*\}$, where $t_p^* = \sqrt{2(1 - \beta) \log p}$.

Analogous to (4.11) in the proof of Theorem 4.1, we have

$$\begin{aligned} \mathbb{P}[\widehat{S} \subseteq S] &= 1 - \mathbb{P}\left[\max_{j \in S^c} x(j) > t_p^*\right] = 1 - \mathbb{P}\left[\max_{j \in S^c} \epsilon(j) > t_p^*\right] \\ &\geq 1 - \mathbb{P}\left[\max_{j \in \{1, \dots, p\}} \epsilon(j) > t_p^*\right] \geq 1 - \mathbb{P}\left[\max_{j \in \{1, \dots, \lfloor p^{1-\beta} \rfloor\}} \tilde{\epsilon}(j) > t_p^*\right] \end{aligned}$$

where $(\tilde{\epsilon})_{j=1}^{\lfloor p^{1-\beta} \rfloor}$'s are independent Gaussian errors; in the last inequality we used the assumption that there are at most $\lfloor p^{1-\beta} \rfloor$ independently distributed Gaussian errors in $(\epsilon_p(j))_{j=1}^p$.

By Example 4.3 (with $\lfloor p^{1-\beta} \rfloor$ taking the role of p), we know that the FWER goes to 0 at a rate of $(2 \log \lfloor p^{1-\beta} \rfloor)^{-1/2}$. Therefore, the probability of no false inclusion converges to 1.

On the other hand, since the signal sizes are no smaller than $(\nu \underline{r} \log p)^{1/\nu}$, similar to (4.13), we obtain

$$\begin{aligned} \mathbb{P}[\widehat{S} \supseteq S] &\geq \mathbb{P}\left[\min_{j \in S} \epsilon(j) > \sqrt{2(1 - \beta) \log p} - \sqrt{2\underline{r} \log p}\right] \\ &= \mathbb{P}\left[\max_{j \in S} (-\epsilon(j)) < \sqrt{2 \log p} (\sqrt{\underline{r}} - \sqrt{1 - \beta})\right] \\ &= \mathbb{P}\left[\frac{\max_{j \in S} (-\epsilon(j))}{u_{|S|}} < \frac{\sqrt{\underline{r}} - \sqrt{1 - \beta}}{\sqrt{1 - \beta}} (1 + o(1))\right], \end{aligned} \quad (5.45)$$

where in the last line we used the quantiles (2.32). Since the minimum signal size is bounded below by $\underline{r} > 4(1 - \beta)$, the right-hand-side of the inequality in (5.45) converges to a constant strictly larger than 1. While the left-hand-side, by Slepian's Lemma Slepian (1962), is stochastically smaller than a r.v. going to 1, i.e.,

$$\frac{1}{u_{|S|}} \max_{j \in S} (-\epsilon(j)) \stackrel{d}{\leq} \frac{1}{u_{|S|}} \max_{j \in S} \epsilon^*(j) \xrightarrow{\mathbb{P}} 1, \quad (5.46)$$

where $(\epsilon^*)_{j=1}^{\lfloor p^{1-\beta} \rfloor}$'s are independent Gaussian errors. Therefore the probability in (5.45) must also converge to 1. \square

CHAPTER 6

The Phase Transition Phenomena in Genome-wide Association Studies

We investigate the fundamental limits of multiple testing problems in high-dimensional chi-square models, and in genome-wide association studies as introduced in Section 1.2.

In Section 6.1, we shall establish the phase transitions of the sparse chi-square model (1.3). Recall that in large-scale screening studies where a large number of association tests are conducted, resulting statistics may be approximated by

$$x(i) \sim \chi_{\nu}^2(\lambda(i)), \quad i = 1, \dots, p, \quad (6.1)$$

where $\chi_{\nu}^2(\lambda(i))$ is a chi-square distributed random variable with ν degrees of freedom and non-centrality parameter $\lambda(i)$. In parallel to results in Chapter 3, we show that several commonly used family-wise error rate-control procedures — including Bonferroni's procedure — are asymptotically optimal for the exact, and exact-approximate support recovery problems (as defined in Definition 2.5) in idealized chi-square models (6.1) with independent components. We further show that the BH procedure is asymptotically optimal for the approximate, and approximate-exact support recovery problems. Under appropriate parametrizations of the signal sizes and sparsity, they establish the phase transitions of support recovery problems in the chi-square model. Remarkably, the degree-of-freedom parameter does not affect the asymptotic boundaries in any of the four support recovery

problems.

All phase transition boundaries coincide with those in the additive error models obtained in Chapter 3 under suitable parametrizations, indicating vanishing differences between the difficulties of the one-sided and two-sided alternatives in the Gaussian additive error model (1.1).

We then return to association screenings of categorical variables in Section 6.2, and present the consequences of the phase transition in the exact-approximate problem in large-scale genetic association studies. We do so by characterizing the relationship between the signal size λ and the marginal frequencies, odds ratio, and sample sizes for association tests on 2-by-2 contingency tables. This result, establishing the relationship between sample sizes and signal sizes, is made precise in Section 6.2.

We elaborate on the implications of this relationship on optimal study designs for association studies in Section 6.3. Perhaps surprisingly, our analysis reveals that balanced designs with equal number of cases and controls are often statistically inefficient. Practical consequences of these results in power analysis will be illustrated with data examples in Section 6.4.

The phase transitions in the chi-square models are demonstrated with numerical simulations in Section 6.5. Proofs of results in this Chapter are collected in Section 6.6.

6.1 Support recovery problems in chi-squared models

Similar to the analysis of additive error models in Chapter 3, we will work with triangular arrays of chi-square models (1.3) indexed by p . We adopt the same parametrization for the sparsity of the non-centrality parameter vectors $\lambda = \lambda_p$,

$$|S_p| = \lfloor p^{1-\beta} \rfloor, \quad \beta \in (0, 1] \quad (6.2)$$

where β parametrizes the problem sparsity. The closer β is to 1, the sparser the support S_p ; conversely, when β is close to 0, the support is dense with many non-null signals.

We parametrize the range of the non-zero and perhaps unequal signals in the chi-square model with

$$\underline{\Delta} = 2\underline{r} \log p \leq \lambda(i) \leq \overline{\Delta} = 2\bar{r} \log p, \quad \text{for all } i \in S_p, \quad (6.3)$$

for some constants $0 < \underline{r} \leq \bar{r} \leq +\infty$.

6.1.1 The exact support recovery problem

The first main result characterizes the phase transition phenomenon in the exact support recovery problem under the chi-square model.

Theorem 6.1. *Consider the high-dimensional chi-squared model (1.3) with signal sparsity and size as described in (6.2) and (6.3). The function*

$$g(\beta) = \left(1 + \sqrt{1 - \beta}\right)^2 \quad (6.4)$$

characterizes the phase transition of exact support recovery problem. Specifically, if $\underline{r} > g(\beta)$, then Bonferroni's, Sidák's, Holm's, and Hochberg's procedures with slowly vanishing (see Definition 3.2) nominal FWER levels all achieve asymptotically exact support recovery in the sense of (2.24).

Conversely, if $\bar{r} < g(\beta)$, then for any thresholding procedure \hat{S}_p , we have $\mathbb{P}[\hat{S}_p = S_p] \rightarrow 0$. Therefore, in view of Lemma 2.6, exact support recovery asymptotically fails for all thresholding procedures in the sense of (2.25).

The procedures listed in Theorem 6.1 were reviewed in Section 2.2. Proof of the theorem can be found in Section 6.6.2.

It is evident that the exact support recovery boundary (6.4) coincides with that in parallel results for the Gaussian additive error models (1.1) in Chapter 3. Implications of these

results will be discussed in Section 6.1.5 below.

Remark 6.2. Theorem 6.1 predicts that the asymptotic boundaries are the same for all values of the parameter ν . In simulations (Section 6.5), we find this asymptotic prediction to be quite accurate for $\nu \leq 3$ even in moderate dimensions ($p = 100$). For $\nu > 3$, the phase transitions take place somewhat above the boundary g . The behavior is qualitatively similar for the other three phase transitions (see Theorems 6.3, 6.4, and 6.5 below).

6.1.2 The exact-approximate support recovery problem

The next theorem describes the phase transition in the exact-approximate support recovery problem.

Theorem 6.3. *In the context of Theorem 6.1, the function*

$$\tilde{g}(\beta) = 1 \tag{6.5}$$

characterizes the phase transition of exact-approximate support recovery problem. Specifically, if $\underline{r} > \tilde{g}(\beta)$, then the procedures listed in Theorem 6.1 with slowly vanishing nominal FWER levels achieve asymptotically exact-approximate support recovery in the sense of (2.24).

Conversely, if $\bar{r} < \tilde{g}(\beta)$, then for any thresholding procedure \hat{S}_p , the exact-approximate support recovery fails in the sense of (2.25).

Theorem 6.3 is proved in Section 6.6.4.

6.1.3 The approximate support recovery problem

Our third main result characterizes the phase transition phenomenon in the approximate support recovery problem in the chi-square model.

Theorem 6.4. *Consider the high-dimensional chi-squared model (1.3) with signal sparsity and size as described in (6.2) and (6.3). The function*

$$h(\beta) = \beta \tag{6.6}$$

characterizes the phase transition of approximate support recovery problem. Specifically, if $\underline{r} > h(\beta)$, then the BHprocedure \widehat{S}_p (defined in Section 2.2) with slowly vanishing (see Definition 3.2) nominal FDR levels achieves asymptotically approximate support recovery in the sense of (2.24).

Conversely, if $\bar{r} < h(\beta)$, then approximate support recovery asymptotically fails in the sense of (2.25) for all thresholding procedures.

Theorem 6.4 is proved in Section 6.6.4 below.

6.1.4 The approximate-exact support recovery problem

A counterpart of Theorem 3.7 also holds in the chi-square models.

Theorem 6.5. *In the context of Theorem 6.4, the function*

$$\tilde{h}(\beta) = \left(\sqrt{\beta} + \sqrt{1 - \beta} \right)^2 \tag{6.7}$$

characterizes the phase transition of approximate-exact support recovery problem. Specifically, if $\underline{r} > \tilde{h}(\beta)$, then the Benjamini-Hochberg procedure with slowly vanishing nominal FDR levels achieves asymptotically approximate-exact support recovery in the sense of (2.24).

Conversely, if $\bar{r} < \tilde{h}(\beta)$, then for any thresholding procedure \widehat{S}_p , the approximate-exact support recovery fails in the sense of (2.25).

Theorem 6.5 is proved in Section 6.6.2.

Notice that all phase transitions boundaries are identical to those in the Gaussian additive error model (1.1) under one-side alternative. We refer readers to Figure 3.2 in Section 3.2 for a visualization of the results in Theorems 6.1 through 6.5.

The all four Theorems so far focus only on the idealized models (1.3) where statistics are *independent*. Support recovery problems under dependent observations remain to be explored. Recall in Chapter 3 we showed that the boundary for the exact support recovery problem in the additive error model (1.1) continues to hold even under severe dependence and general distributional assumptions. We conjecture that similar results would also hold, under classes of dependence structures that are “not too different from independence”, in the chi-square models. As an example, in the GWAS application, dependence among the genetic markers at different locations (known as linkage disequilibrium) decay as a function of their physical distances on the genome Bush and Moore (2012), resulting in locally dependent test statistics. It would be of great interest to extend the current theory to cover important dependence structures that arise in such applications.

6.1.5 Comparison of one- versus two-sided alternatives in additive error models

As alluded to in Section 1.2 in the introduction, we draw explicit comparisons between the one-sided and two-sided alternatives in Gaussian additive error models (1.1).

The exact support recovery problem in the dependent Gaussian additive error model (1.1) was studied in Chapter 3, with parametrization of sparsity identical to that in (6.2), whereas the range of the non-zero (and perhaps unequal) mean shifts $\mu(i)$ was parametrized as

$$\underline{\Delta} = \sqrt{2\underline{r} \log p} \leq \mu(i) \leq \overline{\Delta} = \sqrt{2\overline{r} \log p}, \quad \text{for all } i \in S_p,$$

for some constants $0 < \underline{r} \leq \overline{r} \leq +\infty$. Under this one-sided alternative, a phase transition in the r - β plane was described, where the boundary was found to be identical to (6.4) in

Theorem 6.1 for the chi-square models (6.1).

As discussed in Section 1.2, support recovery problems in the chi-square model with $\nu = 1$, , corresponds to the support recovery problems in the additive model under two-sided alternatives. This implies that the asymptotic signal size requirements are identical between the two-sided alternative and its one-sided counterpart, in order to achieve exact support recovery. As we shall see in numerical experiments (in Section 6.5 below), the difference is not very pronounced even in moderate dimensions, and vanishes as $p \rightarrow \infty$, in accordance with Theorem 6.1.

Comparisons can also be drawn in the approximate, approximate-exact, and exact approximate support recovery problems between the two types of alternatives.

Specifically, the approximate support recovery problem in the Gaussian additive error model (1.1) under one-sided alternatives exhibits a phase transition phenomenon characterized by a boundary that coincides with (6.6) in Theorem 6.4. Similar to the exact support recovery problem, this indicates vanishing difference in the difficulties of the two types alternatives in approximate support recovery problems.

Comparing Theorems 6.3 to 3.5 and Theorems 6.5 to 3.7, we see that the phase transition boundaries under the two types of alternatives are also identical in the exact-approximate and approximate-exact support recovery problems. The additional uncertainty in the two-sided alternatives do not call for larger signal sizes asymptotically in these problems.

To complete the comparisons, we point out that the phase transition boundaries for the sparse signal detection problem in the two types of alternatives are both identical to (3.4). This was analyzed in Donoho and Jin (2004).

6.2 Odds ratios and statistical power

We return to the application of association screenings for categorical variables, and put the results in the previous section to use. In particular, we focus on the exact-approximate sup-

port recovery problem, and demonstrate the consequences of its phase transition (Theorem 6.3) in genetic association studies.

In order to do so, we must first connect the concept of “statistical signal size” λ with some key quantities in association tests. While “signal size” likely sounds foreign to most practitioners, it is intimately linked with the concept of “effect sizes” — or odds ratios — in association studies, which are frequently estimated and reported in GWAS catalogs. We characterize the relationship between the two quantities in the special, but fairly common case of association tests on 2-by-2 contingency tables in Section 6.2.

Consider a 2-by-2 multinomial distribution with marginal probabilities of phenotypes (ϕ_1, ϕ_2) and genotypes (θ_1, θ_2) . The *probability* table (as opposed to the table of multinomial *counts* in the introduction) is as follows.

Probabilities	Genotype		Total by phenotype
	Variant 1	Variant 2	
Cases	μ_{11}	μ_{12}	ϕ_1
Controls	μ_{21}	μ_{22}	ϕ_2
Total by genotype	θ_1	θ_2	1

The odds ratio (i.e., “effect size”) is defined as the ratio of the phenotype frequencies between the two genotype variants,

$$R := \frac{\mu_{11}}{\mu_{21}} \bigg/ \frac{\mu_{12}}{\mu_{22}} = \frac{\mu_{11}\mu_{22}}{\mu_{12}\mu_{21}}. \quad (6.8)$$

The multinomial distribution is fully parametrized by the trio (θ_1, ϕ_1, R) . Odds ratios further away from 1 indicate greater contrasts between the probability of outcomes. Independence between the genotypes and phenotypes would imply an odds ratio of one, and hence $\mu_{jk} = \phi_j\theta_k$, for all $j, k \in \{1, 2\}$.

For a sequence of local alternatives $\mu^{(1)}, \mu^{(2)}, \dots$, such that $\sqrt{n}(\mu_{jk}^{(n)} - \phi_j\theta_k)$ converges to a constant table $\delta = (\delta_{jk})$, the chi-square test statistics converge in distribution to the

non-central chi-squared distribution with non-centrality parameter

$$\lambda = \sum_{j=1}^2 \sum_{k=1}^2 \delta_{jk}^2 / (\phi_j \theta_k).$$

See, e.g., Ferguson (2017). Hence, for large samples from a fixed distribution (μ_{ij}) , the statistic is well approximated by a $\chi_1^2(\lambda)$ distribution, where

$$\lambda = n \sum_{j=1}^2 \sum_{k=1}^2 \frac{(\mu_{jk} - \phi_j \theta_k)^2}{\phi_j \theta_k}. \quad (6.9)$$

Power calculations therefore only depend on the μ_{jk} 's through $\lambda = nw^2$, where we define

$$w^2 := \lambda/n \quad (6.10)$$

to be the *signal size per sample*. Statistical power would be increasing in w^2 for fixed sample sizes.

The next proposition states that the statistical signal size per sample can be parametrized by the odds ratio and the marginals in the probability table.

Proposition 6.6. *Consider a 2-by-2 multinomial distribution with marginal distributions $(\phi_1, \phi_2 = 1 - \phi_2)$ and $(\theta_1, \theta_2 = 1 - \theta_1)$. Let signal size w^2 be defined as in (6.10), and odds ratio R be defined as in (6.8). If $R = 1$, we have $w^2 = 0$; if $R \in (0, 1) \cup (1, +\infty)$, then we have*

$$w^2(R) = \frac{1}{4A(R-1)^2} \left(B + CR - \sqrt{(B + CR)^2 - 4A(R-1)^2} \right)^2, \quad (6.11)$$

where $A = \phi_1 \theta_1 \phi_2 \theta_2$, $B = \phi_1 \theta_1 + \phi_2 \theta_2$, and $C = \phi_1 \theta_2 + \phi_2 \theta_1$.

Proposition 6.6 is derived in Section 6.6.5.

To understand Proposition 6.6, we illustrate Relation (6.11) for selected values of marginals θ_1 and ϕ_1 in Figure 6.1. Observe in the figure that an odds ratio further away from one cor-

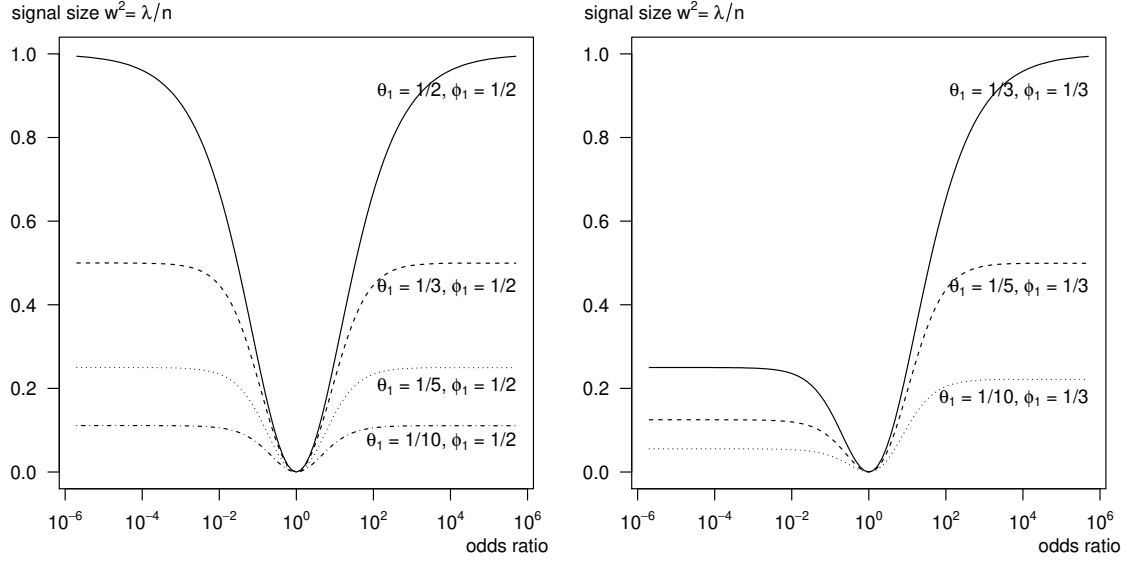


Figure 6.1: Signal sizes per sample w^2 as functions of odds ratios in 2-by-2 multinomial distributions for selected genotype marginals in balanced (left) and unbalanced (right) designs; see Relation (6.11) in Proposition 6.6. For given marginal distributions, extreme odds ratios imply stronger statistical signals at a given sample size. However, the signal sizes are bounded above by constants that depend on the marginal distributions; see Relations (6.12) and (6.13).

responds to stronger statistical signal per sample, *ceteris paribus*. However, this “valley” pattern is in general not symmetric around 1, except for balanced marginal distributions ($\phi_1 = 1/2$ or $\theta_1 = 1/2$). While the odds ratio R can be arbitrarily close to 0 or diverge to $+\infty$ for any marginal distribution, the signal sizes w^2 are bounded from above by constants that depend only on the marginals.

Corollary 6.7. *The signal size as a function of the odds ratio $w^2(R)$ is decreasing on $(0, 1)$ and increasing on $(1, \infty)$, with limits*

$$\lim_{R \rightarrow 0+} w^2(R) = \min \left\{ \frac{\phi_1 \theta_1}{\phi_2 \theta_2}, \frac{\phi_2 \theta_2}{\phi_1 \theta_1} \right\}, \quad (6.12)$$

and

$$\lim_{R \rightarrow +\infty} w^2(R) = \min \left\{ \frac{\phi_1 \theta_2}{\phi_2 \theta_1}, \frac{\phi_2 \theta_1}{\phi_1 \theta_2} \right\}. \quad (6.13)$$

Corollary 6.7 immediately implies that balanced designs with roughly equal number of

cases and controls are not necessarily the most informative.

For example, in a study where a third of the recruited subjects carry the genetic variant positively correlated with the trait (i.e., $\theta_1 = 1/3$), an unbalanced design with $\phi_1 = 1/3$ would maximize w^2 at large odds ratios. This unbalanced design is much more efficient compared to, say, a balanced design with $\phi_1 = 1/2$. In the first case, we have $w^2 \rightarrow 1$ as $R \rightarrow \infty$; whereas in the second design, $w^2 < 1/2$ no matter how large R is. This difference can also be read by comparing the dashed curve ($\theta_1 = 1/3, \phi_1 = 1/2$) in the left panel of Figure 6.1, with the solid curve ($\theta_1 = 1/3, \phi_1 = 1/3$) in the right panel of Figure 6.1.

6.3 Optimal study designs and rare variants

For a study with a fixed budget, i.e., a fixed total number of subjects n , the researcher is free to choose the fraction of cases ϕ_1 to be included in the study. A natural question is how this budget should be allocated to maximize the statistical power of discovery, or equivalently, the signal sizes $\lambda = nw^2$.

In principal, Relation (6.11) can be optimized with respect to the fraction of cases ϕ_1 in order to find optimal designs, if θ_1 is known and held constant. In practice, this is not the case. While the fraction of cases can be controlled, the distributions of genotypes *in the study* are often unknown prior to data collection, and can change with the case-to-control ratio.

Fortunately, the conditional distributions of genotypes in the healthy control groups are often estimated by existing studies, and are made available by consortia such as the NHGRI-EBI GWAS catalog MacArthur et al. (2016). We denote the conditional frequency of the first genetic variant in the control group as $(f, 1 - f)$, where

$$f := \mu_{21}/\phi_2. \quad (6.14)$$

The multinomial probability is fully parametrized by the new trio: (f, ϕ_1, R) .

Probabilities	Genotype		Total by phenotype
	Variant 1	Variant 2	
Cases	$\frac{\phi_1 f R}{f R + 1 - f}$	$\frac{\phi_1 (1 - f)}{f R + 1 - f}$	ϕ_1
Controls	$f(1 - \phi_1)$	$(1 - f)(1 - \phi_1)$	$1 - \phi_1$

Proposition 6.6 may also be re-stated in terms of the new parametrization.

Corollary 6.8. *In the 2-by-2 multinomial distribution with marginals $(\phi_1, \phi_2 = 1 - \phi_1)$, and conditional distribution of the variants in the control group $(f, 1 - f)$, Relation (6.11) holds with $\theta_1 = \phi_1 f R / (f R + 1 - f) + f(1 - \phi_1)$ and $\theta_2 = 1 - \theta_1$.*

The choice of ϕ_1 now has a practical solution.

Corollary 6.9. *In the context of Corollary 6.8, the optimal design (ϕ_1^*, ϕ_2^*) that maximizes the signal size per sample w^2 is prescribed by*

$$\phi_1^* = \frac{f R + 1 - f}{f R + 1 - f + \sqrt{R}}, \quad \text{and} \quad \phi_2^* = 1 - \phi_1^*. \quad (6.15)$$

Corollary 6.9 is proved in Section 6.6.5.

Of particular interest in the genetics literature are genetic variants with very low allele frequencies in the control group (i.e., $f \approx 0$), known as rare variants. In such cases, Equation (6.15) can be approximated using the Taylor expansion,

$$\phi_1^* = \frac{1}{1 + \sqrt{R}} + \frac{(R - \sqrt{R})f}{1 + \sqrt{R}} + O(f^2). \quad (6.16)$$

To illustrate, for rare and adversarial factors ($f \approx 0$ and $R > 1$), the optimal ϕ_1^* is less than $1/2$. Therefore, for studies under a fixed budget, controls should constitute the majority of the subjects, in order to maximize power. On the other hand, for rare and protective factors ($f \approx 0$ and $R < 1$), the optimal ϕ_1^* is greater than $1/2$, and cases should be the majority.

6.4 Phase transitions in large-scale association screening studies

Returning to the problem of *high-dimensional* marginal screenings for categorical covariates, we explore the manifestation of the phase transition in the exact-approximate support recovery problem in the genetic context.

Recall Theorem 6.3 predicts that FWER and FNR can be simultaneously controlled in large dimensions if and only if

$$r = \frac{\lambda}{2 \log p} = \frac{w^2 n}{2 \log p} > 1. \quad (6.17)$$

Therefore, if we were to apply FWER-controlling procedures at low nominal levels (say, 5%), then the FNR would experience a phase transition in the sense that, if

$$r > 1 \iff w^2 > \frac{2 \log p}{n}, \quad (6.18)$$

then the FNR can be close to 0; otherwise, FNR must be close to 1.

Using the parametric relationship described in Corollary 6.8 (and Proposition 6.6), the inequalities in (6.18) implicitly define regions of (f, R) where associations are discoverable with high power, for a given ϕ_1 . Further, the boundary of such discoverable regions sharpens as dimensionality diverges. We illustrate this phase transition through a numerical example next.

Example 6.10. Consider association tests on 2×2 contingency tables at p locations as introduced in Section 1.2, where the counts follow a multinomial distribution parametrized by (f, R, ϕ_1) as in Section 6.3. Assume that the phenotype marginals are fixed at $\phi_1 = \phi_2 = 1/2$. Applying Bonferroni's procedure with nominal FWER at $\alpha = 5\%$ level, we can

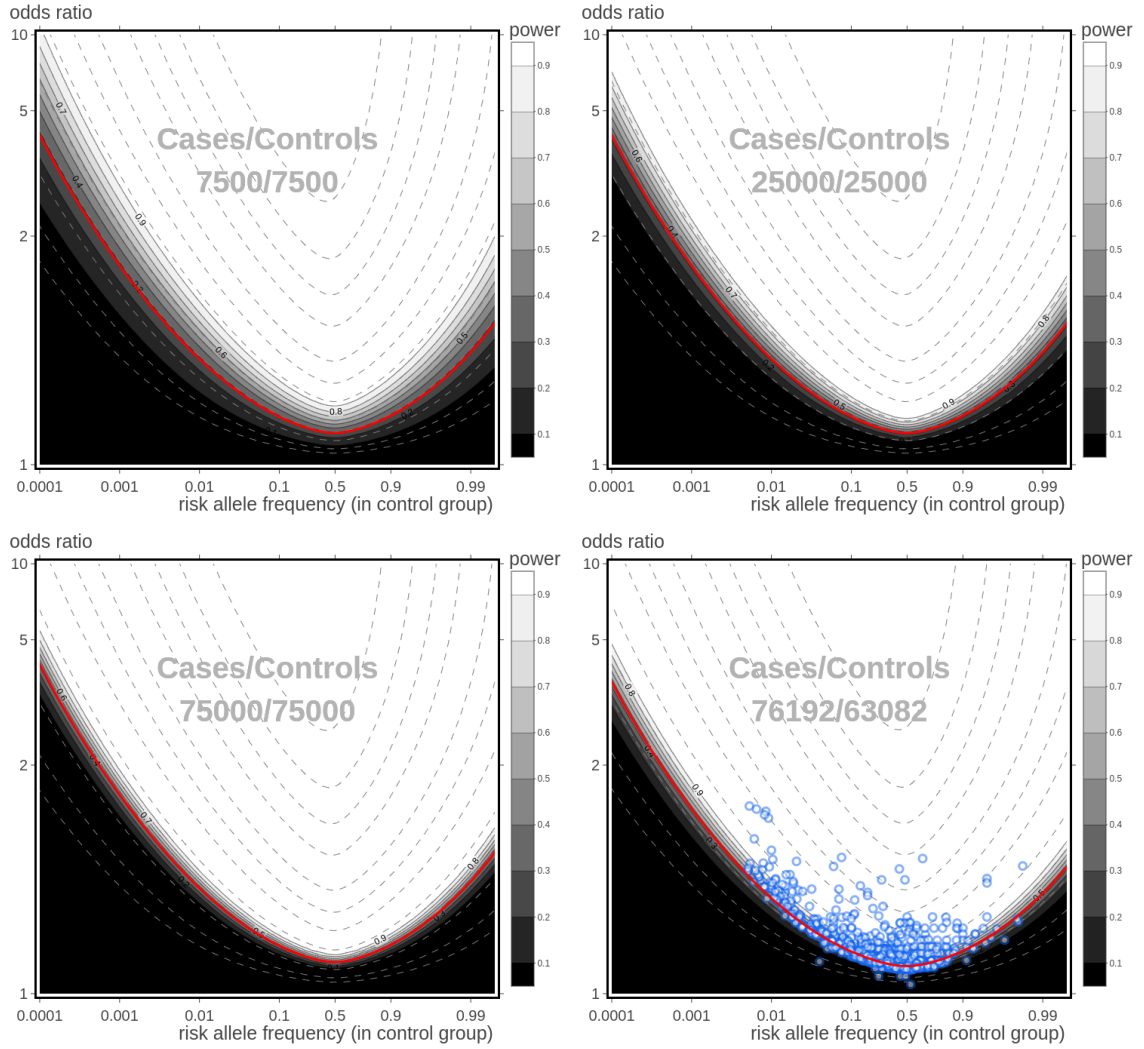


Figure 6.2: The OR-RAF diagram visualizing the marginal power of discovery in genetic association studies, after applying Bonferroni's procedure with nominal FWER at 5% level. Sample sizes are marked in each panel, and the problem dimensions are, respectively, $p = 4$ (upper-left), $p = 10^2$ (upper-right), and $p = 10^6$ (lower-left), so that $n/\log p$ are roughly constant. Red curves mark the boundaries ($r = 1$) of the phase transition for the exact-approximate support recovery problem; dashed curves are the equi-signal (equi-power) curves. The phase transition in signal sizes λ translates into the phase transition in terms of (f, R) , and sharpens as $p \rightarrow \infty$; see Example 6.10. In the lower-right panel, we visualize discovered associations (blue circles) in a recent GWA study (Michailidou et al. (2017)); the estimated odds ratios and risk allele frequencies are subject to survival bias and should not be taken at their face values; see Remark 6.11.

approximate the marginal power of association tests by

$$\mathbb{P}[\chi_1^2(\lambda) > \chi_{1,\alpha/p}^2], \quad (6.19)$$

where $\chi_{1,\alpha/p}^2$ is the upper (α/p) -quantile of a central chi-squared distribution with 1 degree of freedom. We calculate this marginal power as a function of the parameters (f, R) in three scenarios:

- $p = 4, n = 3 \times 10^4$
- $p = 10^2, n = 1 \times 10^5$
- $p = 10^6, n = 3 \times 10^6$

and visualize the results as heatmaps¹ (referred to as OR-RAF diagrams) in Figure 6.2. These parameter values are chosen so that $\log p/n$ are roughly constant (around 4.6×10^{-5}).

We also overlay “equi-signal” curves, i.e., functions implicitly defined by the equations $r = c$ for a range of c (dashed curves), and highlight the predicted boundary of phase transition for the exact-approximate support recovery problem $r = 1$ (red curves). The change in marginal power clearly sharpens around the predicted boundary $r = 1$ as dimensionality diverges.

Remark 6.11. In an attempt to find empirical evidence of our theoretical predictions, we chart the genetic variants associated with breast cancer, discovered in a 2017 study by Michailidou et al. (2017) in an OR-RAF diagram. The estimated risk allele frequencies (f) and odds ratios (R) are taken from the NHGRI-EBI GWAS catalog MacArthur et al. (2016), and plotted against a power heatmap calculated according to the reported sample sizes. See lower-right panel of Figure 6.2.

¹Since genetic variants can always be relabelled such that Variant 1 is positively associated with Cases, we only produce part of the diagram where $R > 1$. Sample sizes marked in the figure are adjusted by a factor of $1/2$, to reflect the genetic context where a pair of alleles are measured for every individual at every genomic location.

It is tempting to believe, on careless inspection, that roughly *all* discovered associations fall inside the high power region of the diagram, therefore demonstrating the phase transition in statistical power. Unfortunately, the estimates here are subject to survival bias — the study in fact uses the same dataset for *both* support estimation and parameter estimation, without adjusting the latter for the selection process. The seemingly striking agreement between the power calculations and the estimated effects of reported associations *should not* be taken as evidence for the validity of our theory. We conjecture, as the theory predicts, that accurate and unbiased parameter estimates from an independent replication will still place the associations in the high power region of the diagram.

Finally, we demonstrate with an example how results in Sections 6.1 and 6.2 may be used for planning prospective association studies.

Example 6.12. In a GWAS with $p = 10^6$ genomic marker locations, researchers wish to locate genetic associations with the trait of interest. Specifically, they wish to maximize power in the region where genetic variants have risk allele frequencies of 0.01 and odds ratios of 1.2. By Corollary 6.9, the optimal design has a fraction of cases $\phi^* = 0.478$, yielding the statistical signal size per sample $w^2 \approx 9.00 \times 10^{-5}$ according to Corollary 6.8.

If we wish to achieve exact-approximate support recovery in the sense of (2.24), Theorem 6.3 predicts that the signal size parameter r has to be at least $\tilde{g}(\beta) = 1$. This signal size calls for a sample size of $n = \lambda/w^2 = 2r \log(p)/w^2 \approx 307,011$. In a typically GWAS, a pair of alleles are sequenced for every marker location, bringing the required number of subjects in the study to $n/2 \approx 153,509$.

In comparison, a more accurate power calculation directly using (6.19) predicts that $n/2 = 165,035$ subjects are needed, under the set of parameters ($p = 10^6$, $f = 0.01$, $R = 1.2$) and FWER = 0.05, FNR = 0.5; this is 7% higher than our crude asymptotic approximation. In general, we recommend using the more precise calculations over the back-of-the-envelope asymptotics for planning prospective studies and performing systematic reviews; a user-friendly web application implementing the more precise approximations is

provided in Gao et al. (2019). Nevertheless, the theoretical results on phase transitions generate simple, accurate, and powerful insights that cannot be easily derived from numerical calculations.

6.5 Numerical illustrations of the phase transitions in chi-square models

We illustrate with simulations the phase transition phenomena in the chi-square model, and compare numerically the required signal sizes in support recovery problems between the two types of alternatives in the additive error model.

6.5.1 Exact support recovery

The sparsity of the signal vectors in the experiments are parametrized as in (6.2). Signal sizes are assumed equal with magnitude $\lambda(i) = 2r \log p$ for $i \in S$. We estimate the support set S using Bonferroni's procedure with nominal FWER level set at $1/(5 \log p)$. The nominal FWER levels vanishes slowly, in line with the assumptions in Theorem 6.1. Experiments were repeated 1000 times at each of the 400 sparsity-signal-size combinations, for dimensions $p = 10^2, 10^3$, and 10^4 .

The empirical probabilities of exact support recovery under Bonferroni's procedure are shown in Figure 6.3. The numerical results suggest not only good accuracy of the predicted boundaries in high-dimensions ($p = 10^4$, right panels of Figure 6.3), but also practical relevance of the theoretical predictions in moderate dimensions ($p = 100$, left panels of Figure 6.3).

We conduct further experiments to examine the optimality claims in Theorem 6.1 by comparing with the oracle procedure with thresholds $t_p = \min_{i \in S} x(i)$. We also examine the claims in Section 6.1.5, and compare the one-sided alternatives in Gaussian additive models with the two-sided alternatives (or equivalently, the chi-square model with $\nu = 1$).

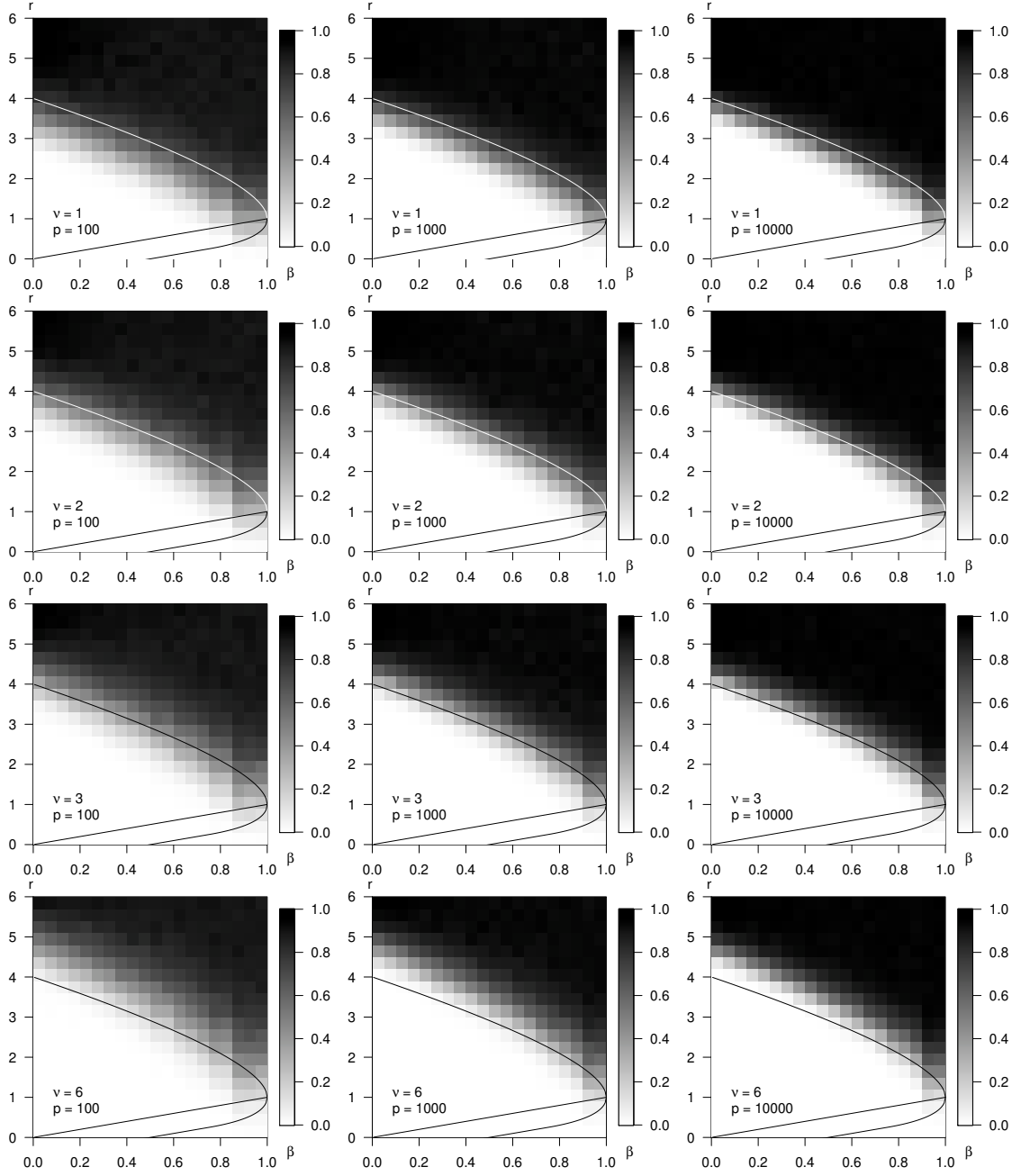


Figure 6.3: The empirical probability of exact support recovery of Bonferroni's procedure in the chi-squared model (1.3). We simulate $\nu = 1, 2, 3, 6$ (first to last row), at dimensions $p = 10^2, 10^3, 10^4$ (left to right column), for a grid of sparsity levels β and signal sizes r . The experiments were repeated 1000 times for each sparsity-signal size combination; darker color indicates higher probability of exact support recovery. Numerical results are in general agreement with the boundaries described in Theorem 6.1; for large ν 's, the phase transitions take place somewhat above the predicted boundaries. The boundary for the approximate support recovery (Theorem 6.4) and the detection boundary (see Donoho and Jin (2004)) are plotted for comparison.

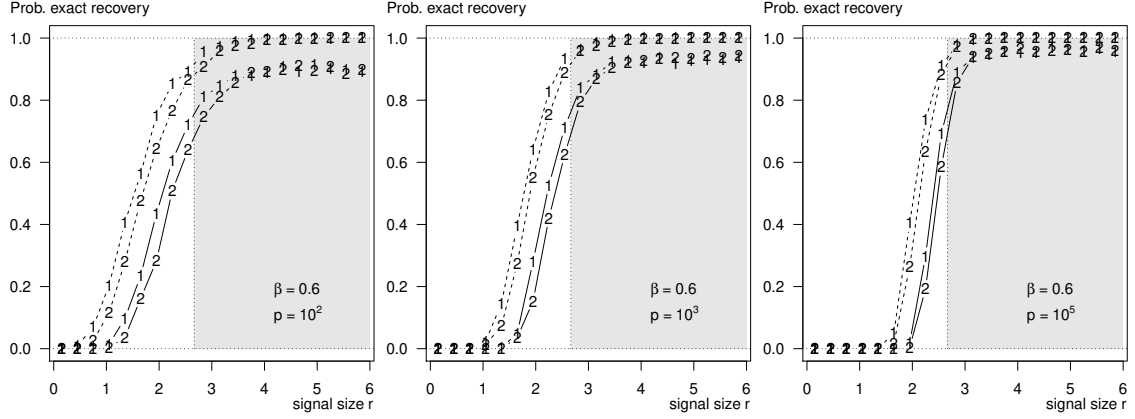


Figure 6.4: The empirical probability of exact support recovery of Bonferroni's procedure (solid curves) and the oracle procedure (dashed curves) in the chi-squared model with one degree of freedom (marked '2') in the additive Gaussian error model and under one-sided alternatives (marked '1'). We simulate at dimensions $p = 10^2, 10^3, 10^5$ (left to right) for a grid of signal sizes r and sparsity level $\beta = 0.6$. The experiments were repeated 1000 times for each method-model-signal-size combination. Numerical results show evidence of convergence to the 0-1 law as predicted by Theorem 6.1; regions where asymptotically exact support recovery can be achieved are shaded in grey. The difference in power between Bonferroni's procedure and the oracle procedure, as well as in the two types of alternatives both decrease as dimensionality increases.

We apply Bonferroni's procedure and the oracle thresholding procedure in both settings.

Experiments were repeated 1000 times for a grid of signal size values ranging from $r = 0$ to 6, and for dimensions $10^2, 10^3$, and 10^5 . Results of the experiments, shown in Figure 6.4, suggest vanishing difference between difficulties of two-sided vs one-sided alternatives in the additive error models, as well as vanishing difference between the powers of Bonferroni's procedures and the oracle procedures as $p \rightarrow \infty$.

6.5.2 Approximate, and approximate-exact support recovery

Similar experiments are conducted to examine the optimality claims in Theorem 6.4, and in Section 6.1.5. We define an oracle thresholding procedure for approximate support recovery, where the threshold is chosen to minimize the empirical risk. That is,

$$t_p(x, S) \in \arg \min_{t \in \mathbb{R}} \frac{|\hat{S}(t) \setminus S|}{\max\{|\hat{S}(t)|, 1\}} + \frac{|S \setminus \hat{S}(t)|}{\max\{|S|, 1\}},$$

where $\widehat{S}(t) = \{i \mid x(i) \geq t\}$; in implementation, we only need to scan the values of observations $t \in \{x(1), \dots, x(p)\}$. The nominal FDR level for the BH procedure is set at $1/(5\log p)$, therefore slowly vanishing, in line with the assumptions in Theorem 6.4; all other parameters are identical to that in the experiments for exact support recovery. Results of the experiments are shown in Figure 6.5 and Figure 6.6.

We also examine the boundary described in Theorem 6.3. Experimental settings are identical to that in the experiments for approximate support recovery. We compare the performance of the BH procedure with an oracle procedure with threshold

$$t_p(x, S) \in \min_{i \in S} x(i),$$

and visualize results of the experiments in Figure 6.7. Notice that the BH procedure sets its threshold somewhat higher than the oracle, especially for small β 's. The empirical risk of the oracle procedure (not shown here in the interest of space) follows much more closely the predicted boundary (6.7).

6.6 Proofs

We review some properties of the chi-square distributions in Section 6.6.1, before presenting the proofs of the main theorems on phase transitions in Sections 6.6.2, 6.6.3, and 6.6.4. Results relating signal sizes and effect sizes in association tests will be justified in Section 6.6.5.

6.6.1 Auxiliary facts of chi-square distributions

We shall recall, and establish, some auxiliary facts about chi-square distributions. These facts will be used in the proofs of Theorem 6.1 and Theorem 6.4.

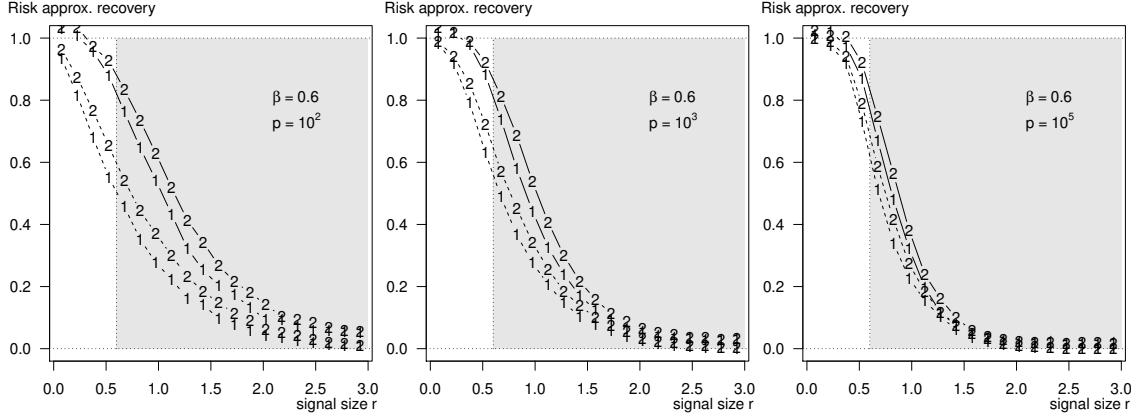


Figure 6.5: The empirical risk of approximate support recovery of Benjamini-Hochberg's procedure (solid curves) and the oracle procedure (dashed curves) in the chi-squared model with one degree of freedom (marked '2') and in the additive Gaussian error model under one-sided alternatives (marked '1'). We simulate at dimensions $p = 10^2, 10^3, 10^5$ (left to right) for a grid of signal sizes r and sparsity level $\beta = 0.6$. The experiments were repeated 1000 times for each method-model-signal-size combination. Numerical results show evidence of convergence to the 0-1 law as predicted by Theorem 6.4; regions where asymptotically approximate support recovery can be achieved are shaded in grey. The difference in risks between Benjamini-Hochberg's procedure and the oracle procedure, as well as in the two types of alternatives, both decrease as dimensionality increases.

Lemma 6.13 (Rapid variation of chi-square distribution tails). *The central chi-square distribution with ν degrees of freedom has rapidly varying tails. That is,*

$$\lim_{x \rightarrow \infty} \frac{\mathbb{P}[\chi_\nu^2(0) > tx]}{\mathbb{P}[\chi_\nu^2(0) > x]} = \begin{cases} 0, & t > 1 \\ 1, & t = 1 \\ \infty, & 0 < t < 1 \end{cases}, \quad (6.20)$$

where we overloaded the notation $\chi_\nu^2(0)$ to represent a random variable with the chi-square distribution.

Proof of Lemma 6.13. When $\nu = 1$, the chi-square distribution reduces to a squared Normal, and (6.20) follows from the rapid variation of the standard Normal distribution. For

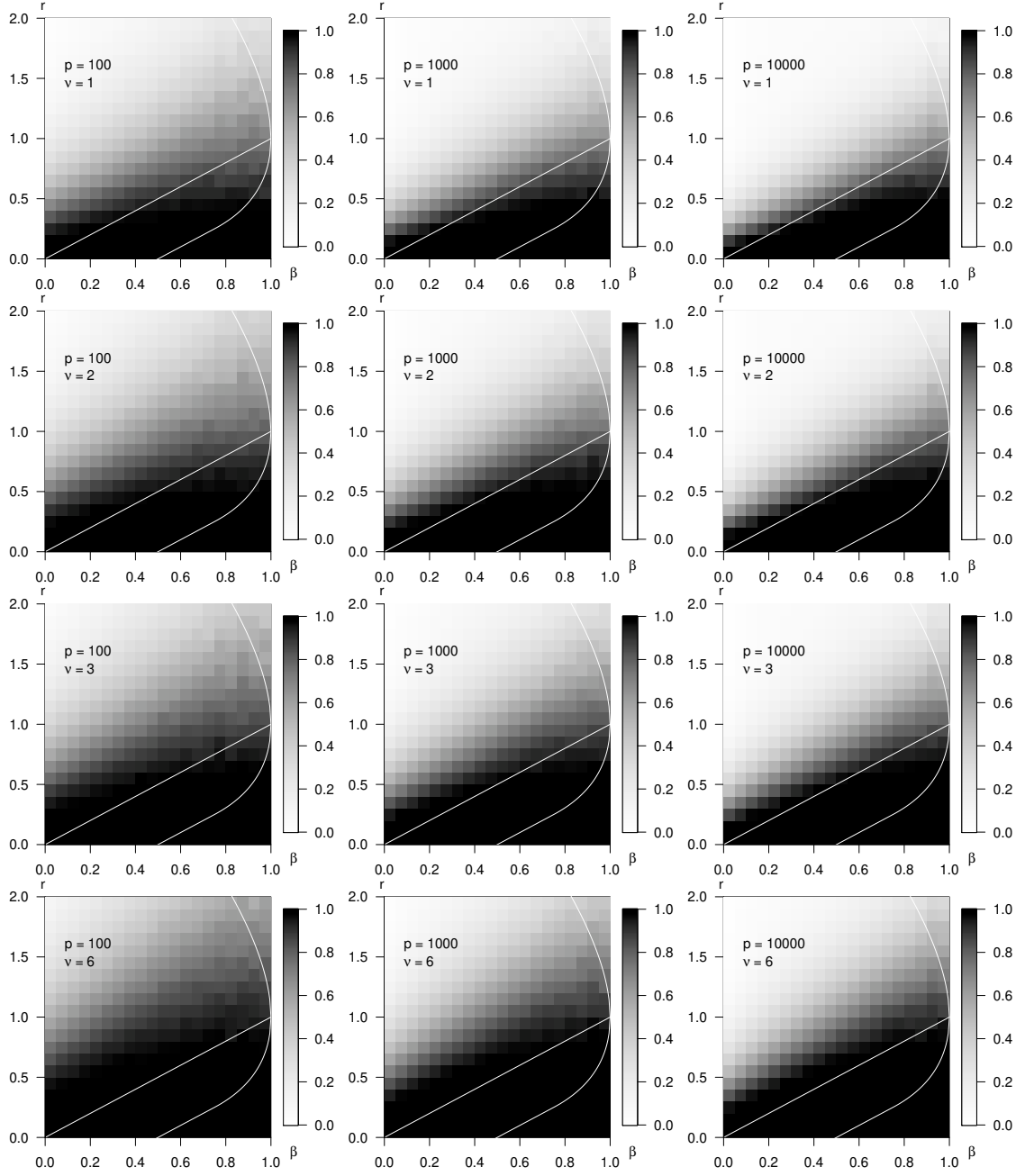


Figure 6.6: The estimated risk of approximate support recovery risk^A (see (2.7)) of the Benjamini-Hochberg procedure in the chi-squared model (1.3). We simulate $\nu = 1, 2, 3, 6$ (first to last row), at dimensions $p = 10^2, 10^3, 10^4$ (left to right column), for a grid of sparsity levels β and signal sizes r . The experiments were repeated 1000 times for each sparsity-signal size combination; darker color indicates higher larger risk^A. Numerical results are generally in agreement with the boundaries described in Theorem 6.4; for large ν 's, the phase transitions take place somewhat above the predicted boundaries. The boundary for the exact support recovery problem (Theorem 6.1) and the detection boundary (see Donoho and Jin (2004)) are plotted for comparison.

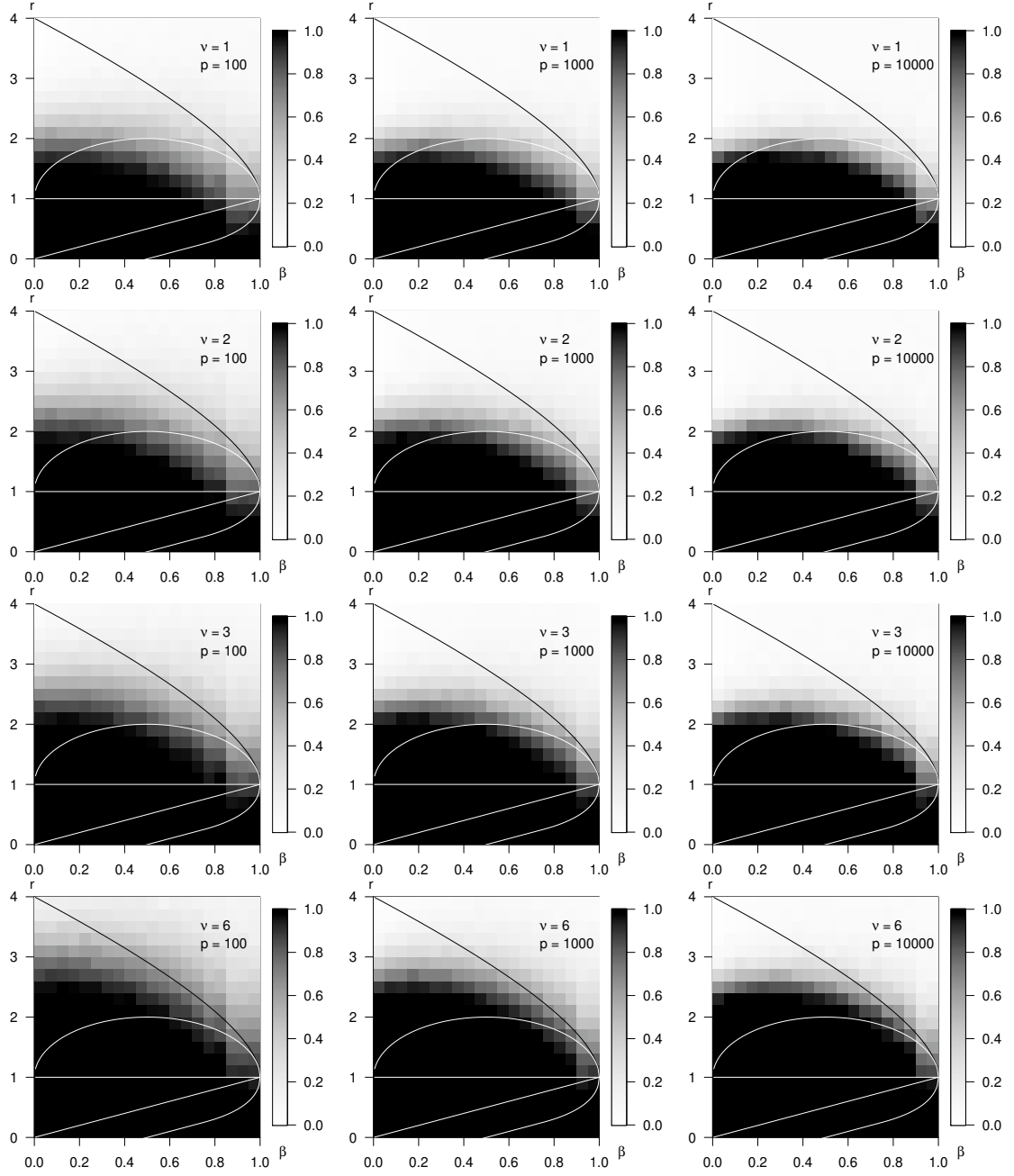


Figure 6.7: The estimated risk of approximate-exact support recovery risk^{EA} (see (2.12)) of the Benjamini-Hochberg procedure in the chi-squared model (1.3). We simulate $\nu = 1, 2, 3, 6$ (first to last row), at dimensions $p = 10^2, 10^3, 10^4$ (left to right column), for a grid of sparsity levels β and signal sizes r . The experiments were repeated 1000 times for each sparsity-signal size combination; darker color indicates higher larger risk^{EA}. Numerical results are generally in agreement with the boundaries described in Theorem 6.5; for small β 's and large ν 's, the phase transitions take place somewhat above the predicted boundaries. Other boundaries in the support recovery and the detection problems are plotted for comparison.

$\nu \geq 2$, we recall the following bound on tail probabilities (see, e.g., (Ingolot, 2010)),

$$\frac{1}{2}\mathcal{E}_\nu(x) \leq \mathbb{P}[\chi_\nu^2(0) > x] \leq \frac{x}{(x - \nu + 2)\sqrt{\pi}}\mathcal{E}_\nu(x), \quad \nu \geq 2, \ x > \nu - 2,$$

where $\mathcal{E}_\nu(x) = \exp\left\{-\frac{1}{2}[(x - \nu - (\nu - 2)\log(x/\nu) + \log \nu)]\right\}$. Therefore, we have

$$\frac{(x - \nu + 2)\sqrt{\pi}}{2x} \frac{\mathcal{E}_\nu(tx)}{\mathcal{E}_\nu(x)} \leq \frac{\mathbb{P}[\chi_\nu^2(0) > tx]}{\mathbb{P}[\chi_\nu^2(0) > x]} \leq \frac{2tx}{(tx - \nu + 2)\sqrt{\pi}} \frac{\mathcal{E}_\nu(tx)}{\mathcal{E}_\nu(x)},$$

where $\mathcal{E}_\nu(tx)/\mathcal{E}_\nu(x) = \exp\left\{-\frac{1}{2}[(t - 1)x - (\nu - 2)\log t]\right\}$ converges to 0 or ∞ depending on whether $t > 1$ or $0 < t < 1$. The case where $t = 1$ is trivial. \square

Lemma 6.13 and Proposition 2.11 yield the following Corollary.

Corollary 6.14. *Maxima of independent observations from central chi-square distributions with ν degrees of freedom are relatively stable. Specifically, let $\epsilon_p = (\epsilon_p(i))_{i=1}^p$ be independently and identically distributed (iid) $\chi_\nu^2(0)$ random variables. Then the triangular array $\mathcal{E} = \{\epsilon_p, p \in \mathbb{N}\}$ has relatively stable (RS) maxima in the sense of (2.37).*

Lemma 6.15 (Stochastic monotonicity). *The non-central chi-square distribution is stochastically monotone in its non-centrality parameter. Specifically, for two non-central chi-square distributions both with ν degrees of freedom, and non-centrality parameters $\lambda_1 \leq \lambda_2$, we have $\chi_\nu^2(\lambda_1) \stackrel{d}{\leq} \chi_\nu^2(\lambda_2)$. That is,*

$$\mathbb{P}[\chi_\nu^2(\lambda_1) \leq t] \geq \mathbb{P}[\chi_\nu^2(\lambda_2) \leq t], \quad \text{for any } t \geq 0. \quad (6.21)$$

where we overloaded the notation $\chi_\nu^2(\lambda)$ to represent a random variable with the chi-square distribution with non-centrality parameter λ and degree-of-freedom parameter ν .

Proof of Lemma 6.15. Recall that non-central chi-square distributions can be written as sums of $\nu - 1$ standard normal random variables and a non-central normal random variable

with mean $\sqrt{\lambda}$ and variance 1,

$$\chi_\nu^2(\lambda) \stackrel{d}{=} Z_1^2 + \dots + Z_{\nu-1}^2 + (Z_\nu + \sqrt{\lambda})^2.$$

Therefore, it suffices to show that $\mathbb{P}[(Z + \sqrt{\lambda})^2 \leq t]$ is non-increasing in λ for any $t \geq 0$, where Z is a standard normal random variable. We rewrite this expression in terms of standard normal probability function Φ ,

$$\begin{aligned} \mathbb{P}[(Z + \sqrt{\lambda})^2 \leq t] &= \mathbb{P}[-\sqrt{\lambda} - \sqrt{t} \leq Z \leq -\sqrt{\lambda} + \sqrt{t}] \\ &= \Phi(-\sqrt{\lambda} + \sqrt{t}) - \Phi(-\sqrt{\lambda} - \sqrt{t}). \end{aligned} \quad (6.22)$$

The derivative of the last expression (with respect to λ) is

$$\frac{1}{2\sqrt{\lambda}} \left(\phi(\sqrt{\lambda} + \sqrt{t}) - \phi(\sqrt{\lambda} - \sqrt{t}) \right) = \frac{1}{2\sqrt{\lambda}} \left(\phi(\sqrt{\lambda} + \sqrt{t}) - \phi(\sqrt{t} - \sqrt{\lambda}) \right), \quad (6.23)$$

where ϕ is the density of the standard normal distribution. Notice that we have used the symmetry of ϕ around 0 in the last expression.

Since $0 \leq \max\{\sqrt{\lambda} - \sqrt{t}, \sqrt{t} - \sqrt{\lambda}\} < \sqrt{t} + \sqrt{\lambda}$ when $t > 0$, by monotonicity of the normal density on $(0, \infty)$, we conclude that the derivative (6.23) is indeed negative. Therefore, (6.22) is decreasing in λ , and (6.21) follows for $t > 0$. For $t = 0$, equality holds in (6.21) with both probabilities being 0. \square

Finally, we derive asymptotic expressions for chi-square quantiles.

Lemma 6.16 (Chi-square quantiles). *Let F be the central chi-square distributions with ν degrees of freedom, and let $u(y)$ be the $(1 - y)$ -th generalized quantile of F , i.e.,*

$$u(y) = F^{\leftarrow}(1 - y). \quad (6.24)$$

Then

$$u(y) \sim 2 \log(1/y), \quad \text{as } y \rightarrow 0. \quad (6.25)$$

Proof of Lemma 6.16. The case where $\nu = 1$ follows from the well-known formula for Normal quantiles (see, e.g., Proposition 1.1 in Gao and Stoev (2019))

$$F^{\leftarrow}(1 - y) = \Phi^{\leftarrow}(1 - y/2) \sim \sqrt{2 \log(2/y)} \sim \sqrt{2 \log(1/y)}.$$

The case where $\nu \geq 2$ follows from the following estimates of high quantiles of chi-square distributions (see, e.g., (Ingolot, 2010)),

$$\nu + 2 \log(1/y) - 5/2 \leq u(y) \leq \nu + 2 \log(1/y) + 2\sqrt{\nu \log(1/y)}, \quad \text{for all } y \leq 0.17,$$

where both the lower and upper bound are asymptotic to $2 \log(1/y)$. □

6.6.2 Proof of Theorem 6.1

Proof of Theorem 6.1. We first prove the sufficient condition. The Bonferroni procedure sets the threshold at $t_p = F^{\leftarrow}(1 - \alpha/p)$, which, by Lemma 6.16, is asymptotic to $2 \log p - 2 \log \alpha$. By the assumption on α in (3.8), for any $\delta > 0$, we have $p^{-\delta} = o(\alpha)$. Therefore, we have $-\log \alpha \leq \delta \log p$ for large p , and

$$1 \leq \limsup_{p \rightarrow \infty} \frac{2 \log p - 2 \log \alpha}{2 \log p} \leq 1 + \delta,$$

for any $\delta > 0$. Hence, $t_p \sim 2 \log p$.

The condition $\underline{r} > g(\beta)$ implies, after some algebraic manipulation, $\sqrt{\underline{r}} - \sqrt{1 - \beta} > 1$. Therefore, we can pick $q > 1$ such that

$$\sqrt{\underline{r}} - \sqrt{1 - \beta} > \sqrt{q} > 1. \quad (6.26)$$

Setting the $t^* = t_p^* = 2q \log p$, we have $t_p < t_p^*$ for large p .

On the one hand, $\text{FWER} = 1 - \mathbb{P}[\widehat{S}_p \subseteq S_p]$ vanishes under the Bonferroni procedure with $\alpha \rightarrow 0$. On the other hand, for large p , the probability of no missed detection is bounded from below by

$$\mathbb{P}[\widehat{S}_p \supseteq S_p] = \mathbb{P}[\min_{i \in S} x(i) \geq t_p] \geq \mathbb{P}[\min_{i \in S} x(i) \geq t^*] \geq 1 - p^{1-\beta} \mathbb{P}[\chi_\nu^2(\underline{\Delta}) < t^*], \quad (6.27)$$

where we have used the fact that signal sizes are bounded below by $\underline{\Delta}$, and the stochastic monotonicity of chi-square distributions (Lemma 6.15) in the last inequality. Writing

$$\chi_\nu^2(\underline{\Delta}) \stackrel{d}{=} Z_1^2 + \dots + Z_{\nu-1}^2 + (Z_\nu + \sqrt{\underline{\Delta}})^2$$

where Z_i 's are iid standard normal variables, we have

$$\begin{aligned} \mathbb{P}[\chi_\nu^2(\underline{\Delta}) < t^*] &\leq \mathbb{P}[(Z_\nu + \sqrt{\underline{\Delta}})^2 < t^*] = \mathbb{P}[|Z_\nu + \sqrt{\underline{\Delta}}| < \sqrt{t^*}] \\ &\leq \mathbb{P}\left[Z_\nu < -\sqrt{\underline{\Delta}} + \sqrt{t^*}\right] \\ &= \mathbb{P}\left[Z_\nu < \sqrt{2 \log p} (\sqrt{q} - \sqrt{r})\right]. \end{aligned} \quad (6.28)$$

By our choice of q in (6.26), the last probability in (6.28) can be bounded from above by

$$\begin{aligned} \mathbb{P}\left[Z_\nu < -\sqrt{2(1-\beta) \log p}\right] &\sim \frac{\phi\left(-\sqrt{2(1-\beta) \log p}\right)}{\sqrt{2(1-\beta) \log p}} \\ &= \frac{1}{\sqrt{2(1-\beta) \log p}} p^{-(1-\beta)}, \end{aligned}$$

where the first line uses Mill's ratio for Gaussian distributions (see Section 3.3.1 and Relation (3.15)). This, combined with (6.27), completes the proof of the sufficient condition for the Bonferroni's procedure.

Under the assumption of independence, Sidák's, Holm's, and Hochberg's procedures

are strictly more powerful than Bonferroni's procedure, while controlling FWER at the nominal levels. Therefore, the risks of exact support recovery for these procedures also vanishes. This completes the proof for the first part of Theorem 6.1.

We now show the necessary condition. We first normalize the maxima by the chi-square quantiles $u_p = F^{\leftarrow}(1 - 1/p)$, where F is the distribution of a (central) chi-square random variable,

$$\mathbb{P}[\widehat{S}_p = S_p] \leq \mathbb{P}[M_{S^c} < t_p \leq m_S] \leq \mathbb{P}\left[\frac{M_{S^c}}{u_p} < \frac{m_S}{u_p}\right], \quad (6.29)$$

where $M_{S^c} = \max_{i \in S^c} x(i)$ and $m_S = \min_{i \in S} x(i)$. By the relative stability of chi-square random variables (Corollary 6.14), we know that $M_{S^c}/u_{|S^c|} \rightarrow 1$ in probability. Further, using the expression for u_p (Lemma 6.16), we obtain

$$\frac{u_{p-p^{1-\beta}}}{u_p} \sim \frac{2 \log(p - p^{1-\beta})}{2 \log p} = \frac{\log p + \log(1 - p^{-\beta})}{\log p} \sim 1.$$

Therefore, the left-hand-side of the last probability in (6.29) converges to 1,

$$\frac{M_{S^c}}{u_p} = \frac{M_{S^c}}{u_{p-p^{1-\beta}}} \frac{u_{p-p^{1-\beta}}}{u_p} \xrightarrow{\mathbb{P}} 1. \quad (6.30)$$

Meanwhile, for any $i \in S$, by Lemma 6.15 and the fact that signal sizes are bounded above by $\overline{\Delta}$, we have,

$$\chi_\nu^2(\lambda(i)) \stackrel{d}{\leq} \chi_\nu^2(\overline{\Delta}) \stackrel{d}{=} Z_1^2 + \dots + Z_{\nu-1}^2 + \left(Z_\nu + \sqrt{\overline{\Delta}}\right)^2.$$

Dividing through by u_p , and taking minimum over S , we obtain

$$\frac{m_S}{u_p} = \min_{i \in S} \frac{\chi_\nu^2(\lambda(i))}{u_p} \stackrel{d}{\leq} \min_{i \in S} \left\{ \frac{Z_1^2(i) + \dots + Z_{\nu-1}^2(i)}{u_p} + \frac{(Z_\nu(i) + \sqrt{\overline{\Delta}})^2}{u_p} \right\}. \quad (6.31)$$

Let $i^\dagger = i_p^\dagger$ be the index minimizing the second term in (6.31), i.e.,

$$i^\dagger := \arg \min_{i \in S} \frac{(Z_\nu(i) + \sqrt{\Delta})^2}{u_p} = \arg \min_{i \in S} f_p(Z_\nu(i)), \quad (6.32)$$

where $f_p(x) := (x + \sqrt{\Delta})^2 / (2 \log p)$. We shall first show that

$$\mathbb{P}[f_p(Z_\nu(i^\dagger)) < 1 - \delta] \rightarrow 1, \quad (6.33)$$

for some small $\delta > 0$. On the one hand, we know (by solving a quadratic inequality) that

$$f_p(x) < 1 - \delta \iff \frac{x}{\sqrt{2 \log p}} \in (-(\sqrt{\bar{r}} + \sqrt{1 - \delta}), -(\sqrt{\bar{r}} - \sqrt{1 - \delta})). \quad (6.34)$$

On the other hand, we know (by relative stability of iid Gaussians Gao and Stoev (2019)) that

$$\frac{\min_{i \in S} Z_\nu(i)}{\sqrt{2 \log p}} \rightarrow -\sqrt{1 - \beta} \quad \text{in probability.} \quad (6.35)$$

Further, by the assumption on the signal sizes $\bar{r} < (1 + \sqrt{1 - \beta})^2$, we have,

$$-(\sqrt{\bar{r}} + 1) < -1 < -\sqrt{1 - \beta} < -(\sqrt{\bar{r}} - 1).$$

Therefore we can picking a small $\delta > 0$ such that

$$-(\sqrt{\bar{r}} + 1) < -(\sqrt{\bar{r}} + \sqrt{1 - \delta}) < -\sqrt{1 - \beta} < -(\sqrt{\bar{r}} - \sqrt{1 - \delta}) < -(\sqrt{\bar{r}} - 1). \quad (6.36)$$

Combining (6.34), (6.35), and (6.36), we obtain

$$\begin{aligned} \mathbb{P} \left[\min_{i \in S} f_p(Z_\nu(i)) < 1 - \delta \right] &= \mathbb{P} [f_p(Z_\nu(i^\dagger)) < 1 - \delta] \\ &\geq \mathbb{P} \left[f_p \left(\min_{i \in S} Z_\nu(i) \right) < 1 - \delta \right] \rightarrow 1, \end{aligned}$$

and we arrive at (6.33). As a corollary, since $u_p \sim 2 \log p$, it follows that

$$\mathbb{P} \left[\min_{i \in S} \frac{(Z_\nu(i) + \sqrt{\Delta})^2}{u_p} < 1 - \delta \right] \rightarrow 1. \quad (6.37)$$

Finally, by independence between $Z_1^2(i) + \dots + Z_{\nu-1}^2(i)$ and $(Z_\nu(i) + \sqrt{\Delta})^2$, and the fact that i^\dagger is a function of only the latter, we have

$$Z_1^2(i^\dagger) + \dots + Z_{\nu-1}^2(i^\dagger) \stackrel{d}{=} Z_1^2(i) + \dots + Z_{\nu-1}^2(i) \quad \text{for all } i \in S.$$

Therefore, $Z_1^2(i^\dagger) + \dots + Z_{\nu-1}^2(i^\dagger) = O_{\mathbb{P}}(1)$, and

$$\frac{Z_1^2(i^\dagger) + \dots + Z_{\nu-1}^2(i^\dagger)}{u_p} \rightarrow 0 \quad \text{in probability.} \quad (6.38)$$

Together, (6.37) and (6.38) imply that

$$\begin{aligned} \mathbb{P} \left[\frac{m_S}{u_p} < 1 - \delta \right] &\geq \mathbb{P} \left[\min_{i \in S} \left\{ \frac{Z_1^2(i) + \dots + Z_{\nu-1}^2(i)}{u_p} + \frac{(Z_\nu(i) + \sqrt{\Delta})^2}{u_p} \right\} < 1 - \delta \right] \\ &\geq \mathbb{P} \left[\frac{Z_1^2(i^\dagger) + \dots + Z_{\nu-1}^2(i^\dagger)}{u_p} + \frac{(Z_\nu(i^\dagger) + \sqrt{\Delta})^2}{u_p} < 1 - \delta \right] \rightarrow 1. \end{aligned} \quad (6.39)$$

In view of (6.29), (6.30), and (6.39), we conclude that exact recovery cannot succeed with any positive probability. The proof of the necessary condition is complete. \square

6.6.3 Proof of Theorem 6.4

We first show the necessary condition. That is, when $\bar{r} < \beta$, no thresholding procedure is able to achieve approximate support recovery.

The proof follows the ideas in Arias-Castro and Chen (2017), and is very similar to the proof of Theorem 3.4. One could in principle obtain the proofs in this section by

referencing arguments that have appeared in Section 3.3. We choose to present the the proof here in full to make this section self-contained.

Proof of necessary condition in Theorem 6.4. Denote the distributions of $\chi_\nu^2(0)$, $\chi_\nu^2(\underline{\Delta})$ and $\chi_\nu^2(\overline{\Delta})$ as F_0 , $F_{\underline{a}}$, and $F_{\overline{a}}$ respectively.

Recall that thresholding procedures are of the form

$$\widehat{S}_p = \{i \mid x(i) > t_p(x)\}.$$

Denote $\widehat{S} := \{i \mid x(i) > t_p(x)\}$, and $\widehat{S}(u) := \{i \mid x(i) > u\}$. For any threshold $u \geq t_p$ we must have $\widehat{S}(u) \subseteq \widehat{S}$, and hence

$$\text{FDP} := \frac{|\widehat{S} \setminus S|}{|\widehat{S}|} \geq \frac{|\widehat{S} \setminus S|}{|\widehat{S} \cup S|} = \frac{|\widehat{S} \setminus S|}{|\widehat{S} \setminus S| + |S|} \geq \frac{|\widehat{S}(u) \setminus S|}{|\widehat{S}(u) \setminus S| + |S|}. \quad (6.40)$$

On the other hand, for any threshold $u \leq t_p$ we must have $\widehat{S}(u) \supseteq \widehat{S}$, and hence

$$\text{NDP} := \frac{|S \setminus \widehat{S}|}{|S|} \geq \frac{|S \setminus \widehat{S}(u)|}{|S|}. \quad (6.41)$$

Since either $u \geq t_p$ or $u \leq t_p$ must take place, putting (6.40) and (6.41) together, we have

$$\text{FDP} + \text{NDP} \geq \frac{|\widehat{S}(u) \setminus S|}{|\widehat{S}(u) \setminus S| + |S|} \wedge \frac{|S \setminus \widehat{S}(u)|}{|S|}, \quad (6.42)$$

for any u . Therefore it suffices to show that for a suitable choice of u , the RHS of (6.42) converges to 1 in probability; the desired conclusion on FDR and FNR follows by the dominated convergence theorem.

Let $t^* = 2q \log p$ for some fixed q , we obtain an estimate of the tail probability

$$\begin{aligned}\overline{F}_0(t^*) &= \mathbb{P}[\chi_\nu^2(0) > t^*] = \frac{2^{-\nu/2}}{\Gamma(\nu/2)} \int_{2q \log p}^{\infty} x^{\nu/2-1} e^{-x/2} dx \\ &\sim \frac{2^{-\nu/2}}{\Gamma(\nu/2)} 2 (2q \log p)^{\nu/2-1} p^{-q}.\end{aligned}\quad (6.43)$$

where $a_p \sim b_p$ is taken to mean $a_p/b_p \rightarrow 1$; this tail estimate was also obtained in Donoho and Jin (2004). Observe that $|\widehat{S}(t^*) \setminus S|$ has distribution $\text{Binom}(p-s, \overline{F}_0(t^*))$ where $s = |S|$, denote $X = X_p := |\widehat{S}(t^*) \setminus S|/|S|$, and we have

$$\mu := \mathbb{E}[X] = \frac{(p-s)\overline{F}_0(t^*)}{s}, \quad \text{and} \quad \text{Var}(X) = \frac{(p-s)\overline{F}_0(t^*)F_0(t^*)}{s^2} \leq \mu/s.$$

Therefore for any $M > 0$, we have, by Chebyshev's inequality,

$$\mathbb{P}[X < M] \leq \mathbb{P}[|X - \mu| > \mu - M] \leq \frac{\mu/s}{(\mu - M)^2} = \frac{1/(\mu s)}{(1 - M/\mu)^2}. \quad (6.44)$$

Now, from the expression of $\overline{F}_0(t^*)$ in (6.43), we obtain

$$\mu = (p^\beta - 1)\overline{F}_0(t^*) \sim \frac{2^{1-\nu/2}}{\Gamma(\nu/2)} (2q \log p)^{\nu/2-1} p^{\beta-q}.$$

Since $\bar{r} < \beta$, we can pick q such that $\bar{r} < q < \beta$. In turn, we have $\mu \rightarrow \infty$, as $p \rightarrow \infty$. Therefore the last expression in (6.44) converges to 0, and we conclude that $X \rightarrow \infty$ in probability, and hence

$$\frac{|\widehat{S}(t^*) \setminus S|}{|\widehat{S}(t^*) \setminus S| + |S|} = \frac{X}{X+1} \rightarrow 1 \quad \text{in probability.} \quad (6.45)$$

On the other hand, we show that with the same choice of $u = t^*$,

$$\frac{|S \setminus \widehat{S}(t^*)|}{|S|} \rightarrow 1 \quad \text{in probability.} \quad (6.46)$$

By the stochastic monotonicity of chi-square distributions (Lemma 6.15), the probability of missed detection for each signal is lower bounded by $\mathbb{P}[\chi_\nu^2(\lambda_i) \leq t^*] \geq F_{\bar{a}}(t^*)$. Therefore, $|S \setminus \widehat{S}(t^*)| \stackrel{d}{\geq} \text{Binom}(s, F_{\bar{a}}(t^*))$, and it suffices to show that $F_{\bar{a}}(t^*)$ converges to 1. This is indeed the case, since

$$\begin{aligned} F_{\bar{a}}(t^*) &= \mathbb{P}[Z_1^2 + \dots + Z_\nu^2 + 2\sqrt{2\bar{r} \log p} Z_\nu + 2\bar{r} \log p \leq 2q \log p] \\ &\geq \mathbb{P}[Z_1^2 + \dots + Z_\nu^2 \leq (q - \bar{r}) \log p, 2\sqrt{2\bar{r} \log p} Z_\nu \leq (q - \bar{r}) \log p], \end{aligned}$$

and both events in the last line have probability going to 1 as $p \rightarrow \infty$. The necessary condition is shown. \square

We now turn to the sufficient condition. That is, when $\underline{r} > \beta$, the Benjamini-Hochberg procedure with slowly vanishing FDR levels achieves asymptotic approximate support recovery. The structure for the proof of sufficient condition follows that of Theorem 2 in Arias-Castro and Chen (2017).

Proof of sufficient condition in Theorem 6.4. The FDR vanishes by our choice of α and the FDR-controlling property of the BH procedure. It only remains to show that FNR also vanishes.

To do so we compare the FNR under the alternative specified in Theorem 6.4 to one with all of the signal sizes equal to $\underline{\Delta}$. Let $x(i)$ be vectors of independent observations with $p-s$ nulls having $\chi_\nu^2(0)$ distributions, and s signals having $\chi_\nu^2(\underline{\Delta})$ distributions. By Lemma 3.9, it suffices to show that the FNR under the BH procedure in this setting vanishes.

Let \widehat{G} denote the empirical survival function as in (3.17). Define the empirical survival functions for the null part and signal part

$$\widehat{W}_{\text{null}}(t) = \frac{1}{p-s} \sum_{i \notin S} \mathbb{1}\{x(i) \geq t\}, \quad \widehat{W}_{\text{signal}}(t) = \frac{1}{s} \sum_{i \in S} \mathbb{1}\{x(i) \geq t\}, \quad (6.47)$$

where $s = |S|$, so that

$$\widehat{G}(t) = \frac{p-s}{p} \widehat{W}_{\text{null}}(t) + \frac{s}{p} \widehat{W}_{\text{signal}}(t).$$

Apply Lemma 3.10 to the two summands in \widehat{G} , we obtain $\widehat{G}(t) = G(t) + \widehat{R}(t)$. where

$$G(t) = \frac{p-s}{p} \overline{F}_0(t) + \frac{s}{p} \overline{F}_a(t), \quad (6.48)$$

where \overline{F}_0 and \overline{F}_a are the survival functions of $\chi_\nu^2(0)$ and $\chi_\nu^2(\underline{\Delta})$ respectively, and

$$\widehat{R}(t) = O_{\mathbb{P}} \left(\xi_p \sqrt{\overline{F}_0(t) F_0(t)} + \frac{s}{p} \xi_s \sqrt{\overline{F}_a(t) F_a(t)} \right), \quad (6.49)$$

uniformly in t .

Recall (see proof of Lemma 3.9) that the BH procedure is the thresholding procedure with threshold set at τ (defined in (3.18)). The NDP may also be re-written as

$$\text{NDP} = \frac{|S \setminus \widehat{S}|}{|S|} = \frac{1}{s} \sum_{i \in S} \mathbb{1}\{x(i) < \tau\} = 1 - \widehat{W}_{\text{signal}}(\tau),$$

so that it suffices to show that

$$\widehat{W}_{\text{signal}}(\tau) \rightarrow 1 \quad (6.50)$$

in probability. Applying Lemma 3.10 to $\widehat{W}_{\text{signal}}$, we know that

$$\widehat{W}_{\text{signal}}(\tau) = \overline{F}_a(\tau) + O_{\mathbb{P}} \left(\xi_s \sqrt{\overline{F}_a(\tau) F_a(\tau)} \right) = \overline{F}_a(\tau) + o_{\mathbb{P}}(1).$$

So it suffices to show that $F_a(\tau) \rightarrow 0$ in probability. Now let $t^* = 2q \log(p)$ for some q

such that $\beta < q < \underline{r}$. We have

$$\begin{aligned} F_a(t^*) &= \mathbb{P}[\chi_\nu^2(\underline{\Delta}) \leq t^*] \leq \mathbb{P}\left[2\sqrt{\underline{\Delta}}Z_\nu \leq t^* - \underline{\Delta}\right] \\ &= \mathbb{P}\left[Z_\nu \leq \frac{t^*}{2\sqrt{\underline{\Delta}}} - \frac{\sqrt{\underline{\Delta}}}{2}\right] = \mathbb{P}\left[Z_\nu \leq \frac{q-r}{2\sqrt{\underline{r}}}\sqrt{2\log p}\right] \rightarrow 0. \end{aligned} \quad (6.51)$$

Hence in order to show (6.50), it suffices to show

$$\mathbb{P}[\tau \leq t^*] \rightarrow 1. \quad (6.52)$$

By (6.48), the mean of the empirical process \widehat{G} evaluated at t^* is

$$G(t^*) = \frac{p-s}{p}\overline{F_0}(t^*) + \frac{s}{p}\overline{F_a}(t^*). \quad (6.53)$$

The first term, using Relation (6.43), is asymptotic to $p^{-q}L(p)$, where $L(p)$ is the logarithmic term in p . The second term, since $\overline{F_a}(t^*) \rightarrow 1$ by Relation (6.51), is asymptotic to $p^{-\beta}$. Therefore, $G(t^*) \sim p^{-q}L(p) + p^{-\beta} \sim p^{-\beta}$, since $p^{\beta-q}L(p) \rightarrow 0$ where $q > \beta$.

The fluctuation of the empirical process at t^* , by Relation (6.49), is

$$\begin{aligned} \widehat{R}(t^*) &= O_{\mathbb{P}}\left(\xi_p\sqrt{\overline{F_0}(t^*)F_0(t^*)} + \frac{s}{p}\xi_s\sqrt{\overline{F_a}(t^*)F_a(t^*)}\right) \\ &= O_{\mathbb{P}}\left(\xi_p\sqrt{\overline{F_0}(t^*)}\right) + o_{\mathbb{P}}(p^{-\beta}). \end{aligned}$$

By (6.43) and the expression for ξ_p , the first term is $O_{\mathbb{P}}(p^{-(q+1)/2}L(p))$ where $L(p)$ is a poly-logarithmic term in p . Since $\beta < \min\{q, 1\}$, we have $\beta < (q+1)/2$, and hence $\widehat{R}(t^*) = o_{\mathbb{P}}(p^{-\beta})$.

Putting the mean and the fluctuation of $\widehat{G}(t^*)$ together, we obtain

$$\widehat{G}(t^*) = G(t^*) + \widehat{R}(t^*) \sim_{\mathbb{P}} G(t^*) \sim p^{-\beta},$$

and therefore, together with (6.43), we have

$$\overline{F}_0(t^*)/\widehat{G}(t^*) = p^{\beta-q}L(p)(1 + o_{\mathbb{P}}(1)),$$

which is eventually smaller than the FDR level α by the assumption (3.8) and the fact that $\beta < q$. That is,

$$\mathbb{P} \left[\overline{F}_0(t^*)/\widehat{G}(t^*) < \alpha \right] \rightarrow 1.$$

By definition of τ (recall (3.18)), this implies that $\tau \leq t^*$ with probability tending to 1, and (6.52) is shown. The proof for the sufficient condition is complete. \square

6.6.4 Proof of Theorems 6.3 and 6.5

As with the proof of Theorem 6.4, one could shorten the presentations in this section by referencing arguments Section 3.3. Again, we choose to present the the proof in full to make this section self-contained.

Proof of Theorem 6.3. We first show the sufficient condition. Similar to the proof of Theorem 6.4, it suffices to show that

$$\text{NDP} = 1 - \widehat{W}_{\text{signal}}(t_p) \rightarrow 0, \tag{6.54}$$

where t_p is the threshold of Bonferroni's procedure.

Since $\underline{r} > \widetilde{g}(\beta) = 1$, we can pick q such that $1 < q < \underline{r}$. Let $t^* = 2q \log p$, we have $t_p < t_p^*$ for large p as in the proof of Theorem 6.1. Therefore for large p , we have

$$\widehat{W}_{\text{signal}}(t_p) \geq \widehat{W}_{\text{signal}}(t^*) \geq \overline{F}_a(t^*) + o_{\mathbb{P}}(1),$$

where the last inequality follows from the stochastic monotonicity of the chi-square family (Lemma 6.15), and Lemma 3.10. Indeed, $F_a(t^*) \rightarrow 0$ by (6.51) and our choice of $q < \underline{r}$.

The proof of the sufficient condition is complete.

Proof of the necessary condition follows a similar structure to that of Theorem 6.4. That is, we show that $\text{FWER} + \text{FNR}$ has \liminf at least 1 by working with the lower bound

$$\text{FWER}(\mathcal{R}) + \text{FNR}(\mathcal{R}) \geq \mathbb{P} \left[\max_{i \in S^c} x(i) > u \right] \wedge \mathbb{E} \left[\frac{|S \setminus \widehat{S}(u)|}{|S|} \right], \quad (6.55)$$

which holds for any thresholding procedure \mathcal{R} and for arbitrary $u \in \mathbb{R}$. By the assumption that $\bar{r} < \widetilde{g}(\beta) = 1$, we can pick q such that $\bar{r} < q < 1$ and let $u = t^* = 2q \log p$. By relative stability of chi-squared random variables (Lemma 6.13), we have

$$\mathbb{P} \left[\frac{\max_{i \in S^c} x(i)}{2 \log p} > \frac{t^*}{2 \log p} \right] \rightarrow 1. \quad (6.56)$$

where the first fraction in (6.56) converges to 1, while the second converges to $q < 1$. On the other hand, by our choice of $q > \bar{r}$, the second term in (6.55) also converges to 1 as in (6.46). This completes the proof of the necessary condition. \square

Proof of Theorem 6.5. We first show the sufficient condition. Since FDR control is guaranteed by the BH procedure, we only need to show that the FWNR also vanishes, that is,

$$\mathbb{P} \left[\min_{i \in S} x(i) \geq \tau \right] \rightarrow 1, \quad (6.57)$$

where τ is the threshold for the BH procedure.

By the assumption that $\underline{r} > \widetilde{h}(\beta) = (\sqrt{\beta} + \sqrt{1 - \beta})^2$, we have $\sqrt{\underline{r}} - \sqrt{1 - \beta} > \sqrt{\beta}$, so we can pick $q > 0$, such that

$$\sqrt{\underline{r}} - \sqrt{1 - \beta} > \sqrt{q} > \sqrt{\beta}. \quad (6.58)$$

Let $t^* = 2q \log p$, we claim that

$$\mathbb{P} [\tau \leq t^*] \rightarrow 1. \quad (6.59)$$

Indeed, by our choice of $q > \beta$, (6.59) follows in the same way that (6.52) did.

With this t^* , we have

$$\mathbb{P} \left[\min_{i \in S} x(i) \geq \tau \right] \geq \mathbb{P} \left[\min_{i \in S} x(i) \geq t^*, t^* \geq \tau \right]. \quad (6.60)$$

However, by our choice of $\sqrt{q} < \sqrt{\bar{r}} - \sqrt{1 - \beta}$, the probability of the first event on the right-hand side of (6.60) also goes to 1 according to (6.27) and (6.28). Together with (6.59), this proves (6.57), and completes proof of the sufficient condition.

The necessary condition follows from the lower bound

$$\text{FDR}(\mathcal{R}) + \text{FWNR}(\mathcal{R}) \geq \mathbb{E} \left[\frac{|\hat{S}(u) \setminus S|}{|\hat{S}(u) \setminus S| + |S|} \right] \wedge \mathbb{P} \left[\min_{i \in S} x(i) < u \right], \quad (6.61)$$

which holds for any thresholding procedure \mathcal{R} and for arbitrary $u \in \mathbb{R}$.

By the assumption that $\bar{r} < \tilde{h}(\beta) = (\sqrt{\beta} + \sqrt{1 - \beta})^2$, we can pick a constant $q > 0$, such that

$$\sqrt{\bar{r}} - \sqrt{1 - \beta} < \sqrt{q} < \sqrt{\beta}. \quad (6.62)$$

Let also $u = t^* = 2q \log p$. By our choice of $q < \beta$, we know from (6.45) that the first term on the right-hand-side of (6.61) converges to 1. It remains to show that the second term in (6.61) also converges to 1.

For the second term in (6.61), dividing through by $2 \log p$, we obtain

$$\mathbb{P} \left[\min_{i \in S} x(i) < t^* \right] = \mathbb{P} \left[\frac{m_S}{2 \log p} < q \right]. \quad (6.63)$$

Similar to (6.31), we have

$$\frac{m_S}{2 \log p} \stackrel{\text{d}}{\leq} \min_{i \in S} \frac{Z_1^2(i) + \dots + Z_{\nu-1}^2(i)}{2 \log p} + \frac{(Z_\nu(i) + \sqrt{\bar{\Delta}})^2}{2 \log p}. \quad (6.64)$$

Define $i^\dagger = i_p^\dagger$ to be the index minimizing the second term in (6.64), i.e.,

$$i^\dagger := \arg \min_{i \in S} f_p(Z_\nu(i)), \quad (6.65)$$

where $f_p(x) := (x + \sqrt{\Delta})^2 / (2 \log p)$.

Since $\sqrt{q} > \sqrt{r} - \sqrt{1 - \beta}$ and $q > 0$, we have $\frac{\sqrt{r} - \sqrt{q}}{\sqrt{1 - \beta}} < 1$. Also, since

$$\frac{\sqrt{r} + \sqrt{q}}{\sqrt{1 - \beta}} > 0, \quad \text{and} \quad \frac{\sqrt{r} - \sqrt{q}}{\sqrt{1 - \beta}} < \frac{\sqrt{r} + \sqrt{q}}{\sqrt{1 - \beta}},$$

we can further pick a constant $\beta_0 \in (0, 1]$ such that

$$\frac{\sqrt{r} - \sqrt{q}}{\sqrt{1 - \beta}} < \sqrt{\beta_0} < \frac{\sqrt{r} + \sqrt{q}}{\sqrt{1 - \beta}}. \quad (6.66)$$

Let $Z_{[1]} \leq Z_{[2]} \leq \dots \leq Z_{[s]}$ be the order statistics of $\{Z_\nu(i)\}_{i \in S}$ and define $k = \lfloor s^{1 - \beta_0} \rfloor$.

Applying Lemma 6.17 (stated below), we obtain

$$\frac{Z_{[k]}}{\sqrt{2 \log p}} = \frac{Z_{[k]}}{\sqrt{2 \log s}} \frac{\sqrt{2 \log s}}{\sqrt{2 \log p}} \rightarrow -\sqrt{\beta_0(1 - \beta)} \quad \text{in probability.} \quad (6.67)$$

Since we know (by solving a quadratic inequality) that

$$f_p(x) < q \iff \frac{x}{\sqrt{2 \log p}} \in \left(-(\sqrt{r} + \sqrt{q}), -(\sqrt{r} - \sqrt{q}) \right), \quad (6.68)$$

combining (6.66), (6.67), and (6.68), it follows that

$$\mathbb{P} [f_p(Z_\nu(i^\dagger)) < q] \geq \mathbb{P} [f_p(Z_{[k]}) < q] \rightarrow 1.$$

Finally, using (6.38), we conclude that

$$\mathbb{P} \left[\min_{i \in S} x(i) < t^* \right] = \mathbb{P} \left[\frac{m_S}{2 \log p} < q \right] \geq \mathbb{P} [o_{\mathbb{P}}(1) + f_p(Z_\nu(i^\dagger)) < q] \rightarrow 1.$$

Therefore, the two terms on the right-hand-side of (6.61) both converge 1. This completes the proof of the necessary condition. \square

It only remains to justify (6.67).

Lemma 6.17 (Relative stability of order statistics). *Let $Z_{[1]} \leq \dots \leq Z_{[s]}$ be the order statistics of s iid standard Gaussian random variables. Let $\beta_0 \in (0, 1]$ and define $k = \lfloor s^{1-\beta_0} \rfloor$, then we have*

$$\frac{Z_{[k]}}{\sqrt{2 \log s}} \rightarrow -\sqrt{\beta_0} \quad \text{in probability.} \quad (6.69)$$

Proof of Lemma 6.17. Using the Renyi representation for order statistics, we write

$$Z_{[i]} = \Phi^{\leftarrow}(U_{[i]}), \quad (6.70)$$

where $U_{[i]}$ is the i^{th} (smallest) order statistic of s independent uniform random variables over $(0, 1)$. Since $U_{[i]}$ has a $\text{Beta}(i, s+1-i)$ distribution, with mean and standard deviation,

$$\mathbb{E}[U_{[k]}] = k/(s+1) \sim s^{-\beta_0}, \quad \text{and} \quad \text{sd}(U_{[k]}) = \frac{1}{s+1} \sqrt{\frac{k(s+1-k)}{s+2}} \sim s^{-\frac{1+\beta_0}{2}},$$

we obtain by Chebyshev's inequality

$$\mathbb{P} \left[s^{-\beta_0}(1-\epsilon) < U_{[k]} < s^{-\beta_0}(1+\epsilon) \right] \rightarrow 1,$$

where ϵ is an arbitrary positive constant. This implies, by representation (6.70),

$$\mathbb{P} \left[\Phi^{\leftarrow}(s^{-\beta_0}(1-\epsilon)) < Z_{[k]} < \Phi^{\leftarrow}(s^{-\beta_0}(1+\epsilon)) \right] \rightarrow 1. \quad (6.71)$$

Using the expression for standard Gaussian quantiles (see, e.g., Proposition 1.1. in Gao

and Stoev (2019)), we know that

$$\begin{aligned}\Phi^{\leftarrow}(s^{-\beta_0}(1-\epsilon)) &\sim -\sqrt{2\log(s^{\beta_0}/(1-\epsilon))} \\ &= -\sqrt{2(\beta_0\log s - \log(1-\epsilon))} \sim -\sqrt{2\beta_0\log s},\end{aligned}$$

and similarly $\Phi^{\leftarrow}(s^{-\beta_0}(1+\epsilon)) \sim -\sqrt{2\beta_0\log s}$. Since both ends of the interval in (6.71) are asymptotic to $-\sqrt{2\beta_0\log s}$, the desired conclusion follows. \square

6.6.5 Proof of Proposition 6.6 and Corollary 6.7

Proof of Proposition 6.6 and Corollary 6.7. We parametrize the 2-by-2 multinomial distribution with the parameter δ ,

$$\mu_{11} = \phi_1\theta_1 + \delta, \quad \mu_{12} = \phi_1\theta_2 - \delta, \quad \mu_{21} = \phi_2\theta_1 - \delta, \quad \mu_{22} = \phi_2\theta_2 + \delta. \quad (6.72)$$

By relabelling of categories, we may assume $0 < \theta_1, \phi_1 \leq 1/2$ without loss of generality. Note that δ must lie within the range $[\delta_{\min}, \delta_{\max}]$, where

$$\delta_{\min} := \max\{-\phi_1\theta_1, -\phi_2\theta_2, \phi_1\theta_2 - 1, \phi_2\theta_1 - 1\} = -\phi_1\theta_1,$$

and

$$\delta_{\max} := \min\{1 - \phi_1\theta_1, 1 - \phi_2\theta_2, \phi_1\theta_2, \phi_2\theta_1\} = \min\{\phi_1\theta_2, \phi_2\theta_1\},$$

in order for $\mu_{ij} \geq 0$ for all $i, j \in \{1, 2\}$. Under this parametrization, Relation (6.8) then becomes

$$R = \frac{\mu_{11}\mu_{22}}{\mu_{12}\mu_{21}} = \frac{\phi_1\theta_1\phi_2\theta_2 + \delta(\phi_1\theta_1 + \phi_2\theta_2) + \delta^2}{\phi_1\theta_1\phi_2\theta_2 - \delta(\phi_1\theta_2 + \phi_2\theta_1) + \delta^2}, \quad (6.73)$$

which is one-to-one and increasing in δ on $(\delta_{\min}, \delta_{\max})$. Equation (6.10) becomes

$$w^2 = \sum_{i=1}^2 \sum_{j=1}^2 \frac{(\mu_{ij} - \phi_i \theta_j)^2}{\phi_i \theta_j} = \delta^2 \sum_i \sum_j \frac{1}{\phi_i \theta_j} = \frac{\delta^2}{\phi_1 \theta_1 \phi_2 \theta_2}, \quad (6.74)$$

Solving for δ in (6.73), and plugging into the expression for signal size (6.74) yields Relation (6.11). Corollary 6.7 follows from the fact that $w^2(\delta)$ is decreasing on $[\delta_{\min}, 0)$, increasing on $(0, \delta_{\max}]$, with limits

$$\lim_{d \rightarrow \delta_{\min}} w^2(\delta) = \frac{\phi_1 \theta_1}{\phi_2 \theta_2}, \quad \text{and} \quad \lim_{d \rightarrow \delta_{\max}} w^2(\delta) = \min \left\{ \frac{\phi_1 \theta_2}{\phi_2 \theta_1}, \frac{\phi_2 \theta_1}{\phi_1 \theta_2} \right\}.$$

The other three cases ($1/2 \leq \theta_1, \phi_1 \leq 1$; $0 < \theta_1 \leq 1/2 \leq \phi_1 \leq 1$; and $0 \leq \phi_1 \leq 1/2 \leq \theta_1 \leq 1$) may be obtained similarly, or by appealing to the symmetry of the problem. \square

Proof of Corollary 6.9. Using the parametrization in (6.72) and in Corollary 6.8, we solve for δ in (6.73) to obtain

$$\begin{aligned} \delta &= \frac{\phi_1 f R}{f R + 1 - f} - \left(\frac{\phi_1 f R}{f R + 1 - f} + f(1 - \phi_1) \right) \phi_1 \\ &= \frac{f(1 - f)\phi_1(1 - \phi_1)(R - 1)}{f R + 1 - f}. \end{aligned} \quad (6.75)$$

Substituting (6.75) into the expression (6.74), after some simplification, yields

$$w^2 = \frac{f(1 - f)\phi_1(1 - \phi_1)(R - 1)^2}{[\phi_1 R + (1 - \phi_1)D][\phi_1 + (1 - \phi_1)D]}, \quad (6.76)$$

where $D = f R + 1 - f > 0$. Therefore, the derivative of (6.76) with respect to ϕ_1 is

$$\frac{dw^2}{d\phi_1} = \frac{f(1 - f)(R - 1)^2}{[\phi_1 R + (1 - \phi_1)D]^2 [\phi_1 + (1 - \phi_1)D]^2} [(D^2 - R)\phi_1^2 - 2D^2\phi_1 + D^2]. \quad (6.77)$$

Further, we obtain the second derivative with respect to ϕ_1 ,

$$\frac{d^2 w^2}{d\phi_1^2} = h(R, f) [(\phi_1 - 1)D^2 - \phi_1 R], \quad (6.78)$$

where h is some function of (R, f) taking on strictly positive values.

Since $[(\phi_1 - 1)D^2 - \phi_1 R] < 0$, the second derivative (6.78) must be strictly negative on $[0, 1]$. This implies that the first derivative (6.77) is strictly decreasing on $[0, 1]$. Since the first derivative (6.77) is strictly positive at $\phi_1 = 0$, and strictly negative at $\phi_1 = 1$, it must have a unique zero between 0 and 1, and hence, the solution to $(D^2 - R)\phi_1^2 - 2D^2\phi_1 + D^2 = 0$ in the interval of $[0, 1]$ must be the maximizer of (6.76) — when $D^2 - R > 0$, the smaller of the two roots maximizes (6.76), and when $D^2 - R < 0$, it is the larger of the two. They share the same expression $D/(D + \sqrt{R})$, which coincides with (6.15). Finally, when $D^2 = R$, the only root $\phi_1^* = 1/2$, which also coincides with (6.15), is the maximizer of (6.76). \square

APPENDIX A

U-PASS: A Software for Unified Power Analysis and Forensics for Qualitative Traits in Genetic Association Studies

We introduce the software we developed for the power analysis of genetic association studies of qualitative traits in this appendix. Section A.1 reviews the typical process of study planning employed by geneticists. Disease models are often used to specify the distribution of observations under the alternative hypothesis in power analysis. In Section A.2, we revisit the use of these disease models and argue for an alternative way of model parametrization that is better suited to conducting systematic reviews and confirmatory studies. Section A.3 provides three example usages of the software. Instructions for downloading, installing, launching, and terminating the software can be found in Section A.4.

A.1 Power analysis in genetic association studies

We briefly review the main steps of a typical power analysis for genetic association studies.

1. Disease model specifications. A typical power analysis for genetic association studies begin by specifying an alternative hypothesis through a disease model (dominant, recessive, multiplicative, additive, etc.), which assumes:

- The genotype relative risks (GRR).

- Risk allele frequency in the general population (p).
- Disease prevalence in the general population (Prev).

The disease model and parameters determine the joint distribution of the genotypes and phenotypes *in the population*, shown in the following table.

Population Prob.	Risk allele copies		
	0 copies	1 copy	2 copies
Cases	π_{10}	π_{11}	π_{12}
Controls	π_{20}	π_{21}	π_{22}

In the disease models, the conditional probabilities of having the disease, given the risk allele copy numbers, satisfy the following relations,

$$\frac{\pi_{10}}{\pi_{10} + \pi_{20}} : \frac{\pi_{11}}{\pi_{11} + \pi_{21}} : \frac{\pi_{12}}{\pi_{12} + \pi_{22}} = \begin{cases} 1 : \text{GRR} : \text{GRR}^2, & \text{Multiplicative} \\ 1 : \text{GRR} : 2 \times \text{GRR} - 1, & \text{Additive} \\ 1 : \text{GRR} : \text{GRR}, & \text{Dominant} \\ 1 : 1 : \text{GRR}, & \text{Recessive} \end{cases} \quad (\text{A.1})$$

where GRR is strictly greater than 1 under the alternative, and equal to 1 under the null hypothesis.

The disease prevalence determines the sum of the probabilities of cases in the population,

$$\pi_{10} + \pi_{11} + \pi_{12} = \text{Prev}. \quad (\text{A.2})$$

The risk allele frequency in the general population, p , assuming Hardy-Weinberg equilibrium, satisfies

$$\pi_{10} + \pi_{20} = (1 - p)^2, \quad \pi_{11} + \pi_{21} = 2p(1 - p), \quad \pi_{12} + \pi_{22} = p^2. \quad (\text{A.3})$$

The population probabilities are determined by the disease model and its parameters (GRR, Prev, and p). The six unknowns ($\pi_{10}, \dots, \pi_{22}$) are solved for using the six equations above: two from Relation (A.1), one from (A.2), and three from (A.3).

2. Sampling adjustments. Next, the probabilities of observing each genotype-phenotype combination are adjusted according the number of cases and controls recruited *in the studies*, where the sample sizes are specified with the number of cases (n_1) and controls (n_2), or equivalently, the fraction of cases (ϕ) and total number of subjects (n).

Prob. in study	Risk allele copies		
	0 copies	1 copy	2 copies
Cases	$\pi_{10} \frac{\phi}{\text{Prev}}$	$\pi_{11} \frac{\phi}{\text{Prev}}$	$\pi_{12} \frac{\phi}{\text{Prev}}$
Controls	$\pi_{20} \frac{1-\phi}{1-\text{Prev}}$	$\pi_{21} \frac{1-\phi}{1-\text{Prev}}$	$\pi_{22} \frac{1-\phi}{1-\text{Prev}}$

As an example, if $\phi > \text{Prev}$, the probabilities are adjusted to account for over-sampling of cases. Conversely, adjustments are needed to account for under-sampling of cases.

The relative frequencies of allele type-phenotype combinations *in the study* are then calculated as follows.

Prob. in study	Allele variant	
	Risk allele	Non-risk allele
Cases	$\phi \left(\frac{\pi_{12}}{\text{Prev}} + \frac{\pi_{11}}{2 \times \text{Prev}} \right)$	$\phi \left(\frac{\pi_{11}}{2 \times \text{Prev}} + \frac{\pi_{10}}{\text{Prev}} \right)$
Controls	$(1 - \phi) \left(\frac{\pi_{22}}{1 - \text{Prev}} + \frac{\pi_{21}}{2(1 - \text{Prev})} \right)$	$(1 - \phi) \left(\frac{\pi_{21}}{2(1 - \text{Prev})} + \frac{\pi_{20}}{1 - \text{Prev}} \right)$

This final table corresponds to the probabilities underlying the 2×2 multinomial counts that we introduced in Chapter 1. We denote the relative frequencies of allele type-phenotype combinations with $\mu = (\mu_{11}, \mu_{12}, \mu_{21}, \mu_{22})$, as we did in Chapter 6.

Prob. in study	Allele variant		Total by phenotype
	Risk allele	Non-risk allele	
Cases	μ_{11}	μ_{12}	$\phi = \mu_{11} + \mu_{12}$
Controls	μ_{21}	μ_{22}	$1 - \phi = \mu_{21} + \mu_{22}$

3. Power calculations. Finally, the power of an statistical test is calculated as the probability of (a correct) rejection, assuming that the data (i.e., tabulated counts of the allele type-phenotype combinations) follow a multinomial or binomial distribution with sample size $2n$, since each individual has a pair of alleles.

These steps form the basis of the calculations implemented in the most existing tools, including the GAS calculator (Johnson and Abecasis, 2017).

Some common association tests include the likelihood ratio test, Pearson’s chi-square test, tests of zero slope coefficient in logistic regressions, as well as t-tests for equal proportions. Although not explicitly stated, the GAS calculator assumes the test of association to be Welch’s t-test. In principal, power analysis has to be tailored to the association test used. Fortunately, many of these tests are asymptotically equivalent in terms of power (Ferguson, 2017; Gao et al., 2019), and results of the power approximation applies to all asymptotically equivalent tests.

A.2 Specification of alternatives in power analysis

In the power calculations outlined in Section A.1, the disease models are used to describe the distribution of the data under the alternative hypothesis. Specifically, they are used to specify the conditional distributions of the allele variants, given the phenotypes. The probability of observing a risk allele in the control group, known as risk allele frequency (RAF), is defined as follows,

$$f := \mathbb{P}[\text{risk allele} \mid \text{control group}] = \frac{\mu_{21}}{1 - \phi} = \frac{\pi_{22} + \pi_{21}/2}{\pi_{22} + \pi_{21} + \pi_{20}}. \quad (\text{A.4})$$

The risk allele frequency is fully determined by the disease model through the probability table μ . This parametrization was also introduced in (6.14).

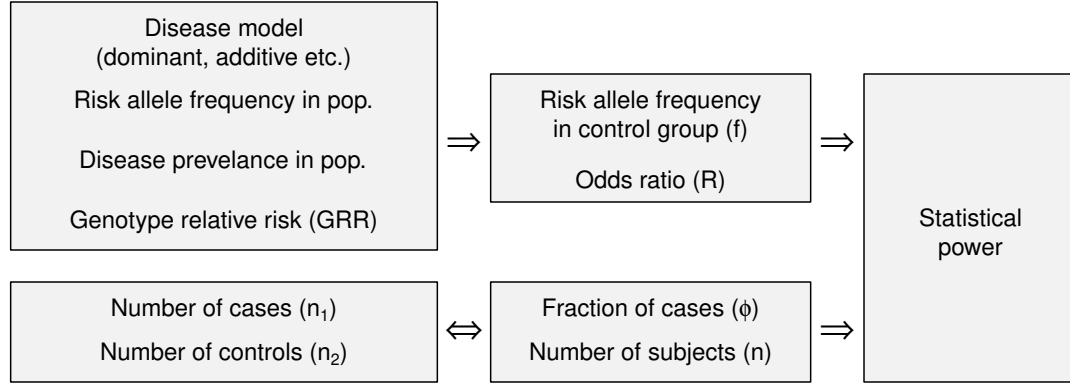


Figure A.1: The process of a typical power analysis for genetic association tests. The quantities depend on, and can be calculated from the values of their parents in the directed graph. Power can be calculated as long as one set of parameters in each branch is known. While there is a one-to-one correspondence between the sample size specifications (n_1, n_2) and (ϕ, n) , the mapping from disease model specifications to (f, R) is many-to-one.

Similarly, the odds ratio between the two allele variants,

$$R := \frac{\mu_{11}\mu_{22}}{\mu_{12}\mu_{21}} = \frac{(\pi_{12} + \pi_{11}/2)(\pi_{20} + \pi_{21}/2)}{(\pi_{10} + \pi_{11}/2)(\pi_{22} + \pi_{21}/2)}, \quad (\text{A.5})$$

is also determined by the disease model and its parameters. See definition in (6.8).

In turn, the parameters (f, R) , together with the sample sizes (ϕ, n) , fully describe the distribution of our data under the alternative hypothesis (by determining the probability vector μ and the sample size n). Power of association tests, therefore, depends on (and only on) the set of “canonical parameters”:

- Risk allele frequency among the controls (f).
- Odds ratio (R) of having the defined trait between the two allele variants.
- One of the two equivalent ways of parametrizing the sample sizes.

We visualize the process of power analysis in Figure A.1. Notice that in power calculations, we can either describe the alternative hypothesis with a disease model, or through the canonical parameters (f, R) . Both approaches are sufficient for the purpose of power

analysis. Unfortunately, these two parametrizations are commonly confused. We emphasize that the risk allele frequency in the control group (f) is not equivalent to the risk allele frequency in the general population (p); odds ratio (R) is not equivalent to genotype relative risk (GRR).

As illustrated in Figure A.1, power calculations are mediated through the canonical parameters, which are invariant to different model specifications. That is, different disease model specifications may lead to the *same* set of canonical parameters (f, R), and consequently the) *same* distributions of the allele variant counts. From a statistical perspective, the disease models that map to the same set of canonical parameters are equivalent in terms of power.

For example, the following set of disease models and parameters imply the same set of canonical parameters ($f = 0.290, R = 1.575$), and therefore enjoy the same power at the same sample sizes ($n_1 = n_2 = 1000$).

Disease Model	(Prev, p , GRR)	(f, R)	Power
Multiplicative	(0.1, 0.3, 1.500)	(0.290, 1.575)	0.990
Additive	(0.1, 0.3, 1.588)	(0.290, 1.575)	0.990
Dominant	(0.1, 0.3, 1.909)	(0.290, 1.575)	0.990
Recessive	(0.1, 0.3, 2.666)	(0.290, 1.575)	0.990

Conversely, different disease models with the same parameters, map to drastically different canonical parameters. For example, the default disease model parameters in the GAS calculator,

$$\text{Disease prevalence in the population : } \text{Prev} = 0.1 \quad (\text{A.6})$$

$$\text{Risk allele frequency in the population : } p = 0.5 \quad (\text{A.7})$$

$$\text{Genotype relative risk : } \text{GRR} = 1.5. \quad (\text{A.8})$$

map to very different canonical parameters under different disease model assumptions (as-

suming the same sample sizes of $n_1 = n_2 = 1000$), which leads to drastically different statistical power.

Disease Model	(Prev, p , GRR)	(f , R)	Power
Multiplicative	(0.1, 0.5, 1.5)	(0.489, 1.568)	0.995
Additive	(0.1, 0.5, 1.5)	(0.491, 1.453)	0.920
Dominant	(0.1, 0.5, 1.5)	(0.495, 1.224)	0.282
Recessive	(0.1, 0.5, 1.5)	(0.494, 1.281)	0.098

In the application, we provide users with a “Disease model converter” that implements this many-to-one conversion from the disease model specifications to the canonical parameters.

While the disease models may carry additional insights into the biological process, the canonical parameters also have their unique advantages. We offer an incomplete list of comparisons of the two approaches, and discuss their usage in practice.

Interpretability and communicability. In general, geneticists and biostatisticians seem to agree that disease models are more interpretable. The concept of genotype relative risks, in particular, seems easier to reason about than odds ratios in the canonical parameters definition. Disease models also seem to be the de facto mode of model specification when performing power analysis for study planning and grant applications.

The “nonparametric” approach to model specification through the canonical parameters is somewhat lesser known to the statistical genetics community. The canonical parameters are typically estimated and reported as outcomes of the research, but not used as inputs to the power analysis for planning purposes.

Availability of parameter estimates. The canonical parameters f and R can be estimated from data collected in the study. They are also reported and curated in GWAS catalogs such as the NHGRI-EBI Catalog (MacArthur et al., 2016).

On the other hand, accurate information regarding the disease model parameters can be

more difficult to obtain, partly because some parameters in the disease models cannot be estimated from the association studies alone.

In particular, disease prevalence in population (Prev), as well as risk allele frequency in population (p), must be obtained from other studies or surveys targeting the general population; the association studies, unless matching the proportion of cases in the population vs in the study ($\phi = \text{Prev}$), cannot produce estimates without using external information. Genetic association studies rarely explicitly estimate the disease model and its parameters. In fact, we are not aware of a GWAS catalog that reports and curates the disease models and their estimated parameters.

This paucity of information on disease model parameters is not an issue if we are planning to study a trait for which we have little prior knowledge. In this case, the purpose of power analysis is to determine the range of models and parameters that lead to discovery of associations, given the study designs.

In contrast, in confirmatory / follow-up studies and systematic reviews, our main interest is in the statistical validity of the reported findings. Power analysis then serves to find efficient designs, and to validate the claims made. Knowledge obtained in prior studies (in the form of parameter estimates) are indeed necessary.

Robustness against model misspecification. Disease models are useful in as much as they help us understand the biology behind the data we observe. Unfortunately, like all models, they can be misspecified. For example, the following genotype relative risks,

$$\frac{\pi_{10}}{\pi_{10} + \pi_{20}} : \frac{\pi_{11}}{\pi_{11} + \pi_{21}} : \frac{\pi_{12}}{\pi_{12} + \pi_{22}} = 1 : 3 : 4,$$

does not follow any of the common disease models. In this case, different studies may come up with different disease models (say, Dominant and Additive), and of course, different parameter estimates.

Suppose a researcher wishes to perform a meta analysis or confirmatory experiment of

the existing results, where the literature reports inconsistent estimates of disease models and parameters, he would have a difficult time pooling the information from these different sources. And even when they are pooled, the resulting model usually does not fall in one of the familiar categories — there is no existing tool with which to perform power analysis. The researcher will likely have to forgo the information from one model, and use estimates from only the other.

On the other hand, the canonical parameters are invariant to the disease model choices, and accommodate models falling outside the usual categories. They can also be easily combined to produce pooled estimates. This universality allows us to perform power analysis in a unified fashion, regardless of the disease models assumed. This also paves the way for the “OR-RAF diagram”, as well as systematic reviews of statistical validity of existing studies; see Section A.3.1 below.

Robustness against human errors. The disparity in availability of parameter estimates we mentioned earlier can lead to unintended consequences, one of which is potentially incorrect usage of power calculators. This issue, although minor, is critical to the correctness of the results of our power analysis.

Recall that the specification of a disease model requires as input the risk allele frequency (RAF) in the general population (p). The RAF reported in the NHGRI-EBI Catalog (MacArthur et al., 2016), in contrast, refers to RAF in the control group (f). With RAF in population often unavailable, it is tempting to substitute the RAF in control group into the calculations. While the two quantities may be close when diseases prevalence and penetrance are low, their difference becomes non-negligible if either of the two conditions are violated, leading to grossly distorted results.

Performing power analysis with the canonical parameters is not guaranteed to prevent this human error, as mistake in the other direction could also happen. But perhaps it is more robust to such mistakes, since what is readily available matches with what is required as input.

Compatibility of parameters. We make another minor comment regarding correct usage of disease models.

We caution users that not all values of the disease model parameter combinations are valid. For example, in a multiplicative model, the parameters

$$p = 0.1, \quad \text{Prev} = 0.5, \quad \text{GRR} = 1.5,$$

would result in the conditional probability of having two risk allele copies greater than 1. (In this case, the GAS calculator (Johnson and Abecasis, 2017) would produce the error message: “I don’t like the genetic model you requested!”, without explicitly pointing to the compatibility issue.)

Although an experienced geneticist would immediately notice the impossibility of the disease model parameter combinations, these contradictions may not be obvious to the untrained eye. The end user of the software – experienced or not – is ultimately responsible for inputting valid values when specifying a disease model.

On the other hand, any combination of

$$f \in (0, 1), \quad \text{and} \quad R \in (0, +\infty)$$

is valid. Parameter compatibility is not an problem for the set of canonical parameters.

Recommendations on model specification in power analysis. Since both the disease models and the canonical parameters are sufficient for the purpose of power analysis, it is natural to ask why (and when) should one take the canonical parameters approach, given that the more familiar disease models would also suffice.

We believe that either approach may be preferred, depending on the use cases. Recall that power analysis is useful in at least three scenarios:

1. *Planning for an exploratory study, where little is known about the associations.*

In this case, the top branch in Figure A.1 is unknown to the researcher. The goal is to find out the range of disease models and parameters that are discoverable given the study designs. Power analysis is also to some extent exploratory in nature.

2. *Planning for a confirmatory study, where something is known about the associations and one wishes to validate the findings with an efficient design.*

In this case, the top branch in Figure A.1 is known, and the variables in the bottom branch is what we are solving for. The goal of power analysis is to provide a set of efficient study designs with sufficient power.

3. *Reviewing the reported findings and verify the statistical validity.*

In the third case, one looks to find out whether the claims of statistical significance are congruent with the evidence from data. A claim supported by very weak or contradictory evidence should invite further investigations. In this case, both branches in Figure A.1 have to be available.

In view of the discussions above, we propose the following general guidelines for power analysis in genetic association studies.

- When designing an association study where little to no prior information is available, either approach is valid. However, disease models may be easier to interpret and communicate.
- When designing a follow-up or confirmatory study, or conducting a systematic review, researchers may wish to choose the approach for which the parameter estimates are available, or of better quality. Typically the canonical parameters are better estimated, reported, and curated.

The comments we made about the two approaches should not be taken as criticisms, but rather as reminders of the potential pitfalls in power analysis. In either approach, care needs to be exercised in order to produce valid results.

A.3 Use case illustrations

The software has three main functionalities, namely, reviewing the GWAS literature, designing prospective association studies, and converting between disease models and canonical parametrizations. We detail each of the three functionalities of the application, and illustrate with examples.

A.3.1 Reviewing reported findings in the GWAS catalog

The “OR-RAF power diagram” tab of the application provides a tool for reviewing reported associations from existing studies. The application calculates statistical power based the core parameters common to models of qualitative traits:

- Sample sizes, i.e., the number of cases and controls i.e., (n_1, n_2) or (ϕ, n) .
- The canonical parameters (f, R) .

Users need only prescribe the sample sizes, by one of two ways provided in the first box, i.e., total sample size + fraction of cases, or number of cases + number of controls.

Statistical power of common association tests, including the likelihood ratio test, chi-square test, Welch’s t-test, and the LR test, have the same asymptotic power curves. This shared power limit is calculated as a function of f and R , and visualized as a heatmap referred to as the OR-RAF diagram.

We provide users the options to load and overlay findings reported in the NHGRI-EBI GWAS Catalog (MacArthur et al., 2016), or upload data from other sources compliant with the Catalog’s data format.

The visualization is adaptive and fully interactive. The initial sample sizes are dynamically adjusted, and automatically determined from texts of the article reporting the user selected loci. Since the sampling structures are many and varied across different studies, and no uniform reporting format is enforced in the catalog, the initial sample sizes are best

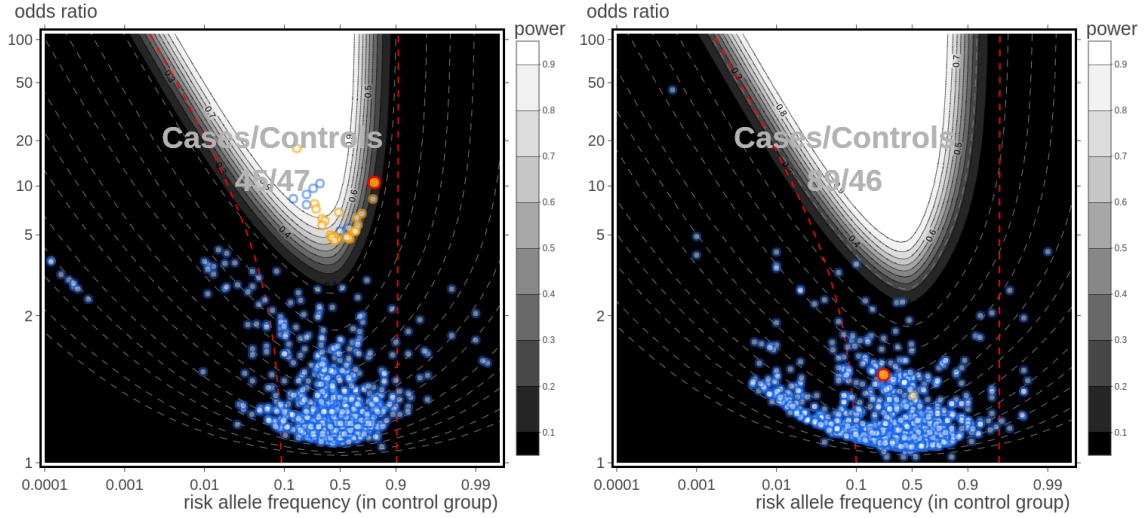


Figure A.2: The OR-RAF diagram of two studies where gross misalignments were identified. Left: Dominguez-Cruz et al. (2018), right: Haryono et al. (2015). The reported odds ratios and risk allele frequencies of the discovered associations in these two papers are charted with orange (and red) circles. Dark regions represent f - R parameter combinations that are predicted to have low power of discovery under the current sample sizes. See text for more comments.

estimates from the extracted texts. Information of the selected loci and the study is also dynamically displayed below the diagram.

The unified power analysis allows us to examine results from different studies employing different models and applicable tests, in the same diagram, with the same power limits. This allows for a systematic review of reported findings for their statistical validity. In particular, a reported association predicted to have low power given the study's sample size – lying in the dark regions of the OR-RAF diagram – while not impossible, invites further scrutiny. Studies where reported associations show misalignment with the predicted powered curves should also be further investigated for potential problems in the data curation process.

We illustrate this forensics feature of the the software with two GWAS studies by Domínguez-Cruz et al. (2018) and Haryono et al. (2015), shown in Figure A.2. Gross misalignments with our power analysis were identified in both cases. Upon contact, Domínguez-Cruz et al. (2018) confirmed that this misalignment is the result of a problem

in the data curation process of the GWAS Catalog (Dominguez-Cruz, personal communication). In particular, the risk allele frequencies reported in the Catalog were based on all subjects in the study, as opposed to only the control group, while the Catalog requires that risk allele frequencies be reported in the control group only. As a consequence, the risk allele frequencies are systematically overestimated, shifting the reported findings to the right in the diagram. The study by Haryono et al. (2015), though may very well hold valid results, calls for further scrutiny of its statistical methodologies given the apparent incongruity of its conclusions at the reported the sample sizes.

In general, however, we expect the forensics aspect of our software to be useful for discovering problems with data entry and catalog curation process, as well as for assessing the reproducibility and robustness of reported findings.

A.3.2 Designing association studies

The “Design my studies” tab of the application provides a tool for finding optimal designs of association studies. The tool requires inputs in a four-step process.

1. Model specification.
2. Sample size constraints specification.
3. False discovery Criteria specification.
4. Power specification.

Each of the steps can be specified in a number of alternative ways.

Step 1: Model specification. We provide two three ways to describe the model for biological process of the disease or trait of interest.

The distribution of observations can be specified through the canonical parameters, risk allele frequency in the control group (f) and odds ratio (R). Estimates for these quantities

in previous studies of the same trait can be found in GWAS catalogs such as the NHGRI-EBI Catalog. See Section 6.3 for their definitions.

Alternatively, users may opt to specify through the disease models, of which we implement the four most popular ones: additive, multiplicative, dominant, and recessive. See Section A.1 below for the definitions of the quantities involved in the disease models. We remind users the difference between the risk allele frequency in the control group (f) versus risk allele frequency in the general population (p); only the latter is used in the disease model specifications.

Advanced users may choose to use a more succinct “signal size per sample” option, which directly parametrizes the signal sizes (λ/n). Definition of signal size λ can be found in Section 6.2.

Step 2: Sample size specifications. The second step requires users input the sample size constraints of the study. The three available options are “Budget / total number of subjects”, “Number of cases”, and “Fraction of cases”. In the subsequent calculations, the selected and specified quantities are treated as fixed. With only one unknown parameter left in the flow of power calculations (recall the flowchart in Fig. A.1), we calculate power as a function of the remaining specified parameter. In particular,

- If the constraint is total budget, power is shown as a function of the fraction of cases.
- If the constraint is number of cases, power is shown as a function of the number of controls.
- If the constraint is fraction of cases, power is shown as a function of the total number of subjects.

Steps 3 and 4: False discovery and power specifications. The final two steps require as input the desired level of false discovery and false non-discovery control. Both specification can be done through the marginal levels, i.e., Type I error and Type II error, or alterna-

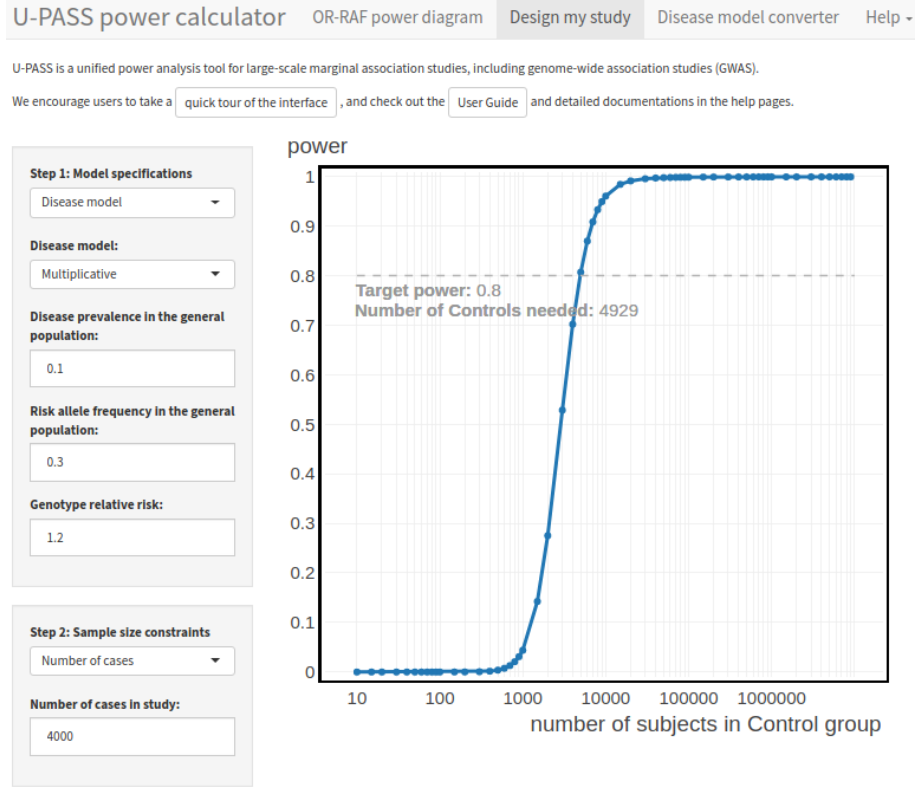


Figure A.3: A screenshot of the user interface for the “Design my study” tab of the software. The inputs are as described in the numerical example in Section A.3.2. Results of the power calculation are visualized in an interactive plot in the application.

tively, through the multiple testing-adjusted levels, i.e., family-wise error rate (FWER) and family-wise non-discovery rate (FWNR).

An example: designing prospective studies. A researcher wishes to find out how many controls are needed in order to detect an association between a risk variant described by a multiplicative model with parameters:

$$\text{GRR} = 1.2, \quad p = 0.3, \quad \text{Prev} = 0.1.$$

The study has recruited 1000 subjects in the case group, and is aiming for power of 80% with FWER controlled at 5% level adjusted for the multiplicity of 10^6 tests.

In the application, we input the disease model parameters in the first step. In the second

U-PASS power calculator OR-RAF power diagram Design my study **Disease model converter** Help -

U-PASS is a unified power analysis tool for large-scale marginal association studies, including genome-wide association studies (GWAS).

We encourage users to take a [quick tour of the interface](#), and check out the [User Guide](#) and detailed documentations in the help pages.

Disease model:

Multiplicative

Disease prevalence in the population:

0.1

Risk allele frequency in the population:

0.3

Genotype relative risk:

1.5

Go to power calculator

Risk allele frequency in controls:

0.29

Odds ratio between allele variants:

1.575

Go to power calculator

Figure A.4: A screenshot of the user interface for the “Disease model converter” tab of the software. See Section A.2 for details of the conversion between disease models and canonical parameters in genome-wide association studies.

step, we select the sample size constraint as “number of cases” and set to 1000. The third step, we selected FWER as the criteria, and set the appropriate levels and multiplicity; a p-value cut off ($0.05/10^6 = 5 \times 10^{-8}$) is automatically calculated and displayed. The final step, we choose “Type II error / (1-power)” as the target and select $1 - 80\% = 20\%$.

The result of the calculation shows that the targeted power cannot be achieved at the current number of cases, no matter how many controls are recruited. Therefore, the researcher should consider recruiting more subjects in the case group in order to increase power. For example, if there are instead 4000 subjects in the case group, then we would need only roughly 4929 controls in order to achieve the desired level of power.

A.3.3 Converting disease models into canonical parametrization

The “Disease model converter” tab of the application provides a tool for converting disease models into their implied canonical parameters. See Figure A.4 for a screenshot.

The converter implements the mapping from disease models to the canonical parameters as detailed in Section A.2 and illustrated in Figure A.1. The tool also allows users to copy the model parameters into the “Design my study” tab for power calculations. Several

numerical examples, discussed in Section A.2, are provided in the tool.

A.4 Download, installation, and usage

Software availability. U-PASS runs as an R Shiny application. It is a free, open source software under the MIT license. A live instance of the application is hosted at <https://power.stat.lsa.umich.edu/u-pass/>. The source code can be obtained from the repository hosting service Github, by running in the computer's terminal:

```
clone https://github.com/Pill-GZ/U-PASS.git
```

or by downloading directly from the GitHub page: <https://github.com/Pill-GZ/U-PASS>.

Should the user choose to run the application from their local machine, we recommend downloading the source code, and follow the next two steps of this user guide.

Installation and dependencies. We have collected the required R packages inside the R script `install_required_packages.R`. These packages can be installed by navigating to the project folder, and running in the computer's terminal:

```
Rscript install_required_packages.R
```

or by running the following command from inside R (RStudio):

```
source("install_required_packages.R")
```

The U-PASS software itself requires no installation.

Start/terminate the application. The application can be started by running in the computer's terminal:

```
Rscript -e 'library(methods);  
          shiny::runApp("./", launch.browser=TRUE)'
```

or by running the following command from inside R (RStudio):

```
shiny::runApp()
```

The application can be terminated by simply closing the browser (or browser tab). Alternatively, the application can be terminated by pressing `Ctrl + C` in the terminal, or by clicking on the red stop button in Rstudio.

BIBLIOGRAPHY

- Adler, R. J. and Taylor, J. E. (2009). *Random fields and geometry*. Springer Science & Business Media.
- Agresti, A. (2018). *An introduction to categorical data analysis*. Wiley.
- Anderson, T. W. and Darling, D. A. (1952). Asymptotic theory of certain "goodness of fit" criteria based on stochastic processes. *The annals of mathematical statistics*, pages 193–212.
- Arias-Castro, E. and Chen, S. (2017). Distribution-free multiple testing. *Electronic Journal of Statistics*, 11(1):1983–2001.
- Arias-Castro, E. and Wang, M. (2017). Distribution-free tests for sparse heterogeneous mixtures. *Test*, 26(1):71–94.
- Arias-Castro, E. and Ying, A. (2019). Detection of sparse mixtures: higher criticism and scan statistic. *Electronic Journal of Statistics*, 13(1):208–230.
- Barber, R. F. and Candès, E. J. (2015). Controlling the false discovery rate via knockoffs. *The Annals of Statistics*, 43(5):2055–2085.
- Barndorff-Nielsen, O. (1963). On the limit behaviour of extreme order statistics. *The Annals of Mathematical Statistics*, 34(3):992–1002.
- Benjamini, Y. and Hochberg, Y. (1995). Controlling the false discovery rate: a practical and powerful approach to multiple testing. *Journal of the royal statistical society. Series B (Methodological)*, pages 289–300.
- Benjamini, Y. and Yekutieli, D. (2001). The control of the false discovery rate in multiple testing under dependency. *Annals of statistics*, pages 1165–1188.
- Berman, S. M. (1964). Limit theorems for the maximum term in stationary sequences. *The Annals of Mathematical Statistics*, pages 502–516.
- Bogdan, M., Chakrabarti, A., Frommlet, F., and Ghosh, J. K. (2011). Asymptotic bayes-optimality under sparsity of some multiple testing procedures. *The Annals of Statistics*, 39(3):1551–1579.
- Bush, W. S. and Moore, J. H. (2012). Genome-wide association studies. *PLoS computational biology*, 8(12):e1002822.

- Butucea, C., Ndaoud, M., Stepanova, N. A., and Tsybakov, A. B. (2018). Variable selection with Hamming loss. *The Annals of Statistics*, 46(5):1837–1875.
- Cai, T. T., Jeng, X. J., and Jin, J. (2011). Optimal detection of heterogeneous and heteroscedastic mixtures. *Journal of the Royal Statistical Society: Series B (Statistical Methodology)*, 73(5):629–662.
- Cai, T. T., Jin, J., and Low, M. G. (2007). Estimation and confidence sets for sparse normal mixtures. *The Annals of Statistics*, 35(6):2421–2449.
- Cai, T. T. and Wu, Y. (2014). Optimal detection of sparse mixtures against a given null distribution. *IEEE Transactions on Information Theory*, 60(4):2217–2232.
- Candés, E. J. (2018). Lecture 3: Global testing, chi-square test, optimality of chi-square test for distributed mild effects. In *Stats 300C: Theory of Statistics (Spring 2018)*, Stanford Lecture notes, <https://statweb.stanford.edu/~candes/teaching/stats300c/index.html>.
- Chatterjee, S. (2014). *Superconcentration and related topics*, volume 15. Springer.
- Comminges, L. and Dalalyan, A. S. (2012). Tight conditions for consistency of variable selection in the context of high dimensionality. *The Annals of Statistics*, 40(5):2667–2696.
- Conlon, D., Fox, J., and Sudakov, B. (2015). Recent developments in graph Ramsey theory. In *Surveys in combinatorics 2015*, volume 424 of *London Math. Soc. Lecture Note Ser.*, pages 49–118. Cambridge Univ. Press, Cambridge.
- Cramér, H. (1928). On the composition of elementary errors: First paper: Mathematical deductions. *Scandinavian Actuarial Journal*, 1928(1):13–74.
- De Haan, L. and Ferreira, A. (2007). *Extreme value theory: an introduction*. Springer Science & Business Media.
- Domingos, P. and Pazzani, M. (1997). On the optimality of the simple Bayesian classifier under zero-one loss. *Machine learning*, 29(2-3):103–130.
- Domínguez-Cruz, M. G., de Lourdes Muñoz, M., Totomoch-Serra, A., García-Escalante, M. G., Burgueño, J., Valadez-González, N., Pinto-Escalantes, D., and Díaz-Badillo, Á. (2018). Pilot genome-wide association study identifying novel risk loci for type 2 diabetes in a maya population. *Gene*, 677:324–331.
- Donoghue, W. F. (2014). *Distributions and Fourier transforms*, volume 32. Academic Press.
- Donoho, D. and Jin, J. (2004). Higher Criticism for detecting sparse heterogeneous mixtures. *The Annals of Statistics*, 32(3):962–994.
- Donoho, D. and Jin, J. (2015). Special invited paper: Higher criticism for large-scale inference, especially for rare and weak effects. *Statistical Science*, pages 1–25.

- Dunn, O. J. (1961). Multiple comparisons among means. *Journal of the American statistical association*, 56(293):52–64.
- Efron, B. (2004). Large-scale simultaneous hypothesis testing: the choice of a null hypothesis. *Journal of the American Statistical Association*, 99(465):96–104.
- Eicker, F. (1979). The asymptotic distribution of the suprema of the standardized empirical processes. *The Annals of Statistics*, pages 116–138.
- Embrechts, P., Klüppelberg, C., and Mikosch, T. (2013). *Modelling extremal events: for insurance and finance*, volume 33. Springer Science & Business Media.
- Erdős, P. and Szekeres, G. (1935). A combinatorial problem in geometry. *Compositio mathematica*, 2:463–470.
- Fan, J. (1996). Test of significance based on wavelet thresholding and neyman’s truncation. *Journal of the American Statistical Association*, 91(434):674–688.
- Ferguson, T. S. (2017). *A course in large sample theory*. Routledge.
- Fox, J. (2009). Lecture 5: Ramsey Theory. In *MAT 307: Combinatorics (Spring 2009)*, MIT Lecture notes, <http://math.mit.edu/~fox/MAT307.html>.
- Gao, Z. (2019). Five shades of grey: Phase transitions in high-dimensional multiple testing. *arXiv preprint arXiv:1910.05701*.
- Gao, Z. and Stoev, S. (2019). Fundamental Limits of Exact Support Recovery in High Dimensions. *Bernoulli*. in press.
- Gao, Z., Terhorst, J., Van Hout, C. V., and Stoev, S. (2019). U-PASS: unified power analysis and forensics for qualitative traits in genetic association studies. *Bioinformatics*. Advance online publication. 10.1093/bioinformatics/btz637.
- Genovese, C. and Wasserman, L. (2002). Operating characteristics and extensions of the false discovery rate procedure. *Journal of the Royal Statistical Society: Series B (Statistical Methodology)*, 64(3):499–517.
- Genovese, C. R., Jin, J., Wasserman, L., and Yao, Z. (2012). A comparison of the lasso and marginal regression. *Journal of Machine Learning Research*, 13(Jun):2107–2143.
- Gnedenko, B. (1943). Sur la distribution limite du terme maximum d’une serie aleatoire. *Annals of mathematics*, pages 423–453.
- Hall, P. and Jin, J. (2010). Innovated higher criticism for detecting sparse signals in correlated noise. *The Annals of Statistics*, 38(3):1686–1732.
- Haryono, S. J., Datasena, I., Santosa, W. B., Mulyarahardja, R., and Sari, K. (2015). A pilot genome-wide association study of breast cancer susceptibility loci in indonesia. *Asian Pac J Cancer Prev*, 16(6):2231–2235.

- He, Y., Xu, G., Wu, C., and Pan, W. (2018). Asymptotically independent u-statistics in high-dimensional testing. *arXiv preprint arXiv:1809.00411*.
- Hochberg, Y. (1988). A sharper bonferroni procedure for multiple tests of significance. *Biometrika*, 75(4):800–802.
- Holm, S. (1979). A simple sequentially rejective multiple test procedure. *Scandinavian journal of statistics*, pages 65–70.
- Hsing, T. (1995). A note on the asymptotic independence of the sum and maximum of strongly mixing stationary random variables. *The Annals of Probability*, pages 938–947.
- Inglot, T. (2010). Inequalities for quantiles of the chi-square distribution. *Probability and Mathematical Statistics*, 30(4):339–351.
- Ingster, Y. I. (1998). Minimax detection of a signal for l_n^p -balls. *Mathematical Methods of Statistics*, 7(4):401–428.
- Ji, P. and Jin, J. (2012). UPS delivers optimal phase diagram in high-dimensional variable selection. *The Annals of Statistics*, 40(1):73–103.
- Jin, J., Zhang, C.-H., and Zhang, Q. (2014). Optimality of graphlet screening in high dimensional variable selection. *The Journal of Machine Learning Research*, 15(1):2723–2772.
- Johnson, J. L. and Abecasis, G. R. (2017). Gas power calculator: web-based power calculator for genetic association studies. *bioRxiv*, page 164343.
- Kallitsis, M., Stoev, S. A., Bhattacharya, S., and Michailidis, G. (2016). AMON: An open source architecture for online monitoring, statistical analysis, and forensics of multi-gigabit streams. *IEEE Journal on Selected Areas in Communications*, 34(6):1834–1848.
- Kartsioukas, R., Gao, Z., and Stoev, S. (2019). On the rate of concentration of maxima in gaussian arrays. *arXiv preprint arXiv:1910.04259*.
- Leadbetter, M. R., Lindgren, G., and Rootzén, H. (2012). *Extremes and related properties of random sequences and processes*. Springer Science & Business Media.
- MacArthur, J., Bowler, E., Cerezo, M., Gil, L., Hall, P., Hastings, E., Junkins, H., McMahon, A., Milano, A., and Morales, J. (2016). The new nhgri-ebi catalog of published genome-wide association studies (gwas catalog). *Nucleic acids research*, 45(D1):D896–D901.
- McCormick, W. and Mittal, Y. (1976). *On weak convergence of the maximum*. Stanford University. Department of Statistics.
- Meinshausen, N. and Bühlmann, P. (2006). High-dimensional graphs and variable selection with the lasso. *The annals of statistics*, 34(3):1436–1462.

- Michailidou, K., Lindström, S., Dennis, J., Beesley, J., Hui, S., Kar, S., Lemaçon, A., Soucy, P., Glubb, D., and Rostamianfar, A. (2017). Association analysis identifies 65 new breast cancer risk loci. *Nature*, 551(7678):92.
- Neuvial, P. and Roquain, E. (2012). On false discovery rate thresholding for classification under sparsity. *The Annals of Statistics*, 40(5):2572–2600.
- Ramsey, F. P. (2009). On a problem of formal logic. In *Classic Papers in Combinatorics*, pages 1–24. Springer.
- Resnick, S. I. (2013). *Extreme values, regular variation and point processes*. Springer.
- Resnick, S. I. and Tomkins, R. (1973). Almost sure stability of maxima. *Journal of Applied Probability*, 10(2):387–401.
- Robbins, H. (1955). A remark on Stirling’s formula. *The American mathematical monthly*, 62(1):26–29.
- Šidák, Z. (1967). Rectangular confidence regions for the means of multivariate normal distributions. *Journal of the American Statistical Association*, 62(318):626–633.
- Skorokhod, A. V. (1956). Limit theorems for stochastic processes. *Theory of Probability & Its Applications*, 1(3):261–290.
- Slepian, D. (1962). The one-sided barrier problem for gaussian noise. *Bell Labs Technical Journal*, 41(2):463–501.
- Smirnov, N. (1948). Table for estimating the goodness of fit of empirical distributions. *The annals of mathematical statistics*, 19(2):279–281.
- Storey, J. D. (2007). The optimal discovery procedure: a new approach to simultaneous significance testing. *Journal of the Royal Statistical Society: Series B (Statistical Methodology)*, 69(3):347–368.
- Sun, W. and Cai, T. T. (2007). Oracle and adaptive compound decision rules for false discovery rate control. *Journal of the American Statistical Association*, 102(479):901–912.
- Tanguy, K. (2015). Some superconcentration inequalities for extrema of stationary gaussian processes. *Statistics & Probability Letters*, 106:239–246.
- Taqqu, M. S. (2003). Fractional Brownian motion and long-range dependence. In Doukhan, P., Oppenheim, G., and Taqqu, M. S., editors, *Theory and Applications of Long-range Dependence*, pages 5–38. Birkhäuser.
- Tsagris, M., Beneki, C., and Hassani, H. (2014). On the folded normal distribution. *Mathematics*, 2(1):12–28.
- Tukey, J. W. (1976). T13N: The higher criticism. In *Statistics 411, Princeton University Lecture notes*.

- Wainwright, M. J. (2009a). Information-theoretic limits on sparsity recovery in the high-dimensional and noisy setting. *IEEE Transactions on Information Theory*, 55(12):5728–5741.
- Wainwright, M. J. (2009b). Sharp thresholds for high-dimensional and noisy sparsity recovery using ℓ_1 -constrained quadratic programming (lasso). *IEEE transactions on information theory*, 55(5):2183–2202.
- Wainwright, M. J. (2019). *High-dimensional statistics: A non-asymptotic viewpoint*. Cambridge University Press, Cambridge, UK.
- Wasserman, L. and Roeder, K. (2009). High dimensional variable selection. *Annals of statistics*, 37(5A):2178.
- Wu, C., Xu, G., and Pan, W. (2019). An adaptive test on high-dimensional parameters in generalized linear models. *Statistica Sinica*, 29:2163–2186.
- Xu, G., Lin, L., Wei, P., and Pan, W. (2016). An adaptive two-sample test for high-dimensional means. *Biometrika*, 103(3):609–624.
- Zhang, J. (2002). Powerful goodness-of-fit tests based on the likelihood ratio. *Journal of the Royal Statistical Society: Series B (Statistical Methodology)*, 64(2):281–294.
- Zhao, P. and Yu, B. (2006). On model selection consistency of lasso. *Journal of Machine learning research*, 7(Nov):2541–2563.
- Zhong, P.-S., Chen, S. X., and Xu, M. (2013). Tests alternative to higher criticism for high-dimensional means under sparsity and column-wise dependence. *The Annals of Statistics*, 41(6):2820–2851.